Roma Tre University
Ph.D. in Computer Science and Engineering
XXV Cycle

Models and algorithms for the efficient operation and planning of energy production systems

Ph.D. Candidate: Arianna Naimo

Advisor: Prof. Giovanni Felici

Ph.D. Coordinator: Prof. Stefano Panzieri

Year 2012/2013

Models and algorithms for the efficient operation and planning of energy
production systems

A thesis presented by
Arianna Naimo
in partial fulfillment of the requirements for the degree of
Doctor of Philosophy
in Computer Science and Engineering
Roma Tre University
Dept. of Informatics and Automation
Spring 2013

A chi, con immenso amore, mi è sempre vicino

Contents

Preamble

Since the last four decades the electrical industry has been characterized by important and rapid changes around the world, regarding generation, transmission and distribution of electricity. These changes create the need for more efficient operation and planning of energy generation systems. Global energy demand is increasing, but most of the energy sources which are used to produce electricity nowadays are characterized by a limited scope, and electric energy is not suitable to be stored. Performing proper operation and planning of energy generation systems leads to a more efficient utilization of the available resources and to a limitation in the global environmental impact.

The recent changes of electrical market structures, like privatization, restructuring and deregulation lead to maximize the expected value of the electricity market profits. Moreover, the integration of different types of energy sources in conventional electrical systems is assuming growing importance, like renewable sources such as wind and solar energy. These aspects have to be considered to perform a proper energy production scheduling, taking into account both the uncertainty related to energy demand load forecast and the uncertainty related to not conventional energy.

For these issues researchers from mathematics, operations research and engineering have focused for many years on applying mathematical modeling and optimization techniques, in order to solve the optimization problems related to energy generation systems.

Different types of optimization problems are considered and solved, according to the energy industry process that is involved; typically, generation, transmission and distribution of electricity, or a combination of them. These optimization problems are characterized by an objective function, variables and constraints. Generally, the economic efficiency or the utilities profits are represented by the objective function, system operating and technical requirements are represented by the constraints, while the variables are used to model decisions, which can be taken in long-term, medium-term, short-term or on-line periods.

In a long-term period (months and years), the Power Expansion Problem is solved, in order to determine the type, the capacity and the number of generating units that the energy system should have.

In a medium-term period (days and weeks), the objective is to determine the best combination of generating units in terms of their status (committed or uncommitted) and their output (power). This schedule has to satisfy the forecast demand at minimum total production cost, under the operating, technical and environmental system constraints. This problem is known as Unit Commitment Problem (UC).

In a short-term and on-line period (hours and minutes), the Economic Dispatch Problem (ED) is solved, in order to determine the power that each unit, scheduled in the previous phase (solving the UC problem) must produce in order to meet the system demand at real time.

Part of our research activities focused on analyzing the modeling aspects related with the

production and the scheduling of electrical systems. In particular, we have studied the limits and the simplifications mainly used in the classical UC models presented in the literature, in order to develop more realistic formulations for this problem.

UC models are usually characterized by a combination of several difficulties like the presence of continuous and binary decision variables at the same time, a very large-scale dimension, several non-linearities (for instance, in fuel costs modeling) and uncertainty of the problem data (for example, in load demand forecasts, fuel pricing models, stream flows to reservoirs and generating units failures). For these reasons, numerous simplified variants of models and algorithms for UC have been proposed in the literature.

Traditional UC models are based on two main hypotheses. First, the power can be instantaneously adjusted. Second, the power output is constant in an assigned time interval (i.e. 1 hour), so that the energy produced in each hour is equal to the power level multiplied by 1 hour. These assumptions greatly simplify the model, because energy and power can be represented by the same entity even if they are different from a physical point of view; nevertheless the model does not properly reflect the realistic operating behavior of the generating units.

For this reason, in our research activities we have defined more realistic mathematical formulations for the UC than the ones proposed in the literature, in order to overcome most of their main drawbacks. In particular, we propose new Mixed-Integer Quadratic Programming (MIQP) models for UC, based on power instead of energy. We have also defined and proposed new UC models integrated with the ED problem, where the variables are associated with the power levels, that are assumed to change linearly in each time period, while the energy levels are then computed accordingly. We have thus derived more realistic models that effectively represent the constraints imposed on the units in order to avoid mechanical stresses to the rotors for conventional units, or to avoid the use of more units in peak hours.

Conventional electrical systems are highly fossil fuel dependent, being the major contributors to the greenhouse gas emissions and to the depletion of global fossil fuel resources which are characterized by more volatile prices. For this reason, the use of clean renewable energy sources for electricity generation is acquiring global relevance. Several world countries actively support the growing use of renewable energy sources, such as wind, in order to meet Kyoto Protocol targets for reducing greenhouse gas emissions. Wind energy contributes to this target with a significant percentage. In some world and European countries, such as Italy, Spain, Germany, and Denmark, wind is an important part of the electricity supply.

Nevertheless, the integration of wind energy into the electrical systems is complex and significantly challenging, especially when large amounts of variable wind generation are introduced. Even if there exist positive aspects related with the utilization of wind energy, it is necessary to take into account some practical considerations. For instance, when wind power plants are connected to the electrical network, it is necessary to improve transmission lines, in order to avoid grid stability problems, needing additional operational costs. Furthermore, when the uncertainty associated with the electricity produced by wind energy sources becomes greater than the uncertainty of the demand, it is no longer possible to maintain the same power system reliability with the conventional power plant scheduling techniques.

For these reasons, even if the integration of wind energy sources into conventional electrical system is growing in importance - due to its economical and environmental development benefits - particular attention must be devoted to the related practical operational aspects. This leads to the necessity to modify the current industry procedures, such as the UC and the ED, to take into account large amounts of wind power production. Even if an exhaustive literature exists on the general UC problem, focused on how improve its mathematical formulation and its solution

algorithm, the research that considers the UC problem in presence of wind energy resources is limited.

Part of our research activities has then focused on the development of new UC models in presence of wind energy sources. The objective of the new proposed UC models is to integrate renewable energy sources in a conventional electrical system. These models formulate and solve the problem of determining the best configuration (optimal mix) of available thermal, hydro and wind power plants.

The ongoing integration and deregulation of electricity markets in Europe and in the world requires that part of the electricity production is traded daily on power pools where producers state how much electricity they will provide up to 36 hours in advance. This market structure induces additional costs for wind power producers due to the greater unpredictability of wind power at these time horizons. These issues motivate the importance of wind power forecasting techniques that are fundamental to provide accurate forecasts on wind production. In particular, wind generation requires complex forecasting techniques which take into account wind speed, wind direction, hub height, geographical conditions, wind farm size, wind turbine technical and operational characteristics and so on.

Since the use of wind energy sources and its integration into power generation systems is assuming increasing importance, new generation models for synthetic wind data are needed, in order to properly generate forecasts of wind speed and power. This data is fundamental in simulations carried out to analyze and improve the performances of wind generating units, individuating the technical parameters of wind turbines that directly affect power production.

Part of our research activities focused also on developing a new model in order to generate realistic synthetic wind data. In this model, wind speed is assumed to behave as a Weibull distribution, while wind speed forecast error is simulated using First-Order Auto-Regressive Moving Average - ARMA time-series models. Mathematical Operations Research formulations of the Assignment Problem are used to model wind speed persistence features, which, as shown by simulation results, are essential to properly obtain wind speed and power output forecasts.

Furthermore, wind synthetic data, generated with the new generation model proposed, has been used to carry out simulations studies to individuate wind turbines operational parameters that mainly affect wind generators performances. In particular, an experimental function which expresses the average energy produced by a wind turbine in a 24 hours time horizon in a typical day has been determined, considering the main simulation parameters related with Weibull distribution and wind turbines.

Below we describe the structure of this dissertation.

In Part I we describe how conventional electrical systems work, focusing our attention on the UC problem which is solved for their efficient operation and planning. In particular, in Chapter 1 we present the main characteristics of a conventional electrical system and we illustrate how the energy is traded in the electrical market and how the electricity production is properly scheduled. Chapter 2 and Chapter 3 illustrate the basic features of the UC, presenting the state of the art of the models and for methods use to solve this problem, respectively.

Part II deals with the new proposed models for the UC, which represent an improvement of the conventional electrical systems, since - as previously anticipated - they are based on novel assumptions which have been neglected in the literature so far. In particular, Chapter 4 illustrates the novel formulations for the UC with power variables, while in Chapter 5 the new model for the UC integrated with the ED is presented.

In Part III, the integration of wind energy sources into conventional electrical systems is treated. In particular, the problems and the challenges that this integration imposes to the

already existing systems are presented in Chapter 6, where the new model for the UC in presence of wind energy sources is proposed. The importance of wind speed and power output forecasts for a proper energy production scheduling is described in Chapter 7, where the new model to generate synthetic wind data is presented. Chapter 8 describes how this new generation model can be applied to properly compute the average energy of a typical wind turbine, illustrating the main parameters of the wind generator that affect the calculation of the energy.

Finally, in the last part of this dissertation, conclusions are drawn and interesting directions for future research are discussed.

Part I

Planning the production of conventional electrical systems

Chapter 1

Planning the production of the energy systems

In this chapter we present the main characteristics of a conventional electrical system, describing its strengths and its weaknesses, and focusing our attention on the dispatch problem, which is fundamental for the proper operation and planning of the electricity production. We also illustrate how the energy is traded in the electrical market and how the energy production is properly scheduled, introducing the UC problem.

1.1   How the electrical system works

In a typical electrical system, the energy taken from the final customers is produced and put into the electrical network by the generating units [ST10] [WW84]. An electrical system is generally composed by three main subsystems which constitute the value chain of the electrical industry, as shown in Fig. 1.1:

- *production nodes*: they are represented by the power plants (thermal, hydro, wind, solar, and so on);

- *transmission lines and interconnections*: they are necessary to send the electrical power from the production nodes to the consumption nodes;

- *distribution lines*: they constitute the final part of the electrical system and distribute the energy at each block of loads.

Generally, the production nodes are not numerous and they produce power in a concentrated point of the network. They are distant from the consumption nodes, which vice versa are really numerous and dislocated in the whole territory, being mainly concentrated in the urban and industrial areas.

Two types of transmission lines exist:

- *primary transmission lines*: they connect the power plants to the primary sorting nodes which are called distribution substations (or substations);
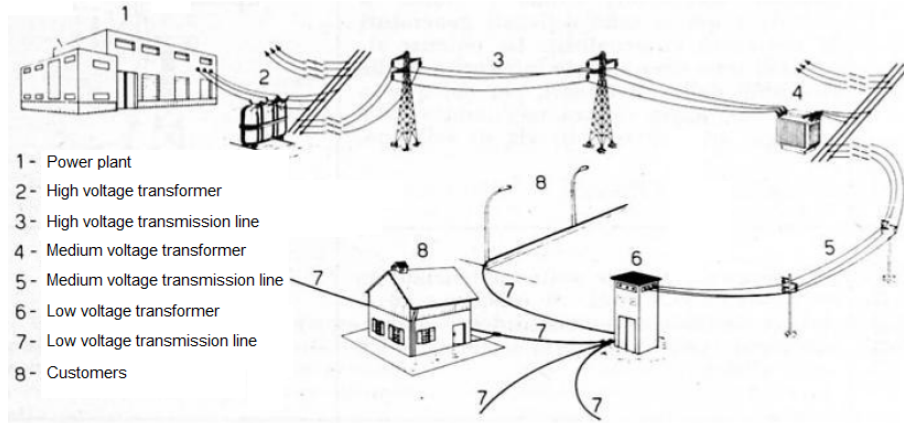
Figure 1.1: A typical conventional electrical system.
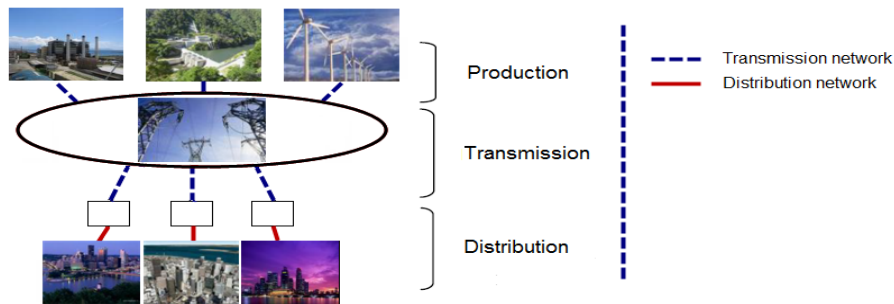
Figure 1.2: Phases of the electrical system.

- *secondary transmission lines*: they start from the substations and feed the distribution of the electric energy at a local level.

Normally, the transmission lines never follow only radial paths. In order to have a greater flexibility in the electrical distribution, networks where the nodes are interconnected are realized. For this reason, the transmission lines are properly called interconnection transmission lines and they can exchange energy also between different power plants. As a matter of fact, all the European electrical systems are interconnected.

Based on its general structure, the electrical system thus consists of three phases: production, transmission and distribution of the electrical energy, as shown in Fig. 1.2.

- *Producing energy* means transforming the energy obtained form primary sources, such as coal, gas, nuclear, water, into electricity. This transformation happens in the thermal or hydro power plants, or in wind and solar generating units. The production phase is connected with the companies that produce electricity; each of them owns several production groups (usually, from 2 to 5, which belongs to a power plant), dislocated in places distant from the consumption centers, to respect the environmental constraints.

- *Transmitting energy* means transferring the energy produced by the production centers to

the consumption zones. In order to perform this operation it is necessary to build transmission lines, electrical stations and transformation stations, which are the elements that compose the transmission network. A large amount of energy is transferred to distant places, with high values of voltage, using overhead lines or cables. The development of the electrical transmission network has several objectives, such as

- to guarantee the security and the continuity of the electricity supply;
- to increase the efficiency and the economy of the transmission service;
- to reduce the network overloads;
- to develop and strengthen the interconnections with other countries.

- *Distributing energy* represents the last phase of the electrical system; it is the delivery of the electricity at a medium and low voltage to the customers, and it is realized with overhead lines or cables characterized by a length and a power lower than those used for the transmission. The planning of the development of the electrical transmission network is based on

  - the energy demand required by the customers;
  - the forecast of the energy demand to be satisfied;
  - the necessity to strengthen the network;
  - the requirement of connections of new generating units to the network.

After being distributed, the electrical energy is utilized in various applications such as the illumination, the movement of machines, the warming of indoor environments.

1.1.1 Strengths and weaknesses of the electrical system

Due to its structure, the electrical system generally presents several strengths which are mainly related with

- flexibility in the production;

- good quality in the transmission and distribution of the electrical energy;

- security in the utilization of the electrical energy.

As far as the first aspect is concerned, the flexibility in the production is due to the possibility to produce electrical energy using all the primary energy sources also in places that are distant from the sources themselves, concentrating the production in a small number of power plants.

The good quality in the transmission and distribution of the electrical energy is related with the possibility to transfer efficiently the electrical energy in places that are distant from the point where it has been produced.

Furthermore, the conversion of the electrical energy into its final form that is utilized by customers is performed in security.

Nevertheless, the electrical system presents also some weaknesses, which represent strong constraints:

- first, the global efficiency of a system which produces, transmits and distributes electrical energy is rather low and it can vary from 35% up to 45% with respect to the primary energy source utilized and to the technology employed; most of the energy losses happen in the production process, within the physical boundaries of the power plants;

- second, it is necessary to instantly and continuously perform a balance between the amount of energy introduced into the network and the amount that is taken from the network itself, taking into account the losses in the transmission and distribution phases; furthermore, the electrical energy can be stored only in limited quantities and at a high cost; storing electricity with proper plants and batteries requires high costs;

- the frequency and the voltage of the energy in the network must be maintained within a strict interval, in order to guarantee the security of the plants;

- it is necessary that the energy fluxes on a single network do not overcome the maximum admissible limits;

- finally, only the already existing transmission network can be utilized: building new lines requires long time periods and high investments.

If the electrical energy production scheduling respects these constraints it is considered feasible. Nevertheless, it could happen that *real time*, when the energy is distributed, these constraints are no longer respected since the values of power absorbed by the load and/or the values of the production differ from what has been scheduled, or a failure of a transmission line occurred. Respecting these constraints is also difficult because of the characteristics of the technologies and of the modalities in which the electrical energy is produced, transmitted and consumed. For this reason, a correct planning of the generating units is needed.

1.1.2   The dispatch problem

The high grade of complexity in guaranteeing the correct working of the electrical system imposes the individuation of a central coordinator that owns a control power on all the production plants of the system. This coordinator, called '*dispatcher*', represents the crucial actor of the electrical system in the monopolistic regime: it guarantees that the production always equals the consumption (for all the 365 days of the year, for all the 24 hours of each day) and that the frequency and the voltage always reach the optimal values, respecting the transmission constraints of the network and the dynamic constraints of the generating units. In order to achieve this goal, the dispatcher performs the following two fundamental activities:

- *definition of the programs of introduction and extraction of electrical energy*, solving the *Unit Commitment (UC)* and the *Scheduling* problems: a week before (or the day before), the dispatcher defines the programs of production of each generating unit in order to satisfy the required energy demand, taking into account also the losses, at a minimum total cost. These programs define, for each hour of the following day, the amount of energy that has to be introduced into the network. The *load forecasting* is related with the individuation of a possible load diagram for a given day or a given week, that is the most realistic possible, while by the solution of the UC the optimal set of generating units is individuated in order to satisfy the forecast demand;
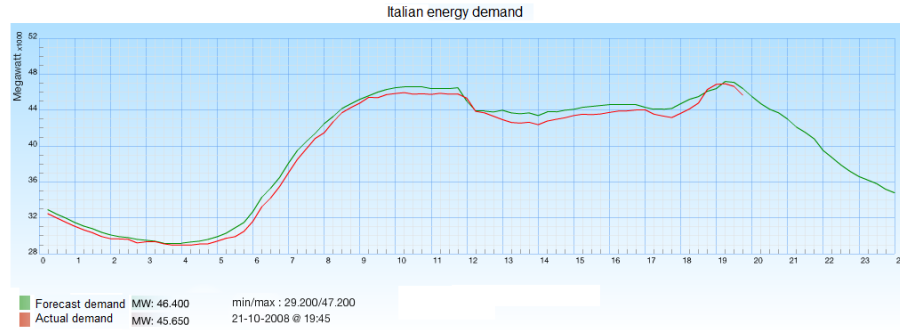
Figure 1.3: Example of load curve.

- *real-time balancing of the system*: the needed equilibrium between the energy introduced and extracted at each time instant and in each node of the network is guaranteed by the regulation and automatic control systems of the generating units (primary and secondary reserve), which increase or decrease the introduction of the energy into the network in order to compensate each disequilibrium on the network itself. The dispatcher actively operates, sending the start-up, increasing or decreasing of the generated power commands to the reserve units, only when the operating margins of the automatic regulation systems are lower than the security standards, in order to reintegrate them. This way, the optimal subdivision of the total load between the set of generating units individuated in the previous phase is guaranteed.

High attention must be devoted to the individuation of the load curve since the analysis of the following phases will be based on this curve. The scheduling of the active generating units will be more complete if this curve is the most realistic possible, being highly similar to the actual load curve. Fig. 1.3 shows an example of load curve.

These forecast curves are determined considering that, as it happens in many other activities, also the electrical system is cyclical and thus generally the total load will be high when industrial and working activities are performed, while it will be lower at night. Furthermore, the weekly cycles have also to be considered: the demand is lower during the week-end and higher during the week when working activities are done. For these reasons, the dispatch problem is very complex and it is subjected to a high number of constraints and variables during the given time period that have to be properly considered in order to obtain a correct scheduling. In the following sections we will explain how the electrical energy is traded and the characteristics of the electrical markets which, in general, constitute a typical electrical system.

1.2 How the electrical energy is traded

The world electrical industry has been always considered monopolistic, nevertheless it is nowadays characterized by a restructuring phase in order to take into account competition rules. This phenomenon is known as the liberalization of the electrical market, which is a well organized system where the exchange between the demand and the supply of electrical energy is performed.

The electrical market is a place where the producers supply and the customers demand of energy meet [dMEG]. In this place, the price of the energy of a given country is determined. Fig.
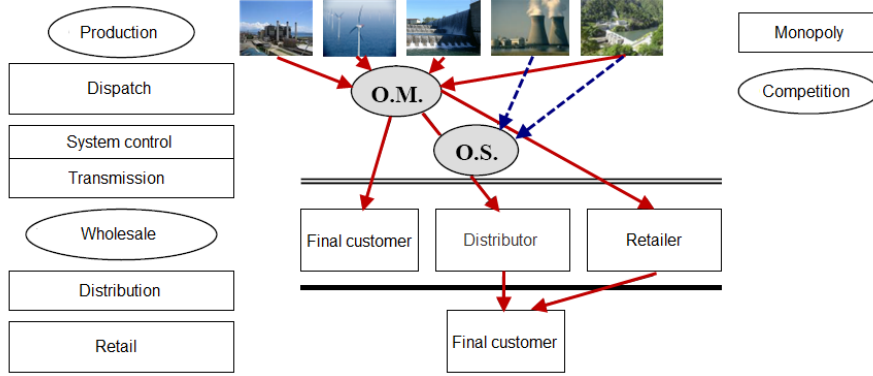
Figure 1.4: Characteristics of the electrical market.

1.4 represents the different parts that compose the electrical market correlated with the various phases of the electrical system.

In order to respect the technical constraints, a centralized coordination of the system is required. Regardless the typology of the electrical market (monopolistic or not), all the electrical systems present a *grid operator*), called also *System Operator* (SO). The SO continuously maintains the balancing between the demand and the supply, ensures the stability of the electrical parameters of the network (in particular, the value of the voltage) and solves the network overloads. In most of the electrical markets, the SO is associated to the *Market Operator* (MO), which manages one or more electrical markets to perform the short-term production scheduling. The functions of the SO and MO are strictly related; the grade of established coordination is maximum in those systems where these functions are assigned to an unique entity, or they are performed by entities that are strictly related, while this grade is minimum if these functions are assigned to two independent entities.

Currently, more than a dozen of working electrical markets exist in the world, and each market presents its own characteristics. The number of electrical markets increases if also the markets that currently are in the implementation phase are considered. The differences between these markets depend both on local and technological factors, and on political choices.

1.2.1   Types of electrical markets

The introduction of the competition in producing and selling electrical energy implies the passage from a traditional monopolistic system, based on the minimization of the cost, to one system based on the prices determined in the electrical market. The creation of an electrical market responds to two main needs:

- to promote the competition in producing and selling electrical energy, respecting neutrality, transparency, and objectivity criteria;

- to ensure the economic management of an adequate availability of the dispatch services.

In general, the electrical system consists of the following three markets [dMEG]:

- *day-ahead market*: it is the main market, and it is connected with the constraints of the electrical network; most of the transactions of the electrical energy take place in this market;

- *adjustment market*: it allows the generation companies to modify the programs defined in the day-ahead market, performing other transactions of electrical energy;

- *auxiliary services market*: it allows the generation companies to obtain the necessary resources to manage and control the system (resolution of the overloads between zones, creation of the energy reserve, real-time balancing). The auxiliary services market consists of the balancing market, the market for the resolution of the overloads, and the reserve market.

  In the *balancing market*, the day-ahead, the SO obtains from the producers the resources necessary to execute real-time, by the regulation, the balancing between the energy generated and the load.

  The *market for the resolution of the overloads* takes place, in an unique session, the day before the transactions. In this market, the generation companies have the possibility to receive an economic compensation for the cancellation of a right obtained on the electrical energy markets, due to the presence of overloads.

  The *reserve market* takes places in an unique session after the first session of the adjustment market. Based on the supply presented by the generation companies, the network manager obtain the reserve power, in order to guarantee the security of the electrical service.

These markets generally constitute a typical electrical system, nevertheless the number and the type of these markets and structure of the electrical system itself could vary according to the country considered. In this thesis, we mainly refer to the Italian electrical system and to the structure previously described.

1.3   How to plan electrical energy production

The efficient planning of the electrical energy production is a complex activity. It requires a proper co-ordination of the operations of many generating units, that can be distributed in different geographical areas. This operation must satisfy the required electrical energy demand, which is always subject to continuous variations, as previously described.

The problem of the scheduling of the production of electrical energy is generally based on three different sets of decisions, which depends on the length of the time horizon. The first set consists of the long-term decisions in which the decisional variables to be determined are represented by the capacity, the type, and the number of generating units that the electrical system has to own. In the mean-term (days or weeks), it is necessary to decide how to schedule (*commitment*) the available units in the given time horizon. The term *commitment* indicates the start-up of a given unit, so that it synchronously operates with the electrical system. Finally, in the short-term (minutes or hours), the objective is to properly determine the amount of power that each scheduled unit has to produce in order to satisfy the real-time demand. Generally, the long-term problem is identified as the *Power Expansion Problem*, the mean-term problem is identified as the *Unit Commitment Problem* - UC, while the short-term problem is called *Economic Dispatch Problem* - ED, or *Generator Allocation Problem*.

Once that the electrical agents (or generation companies) obtain the scheduling that derives from the resolution of the UC, they solve the ED on a 15 minutes time horizon and they change the outputs of the scheduled units in order to respect the demand estimations.

The generation companies typically posses numerous units and they have to schedule them. This is due to the fact that the electricity cannot be stored in a large-scale system, that the demand

varies and that the generating units cannot produce the same amount of power in all the time instants. Furthermore, the generators cannot be started-up instantly to satisfy the demand and the commitment of a unit that is not needed represents an economical loss. Moreover, another source of uncertainty for the problem is related with the supply. For instance, in the case in which the power system includes wind unit, the power produced by these generators varies in time according to the wind speed.

For these reasons, the scheduling of the power generators is a crucial economical decision for the generation companies. Neglecting the importance of this problem can lead to serious consequences. For instance, if an operator effectuates the *over-committing* of the generators using the rule to schedule the demand and in addition a certain percentage of the load peak, then the result will have a higher production cost. On the other hand, the *under-committing* of the generators can lead to a *black-out* if a failure of a unit or a high peak of the demand occur.

The *Unit Commitment* (UC) is one of the most important problem to be solved in order to obtain a proper energy production scheduling. The objective of this problem is to determine a combination of the available electrical generators, scheduling their respective outputs in order to satisfy the forecast load demand at minimum total production cost in a specific time period, which usually varies from 24 hours to one week. The scheduling not only must minimize the total production cost, but it also should satisfy the operating constraints of the whole electrical system. These constraints reduce the freedom in the choice of starting-up or shutting-down the units. Usually, the constraints that have to be satisfied are related with the status of the units, to the minimum *minimum up time* and *minimum down time* of the units, to the capacity and power production limits, to the *maximum ramp up rate* and to the *maximum ramp down rate*, to the *spinning reserve*, and to the other operating characteristics such as those of the hydro units.

In order to meet the needs of the electrical industry, many researches have been focused on this problem. The computational effort to solve the UC is stronger when it is formulated for a large-scale system, with hundreds of binary and continuous variables, due to its NP-*hard* nature [Tse96]. Furthermore, the resolution time exponentially increases with the dimension of the system, for this reason, the UC requires efficient and effective methods to be solved. Moreover, the problem is dynamic and this means that the current optimal configuration of the set of generating units is influenced by the previous one and influences the following one.

The problem is challenging because in a typical electrical system various types of generating units are available to generate electrical energy and each unit has its own characteristics. For instance, a nuclear power plants can produce energy at a very low incremental cost for each MWh of additional energy, but it presents a high cost of *start-up* once it has been shut-down, it takes some time before it reaches the regime status, producing the maximum power. A typical power plant should be shut-down only in spring or in autumn, when the demand for the warming or for the air conditioning is lower.

On the opposite side, a power plant based on turbines can be started-up in a few minutes. Nevertheless, the incremental cost for MWh is higher. According to the most convenient scheduling, the most efficient units, with a higher start-up cost, should be started-up first as far as the demand increases, then the remaining units. As far as the demand decreases, the units should be shut-down in the reverse order.

Decisions are more interesting if a modest load peak of short duration is present. In this case, it should be more economical to not consider an intermediate unit and instead start-up an inefficient generator, which is characterized by a lower start-up cost, for all the duration of the demand peak. The decisions can be complicated by other characteristics and by other types of units (which for instance can be nuclear, thermal or hydro).

Chapter 2

Models for formulating the Unit Commitment

Mathematical models are fundamental to understand the optimization problems related to generation, transmission and distribution of electricity. Different mathematical models of Unit Commitment (UC) exist, due to the diversity of power systems regarding technological design and economic requirements, but there are quite a few basic features that UC problems in hydro-thermal power systems have in common.

In this chapter we illustrate the basic features of the UC, presenting the state of the art on the models to formulate this problem, analyzing the basic assumptions and simplifications that have been made in the literature so far.

2.1   Basic features of Unit Commitment models

The UC problem can be formulated as an optimization problem with an objective function, variables and constraints. The objective of the UC is to schedule at minimum total cost a given set of generating units, such as thermal, hydro, wind, and so on, ensuring that the required energy demand is satisfied, on a given time horizon. This goal is reached when the best combination of generating units in terms of their status (committed/uncommitted) and their output (power) is found. This schedule has to satisfy the forecast demand at minimum total production cost, under the operating system constraints, in a specified time horizon (usually 24 hours or one week). Each type of generating unit considered in the UC problem presents different technical and operating characteristics that have to be modeled with specific constraints and a proper objective function. This leads to the existence of different forms of UC problems, depending on the accuracy considered in the representation of certain aspects of the operating characteristics of the units. In the literature various types of UC models exist, which take into account for instance thermal units [AC04] [LS03] [LS05] and hydro units [AOS02] [CMMF05] [CPM10] [FdS06] [FdSS05]. Nevertheless, there exist some basic features that UC models have in common, as shown in the following sections.

2.1.1 Objective function

The objective of the UC decision process is to select the generating units that have to be on or off, the type of fuel that has to be utilized, the power generation level for each unit and the spinning reserve margins. The objective function of the UC problem consists in minimizing the total operational cost, subjected to the system operating constraints. Total energy production costs may include fuel costs, maintenance and start-up costs of generating units. Fuel costs are normally represented either by a polynomial cost curve (quadratic or cubic), a piecewise constant curve or a piecewise linear curve.

However, in recent years, because of environmental considerations and market liberalization, literature has focused attention also on UC problems whose objective is not only reaching minimum total operational cost, but maximizing the expected value of the overall electricity market profits, including costs related to environmental impacts [CHR12]. Moreover, the great complexity of power networks leads to maximize also reliability and security of the system, keeping them above a certain minimum level.

The form of the UC model shown in this chapter is the classical UC formulation, which originated from the era of monopolistic producers. In our model, we assume that the objective function has a quadratic form with respect to the power p_t^i produced by the thermal unit i at time period t, as explained in [HRNC01]. As far as this aspect is concerned, recent trends in the literature have focused attention on the piecewise linear approximation of the quadratic cost curves of the UC problem, as shown in [Wu11].

Consider a set $\mathcal{P}$ of thermal units and a set $\mathcal{H}$ of hydro cascades, each comprising one or more basin units. $\mathcal{T} = \{1, \ldots, n\}$ is the set of time periods defining the time horizon (the time period "0" will be used to indicate the initial conditions of the power system).

We introduce the binary variable u_t^i to express the status of the thermal unit i at time period t, with $i \in \mathcal{P}$, $t \in \mathcal{T}$. If $u_t^i = 1$ the thermal unit i is on at time period t, otherwise, if $u_t^i = 0$ the thermal unit i is off at time period t. We also introduce the continuous variable p_t^i to indicate the power produced by the thermal unit i at time period t, expressed in MW, with $i \in \mathcal{P}$, $t \in \mathcal{T}$.

Introducing these variables for the thermal units, the objective function of the UC, representing the total power production cost to be minimized, has the following form

$$\sum_{i \in \mathcal{P}} c^i(p^i, u^i) = \sum_{i \in \mathcal{P}} \left(s^i(u^i) + \sum_{t \in \mathcal{T}} a_t^i(p_t^i)^2 + b_t^i p_t^i + c_t^i u_t^i \right) \tag{2.1}$$

where

- $s^i(u^i)$ is the start-up costs function of unit i, possibly time-dependent;

- a_t^i is the quadratic term of power cost function of thermal unit i at period t, expressed in €$/MW^2$;

- b_t^i is the linear term of power cost function of thermal unit i at period t, expressed in €$/MW$;

- c_t^i is the constant term of power cost function of thermal unit i at period t, expressed in €.

In the following sections the basic constraints of the UC problem, such as the operating constraints for the units and the power balance constraints are explained.

2.1.2   Operating constraints for thermal units

The solution of the UC problem is represented by an optimal production schedule that takes into account all the system constraints, like practical device and operational assumptions, environmental considerations and reliability and security assumptions.

In the classical UC model, presented previously, the constraints can be partitioned as follows [Pad04]:

1. *operating constraints for thermal units*: these constraints represent operating requirements related with the utilization of thermal generating units;

2. *operating constraints for hydro units*: these constraints represent operating requirements related with the utilization of hydro generating units;

3. *power balance constraints*: these constraints represent the power balance equation that has to be satisfied in order to fulfill the required system load demand.

UC can be modeled also with additional constraints which represent further operating requirements of the generating units; the meaning of these constraints is explained in section 2.1.4.

The operating requirements of thermal generating units are usually expressed by inequality constraints, which are used to model the technical characteristics of the units. In the formulation of the constraints shown below, the complete state of each unit before the beginning of the current operation is assumed known, i.e. its commitment u_0^i and the generated power p_0^i. In order to formulate minimum up-and down-time constraints (2.2) and (2.3) it is also necessary to know how long the unit has been on or off at time period 0.

Minimum up and down time constraints

The most important non-linear constraints for thermal units are the minimum up-time and down-time restrictions. The start-up of a unit is efficient only if it is required to run for a certain minimum number of hours continuously (minimum up-time requirement), while minimum down-time is the number of hours a unit must be off-line before it can be started-up again (minimum down-time requirement), as in [DT05] [LLM04]. These constraints represent mechanical requirements to prevent damages of the most solicited parts of a conventional unit (such as turbine, compressor and alternator).

For each thermal unit $i \in \mathcal{P}$, let τ_+^i and τ_-^i be respectively the minimum up- and down-time requirements. The minimum up- and down-time constraints can be expressed as follows:

$$u_t^i \geq u_r^i - u_{r-1}^i \qquad t \in \mathcal{T}, r \in \left[t - \tau_+^i, t - 1\right] \tag{2.2}$$

$$u_t^i \geq 1 - u_{r-1}^i - u_r^i \qquad t \in \mathcal{T}, r \in \left[t - \tau_-^i, t - 1\right] \tag{2.3}$$

$$u_t^i \in \{0, 1\} \qquad t \in \mathcal{T} \tag{2.4}$$

Unit generation capability limits

A generating unit is forced to operate within a lower and an upper limit of power, in order to avoid technical damages.

For each thermal unit $i \in \mathcal{P}$, let $\overline{p}^i_{min}$ and $\overline{p}^i_{max}$ be respectively the minimum and maximum power output of the unit when operating in steady state, expressed in MW. The unit generation capability limits can be expressed as follows:

$$\overline{p}^i_{min} u^i_t \leq p^i_t \leq \overline{p}^i_{max} u^i_t \qquad t \in \mathcal{T} \tag{2.5}$$

Ramp rate constraints

The rate of increasing or decreasing electrical power output from the unit is limited by ramp rate constraints. Ramp-up constraints limit the maximum increase of the unit electrical output, while ramp-down constraints limit the maximum decrease of this output.

For each thermal unit $i \in \mathcal{P}$, let Δ^i_+ and Δ^i_- be respectively the maximum ramp-up and ramp-down rates, expressed in MW/h, and let $\overline{l}^i$ and $\overline{u}^i$ be the maximum power that can be produced by the unit in the time period immediately where it is committed or uncommitted, respectively, expressed in MW. The ramp rate constraints can be expressed as follows.

- *Ramp-up constraints*: when the unit is committed in both time periods $t-1$ and t, the maximum increase of generated energy from time instant $t-1$ to the next is limited to $\Delta^i_+ > 0$, as expressed in formula (2.6) and depicted in Fig. 2.1(a)

$$p^i_t \leq p^i_{t-1} + u^i_{t-1}\Delta^i_+ + (1 - u^i_{t-1})\overline{l}^i \qquad t \in \mathcal{T} \tag{2.6}$$

- *Ramp-down constraints*: when the unit is committed in both time periods $t-1$ and t, the maximum decrease of generated energy from time instant $t-1$ to the next is limited to $\Delta^i_- > 0$, as expressed in formula (2.7) and depicted in Fig. 2.1(b)

$$p^i_{t-1} \leq p^i_t + u^i_t\Delta^i_- + (1 - u^i_t)\overline{u}^i \qquad t \in \mathcal{T} \tag{2.7}$$

In other words, when the unit i is committed, Δ^i_+ represents the most rapid power path that the unit can follow to increase its power output in a given time interval. Analogously, the same concept can be applied to explain Δ^i_-, when the unit decreases its power output. Instead, when the unit i is not committed, just started, the maximum power level can be only the $\overline{l}^i$ (often assumed equal to the minimum power output). On the other hand, when the unit i has to be uncommitted in the next period, the last power level output before the shut-down can be only the $\overline{u}^i$.

2.1.3   Operating constraints for hydro units

As it happens for the thermal generating units, the operating requirements of hydro generating units are usually expressed by inequality constraints, which are used to model the technical characteristics of the generators themselves. In the formulation of the constraints shown below, it is assumed that each cascade $h \in \mathcal{H}$ is composed by a set $\mathcal{H}(h)$ of individual hydro units. $\mathcal{S}(j)$ is the set of the immediate predecessors of unit j and t_{kj} is the water time delay from plant $k \in \mathcal{S}(j)$ to the basin feeding plant j.

(a) *Representation of the concept of ramp-up constraints.*

(b) *Representation of the concept of ramp-down constraints.*
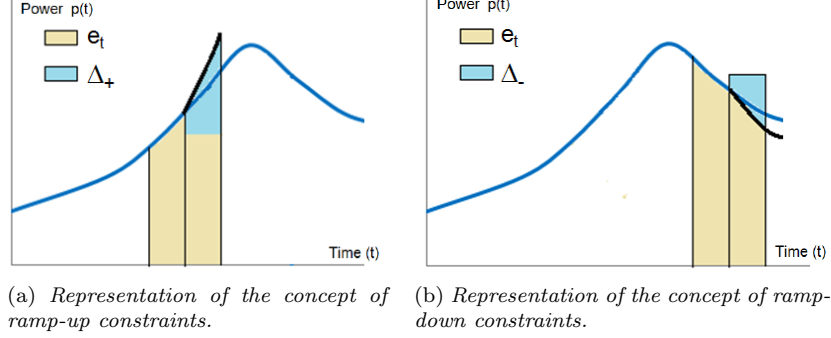
Figure 2.1: Representation of the concept of ramp-up and ramp-down constraints.

Constraints on discharged water

The amount of discharged water of a hydro unit is limited within a lower and an upper level, in order to avoid technical damages.

For each hydro unit $j \in \mathcal{H}(h)$, let q_t^j be the variables that represent discharged water of hydro unit j at time period $t \in \mathcal{T}$, expressed in m^3. Constants $\overline{q}_{max}^j$ represent the technical maximum of discharged water of hydro unit j, expressed in m^3 (the technical minimum is assumed to be zero in order to simplify the model). The constraints on discharged water can be expressed as follows:

$$0 \leq q_t^j \leq \overline{q}_{max}^j \qquad t \in \mathcal{T} \tag{2.8}$$

Constraints on reservoir volume

The volume of the reservoir of a hydro unit is limited within a lower and an upper level, in order to avoid technical damages.

For each hydro unit $j \in \mathcal{H}(h)$, let v_t^j be the variables that represent the volume of the reservoir of hydro unit j at time period $t \in \mathcal{T}$, expressed in m^3. Constants $\overline{v}_{min}^j$ and $\overline{v}_{max}^j$ represent respectively the minimum and maximum volume of the reservoir of hydro unit j, expressed in m^3. The constraints on reservoir volume can be expressed as follows:

$$\overline{v}_{min}^j \leq v_t^j \leq \overline{v}_{max}^j \qquad t \in \mathcal{T} \tag{2.9}$$

Hydro balance constraints

According to the hydro balance constraints, water that feeds the hydro power plant must balance water that is used to produce energy and spilled water.

For each hydro unit $j \in \mathcal{H}(h)$, let w_t^j be the variables that represent spilled water of hydro unit j at time period $t \in \mathcal{T}$, expressed in m^3, while $\overline{w}_t^j$ represents the natural inflows to hydro unit j at time period $t \in \mathcal{T}$, expressed in m^3. The hydro balance constraints can be expressed as follows:

$$v_t^j - v_{t-1}^j = \overline{w}_t^j - w_j^t - q_j^t + \sum_{k \in \mathcal{S}(j)} \left(q_{t-t_{kj}}^k + w_{t-t_{kj}}^k \right) \qquad t \in \mathcal{T} \tag{2.10}$$

In order to properly define the balance equations (2.10), the volume of each reservoir at time period $t = 0$ is assumed known, and water discharged and spilled at all time periods before $t = 1$ for which the water is still arriving to one of the downstream basis (i.e., those $k \in \mathcal{S}(j)$ such that $t < t_{kj}$).

2.1.4   Power balance constraints

According to the power balance constraints, the power produced by thermal and hydro units must balance the total system load demand. For each time period $t \in \mathcal{T}$, let $\bar{d}_t$ be the forecast energy load demand to be satisfied, expressed in MWh. Then, for each hydro unit j, let α^j be the term that expresses the efficiency of the hydro unit j in generating power from the discharged water, expressed in MWh/m^3 (which is assumed constant). The power balance constraints, linking the different units among themselves, are expressed as follows:

$$\sum_{i \in \mathcal{P}} p_t^i + \sum_{h \in \mathcal{H}} \sum_{j \in \mathcal{H}(h)} \alpha^j q_t^j = \bar{d}_t \qquad t \in \mathcal{T} \tag{2.11}$$

Additional constraints

The classical UC model can be formulated with additional constraints that are used to model specific technical and operating characteristic of the units or the whole energy system. For instance, it could be required to respect a certain reliability and security level of the system, satisfying system reserve constraints. Some power network characteristics may need to be taken into account, considering transmission constraints, in order to avoid transmission lines overloading. Furthermore, other constraints may be considered in order to impose which types of units must be on or off during the commitment of the whole system.

System reserve constraints

System reserve constraints impose to supply the load throughout the scheduling period with a certain degree of reliability even during the outage of some committed units. Spinning reserve requirements are necessary in the operation of a power system if load interruption has to be minimal. These requirements may be specified in terms of excess of capacity (expressed in MW) or in some form of reliability measures. This is made considering Spinning Reserve and Non-Spinning Reserve margins. Spinning Reserve is the on-line reserve capacity that is synchronized to the grid system and ready to meet electric demand within 10 minutes. Non-Spinning Reserve is off-line generation capacity that can be synchronized to the grid within 10 minutes, and that is capable of maintaining that output for at least two hours.

Transmission constraints

Since generating units of a utility company are normally located in different areas interconnected via transmission lines, power flows are subject to thermal limits of transmission lines.

However, the transmission constraints are usually left out in the UC models, in order to simplify the mathematical formulation of the problem. Nevertheless, if the transmission constraints are not considered, the schedule obtained might cause some transmission lines to be overloaded. This could result in rescheduling of some generating units that may produce significant additional operating costs.

Crew constraints

Certain plants may have limited crew size which prohibits the simultaneous starting up and/or shutting down of two or more units at the same plant. Such constraints are specified by the times required to bring a unit on-line and to shut down the unit.

Must run/must out constraints

In order to impose which types of units must be on or off during the commitment of the whole system *must run* and *must out* constraints may be introduced in the UC model. *Must run* units include already scheduled units which must be on-line, due to operating reliability and/or economic considerations. *Must out* units include already scheduled units which must be off-line and that are unavailable for commitment, since they are on forced outages and maintenance.

2.2 State of the art on Unit Commitment models

Different models for UC have been developed so far, nevertheless, they present some sort of approximations and simplifications. For this reason, novel UC models present some characteristics that have been left out in the literature until now. For instance, UC which involves more generating areas or a multiple objective function has been recently devoted some attention. Constraints related to fuel, pollutant emissions and security level are considered too. In this section, a brief overview on the state of the art on UC models is presented.

2.2.1 Multi-area Unit Commitment

Many utilities and power pools have limits on power flow between different areas or regions. Each area or region has its own pattern of load variation and generation characteristics. They also have separate spinning reserve constraints. The units in each area should be selected in such a way that reserve requirement and transmission constraints will be satisfied. Some works have addressed multi-area UC problem, such as [LF92] [LHA94], where different generation area for units are taken into account.

2.2.2 Fuel-constrained Unit Commitment

Many utilities have various fuel-supply constraints that affect the commitment of the units. Examples of this type of requirements are represented by the limits in fuel and gas supplies or by take-or pay requirements, which can be constrained over a period much longer than one week. In the case of multiple fuels supplying a unit, the fuel price could vary over different time intervals of the planning horizon, making the problem more complex. Cohen and Wan [CW87], Vemuri and Lemonidis [VL91] and Lee [Lee89] tried to solve this problem, proposing some generalized methods to solve the fuel-constrained UC problem.

2.2.3   Emission-constrained Unit Commitment

The process of generating energy from fossil fuel produces several pollutants which are released into the atmosphere. Kuloor *et al.* [KHM92] describe a method of solving the UC problem including all of the emission considerations in the UC objective function. In this case, emissions are considered as a second objective function and are added to the main objective function with a weighting factor. Gijengedal [Gij96] suggests an emission-constrained approach using an algorithm based on Lagrangian Relaxation that identifies the least-cost action in order to achieve daily or weekly emission targets. The problem formulation includes all standard system constraints, and addresses variable emission during start-up, operation and shut-down of units.

2.2.4   Security-constrained Unit Commitment

UC problem is frequently solved without taking into account security and transmission constraints. Nevertheless, if the resulting schedule ignores these requirements, the utility may overload critical transmission lines. Without advanced planning, the utility may have the necessity to reschedule the production, incurring in significant additional operational costs. Cohen *et al.* [CBC99] and Lei *et al.* [LLX02] presented a security-constrained UC program, while Shaw [Sha95] developed an algorithm for solving the security-constrained UC problem utilizing a Lagrangian Relaxation approach. Bertsimas *et al.* [BLS$^+$13] propose a two-stage adaptive robust model for the security-constrained UC problem, while in [KS10] transmission switching is introduced in security-constrained UC in order to avoid transmission violations and to reduce operating costs. Lotfjou *et al.* [LSFL10] present a model for the security-constrained UC problem representing also the characteristics of the high voltage direct current (DC) transmission system. A novel combinatorial solution strategy for security-constrained UC problem is presented in [SAS13] where the unit states are determined by an enhanced harmony search technique.

2.2.5   Multi-objective Unit Commitment

Multi-objective UC problem is modeled in order to take into account different goals in the objective function. In [SCL94], Srinivasan presented a fast and efficient approach to solve the multi-objective UC problem. This approach integrates a fuzzy expert system in order to obtain an optimum generation scheduling and to evaluate security transfer requirements in an interconnected system. In contrast to the existing UC models, this method considers economy, security, emission and reliability constraints as competing objectives for optimal UC solution. A preference of an operator is required in order to find a solution which does not produce a conflict between the different objectives, since an improvement of one objective may degrade the performance of another.

Chapter 3

Methods for solving the Unit Commitment

Traditionally, the UC problem has been solved considering only thermal units to determine when generators should be on or off and how to dispatch their production output in order to meet load system demand and spinning reserve requirements. The resultant schedule should satisfy technical operating constraints of units such as production and ramping limits and minimum up and down time requirements, over a specific short-term time horizon, minimizing the total operation cost. Currently, the solution of the traditional UC problem is important in the new competitive power industry, for this reason, more accurate models and more efficient methods to determine a proper power production scheduling are needed in order to fulfill new requirements in the current power systems environment. UC has been an active research topic for several decades (over 30 years) due to the potential savings in operation costs that could be obtained by properly solving this problem. The UC problem is characterized by a combination of several difficulties like continuous as well as binary decision variables, very large dimension, nonlinearities (for instance in hydro modeling, fuel costs) and the uncertainty of problem data (for instance uncertainty of load forecasts, stream-flows to reservoirs, pricing schemes and generator failures). These characteristics make the UC a large-scale, mixed-integer, combinatorial and nonlinear programming problem (MINLP), which still cannot be considered a well-solved problem for all practical sizes and operating environments. Several solution techniques have been proposed such as Dynamic Programming and Lagrangian Relaxation, heuristics, mixed-integer linear programming approaches, simulated annealing and evolution-inspired approaches. Recent literature surveys on methods used to solve the UC problem can be found in [Pad04], [Sal07], [SDSK13], [SM12], [BKS$^+$12], and [BTK12].

The available methods for solving the UC can usually be classified as follows:

- optimization methods: these approaches are represented by the mathematical programming methods such as Lagrangian Relaxation, Dynamic Programming, and Mixed Integer Programming;

- heuristic/meta-heuristic methods: these approaches are represented by the heuristic approaches such as Tabu Search, Simulated Annealing, and Genetic Algorithms.

In the following sections, the main methods used to solve the UC problem will be briefly described, in order to show the state of the art and the recent trends in this field.

3.1   Exhaustive Enumeration and Priority Listing

The Exhaustive Enumeration approach was one of the earliest methods to be applied to solve the UC problem [Pad04]. The first phase of this approach consists in enumerating all the possible combinations of the generating units. In the second phase, the combinations of units that are associated with the least operational cost are chosen as the optimal solution, which is found once all the system constraints are satisfied [HJW71] [WW84]. This method is not suitable to solve UC problems in large scale systems, since the computational effort increases when a high number of units is considered. However in some cases it could provide accurate solutions, as shown by Kerr *et al.* [KSF66] and Hara *et al.* [HKH66] who successfully solved the UC by the Exhaustive Enumeration method considering Florida Power Corporation system.

Priority Listing approaches are the simplest methods to solve the UC problem. These algorithms are based on priority lists of generating units, which are ordered according to a start-up/shut-down heuristic with increasing/decreasing order by operational cost characteristics, including state transition costs. This initial order is then used to commit the units to obtain the solution of UC, satisfying the system load demand and the reserve requirements [Lee88]. The Commitment Utilization Factor (CUF) and the Average Full Load Cost (AFLC) index or a combination of both can be used to determine the priority order of units. For instance, the CUF algorithm can be applied in the solution of single-area and multi-area UC [HJW71] [LHA94] [LF92] [Lee91]. Burns *et al.* [BG75] and Lee [Lee88] solved the UC problem considering a Priority Listing approach. Shoults *et al.* [SCHG80] developed an efficient algorithm based on priority ordering including import/export constraints in the formulation of UC. One of the disadvantages of the Priority Listing method is related with its sub-optimality in the scheduling solution of the UC, as it is based on many assumptions. However, this approach is still used by some utilities due to its ease of application and understanding and its simplicity. Moreover, the resultant schedule is adequate in many situations.

3.2   Branch and Bound and Benders Decomposition

The Branch and Bound approach is a widely applied method to solve various optimization problems, such as the UC [Pad04].

Lauer *et al.* [LJBP82] and Cohen *et al.* [CY83] developed an enhanced approach to solve the UC problem based on Branch and Bound algorithm. This method includes all time-dependent constraints and does not require a priority ordering of units. In order to develop an efficient approach to solve the UC problem, Huang *et al.* [HYH98] proposed a Branch and Bound method integrated with constraint logic programming.

Branch and Bound method is comparable to Dynamic Programming approaches since it is based on structured searches in the space of feasible solution [DE76] [DEKT78]. Nevertheless, Branch and Bound algorithms differ from most of the approaches for the solution of the UC problem since they do not need a priority ordering and they allow to introduce time-dependent start-up costs in the mathematical formulation.

Benders Decomposition approaches decompose the UC problem into a master problem including only discrete commitment variables and a sub problem involving continuous generation variables [Tur78] [MS98]. This sub problem corresponds to the Economic Dispatch (ED) problem for a given commitment. The master problem and the ED sub problem are solved iteratively until the solution converges. The major disadvantage in Benders Decomposition approaches is

the determination of the solution of the master problem, which is a large scale integer optimization problem. In order to overcome this difficulty, Turgeon [Tur78] solved the master problem considering a Branch and Bound algorithm. Baptistella and Geromel [BG80] solved the master problem by relaxation in the master level of Benders Decomposition approach. Some of the constraints like minimum up and down time constraints, which are difficult to handle, are replaced by simpler constraints, in order to improve the efficiency of the approach. For example, in [HB86] minimum up and down time constraints are not considered in the mathematical model, and they are substituted by a constraint that allows only one commitment per day for each unit. In [AA13] a novel approach based on Benders Decomposition is presented in order to solve hydrothermal UC problem with AC power flow and security constraints, decomposing the problem into a master problem and two sets of sub-problems.

3.3 Dynamic Programming

Dynamic Programming (DP) is a very important optimization approach which is applied in many areas [BD46]. DP techniques, as well as Lagrangian Relaxation, have been the first optimization techniques to be used extensively to solve the UC problem at industry level.

From a mathematical point of view, the objective of DP approaches is to minimize the following expression [Pad04]:

$$F_N(x) = \min[g_N(y) + f_{N-1}(x - y)]$$

where

- $F_N(x)$ is the minimum running cost of carrying a load of x MW on N generating units;

- $g_N(y)$ is the cost of carrying a load of y MW on unit N;

- $f_{N-1}(x - y)$ is the minimum cost of carrying the load of $(x - y)$ MW on the remaining $(N - 1)$ units.

The assigned UC problem is thus decomposed into more sub problems of smaller dimension. These sub problems are solved and the optimal solution to the original problem is recursively developed from these sub problems step-by-step. Usually, in DP approaches for UC, every possible state in the solution space is examined in each time interval. This search can be carried out in a forward or a backward direction. The states are combinations of units within a time period. Time periods are called stages of the problem [HSLH91] [Guy71].

Lowery first analyzed the applicability of DP approaches to solve UC problems, from a practical point of view [Low66]. The approach developed by Lowery considered the output of the generating unit as a state variable and the on-line capacity as the stages. The DP approach for UC has been then improved by Ayoub and Patton [AP71], including also probabilistic methods to determine reserve requirement. In the literature, a typical DP approach for the UC determines a nominal commitment which is good for each hour [PC76] [PSA81]. A commitment is good when some criteria are met, such as the minimum number of units considered in a priority ordering which is needed to satisfy the reserve requirements. A set of units belonging to this priority list of the nominal commitment are then chosen, in order to find the optimal solution to the UC. The units that are below that set are assumed to be committed, while the other units are assumed to be off. Other DP approaches choose the most promising states from the set of all possible states using

selection techniques [SPR87] [HHWS88]. In order to reduce computational times, approximate subroutines for Economic Dispatch are integrated into DP methods.

Nagrath *et al.* have shown that DP has more advantages than priority list and enumeration techniques in the solution of UC problems [NK94]. One of the advantages of DP is the possibility to maintain the feasibility of the solution and to easily allow to add constraints like power balance constraints [LHA94]. DP also allows to solve problems of various sizes and can be modified to model specific characteristics of the system and the utilities [NIF86] [SPR87]. Nevertheless, one of the drawbacks of the DP approaches is the handling of minimum up and down-time constraints and time-dependent start-up costs which are usually treated in a suboptimal way [LJS+98]. Moreover, the size of the problem, expressed by the number of states, increases with the number of available units, requiring a large computational effort. For this reason, some simplifications and approximations to the traditional DP approach are applied [SPR87]. Several approaches have been developed in order to reduce dimension, search space and running times. Most of these approaches are based on truncation and fixed priority ordering. They can be classified as follows:

- DP-SC: it is a combination of DP approaches and sequential combination methods [PSA81];

- DP-TC: it is a combination of DP approaches and truncated combination methods [PC76];

- DP-STC: it is a combination of DP-SC and DP-TC approaches [PSA81];

- DP-VW: it is a combination of truncated DP approaches and variable window methods; in this case, UC planning time window size is variated according to the increment of load demand reducing running times and obtaining a solution of acceptable quality [OS91].

The solution obtained by the DP approaches mentioned above is suboptimal, in particular when large-scale systems are considered, since these algorithms are based on priority lists or truncated combination methods. When the UC problem is decomposed into smaller sub problems which are solved by these DP approaches, Successive Approximation methods (SA) and Hierarchical approaches methods (HA) can be used in order to coordinate these sub problems, respectively either sequentially or in parallel [BH85] [HB86]. In order to reduce the solution space Lagrangian reduction can be combined with SA approaches considering the dual nature of the UC [NaIG87].

Recent trends on methods to solve the UC have been focused attention on the integration of fuzzy logic, expert systems and neural networks into DP approaches. Fuzzy logic can be applied to DP when load demands and generation parameters are known with uncertainty [SH91]. Nevertheless, the fuzzy approach requires a larger computational effort than the conventional DP method. The utilization of expert systems has been taken into account too, in order to enhance DP approaches, especially when truncated DP methods are developed. Constraints that are difficult to implement in a DP algorithm for the UC can be easily managed by this expert system [MSW88] [SHN91]. Neural networks have been integrated into DP algorithm too to generate economic dispatch schedules and the whole UC solution [KP07].

3.4   Lagrangian Relaxation

Lagrangian Relaxation (LR) optimization techniques have been used more recently than Dynamic Programming (DP) approaches. Currently, some utilities use LR approaches to solve the UC problem, since the degree of sub optimality of the obtained solution is close to zero when a large number of units is considered and the characteristics of the specific utilities can be easily modeled,

adding unit constraints [CW87] [NaIG87] [TS89]. For instance, Merlin *et al.* proposed a new method for solving UC based on LR which was validated at Electricite De France [MS83]. Tong and Shahidehpour [TS90b] developed an algorithm based on Lagrangian Relaxation for solving UC in large scale systems including different types of units, such as thermal, fuel constrained and hydro generating units. A similar study was carried on by Aoki *et al.* who applied a LR approach to a UC problem taking into account the same set of generating units (thermal, fuel-constrained and pumped storage hydro units) [AIS+89] [ASI87]. Yan et al. [YLGR93] too developed a LR approach including hydro units in the UC formulation, in addition to thermal units, in order to solve UC in a realistic large scale system.

In contrast to DP approaches, LR methods do not need priority lists. LR methods are more flexible in handling operating constraints of different types of units than other solution approaches. Moreover, these algorithms present a higher computational efficiency and faster solution times. Large-scale UC problems can be decomposed in more sub problems easier to solve because of the dual formulation obtained with LR approaches.

In fact, LR methods decompose the assigned UC problem into a master problem and more sub problems, which are solved iteratively in order to obtain a solution for the master problem. Each sub problem is solved independently in order to determine the commitment of a single unit. Lagrange multipliers, that are used to link the sub problems, are added to the master problem to determine the dual problem. This dual problem is easier to solve than the primal problem since it has lower dimensions. The Lagrange multipliers are determined in the master problem and then passed to the sub problems which are solved by forward DP approach. The solution obtained for the sub problems is then passed to the master problem in a backward direction, the Lagrange multipliers are updated and used by the sub problems again. This process is repeated recursively until a solution for the master problem is obtained.

However, even if LR methods present several advantages than other solution approaches, the dual nature of the algorithm leads to some difficulty in obtaining solution feasibility. In particular, an unnecessary commitment of generating units could be determined, resulting in higher production costs.

In order to overcome these difficulties, recently, a new approach, called Augmented Lagrangian Relaxation (ALR), has been developed [WSKI95]. In this method, quadratic penalty terms associated with energy system demand are added to the objective function, in order to improve the commonly used LR algorithms.

Some works have focused attention in refining traditional LR methods, in order to obtain better solutions, requiring less computational effort. Takriti [TB00] and Cheng [CLL00] developed refined LR approaches with reduced complexity than traditional LR methods. Muckstadt and Koenig replaced the common linear programming relaxation approach with the LR method with a significant improvement of computational efficiency in the solution of UC [MK77]. Zhuang *et al.* improved LR approach for UC, proposing a three phases LR algorithm [ZG88].

Wang *et al.* proposed a LR method which takes into account also ramp rate constraints in UC and rotor fatigue constraints in the Economic Dispatch [WS94], while Ma *et al.* included optimal power flow constraints in the formulation of UC, using Bender's Decomposition approach [MS99]. A LR method to solve the environmentally constrained thermal UC is shown in [KHM92], where environmental requirements are considered as a second objective function which is added to the traditional UC objective function. Furthermore, recently, a Lagrangian algorithm has been applied to solve the unit schedule problem in an electrical power system, as shown in [TBB13].

3.5 Mixed Integer Programming and Interior Point Optimization

The UC can be formulated and solved using Linear Programming approaches, as shown in [Mee84] [WAB81] [FBC95]. However, the main disadvantage of Linear Programming methods is the large number of variables that are needed to represent the piece-wise linear input-output curves, which leads to a strong computational effort [BF86].

For these reasons, literature has focused attention on Mixed Integer Programming (MIP) approaches in order to solve the UC problem. Mixed Integer Programming approach is used to solve the UC reducing the search in the space of solutions rejecting infeasible states. Bond and Fox [BF86] developed an algorithm that combines Mixed Integer Linear and Dynamic Programming. Feasible combinations of units are determined by Mixed Integer Linear Programming, while dynamic programming identifies promising scheduling solutions in the solution space.

Dillon et al. [DEKT78] formulated the UC problem as a linear MIP problem and developed an Integer Programming method to solve the UC problem, taking into account an extension and modification of the Branch and Bound method. In [LN84] the proposed MIP method transforms the linear optimization problems that arise in the search procedure of the Branch and Bound algorithm into capacitated transshipment problems, which are solved by a network-based solution procedure.

Recent trends in MIP approaches employ more accurate cost models, like quadratic cost curves, than the traditional linear cost functions. Currently, literature is focusing attention on improved modeling of unit input/output characteristics with more detailed non-linear models. The MIP approaches with non linear models, if applied to a typical generation mix consisting of a large number of units, may require a major computational effort. However, recent works in literature have shown that accurate and proper MIP for UC can be developed in order to significantly save computational time [CA06].

In [OAV12] the UC is formulated as a mixed-integer linear programming (MILP) problem, while Morales et al. [MELR12] present a MILP formulation of specific constraints of UC such as start-up and shut-down power trajectories of thermal units. A mixed integer quadratically constrained program (MIQCP) model to solve the Unit Commitment problem has been also presented in [lLCMMG12].

The Interior Point method is currently applied to solve combinatorial and non-differentiable problems, such as the UC. This method is used to determine proper production schedule in electric power systems. Madrigal *et al.* [MQ00] applied the interior point method to solve the UC problem, observing that this approach presents two main advantages such as better convergence characteristics and fine parameters tuning.

3.6 Tabu Search and Simulated Annealing

Tabu Search is an optimization heuristic procedure that has been successfully applied to various combinatorial optimization problems. This approach is characterized by avoiding entrapment in local minima by employing a flexible memory system, called *Tabu List* [MAMS98]. Mori *et al.* [MM00] [MU96] developed an algorithm based on Tabu Search method in order to solve the UC problem. Rajan *et al.* [RMM02] improved Tabu Search approaches for UC developing an algorithm using a neural-based tabu search method. Lin *et al.* [LCT02] solved Economic Dispatch using a Tabu Search algorithm. Mantawy *et al.* [MAMS98] [MAMS99] [MSH02] efficiently solved the

UC problem with a Tabu Search method, taking into account also hydro generating units, over a long-term time horizon.

From a physical point of view, annealing refers to the process of heating up a solid to a high temperature followed by slow cooling achieved by decreasing the temperature of the environment in steps [WW94] [ANP95]. By making an analogy between the annealing process and the optimization problem, Simulated Annealing was independently introduced by Kirkpatrick, Gela, and Vecchi in 1982 and Cerny in 1985. A large class of combinatorial optimization problems, like the UC, can be solved following the same heuristic procedure of transition from equilibrium state to another, reaching minimum energy of the system. In order to solve the UC with the Simulated Annealing procedure, the problem is decomposed into two subproblems, a combinatorial optimization problem with variables representing the status of the units, and a nonlinear optimization problem in the variables indicating the power output of the generators. Mantawy *et al.* [HAMS98] developed a Simulated Annealing algorithm to solve the UC problem, concluding that even if this procedure takes a long computational time, it is independent of the initial solution.

3.7 Expert Systems and Fuzzy Systems

An expert system is an intelligent computer program which, using knowledge and inference procedures, is able to solve problems that require significant human expertise for their solutions [CA91]. The expert system knowledge is usually derived from human experts and encoded in a formal language, in order to emulate their methodology and performance [LC91] [WD91] [PP95]. Expert system approaches have been recently applied to solve the UC problem [GLYA92] [OS91]. The real-time processing capability of these approaches is challenging with those of mathematical programming methods [LS93] [BS97]. Mokhtari *et al.* developed an expert system-based approach to assist power systems operators in the generating units scheduling [MSW88]. Ouyang *et al.* proposed an expert system for UC consisting of a commitment schedule database, a dynamic load pattern matching process, and an interface optimization process [OS90]. Tong *et al.* developed an algorithm for solving the UC using priority listing heuristics in the form of interface rules [TS90a]. Salam *et al.* used a Dynamic Programming approach integrated into an expert system to obtain a feasible solution to the schedule of the operations of the generating units [SHN91].

UC is a complex decision-making process. When it is solved, the load demand and some other variables like the outage of the units are uncertain [LDCG83] [CB90]. This raises the question of how to tackle the UC when these aspects are imprecise [MK95] [Pad99] [PRP99] [PRP95]. Stochastic models have been observed by researchers to perform better than deterministic models under uncertainty but they present some limitations [TBL96]. For this reason, in order to manage uncertainty, some other approaches have been recently applied to the UC problem, such as fuzzy logic, which has been first introduced in the literature by Zadeh in 1965, who presented the concept of fuzzy sets as a mathematical means to describe vagueness in linguistics. Taking into account fuzzy logic, Tong *et al.* developed a rational model in order to consider the outage of thermal units and the uncertainty of the load demand [TS90a]. Saneifard *et al.* demonstrated that it is possible to apply fuzzy logic in order to solve the UC problem, allowing a qualitative description of the behavior and the characteristics of a system, without the necessity to determine an exact mathematical formulation [SPS97]. In some recent works enhanced algorithms based on fuzzy logic have been successfully applied in order to solve the UC problem, as shown in [LG13] [KK13] [KK12].

3.8 Artificial Neural Networks and Ant Colony Search Algorithms

Artificial Neural Networks (ANNs) have been developed in order to model the behavior of biological neural networks. Over the years, several models of ANNs and the associated learning algorithms have been developed [SWK$^+$91]. ANNs have been recently applied to solve combinatorial optimization problem such as the UC. Sasaki *et al.* applied the Hopfield neural network to solve a UC problem consisting of 30 units over a 24 periods [SWY92]. C. Wang *et al.* developed a model based on ANNs to solve the UC with ramp rate constraints [WS93]. Walsh *et al.* improved the conventional Hopfield neural network developing an augmented network architecture with a new form of interconnection between neurons in order to obtain a more general energy function [WM97]. The UC was also successfully solved by Liang *et al.* using an extended mean field annealing neural network approach [LK00]. Artificial neural networks and artificial intelligence algorithms have been recently applied to solve the UC problem in [JBRF13] and [Hua13].

An ant system has been inspired by the behavior of real ants, which are capable of finding the shortest path from a food source to their nest without using visual cues, but by exploiting pheromone information. In an ant system, a set of artificial ants cooperate to the solution of a problem by exchanging information via pheromone deposited on graph edges. Ant systems have been applied to solve combinatorial optimization problems like UC. Sisworahardjo and El-Kaib have applied ant colony search algorithm to solve the UC [SEK02], while Huang has solved the problem with ant colony approaches considering also hydroelectric generating units [Hua01]. Recently, enhanced ant colony system algorithms have been applied to solve the UC problem, as shown in [YKCCCL13] [CHSP12] [CCS12].

3.9 Genetic Algorithms and Evolutionary Programming

Over the last 30 years, systems based on the principles of evolution and machine learning have been devoted a growing interest [OI97] [SPG03]. These systems maintain a population of potential solutions and they have a selection process based on the fitness of individuals and some genetic operators. Genetic algorithms which are involved in these systems imitate the evolution strategies and the principles of natural evolution in order to solve optimization problems, such as the UC for both small and large size systems [DM94]. Sheble *et al.* applied a genetic algorithm to solve the UC in a time horizon from one to seven days [She96]. Maifeld *et al.* solved the UC applying a genetic algorithms which considers domain-specific mutation operators [MS96]. Yang *et al.* proposed a parallel genetic algorithm to solve the UC, using a constraint handling technique [YYH97]. Rudolf *et al.* developed a genetic algorithm to solve the UC in a hydrothermal power system [RB99]. Swarup *et al.* handled the large-scale UC employing a new strategy for representing chromosomes and encoding the search space of the problem [SY02].

An evolutionary programming approach to solve the UC problem has been proposed by Yang *et al.* [YYH96] and Juste *et al.* [JKTH99]. In this approach, populations of contending solutions evolve through random changes, competition and selection. Chen *et al.* [CW02] extended the traditional evolutionary programming approach [VGP03] presenting a cooperative co-evolutionary algorithm for UC, formulating and solving the problem by modeling the co-evolution of cooperating spices. Recent trends in the application of the evolutionary programming for solving the UC problem are shown in [LPZ13] and [GR12].

Part II

Enhanced models for the Unit Commitment Problem in conventional electrical systems

Chapter 4

Unit Commitment models with power variables *

In the literature, ramp-rate constraints have been usually neglected in the UC models [ZG88], this has produced mathematical models for UC that overestimate the actual behavior of the units, obtaining commitment decisions that are not feasible and therefore cannot be implemented from a practical point of view. Nevertheless, if ramp-rate constraints are considered in the model, the corresponding optimization problem presents more difficulties, especially if Lagrangian techniques are applied for the resolution [ZG88] [BLRS01] [BFLN03].

For these reasons, an assumption of the models for the UC is given by the form of the ramp-rate constraints usually employed, that is an approximated one, assuming that the difference between the total energy produced by a unit at two consecutive hours must be bounded. This means that the changes in the power production are represented by a step discontinuous function and the power produced by a unit is constant in each hour and can be adjusted instantaneously passing between two consecutive hours, as depicted in Fig. 4.1. In our dissertation, for these characteristics, we refer to the classical UC model presented in the literature as a '*discontinuous*' model or energy-based model.

The assumption mentioned above leads to a numerical coincidence (though not physical) between the energy e produced by the unit in a given hour and the power p (multiplied by one hour) produced in the same time period. This aspect greatly simplifies the formulation of the UC model, since, from a mathematical point of view, a smaller number of variables is required (the same variable is used to represent energy and power at the same time) and computational effort in the solution is limited, due to the numerical coincidence between energy and power.

Moreover, these simplifications lead to some approximations and several drawbacks that make these '*discontinuous*' models not realistic enough. In particular, some technical restrictions of the generating units are neglected, since in practice power trajectories are continuous along sets of consecutive time periods for which a generating unit is continuously active. In fact, a generator usually does not produce a power on a constant level in each time period and it needs a technical time to change its power output, it cannot instantly pass from a power level into another. These simplifications may lead the model to either under-estimate or over-estimate the actual amount of

---

*Part of the material presented in this chapter is based on the following publication *A. Frangioni, C. Gentile, F. Lacalandra, A. Naimo. Unit Commitment models with power variables. Technical Report R. 11-26, IASI-CNR, 11/2011.*
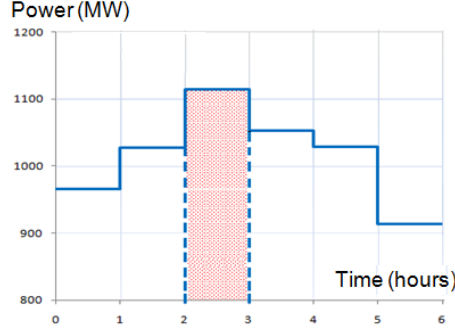
Figure 4.1: Power trajectories in the classical (discontinuous) UC model.

energy that a generating unit can actually provide depending on the exact shape of its real power trajectory. Thus we propose a new Mixed-Integer Quadratic Programming (MIQP) model for UC, based on power instead of energy. We refer to this model as a '*continuous*' model or power-based model.

In this chapter we present how we have defined a transition from an energy-based UC model to a power-based UC model; hence we illustrate the detailed formulation of our power-based UC model; finally we present simulation results and outline the conclusions.

4.1 Transforming an energy-based model in a power-based one

To formulate a power-based model, it is necessary to further investigate some aspects related to the UC discontinuous energy-based model.

In particular, we better explain why the previously mentioned simplifications may lead the model to either under- or over-estimate the actual amount of energy produced by a generating unit, using the example depicted in Fig. (4.2).
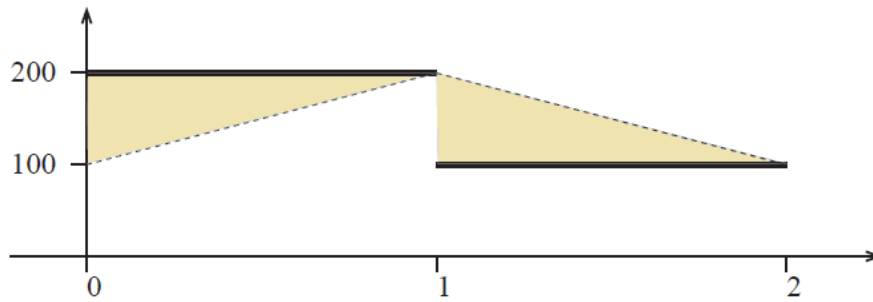

Figure 4.2: Power generation with instantaneous jump (thick continuous lines) vs. actual power generation (thin dashed lines).

We assume that the generating unit has uniformly produced 100 MW for one hour, called hour 0, producing 100 MWh of energy. If its production needs to be increased at the following hour

1, and the ramp-rate is 100 MW/h, the '*discontinuous*'' model will assume that the produced power can be made to instantaneously jump to 200 MW (thick line), producing 200 MWh during the hour. However, the unit will instead ramp-up during the hour. If we assume continuous ramping at the maximum rate, the unit will only reach 200 MW of power at the end of the hour (thin dashed line). Hence, the unit will have produced only 150 MWh, leaving a gap between the expected energy production and the real one (left yellow triangle). The reverse happens if the generating unit needs to be ramped down at the subsequent hour 2. If we assume, for instance, a ramp-down rate equal to the ramp-up rate, while the usual model stipulates that as low as 100 MWh can be generated, the generating unit will produce at least 150 MWh, since it can only reach 100 MW of power at the end of the hour. Hence a surplus of energy is generated (right yellow triangle).

This example has shown that this way of modeling ramp-rate limits, even if it is still used in the literature, is an approximated one. In fact, the crucial point is that ramp-rates are actually applied to the produced energy rather than, as it should, to the power. We refer to the UC models employing this simplification as the '*energy-based*' (discontinuous) models. The drawbacks related to this way of modeling ramp-rate limits could be solved by disregarding the problem and limiting the ramp-rate to lower values than the ones that are technical and economically feasible. Even if this should limit the practical impact of the issue, studies that provide guidelines about how this should be done are not currently available in the literature. Furthermore, it can be easily verified that artificially limiting the dynamic of the generating units beyond what is required by technical and economical considerations may lead to suboptimal decisions. Indeed, Wang and Shahidehpour [WS95] have already observed that using '*energy-based*' models leads to a nontrivial trade-off between two opposite problems:

- if the ramp-rates are underestimated, then the total production costs may increase and it should be necessary to use additional units during peaks hours, even if the optimal solution does not require them;

- if the ramp-rates are not underestimated, then the total energy produced in one hour can be significantly higher or lower than the required one. This could lead to uneconomical behavior like shedding valuable energy, requiring reserve energy to be consumed and therefore diminishing the safety margins of the system. Indeed, ramp-rate limits could be disregarded in peak hours, reducing the life-cycle of the generating units.

Several ways to overcome these difficulties have been proposed in the literature. In [WS93] an algorithm based on three steps has been developed:

- at first step, artificial intelligence techniques are applied to produce a UC schedule which satisfies all the constraints of the system and the units operation, except ramp-rate limits;

- at second step, a dynamic procedure is used to consider the ramp limits when units are started up and shut down;

- at third step, a dynamic dispatch procedure is applied to obtain a feasible solution which includes the units generating capability information given by the UC, the ramp-rate constraints and the economical considerations.

In [WS94] an algorithm based on the Lagrangian Relaxation of demand and spinning reserve constraints has been proposed. The single UC is solved by Dynamic Programming, where the power levels are discretized depending on the number of hours needed to reach the maximum
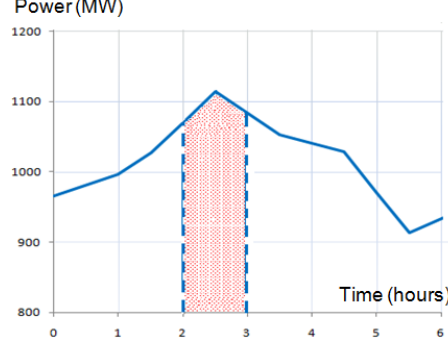
Figure 4.3: Power trajectories in a power-based (continuous) UC model.

production level. Finally, the solution is adjusted by a heuristic procedure based on Linear Programming, in order to satisfy the relaxed constraints. In [WS95] a Mixed-Integer Non Linear Programming (MINLP) model with non-convex constraints is developed and a heuristic algorithm based on Lagrangian Relaxation and Dynamic Programming is proposed for its solution. With respect to [WS94], this algorithm also deals with ramping costs depending on the ramp speed. Finally, in [XGK01] a heuristic algorithm was proposed to adjust the solution of a non-ramp-constrained UC in order to consider ramp-rate limits.

In our research activities, the aforementioned drawbacks of the UC energy-based discontinuous models will be overcome, defining more realistic mathematical formulations than the ones proposed in the literature. In particular, we propose new Mixed-Integer Quadratic Programming (MIQP) models for UC, where decision variables represent power levels instead of energy. The basic assumption of these models is that the unit is always ramping linearly during each time period. This means that the power increases -or decreases- uniformly from p_{t-1} to p_t during all the period, as shown in Fig. 4.3. If $p_{t-1} = p_t$ the unit is actually not ramping. The energy is computed by assuming linear ramp-up and ramp-down trajectories, i.e., piecewise-linear continuous power curves whose integral (the produced energy) can be easily computed. We refer to this model as a '*power-based*' (continuous) model.

The advantage of the proposed models is that the physical constraints on power generation, such as ramp rate requirements, are directly modeled, so the trajectories of power p constructed by the model and the energy decisions are surely feasible. Moreover, the resulting MIQP problems can be solved with commercial solvers, possibly using semi-infinite or second-order cone programming formulations to improve their efficiency. This means that these models, that are relatively easy to implement, can be solved at optimality, as opposed to all previous approaches which are based on heuristics. Furthermore, the approach of these formulations is general and can be easily extended to model more detailed aspects of the behavior of thermal units, like start-up and shut-down power trajectories [AC04], thermal stress constraints [LS03], combined-cycle units [LS05], and many others.

In order to simplify further reading, in the following section we recall the classical energy-based formulation of UC, which has been previously described in section 2 of chapter 1. For the sake of simplicity, the model is presented considering only thermal units and neglecting the constraints related with other types of units such as hydro generators.

4.1.1 Foundations and objectives of the UC power-based model

A set $\mathcal{P}$ of thermal generating units, burning some type of fuel (oil, gas, coal,...) is given upon a time horizon $\mathcal{T}$ (e.g., a day or a week) discretized into a finite number of time instants (e.g., hours or half-hours), i.e., $\mathcal{T} = \{1, \ldots, n\}$. Each unit is characterized by a minimum and a maximum energy output (typically measured in MWh), e^i_{min} and e^i_{max}, respectively, for each of the time instants. If a unit is committed (actively generating power) at time instant t, it is subject to a convex energy generating cost function $f^i(e^i_t)$, typically a convex quadratic function, where e^i_t is the total amount of energy produced during all the time period. The operation of the units must satisfy a number of technical constraints, typically the minimum up- and down-time ones: whenever the unit i is turned on it must remain committed for at least τ^i_+ consecutive time instants, and, analogously, whenever the unit i is turned off it must remain uncommitted for at least τ^i_- consecutive time instants. Therefore, binary variables u^i_t, indicating the commitment of the unit i at time instant t (if their value is equal to 1), have to be introduced.

The other set of technical requirements are the ramp-rate constraints. These require that the maximum increase of the generated energy from time instant t to the next is limited to $\Delta^+_i > 0$, and, analogously, the maximum decrease of generated power from time instant t to the next is limited to $\Delta^-_i > 0$. Note that this definition can be applied only if the unit i is committed in both time periods t and $t+1$. Therefore, a general form of ramp-rate constraints is considered where an upper bound $\bar{l}^i$, $e^i_{min} \leq \bar{l}^i \leq e^i_{max}$, is known on the maximum amount of energy that can be generated if the unit i is turned on in a time period t (that is, it was uncommitted in $t-1$) and, analogously, an upper bound $\bar{u}^i$, $e^i_{min} \leq \bar{u}^i \leq e^i_{max}$, is known on the maximum amount of energy that can be generated if the unit is turned off at the end of time period t (that is, it will be uncommitted in $t+1$).

The classical energy-based formulation of UC is the following

$$\min \sum_{i \in \mathcal{P}} c^i(u^i) + \sum_{t \in \mathcal{T}} f^i(e^i_t) \tag{4.1}$$

$$\sum_{i \in \mathcal{P}} p^i_t = \bar{d}_t \qquad t \in \mathcal{T} \tag{4.2}$$

$$\bar{e}^i_{min} u^i_t \leq e^i_t \leq \bar{e}^i_{max} u^i_t \qquad i \in \mathcal{P}, t \in \mathcal{T} \tag{4.3}$$

$$e^i_{t+1} \leq e^i_t + u^i_t \Delta^i_+ + (1 - u^i_t)\bar{l}^i \qquad i \in \mathcal{P}, t = 0, \ldots, n-1 \tag{4.4}$$

$$e^i_t \leq e^i_{t+1} + u^i_{t+1} \Delta^i_- + (1 - u^i_{t+1})\bar{u}^i \qquad i \in \mathcal{P}, t = 0, \ldots, n-1 \tag{4.5}$$

$$u^i_t \geq u^i_r - u^i_{r-1} \qquad t \in \mathcal{T}, r \in \left[t - \tau^i_+, t-1\right] \tag{4.6}$$

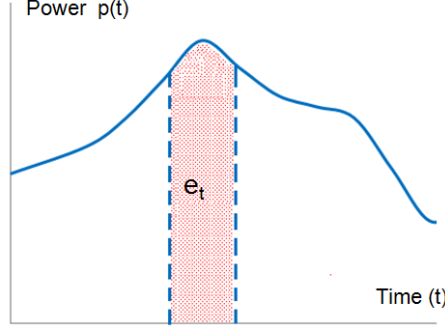$$u^i_t \geq 1 - u^i_{r-1} - u^i_r \qquad t \in \mathcal{T}, r \in \left[t - \tau^i_-, t-1\right] \tag{4.7}$$

Figure 4.4: Power trajectories in a realistic UC model.

$$u_t^i \in \{0, 1\} \qquad t \in \mathcal{T} \tag{4.8}$$

Constraints (4.4) and (4.5) are, respectively, ramp-up and ramp-down requirements, while constraints (4.6) and (4.7) are minimum up- and down-time requirements, respectively.

In order to transform the energy-based formulation into a power-based one, it is necessary to examine in details the data of the problem and how they are related with the actual operation of the units. In particular, it is necessary to study the following problem: given the power ramp-rate limits (expressed in MW/h), determine the energy ramp-rate limits (expressed in MWh/h) so that any feasible commitment satisfying the latter always admits a feasible power trajectory satisfying the former. Even if this problem does not have any obvious optimal solution, conservative estimates can be obtained in order to guarantee the property. Nevertheless, these estimates severely restrict the dynamic of the generating units.

The numerical coincidence between energy and power makes it possible to consider the main variables of the energy-based UC model as the total energy output of the given generating unit in each time period of the planning horizon.

Nevertheless, form a practical point of view, the energy output of a given unit is determined by the integral of the functions that represent the actual power output of the unit, during each of the time periods, as indicated in the following expression

$$e_t^i = \int_{t-1}^t p^i(\tau) d(\tau) \tag{4.9}$$

where e_t^i represents the total energy output of the unit i during one time period (measured in MWh), while $p^i(\tau)$ is a continuous curve that represents the actual power output of the unit i (measured in MW), as depicted in Fig. 4.4.

It means that there are different actual trajectories $p(\tau)$ of the power p that provide the same amount of energy e, and some of these actual trajectories are not feasible, since they cannot be realized from a practical point of view, because of the technical restrictions of the units, like the ramping constraints. In the classical energy-based model, the ramping limits of the units are Δ_+^i and Δ_-^i, typically measured in MWh/h, as expressed in (4.4) and in (4.5). Nevertheless, as long as a unit is active, each p_t^i has to be a continuous curve, and continuity has to be enforced on the boundaries of each time instant, that is $p_{t-1}^i(1) = p_t^i(0)$ has to hold for each $t \in \mathcal{T}$ such that

$u_{t-1}^i = u_t^i = 1$. Furthermore, it is actually the instantaneous power variation that is bounded; one typically has $p_t^i(\tau) \in [\delta_-^i, \delta_+^i]$ (or, allowing p_t^i to be non-differentiable, $\partial p_t^{'i}(\tau) \subseteq [\delta_-^i, \delta_+^i]$) for all $\tau \in [0,1]$ and units $i \in \mathcal{P}$. Thus, in a power-based model, the actual data describing the ramping limits of the units are δ_-^i and δ_+^i, typically measured in MW/h or (MW/min), as expressed in (4.10) and in (4.11)

$$p_{t+1}^i \le p_t^i + u_t^i \delta_+^i + (1 - u_t^i)\bar{l}^i \tag{4.10}$$

$$p_t^i \le p_{t+1}^i + u_{t+1}^i \delta_-^i + (1 - u_{t+1}^i)\overline{u}^i \tag{4.11}$$

The main differences between an energy-based model and a power-based model, described above, are briefly resumed in table (4.1).

According to the assumption that the typical duration of the time interval is one hour, one could think that it is possible to easily operate a translation between an energy-based model and a power-based model, considering a proper mathematical relationship between ramp-rates expressed in energy (Δ_+^i, Δ_-^i) and the respective limits expressed in power (δ_+^i, δ_-^i). Nevertheless, this transformation is not trivial, as shown in the examples below. The following sections describe that, making some assumptions, it is possible to mathematically relate the ramp limits, in order to properly formulate a power-based model.

4.1.2 How to transform the energy ramp-rates into power ones

In order to describe a relationship between ramp-rates expressed in energy (Δ_+^i, Δ_-^i) and ramp limits expressed in power (δ_+^i, δ_-^i), one could think that it is possible to consider that $\Delta^i = \delta^i$. Nevertheless, this choice does not allow a correct transformation between an energy-based model and a power-based model. In fact, consider for example a unit with a maximum instantaneous power output of 450 MW that produces 450 MWh of energy in the typical time period. If the unit can ramp up or down its power at 100 MW/h, one could at first assume that $\Delta_+^i = \Delta_-^i = 100$ MWh. But, this is not the case, because if the unit keeps up ramping up (or down) for an entire hour at its maximum speed, the corresponding increase (decrease) of the generated energy will be the integral of the extra (missing) power produced, that is only 50 MWh, as depicted in Fig. 4.5.

The example described above shows that translating the bounds δ_+^i and δ_-^i over power variations into bounds Δ_+^i and Δ_-^i over energy is not immediate. We could assume that $\Delta^i = \frac{1}{2}\delta^i$, but also this choice does not always allow a correct transformation between the two models for UC. In fact, let us consider a unit with the same characteristics mentioned above, such as $\delta^i = 100$ MW/h, that is committed at the beginning of the time horizon ($t = 1$) and that produced 200 MWh ($= e_0$) of energy in the previous time period ($t - 1$). Based on the previous assumption we have, in the first period, $e_0 - \Delta^i \le e_1 \le e_0 + \Delta^i$, this leads to $150 \le e_1 \le 250$. If we assume that $e_1 = 200$ MWh, to keep the same energy output, in the second period we have again $150 \le e_2 \le 250$. Nevertheless, this result is not realistic, because there are different actual trajectories p that provide the same amount of energy, as shown in Fig. 4.6:

- a_1 is the trajectory corresponding to a continuous output of 200 MW for all the period;

- b_1 is the trajectory corresponding to starting at 250 MW and continuously ramping down at full rate to 150 MW;
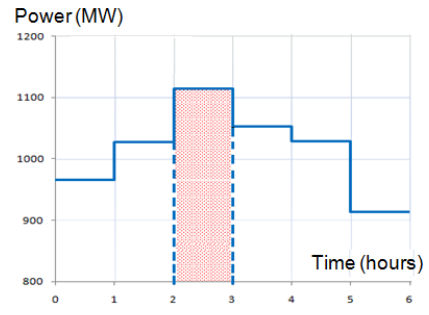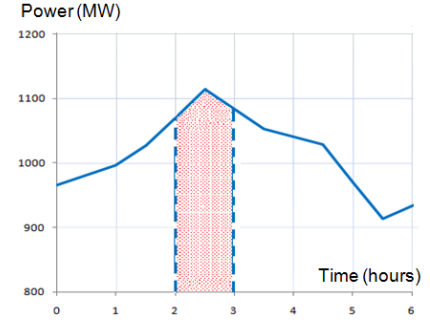
UC energy-based model	**UC power-based model**

Balance constraints

$e_t^i = p_t^i$	$e_t^i = \int_{t-1}^{t} p^i(\tau)d(\tau)$

Ramp-up constraints

$e_{t+1}^i \leq e_t^i + u_t^i \Delta_+^i + (1 - u_t^i)\bar{l}^i$	$p_{t+1}^i \leq p_t^i + u_t^i \delta_+^i + (1 - u_t^i)\bar{l}^i$

Ramp-down constraints

$e_t^i \leq e_{t+1}^i + u_{t+1}^i \Delta_-^i + (1 - u_{t+1}^i)\overline{u}^i$	$p_t^i \leq p_{t+1}^i + u_{t+1}^i \delta_-^i + (1 - u_{t+1}^i)\overline{u}^i$

Table 4.1: Main differences between an energy-based model and a power-based model
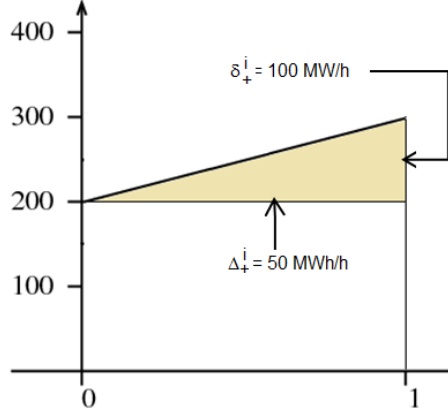
Figure 4.5: Transformation between ramp rates: $\Delta^i = \delta^i$.

- c_1 is the symmetric trajectory corresponding to starting at 150 MW and continuously ramping up at full rate to 250 MW.

This means that the maximum and minimum amount of energy e_2 that can be produced in the second period is different according to the 'scenario' realized in the first period, as shown in Fig. 4.7. In fact, the trajectory $a_1 : a_2$ corresponds to a production of $e_2 = 200$ MWh, the trajectory $b_1 : b_2$ corresponds to a production of $e_2 = 100$ MWh, while the trajectory $c_1 : c_2$ corresponds to a production of $e_2 = 300$ MWh. In particular, if we consider the scenario $c_1 : c_2$, it is possible to observe that the power produced at the end of the second period is 350 MW. This means that the minimum amount of energy that can be produced in the third period is 300 MWh (corresponding to a scenario $c_1 : c_2 : b_3$ where the unit is ramping down at full rate during all the third period), while the estimate based on energy gives $300 - 100 = 200$ MWh. All this leads to the following observation.

Observation 1 *The maximum and minimum amounts of energy that can be produced in a period t do not have the form $e_{t-1} + \Delta^i_+$ and $e_{t-1} - \Delta^i_-$, respectively, for fixed Δ^i_+ and Δ^i_-.*

It is thus necessary to understand if the knowledge of the power level of the unit at the beginning of a period could help in the definition of the values of Δ^i_+ and Δ^i_-. In particular, it could be useful to know if it is possible to have $\Delta^i = f(\delta^i)$ for particular trajectories of $p(t)$, that is to say, if there exists a particular trajectory of $p(t)$ for which the total energy produced by the unit is numerically equal to the instantaneous power at the end of the period (even if it is expressed in a different unit of measure).

In order to further investigate this aspect, assume that the unit was producing 200 MW at the beginning of the first period (end of period 0), and that has produced 200 MWh of energy during all the first period. It is easy to observe that this makes scenarios b_1 and c_1 unfeasible, as shown in Fig. 4.6.

However, there exist many different ways in which a unit that starts at 200 MW can produce 200 MWh of energy. This means that there are many different feasible curves $p(\tau)$ such that their integral is 200 MWh and $p_1(0) = 200$ MW. For instance, consider the scenario d_1, as shown in Fig. 4.8, corresponding to the unit ramping down at full rate α for the first fraction
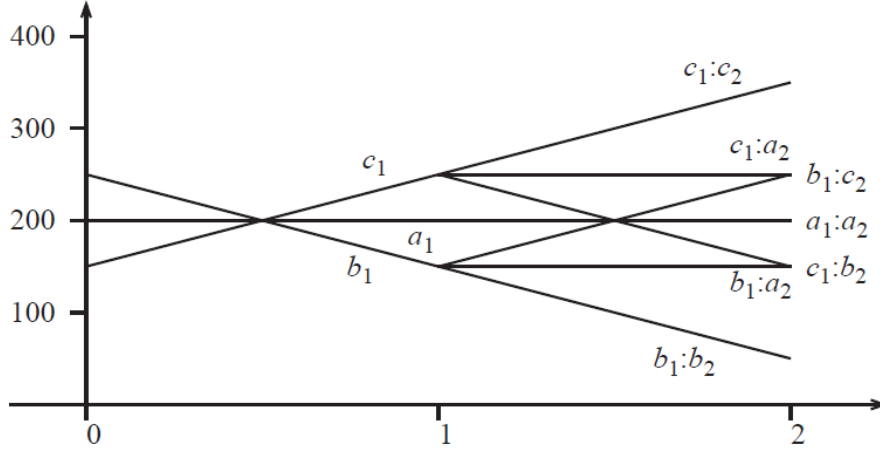
Figure 4.6: Different possibilities for trajectories p.

(a) *Scenario 1: trajectory $b_1 : b_2$.*   (b) *Scenario 2: trajectory $c_1 : c_2$.*
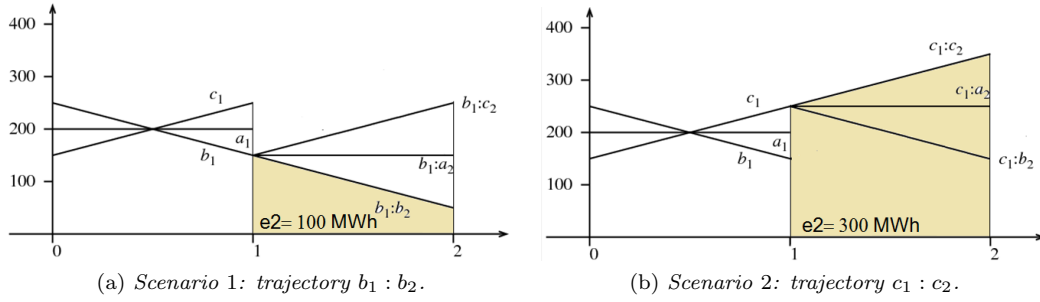
Figure 4.7: Different possibilities for trajectories p in the second period.

of $1 - \frac{1}{\sqrt{2}} \approx 0.293 \approx 0.3$ of the time period, and, after that, ramping up at full rate α for the remaining $\frac{1}{\sqrt{2}} \approx 0.7$ of the time period.

It is easy to observe that the integral of the curve d_1 is the same as that of a_1. In fact, the triangle 'below' curve a_1, of basis $2v$ and height αv ($v = 1 - \frac{1}{\sqrt{2}}$), has the same area as the triangle 'above' the curve, of basis $1 - 2v$ and height $\alpha(1 - 2v)$. This result does not depend on α, but on the fact that the maximum ramp-up and ramp-down rates are equal. The final power is $\alpha(\sqrt{2} - 1) \approx \alpha \cdot 0.414 \approx \alpha \cdot 0.4$ larger than that of a_1 (for the instance at hand, this makes roughly 240 MW).

Obviously, there exists an external curve f_1, symmetric to d_1 with respect to a_1, which gives the minimal possible final power (≈ 160 MW) compatible with the initial conditions and the value of e_1.

Then, the conditions $p_1(0) = 200$ MW and $e_1 = 200$ MWh are compatible with a final power ranging between 240 and 160 MW. This means that the two 'extreme' scenarios for time period 1, coupled with the corresponding extreme scenarios for time period 2 (see Fig. 4.8), give a maximum and minimum energy output for the unit respectively of about 290 and 110 MWh.
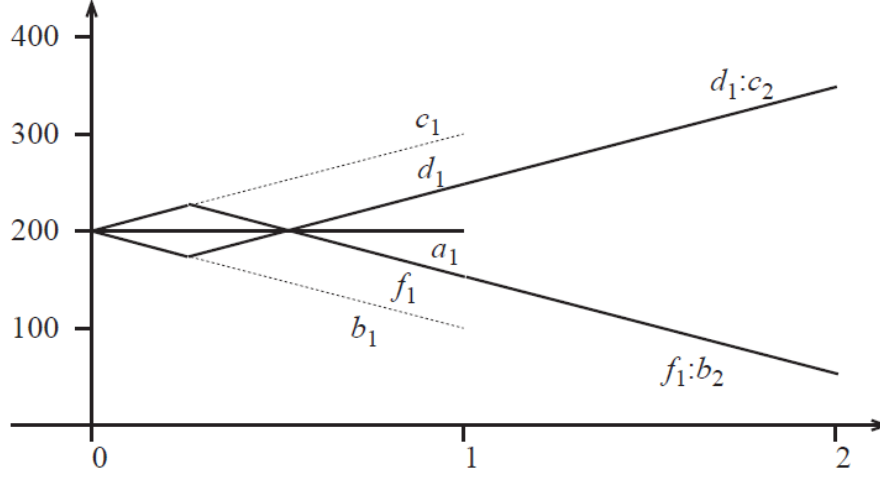
Figure 4.8: Another trajectory p_1.

Again, this is far beyond what the initial estimates gave. And again, one cannot simply enlarge the estimates at about 90 MWh. For scenario $d_1 : c_2 : b_3$ the estimate gives the minimal energy production at period 3 of 290 MWh, while the estimate from the 290 MWh produced at period 2 (under this scenario) is 200 MWh. All this gives:

Observation 2 *The maximum and minimum amounts of energy that can be produced in a period* t *do not have the form* $e_{t-1} + \Delta_+^i(p_{t-1}(0))$ *and* $e_{t-1} - \Delta_-^i(p_{t-1}(0))$, *respectively.*

The previous examples have shown that under the assumption that $\delta_+^i = \delta_-^i$, after one period t where the unit has been ramping up (down) at full rate, the minimum (maximum) energy produced in period $t + 1$ will be at least (at most) equal to that produced in period t. This means that for every sequence of energy decisions e_t which cannot rule out the possibility of the unit ramping up or down at full rate for a whole period, no positive value of Δ_+^i and Δ_-^i can be chosen. So, one may wonder whether small values of Δ_+^i and Δ_-^i may solve the problem, by ensuring that the unit will never be forced to ramp up (or down) at full rate for one entire period. This is indeed the case, as shown below.

Lemma 3 *If the unit starts a period at power* $\overline{p}$, *it can end the same period at any power* $p \in$ $\left[\overline{p} - \left(\sqrt{\delta_+^i \left(\delta_+^i + \delta_-^i \right)} - \delta_+^i \right), \overline{p} + \left(\sqrt{\delta_-^i \left(\delta_+^i + \delta_-^i \right)} - \delta_-^i \right) \right]$, *having produced exactly* p *(that is,* p *times the duration of the period) energy.*

Proof. Consider the generic trajectory where the unit ramps up at full rate δ_+^i for a fraction $\tau \in [0, 1]$ of the period, then starts ramping down, again at full rate δ_-^i, for the remaining fraction $1 - \tau$ of the period. By trivial calculations one has that the power reached at the end of the period is

$$p(\tau) = \overline{p} + \delta_+^i \tau - \delta_-^i (1 - \tau)$$
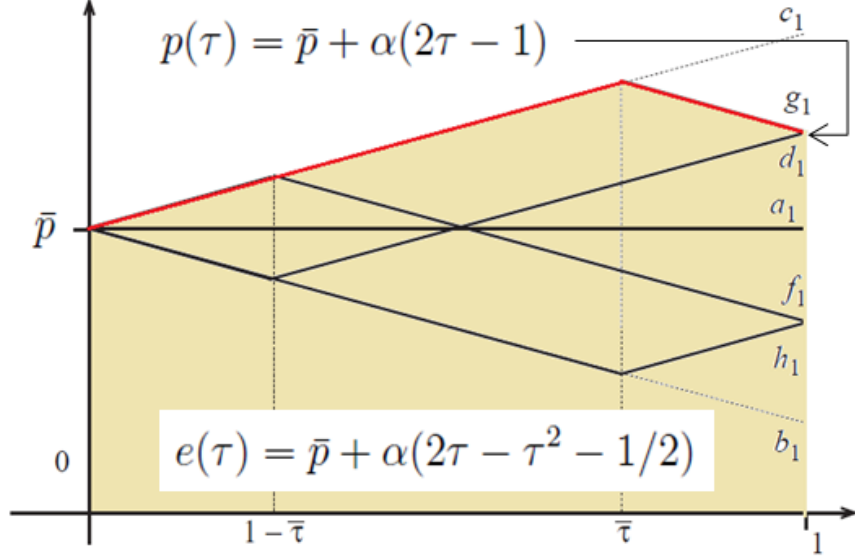
Figure 4.9: Extremal trajectories for Lemma 3 when $\delta_+^i = \delta_-^i$.

while the total energy produced during the period is

$$e(\tau) = \bar{p} + \delta_+^i \left(\tau - \frac{\tau^2}{2} \right) - \delta_-^i \frac{(1-\tau)^2}{2}$$

By solving the simple equation $e(\tau) = p(\tau)$, one shows that for $\bar{\tau} = \sqrt{\frac{\delta_-^i}{\delta_+^i + \delta_-^i}}$ the total energy produced by the unit is numerically equal (though in a different unit of measure) to the instantaneous power at the end of period, both at

$$\bar{p} + \left(\sqrt{\delta_-^i \left(\delta_+^i + \delta_-^i \right)} - \delta_-^i \right)$$

This corresponds to trajectory g_1 in Fig. 4.9; clearly, there exists the symmetric extremal trajectory h_1 with the unit ramping down for $\bar{\tau}$ and up for the rest of the period that gives power and energy both at $\bar{p} - \left(\sqrt{\delta_+^i \left(\delta_+^i + \delta_-^i \right)} - \delta_+^i \right)$. Note that, as depicted in figure, these trajectories are 'reverse' of the previously described extremal ones giving maximal power variation for fixed energy output.

Now, fix some $\epsilon > 0$ and consider the following modification of trajectory g_1:

- for the first $\frac{\epsilon}{\delta_+^i}$ fraction of the period, keep producing at the initial power level $\bar{p}$;

- then, start ramping up at full rate δ_+^i until instant $\bar{\tau} \left(1 - \frac{\epsilon}{\delta_+^i} \right)$;

- then, keep the attained power level stable until instant $\bar{\tau} \left(1 + \frac{\epsilon}{\delta_-^i} \right)$;

- finally, ramp down at full rate δ_-^i until the end of the period.

It is easy to verify that the final power level attained by this trajectory $g(\epsilon)$ is just the final power level of $g_1 \left(= \bar{p} + \left(\sqrt{\delta_-^i \left(\delta_+^i + \delta_-^i\right)} - \delta_-^i\right)\right)$ minus ϵ, and it is numerically identical to the total energy produced by the unit during the period.

In order to prove that the trajectory produces $g_1 - \epsilon$ energy, where g_1 is the energy produced by the trajectory with maximum ramp-up speed in the interval $[0, \bar{\tau}]$ and with maximum ramp-down speed in the interval $[\bar{\tau}, 1]$, the area between the two trajectories is computed.

This area can be divided into four regions. The first one is a parallelogram with base from $t = 0$ and $t = \frac{\epsilon}{\delta_+^i}$ and height from $\bar{p}$ to $\bar{p} + \delta_+^i \left(\bar{\tau}\left(1 - \frac{\epsilon}{\delta_+^i}\right) - \frac{\epsilon}{\delta_+^i}\right)$. Its area is denoted by A_1 and it is equal to:

$$A_1 = \frac{\epsilon}{\delta_+^i} \delta_+^i \left(\bar{\tau}\left(1 - \frac{\epsilon}{\delta_+^i}\right) - \frac{\epsilon}{\delta_+^i}\right) = \epsilon\bar{\tau} - \frac{\epsilon^2}{\delta_+^i}(\bar{\tau} + 1)$$

The second region is a triangle with base from $t = \bar{\tau}\left(1 - \frac{\epsilon}{\delta_+^i}\right) - \frac{\epsilon}{\delta_+^i}$ to $\bar{\tau}$ and height from $\bar{p} + \delta_+^i \left(\bar{\tau}\left(1 - \frac{\epsilon}{\delta_+^i}\right) - \frac{\epsilon}{\delta_+^i}\right)$ to $\bar{p} + \delta_+^i \bar{\tau}$. Its area is denoted by A_2 and it is equal to:

$$A_2 = \left(\bar{\tau} - \left(\bar{\tau} - \frac{\epsilon}{\delta_+^i}\bar{\tau}\right) + \frac{\epsilon}{\delta_+^i}\right)^2 \frac{\delta_+^i}{2} = \frac{\epsilon^2}{2\delta_+^i}(1 + \bar{\tau})^2$$

The third region is a trapezium (rotated by 90°) with height from $\bar{\tau}$ to $\bar{\tau}\left(1 + \frac{\epsilon}{\delta_-^i}\right)$, first base from $\bar{p} + \delta_+^i \left(\bar{\tau}\left(1 - \frac{\epsilon}{\delta_+^i}\right) - \frac{\epsilon}{\delta_+^i}\right)$ to $\bar{p} + \delta_+^i \bar{\tau}$, and second base from $\bar{p} + \delta_+^i \left(\bar{\tau}\left(1 - \frac{\epsilon}{\delta_+^i}\right) - \frac{\epsilon}{\delta_+^i}\right)$ to $\bar{p} + \delta_+^i \bar{\tau} - \delta_-^i \left(\bar{\tau}\left(1 + \frac{\epsilon}{\delta_-^i}\right) - \bar{\tau}\right)$. It can be checked that the second base is large exactly ϵ. Its area is denoted by A_3 and it is equal to:

$$A_3 = \frac{1}{2}\bar{\tau}\frac{\epsilon}{\delta_-^i}\left(\epsilon + \delta_+^i \bar{\tau} - \delta_+^i \left(\bar{\tau}\left(1 - \frac{\epsilon}{\delta_+^i}\right) - \frac{\epsilon}{\delta_+^i}\right)\right) = \frac{1}{2}\bar{\tau}\frac{\epsilon}{\delta_-^i}\left(\epsilon + \epsilon\bar{\tau} + \epsilon\right) = \frac{1}{2}\frac{\epsilon^2}{\delta_-^i}\bar{\tau}(2 + \bar{\tau})$$

The fourth region is a parallelogram with base of length ϵ (see second base of the previous trapezium) and height equal from $\bar{\tau}\left(1 + \frac{\epsilon}{\delta_-^i}\right)$ to 1. Its area is denoted by A_4 and it is equal to:

$$A_4 = \epsilon\left(1 - \bar{\tau}\left(1 + \frac{\epsilon}{\delta_-^i}\right)\right) = \epsilon - \epsilon\bar{\tau} - \frac{\epsilon^2}{\delta_-^i}\bar{\tau}$$

The sum of the four areas is easily computed and it is equal to ϵ:

$$\sum_{i=1}^{4} A_i \;=\; \epsilon\left(\overline{\tau}+1-\overline{\tau}\right)+\epsilon^2\left(-\frac{1}{\delta_+^i}\overline{\tau}-\frac{1}{\delta_+^i}+\frac{1}{2\delta_+^i}\left(1+\overline{\tau}^2+2\overline{\tau}\right)+\frac{1}{2\delta_-^i}\left(2\overline{\tau}+\overline{\tau}^2\right)-\frac{1}{\delta_-^i}\overline{\tau}\right)=$$

$$=\;\epsilon+\epsilon^2\left(-\frac{1}{\delta_+^i}\overline{\tau}+\frac{1}{\delta_+^i}\overline{\tau}-\frac{1}{\delta_+^i}+\frac{1}{2\delta_+^i}\left(1+\overline{\tau}^2\right)+\frac{1}{2\delta_-^i}\overline{\tau}^2+\frac{1}{\delta_-^i}\overline{\tau}-\frac{1}{\delta_-^i}\overline{\tau}\right)=$$

$$=\;\epsilon+\epsilon^2\left(-\frac{1}{2\delta_+^i}+\frac{\delta^-}{2\delta_+^i\left(\delta_+^i+\delta_-^i\right)}+\frac{1}{2\left(\delta_+^i+\delta_-^i\right)}\right)=$$

$$=\;\epsilon+\frac{\epsilon^2}{2}\left(-\frac{1}{\delta_+^i}+\frac{\delta_-^i}{\delta_+^i\left(\delta_+^i+\delta_-^i\right)}+\frac{\delta_+^i}{\delta_+^i\left(\delta_+^i+\delta_-^i\right)}\right)=\epsilon$$

Finally, we should see that if $\epsilon=\frac{\delta_+^i\,\overline{\tau}}{1+\overline{\tau}}$ then the trajectory is constant. Indeed, the trajectory producing $g_1-\epsilon$ energy has two constant pieces. The first one starts at zero and ends at $\frac{\epsilon}{\delta_+^i}=\frac{\overline{\tau}}{1+\overline{\tau}}$. The second one starts at $\overline{\tau}\left(1-\frac{\epsilon}{\delta_+^i}\right)=\overline{\tau}\left(1-\frac{\overline{\tau}}{1+\overline{\tau}}\right)=\frac{\overline{\tau}}{1+\overline{\tau}}$ and ends at $\overline{\tau}\left(1+\frac{\epsilon}{\delta_-^i}\right)=1$. The last relation can be easily obtained by substituting the value of $\overline{\tau}=\sqrt{\frac{\delta_-^i}{\delta_+^i+\delta_-^i}}$ and multiplying both numerator and denominator by $1-\overline{\tau}$. We have thus shown that the two constant pieces cover all the interval $[0,1]$.

All this is possible as long as $\frac{\epsilon}{\delta_+^i}\leq\overline{\tau}\left(1-\frac{\epsilon}{\delta_+^i}\right)$, which gives $\epsilon\leq\delta_+^i\frac{\overline{\tau}}{1+\overline{\tau}}=\sqrt{\delta_-^i\left(\delta_+^i+\delta_-^i\right)}-\delta_-^i$ (and, as expected, the 'flat' trajectory a_1 for the largest value of ϵ). Repeating similar arguments for the symmetrical trajectory h_1, the Lemma is proved. ∎

Theorem 4 *Let e_0 be chosen as the numerical value of the power p_0 of the unit at the beginning of the first period; then, for each energy vector $e=[e_1,\ldots,e_n]$ satisfying the ramping constraints with $\Delta_+^i=\sqrt{\delta_-^i\left(\delta_+^i+\delta_-^i\right)}-\delta_-^i$ and $\Delta_-^i=\sqrt{\delta_+^i\left(\delta_+^i+\delta_-^i\right)}-\delta_+^i$, there exists a feasible trajectory attaining exactly those energy production levels.*

Proof. From the previous Lemma, it is easy to prove by recursion that one can always build a trajectory where at the end of period t the power level of the unit is exactly e_t. ∎

For instance, if $\alpha=\delta_+^i=\delta_-^i$, choosing $\Delta_+^i=\Delta_-^i=\sqrt{2\alpha^2}-\alpha=\alpha\left(\sqrt{2}-1\right)\approx0.4\alpha$ ensures that there exist technically feasible trajectories $p(t)$ that satisfy the stipulated energy decisions $e(t)$. Clearly, the estimate is conservative, and energy decisions respecting ramp constraints with larger values of $\Delta_\pm^i$ need not necessarily result in unfeasible trajectories. However, it is easily proved with the only slightly larger 'conservative' estimate $\Delta_+^i=\Delta_-^i=0.5\delta$ that one cannot always get feasible power trajectories corresponding to feasible energy levels according to constraints (4.4) and (4.5).

Proposition 5 *Let $\alpha=\delta_+^i=\delta_-^i$; then, there exists one energy vector $e=[e_1,\ldots,e_n]$ satisfying the ramping constraints with $\Delta^i=\Delta_+^i=\Delta_-^i=\frac{\alpha}{2}$ such that no feasible trajectory attaining exactly those energy production levels exists.*

Proof. We have basically already seen this in the initial examples, so let us use the data of the unit: $\alpha=100$ MW, $p_0=200$ MW, $\Delta=\frac{\alpha}{2}=50$ MWh. Clearly, one should choose $e_0=p_0=200$

(MWh); in fact, choosing, say, $e_0 = 201$ MWh results in a feasible energy decision $e_1 = 251$ MWh that is unattainable by the unit even if ramping up at full rate for all the first period, and an analogous effect occurs with ramp downs for $e_0 = 199$ MWh. So, let $e_0 = 200$ MWh and consider the feasible energy decision vector $[e_1, e_2] = [250, 200]$; as already seen, no feasible trajectory exists that produces those energies, since in order to have $e_1 = 250$ MWh the unit has to be ramping up at full rate for all period 1, hence in period 2 it cannot produce less than 250 MWh. ∎

Thus, already the choice $\Delta = \frac{\alpha}{2}$ is 'unsafe', while of course not necessarily resulting in technically unfeasible decisions. No choice for the values of Δ_+^i and Δ_-^i can entirely reflect the actual flexibility of the ramping of one unit and at the same time be entirely safe. Therefore, a modeler should:

- use larger values than those suggested by the Theorem 4, incurring the risk that no feasible trajectory can be found to actually instantiate the energy decisions;

- use smaller values, unnecessarily restricting the flexibility of the unit in the decision model, which may possibly force to fire up some units that could have been left uncommitted by fully exploiting the dynamic range of those already producing, thus paying the corresponding additional start-up costs.

This is even more striking if we consider that, as shown in the previous examples, the maximal energy that can eventually be produced in time instant 2 by a unit starting at power p_0 is $p_0 + 1.5\alpha$. Thus, in order to allow this - technically feasible - ramping rate to be exploited by the mathematical model, one would need to choose $\Delta^i = 0.75\alpha$, a full 50% larger than the already 'unsafe' estimate $\Delta^i = 0.5\alpha$, and a whopping 81% larger than the 'safe' estimate $\Delta^i = 0.4\alpha$ suggested by the Theorem 4.

4.1.3 Analysis of the relationships between the ramp-rate limits

In order to analyze how the choice of Δ^i influences the decisions in an energy-based model, different simulations over realistic instances have been made. The energy-based model and the power-based model described in section 4.1.1 (table (4.1)) have been implemented in a C++ programming language code, and they have been solved with the CPLEX 11.0 commercial solver, over a machine with standard computational characteristics. A typical realistic instance consisting of 10 thermal units has been used as input to the two models. In order to study the behavior of the models to the different values of Δ^i, various choices for the amount of the energy-ramp rate have been selected, while the value of δ^i has been left unaltered during all simulations. In this way, we could analyze how the value of $\frac{\Delta^i}{\delta^i}$ may affect the solution of the energy-based model, specially in feasibility terms. The main results obtained in the simulation phase have been briefly resumed in table (4.2), where the values of the objective functions obtained for the two models, with respect to $\frac{\Delta^i}{\delta^i}$, are shown. The form of the objective function (expressed in €) of the two models with respect to $\frac{\Delta^i}{\delta^i}$ is depicted in Fig. 4.10.

It is thus possible to observe the following interesting aspects:

- even if choosing larger values for $\frac{\Delta^i}{\delta^i}$ of than those suggested by the Theorem 4 is 'unsafe', not necessarily technically unfeasible decisions could be found to actually instantiate the energy decisions;

$\frac{\Delta^i}{\delta^i}$	O.F. (power-based)	O.F. (energy-based)
0.015	1870995.240	n.a.
0.020	1870995.240	2193925.296
0.025	1870995.240	2117702.497
0.030	1870995.240	2100790.505
0.040	1870995.240	2071474.034
0.050	1870995.240	2042716.357
0.100	1870995.240	1946469.994
0.200	1870995.240	1874453.927
0.300	1870995.240	1860405.253
0.400	1870995.240	1853614.646
0.500	1870995.240	1848661.142
0.600	1870995.240	1848104.181

Table 4.2: Comparison between objective functions with respect to the ramp rates values
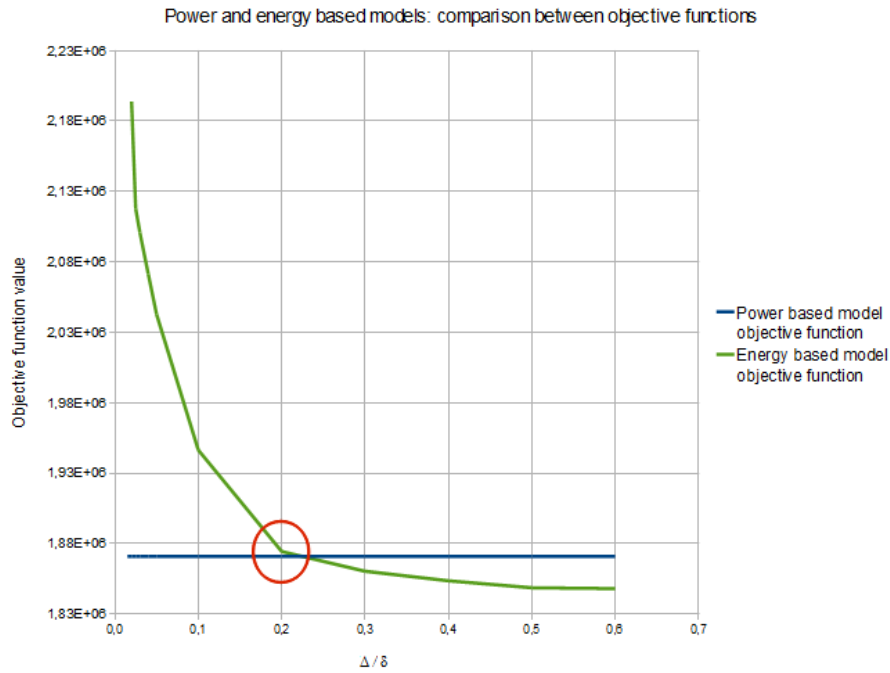
Figure 4.10: Power and energy based models: comparison between objective functions.

- large values of $\frac{\Delta^i}{\delta^i}$ could lead to the advantage in increasing the flexibility of the units, since ramping constraints are well satisfied, making possible to use a small set of units, consequently reducing the operational costs (this means that the value of the objective function decreases);

- using smaller values for $\frac{\Delta^i}{\delta^i}$ of than those suggested by the Theorem 4, could restrict the flexibility of the units, since it is more difficult to satisfy the ramping constraints; in this case it could be necessary to switch on other units that could have been left off, utilizing the units already producing at their maximum power, consequently increasing the operational costs (this means that the value of the objective function increases);

- using too small values for $\frac{\Delta^i}{\delta^i}$ could severely limit the operation of the units, such that the solution of the respective problem is unfeasible;

- from a global point of view, the objective function of the power-based model presents smaller values than those of the energy-based model, for values of $\frac{\Delta^i}{\delta^i} < 0.2$; this means that the power-based model ensures more flexibility to the units, since the ramping-constraints, with ramp-rate expressed in power, are alway satisfied, in contrast with what happens in a typical energy-based model.

4.2 Unit Commitment power-based models formulation

In the UC models with power variables, the decisional variables represent the power output of each generator instead of energy, in contrast with what happens in the classical model for UC, as described previously in section 2 of chapter 1.

For each time period t, a variable called p_t^i is introduced, in order to represent the power generated by the thermal unit i at the end of the time period t. The binary variables u_t^i represent the status (on or off) of the thermal unit i at time t, with $u_t^i \in \{0, 1\}$.

The model is based on the assumption that the power output increases - or decreases - uniformly from p_{t-1}^i to p_t^i during all the time period t; if $p_{t-1}^i = p_t^i$, then the unit is not ramping at all.

The main difference with respect to the classical model for UC concerns the computation of the energy in the demand constraints, as described in the following sections. In fact, the energy balance constraints must be modified in order to compute the total energy produced by all the thermal units in each time period, since the units are always ramping linearly.

Various models for UC with power variables are proposed below, each model is different from the others, according to the way in which the demand constraints are calculated.

4.2.1 A simple continuous power-based model

The first power-based model that we propose is the *'simple continuous'* model. This model is called 'simple continuous' because it represents the standard simplest formulation of the power-based model, which all the other models that we will propose in the following sections are based on. The simple continuous power-based model is based on the aforementioned assumption that all the generating units are always ramping linearly during each time period. This means that the power output increases - or decreases - uniformly from p_{t-1}^i to p_t^i during all the time period t. If $p_{t-1}^i = p_t^i$, then the unit is not ramping. Moreover, another assumption is that the generating units are all always committed during time periods.
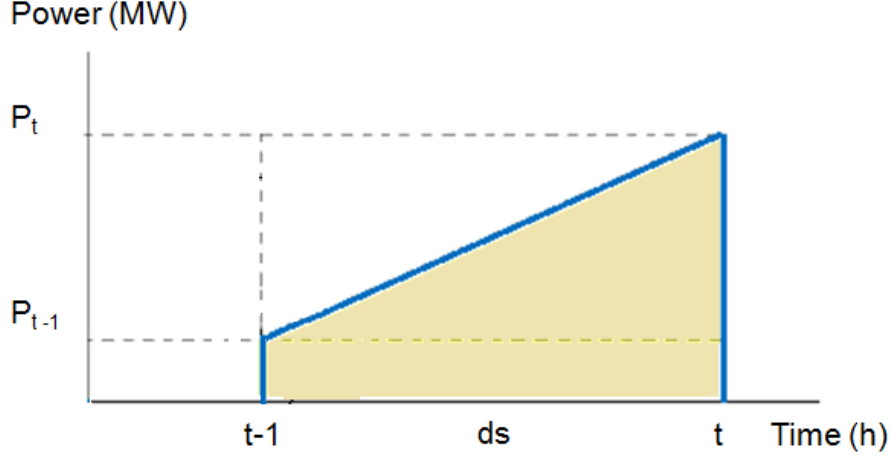
Figure 4.11: Standard case of the demand constraints in the simple continuous model.

In this standard case, the demand constraints, which estimate the energy produced by a thermal unit i, are expressed as follows [WS93] [WS94] [WS95]:

$$\frac{d_s}{2}(p_{t-1}^i + p_t^i) \tag{4.12}$$

where d_s is the duration of the time interval starting at $t-1$ and ending at t, which is normally equal to 1 hour. According to the expression (4.12), the energy produced during the time period t is calculated as the area of the trapezium with base from p_{t-1}^i to p_t^i and height equal to the time duration d_s, as depicted in Fig. 4.11.

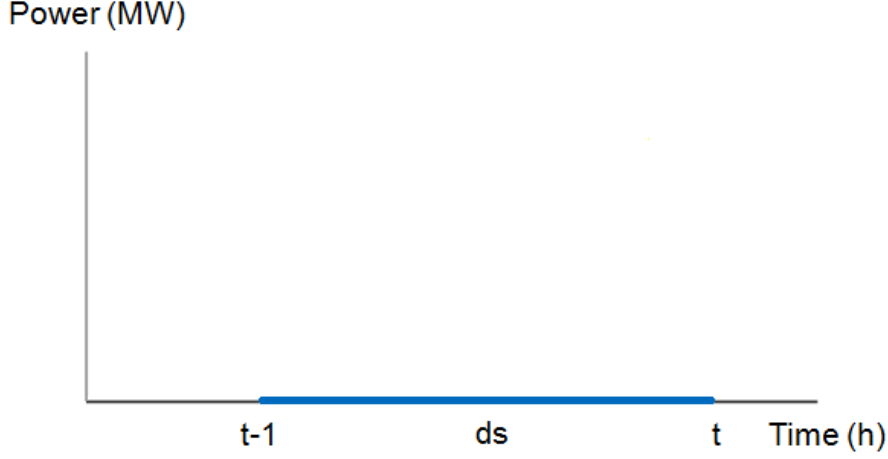Thus, the standard formulation of the *'simple continuous'* power-based model is the following

$$\min \sum_{i \in \mathcal{P}} c^i(u^i) + \sum_{t \in \mathcal{T}} f^i(p_t^i) \tag{4.13}$$

$$\sum_{i \in \mathcal{P}} \frac{d_s}{2}(p_{t-1}^i + p_t^i) = \bar{d}_t \qquad t \in \mathcal{T} \tag{4.14}$$

$$\bar{p}_{min}^i u_t^i \le p_t^i \le \bar{p}_{max}^i u_t^i \qquad i \in \mathcal{P}, t \in \mathcal{T} \tag{4.15}$$

$$p_{t+1}^i \le p_t^i + u_t^i \delta_+^i + (1 - u_t^i)\bar{l}^i \qquad i \in \mathcal{P}, t = 0, \dots, n-1 \tag{4.16}$$

$$p_t^i \le p_{t+1}^i + u_{t+1}^i \delta_-^i + (1 - u_{t+1}^i)\bar{u}^i \qquad i \in \mathcal{P}, t = 0, \dots, n-1 \tag{4.17}$$

Figure 4.12: Case when $u_{t-1}^i = 0$ and $u_t^i = 0$.

$$u_t^i \geq u_r^i - u_{r-1}^i \qquad t \in \mathcal{T}, r \in \left[t - \tau_+^i, t - 1\right] \tag{4.18}$$

$$u_t^i \geq 1 - u_{r-1}^i - u_r^i \qquad t \in \mathcal{T}, r \in \left[t - \tau_-^i, t - 1\right] \tag{4.19}$$

$$u_t^i \in \{0, 1\} \qquad t \in \mathcal{T} \tag{4.20}$$

Nevertheless, the standard formulation of the simple continuous power-based model presents some drawbacks, that cannot be neglected. In fact, the expression (4.12) provides exactly the amount of energy generated by a thermal unit i during time period t, if no start-ups or shutdowns occur at the beginning/end of the period. This means that the model works correctly only in the cases when $u_{t-1}^i = 1$ and $u_t^i = 1$ or $u_{t-1}^i = 0$ and $u_t^i = 0$, respectively shown in figures 4.11 and 4.12.

In the other cases, e.g., when the unit changes its status passing from $t - 1$ to t, (this means that $u_{t-1}^i = 0$ and $u_t^i = 1$; or that $u_{t-1}^i = 1$ and $u_t^i = 0$), the expression (4.12) is incorrect.

In order to explain this concept, consider the case when $u_{t-1}^i = 0$ and $u_t^i = 1$. In this case, the thermal unit i is off at time period $t - 1$ ($u_{t-1}^i = 0$) and it is on at time period t ($u_t^i = 1$), as shown in Fig. 4.13.

At time interval $t - 1$, we have $p_{t-1}^i = 0$, nevertheless $p_t^i > 0$ from $t - 1 + \epsilon$ to t; in particular, at time interval $t - 1 + \epsilon$ a discontinuity is generated due to the fact that the unit is turned on. The problem with start-ups is that (4.12) is incorrect when $p_{t-1}^i = 0$, because the unit begins to feed energy in the electrical network only after having reached a power level that belongs to a specific subinterval $\left[\overline{p}_{min}^i, \overline{l}^i\right]$ of the production range $\left[\overline{p}_{min}^i, \overline{p}_{max}^i\right]$. If we assume that $\overline{l}^i = \overline{p}_{min}^i$, the energy produced by the thermal unit i in the first period t following a start-up is actually
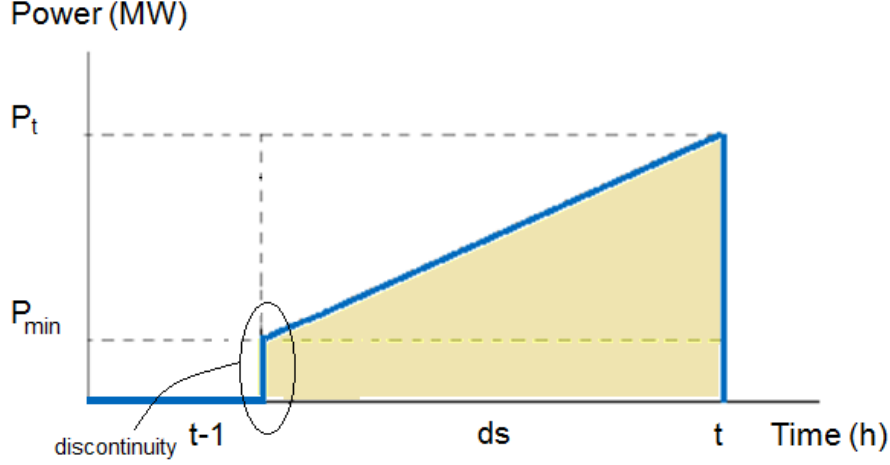
Figure 4.13: Case when $u_{t-1}^i = 0$ and $u_t^i = 1$.

$$\frac{d_s}{2}(\overline{p}_{min}^i + p_t^i) \tag{4.21}$$

that is more than what predicted by the term (4.12). In fact, the energy determined by the power curve is given by the area of the trapezium with base from $\overline{p}_{min}^i$ to p_t^i and height d_s.

Consider now the case when $u_{t-1}^i = 1$ and $u_t^i = 0$. In this case, the thermal unit i is on at time $t-1$ ($u_{t-1}^i = 1$) and it is off at time t ($u_t^i = 0$), as shown in Fig. 4.14.

If we consider the time interval $t-1$, we have $p_{t-1}^i > 0$, nevertheless $p_t^i = 0$ in the time period between $t-1+\epsilon$ and t; in particular, at time instant ϵ a discontinuity is generated due to the fact that the unit is off. For this reason, a symmetric problem occurs with respect to what shown in the previous case. In fact, a shut-down occurs in period t, after period $t-1$: the term (4.12), having $p_{t-1}^i > 0$ (and $p_t^i = 0$), seems to provide a fictitious amount of energy during period t while in fact none is produced.

All the cases shown above have demonstrated that the expression (4.12) must be properly modified in order to model also the special cases in which the unit is not running, either in time period $t-1$ or in time period t.

In particular, the UC formulation with power variables should be able to model the special cases shown in figures 4.13 and 4.14.

A more formal modification of the model requires a quite reasonable assumption: the exact amount of power produced at the beginning of start-up period and at the end of a shut-down period is exactly known, i.e. it is a constant. This can be simply obtained by requiring $\overline{u}^i = \overline{l}^i = \overline{p}_{min}^i$, i.e., that each unit exactly reaches its thermal minimum before being put on/off line, thereby ensuring the exact computation of the 'correction terms' between (4.12) and the true amount of energy that is going to be produced. Then, consider the following modified expression for the amount of energy produced in period t by the thermal unit i:

$$\frac{d_s}{2}(p_{t-1}^i + p_t^i) + d_s \frac{\overline{p}_{min}^i}{2}(u_t^i - u_{t-1}^i) \tag{4.22}$$
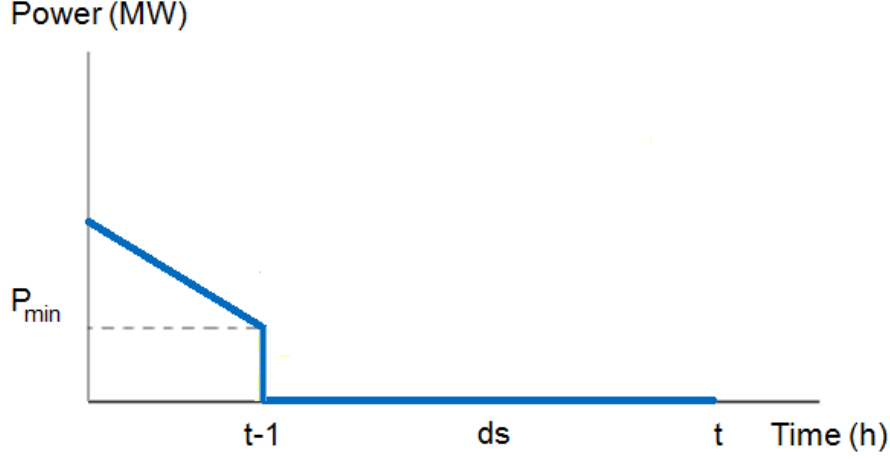
Figure 4.14: Case when $u_{t-1}^i = 1$ and $u_t^i = 0$.

The form (4.22) coincides with (4.12) if unit i is continuously off ($u_{t-1}^i = u_t^i = 0$) or on ($u_{t-1}^i = u_t^i = 1$) in the two consecutive time periods $t-1$ and t. If start-up occurs at time period t, i.e., $u_{t-1}^i = 0$ ($\to p_{t-1}^i = 0$) and $u_t^i = 1$, then an extra correction term $d_s \frac{\overline{p}_{min}^i}{2}$ is added to the amount of energy produced in period t, as justified by the fact that the unit is already producing $\overline{p}_{min}^i$ power at the beginning of the period. Conversely, if a shut down occurs at the end of time period $t-1$, i.e., $u_{t-1}^i = 1$ and $u_t^i = 0$ ($\to p_t^i = 0$), then an extra correction term $-d_s \frac{\overline{p}_{min}^i}{2}$ is added to the amount of energy produced in period t, balancing the fictitious production due to the fact that $p_{t-1}^i = \overline{p}_{min}^i > 0$ while $p_t^i = 0$.

With these stipulations, the model is as follows:

$$\min \sum_{i \in \mathcal{P}} c^i(u^i) + \sum_{t \in \mathcal{T}} f^i(p_t^i) \tag{4.23}$$

$$\sum_{i \in \mathcal{P}} \frac{d_s}{2}(p_{t-1}^i + p_t^i) + d_s \frac{\overline{p}_{min}^i}{2}(u_t^i - u_{t-1}^i) = \overline{d}_t \quad t \in \mathcal{T} \tag{4.24}$$

$$(4.15)(4.16)(4.17)(4.18)(4.19)(4.20)$$

In section 4.3.1, the simulations results obtained with the simple continuous power-based model are described and commented.

4.2.2   A semi-continuous power-based model

In a 'pure' continuous power-based model, that is to say, a model in which all the units are always on, the power at the beginning of the current time interval t is equal to the power at the end of the previous time interval $t-1$, e.g., it is expressed by p_{t-1}^i. Nevertheless, it is necessary to consider all the scenarios analyzed in section 4.2.1, with particular attention to the cases in which

the unit changes its status, being turned on or off, as depicted in figures 4.13 and 4.14. In fact, in these cases, a discontinuity is determined, due to a variation of the power in the time interval $t-1+\epsilon$; from a practical point of view, ϵ it is not represented by an instant, but it is a finite time interval.

The simple continuous power-based model for UC proposed in section 4.2.1 modeled these discontinuity cases making some simplifications, as previously described. Nevertheless, for the issues mentioned above, it is necessary to formulate a more accurate power-based model, that we call *'semi-continuous'*, in which the power at the beginning of the current time interval t is defined in a different way than it happens in the 'pure' continuous formulation.

In fact, if the assumption $\overline{u}^i = \overline{l}^i = \overline{p}^i_{min}$ for each $i \in \mathcal{P}$ is not verified we have to directly model the power levels at the beginning of each period by adding a proper vector of auxiliary variables called γ^i_t for $i \in \mathcal{P}, t \in \mathcal{T}$.

This variable, subjected to proper constraints, as described below, guarantees that the value of the energy, in the current time interval where the power curve is individuated, is coherent with the status of the unit, from a practical point of view. In particular, the new variable γ^i_t will assume different values, according to the status of the unit i at time $t-1$ and at time t. In fact, the variable γ^i_t must be equal to p^i_{t-1} if unit i is on in both periods t and $t-1$ and the same holds when unit i is off in both t and $t-1$. When the unit i is switched off in period t then $\gamma^i_t = 0$, while if the unit i is switched on in period t then γ^i_t must be in the interval $\left[\overline{p}^i_{min}, \overline{l}^i\right]$.

All these conditions can be summarized in the following constraints

$$\overline{p}^i_{min} u^i_t \leq \gamma^i_t \leq \overline{p}^i_{max} u^i_t \qquad i \in \mathcal{P}, t \in \mathcal{T} \tag{4.25}$$

$$0 \leq \gamma^i_t \leq p^i_{t-1} + \overline{p}^i_{min}(1 - u^i_{t-1}) \qquad i \in \mathcal{P}, t \in \mathcal{T} \tag{4.26}$$

$$\gamma^i_t \geq p^i_{t-1} - \overline{u}^i(1 - u^i_t) \qquad i \in \mathcal{P}, t \in \mathcal{T} \tag{4.27}$$

Constraints (4.25) express the unit capability limits, according to which a unit can produce a power that is limited between a minimum and a maximum level. Constraints (4.26) and (4.27) make it possible that the variable γ^i_t is equal to p^i_{t-1} if the unit i is on in both periods t and $t-1$ and when is off in both t and $t-1$. When the unit i is switched off in period t then $\gamma^i_t = 0$, while if the unit i is switched on in period t then γ^i_t must be in the interval $\left[\overline{p}^i_{min}, \overline{l}^i\right]$.

All this means that the demand constraints expressed in (4.12) should be properly modified, in order to satisfy all the cases described before. These constraints could be written so that the power associated with the time instants $t-1$ and t depend on u^i_{t-1} and on u^i_t, nevertheless, in this way we obtain a bilinear form in the terms of $p^i_{t-1}u^i_{t-1}$ and $p^i_t u^i_t$, or with quadratic terms in the variables u^i_{t-1} and u^i_t, which are not easily solvable with the available MILP solvers. In order to obtain a constraint in a linear form, it is possible to use the auxiliary variable γ^i_t, whose meaning has been described before, in order to express the energy produced by a thermal unit i in the demand constraints as follows

$$\frac{d_s}{2}(\gamma^i_t + p^i_t) \tag{4.28}$$

The *'semi-continuous'* power-based model for UC is thus the following

$$\min \sum_{i \in \mathcal{P}} c^i(u^i) + \sum_{t \in \mathcal{T}} f^i(p_t^i) \tag{4.29}$$

$$\sum_{i \in \mathcal{P}} \frac{d_s}{2}(\gamma_t^i + p_t^i) = \overline{d}_t \quad t \in \mathcal{T} \tag{4.30}$$

$$\overline{p}_{min}^i u_t^i \leq \gamma_t^i \leq \overline{p}_{max}^i u_t^i \qquad i \in \mathcal{P}, t \in \mathcal{T} \tag{4.31}$$

$$0 \leq \gamma_t^i \leq p_{t-1}^i + \overline{p}_{min}^i(1 - u_{t-1}^i) \qquad i \in \mathcal{P}, t \in \mathcal{T} \tag{4.32}$$

$$\gamma_t^i \geq p_{t-1}^i - \overline{u}^i(1 - u_t^i) \qquad i \in \mathcal{P}, t \in \mathcal{T} \tag{4.33}$$

$$(4.15)(4.16)(4.17)(4.18)(4.19)(4.20)$$

The advantage of this model is that the physical constraints on power generation are directly modeled so that the trajectories of the power p constructed are surely feasible. Nevertheless, the formulation requires to use more constraints and more variables and the structure of the demand constraints, that link the variables of different units, is more complicated.

In section 4.3.2, the simulations results obtained with the semi-continuous power-based model are described and commented.

4.2.3 A two-sloped continuous power-based model

The simple-continuous model presents some aspects that do not proper reflect the operating behavior of the units, from a practical point of view. In order to overcome this difficulty, an extension of this model, called *'two-sloped'* continuous power-based model, is proposed. This model is based on the assumptions that a generating unit could reach its maximum (minimum) power output in a given time period during its ramp-up (ramp-down) phase; furthermore, power trajectories are characterized by different ramp rates into the same time period.

In order to formulate this model, it is assumed that the value of the energy e_t^i of the thermal unit i associated with a given power trajectory is limited between a minimum and a maximum function, as depicted in Fig. 4.15. In the picture, two power curves $f_1^i(\gamma_t^i, p_t^i)$ (red curve) and $f_2^i(\gamma_t^i, p_t^i)$ (blue curve) are shown, that respectively represent the lower and the upper bounding functions on the energy e_t^i.

According to this, the two-sloped power-based model can be formulated as follows

$$\min \sum_{i \in \mathcal{P}} c^i(u^i) + \sum_{t \in \mathcal{T}} f^i(p_t^i) \tag{4.34}$$

$$f_1^i(\gamma_t^i, p_t^i) \leq e_t^i \leq f_2^i(\gamma_t^i, p_t^i) \tag{4.35}$$
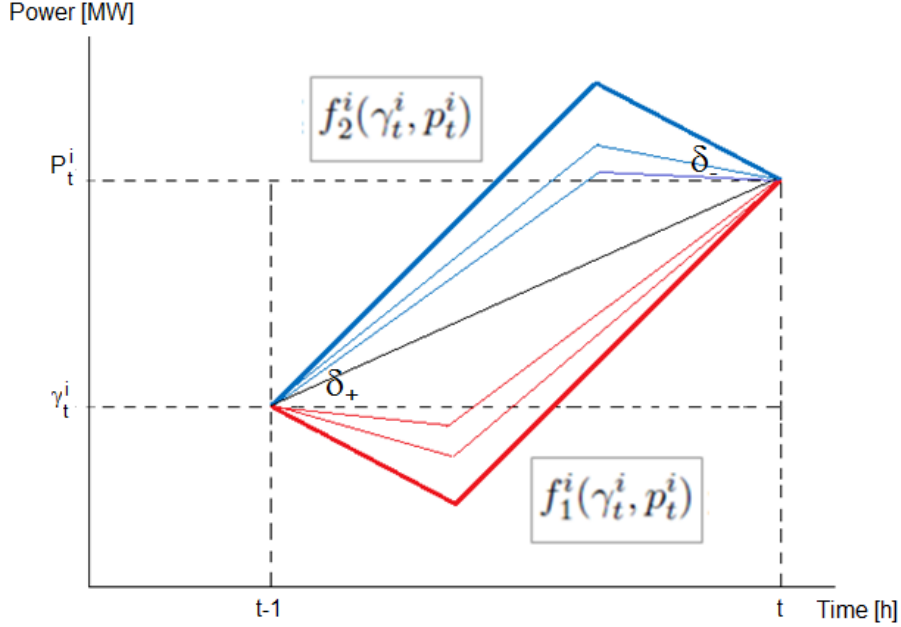
Figure 4.15: Upper and lower bounding functions on the energy e_t^i.

$$\sum_{i \in \mathcal{P}} e_t^i = \overline{d}_t \tag{4.36}$$

$$(4.15)(4.16)(4.17)(4.18)(4.19)(4.20)(4.31)(4.32)(4.33)$$

If the assumption that a generating unit could reach its maximum (minimum) power output in a given time period during its ramp-up (ramp-down) phase is neglected and it is only assumed that power trajectories are characterized by different ramp rates into the same time period, it is possible to calculate the expression of $f_1^i(\gamma_t^i, p_t^i)$ and $f_2^i(\gamma_t^i, p_t^i)$, considering the case shown in picture (4.15). In fact, it is easy to verify that the functions $f_1^i(\gamma_t^i, p_t^i)$ and $f_2^i(\gamma_t^i, p_t^i)$ are described by the following expressions:

$$f_1^i(\gamma_t^i, p_t^i) = \frac{1}{2(\delta_+^i + \delta_-^i)}(\gamma_t^{i\,2} + p_t^{i\,2} - 2\gamma_t^i p_t^i + 2\delta_+^i \gamma_t^i + 2\delta_-^i p_t^i - \delta_+^i \delta_-^i) \tag{4.37}$$

$$f_2^i(\gamma_t^i, p_t^i) = \frac{1}{2(\delta_+^i + \delta_-^i)}(-\gamma_t^{i\,2} - p_t^{i\,2} + 2\gamma_t^i p_t^i + 2\delta_-^i \gamma_t^i + 2\delta_+^i p_t^i + \delta_+^i \delta_-^i) \tag{4.38}$$

Nevertheless, the model should take into account also the case in which a generating unit could reach its maximum (minimum) power output in a given time period during its ramp-up
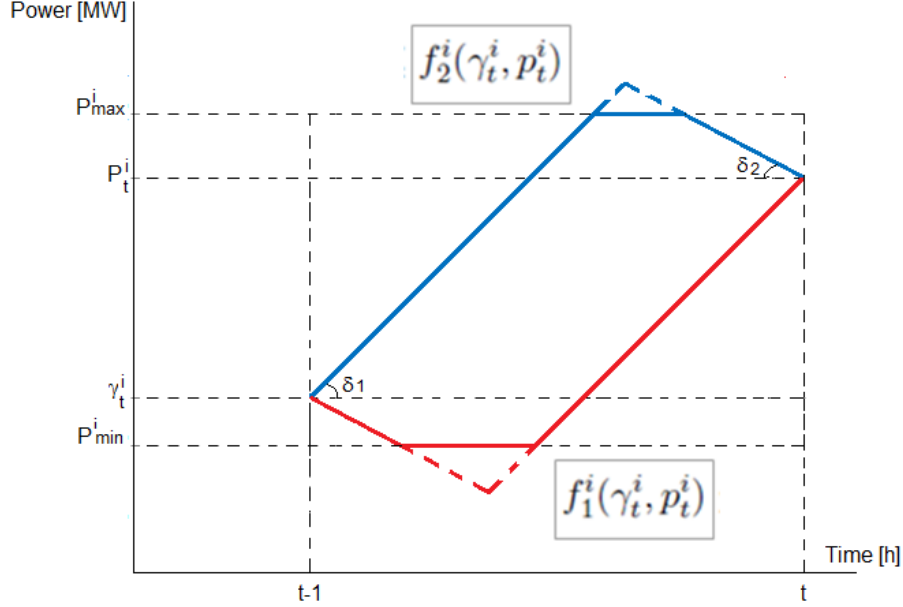
Figure 4.16: Upper and lower bounding functions on the energy e_t^i when the maximum (or minimum) power are reached.

(ramp-down) phase. These cases are shown in Fig. 4.16. Observing this picture, it is possible to notice that the power curves $f_1^i(\gamma_t^i, p_t^i)$ and $f_2^i(\gamma_t^i, p_t^i)$ are 'cut', this means that they are limited since the minimum (or the maximum) power is reached in the current time period.

In the following sections, we describe how the expression of $f_1^i(\gamma_t^i, p_t^i)$ and $f_2^i(\gamma_t^i, p_t^i)$ can be determined, taking into account the assumptions previously mentioned.

Determination of the lower bounding function

In order to calculate the expression of the function $f_1^i(\gamma_t^i, p_t^i)$, consider Fig. 4.17, where, for the sake of simplicity, only the curve $f_1^i(\gamma_t^i, p_t^i)$ has been drawn (in the figure, for simplicity, δ_+^i and δ_-^i have been substituted with δ_1 and δ_2). It is easy to observe that the area determined by the curve $f_1^i(\gamma_t^i, p_t^i)$ consists of the sum of two trapeziums ($ABCD$ and $EGHF$) and a rectangle ($BEFC$).

Since the value of the time duration x is given by $x = \frac{\gamma_t^i - \overline{p}_{min}^i}{\delta_1}$, the area of the trapezium $ABCD$ can be expressed as follows

$$A_{ABCD} = \frac{(\gamma_t^i + \overline{p}_{min}^i) \cdot x}{2} = \frac{\gamma_t^{i^2} - \overline{p}_{min}^{i^2}}{2\delta_1} \tag{4.39}$$

Moreover, considering that the value of the time duration y is given by $y = \frac{p_t^i - \overline{p}_{min}^i}{\delta_2}$, the area of the trapezium $EGHF$ can be expressed as follows

$$A_{EGHF} = \frac{(p_t^i + \overline{p}_{min}^i) \cdot y}{2} = \frac{p_t^{i^2} - \overline{p}_{min}^{i^2}}{2\delta_2} \tag{4.40}$$
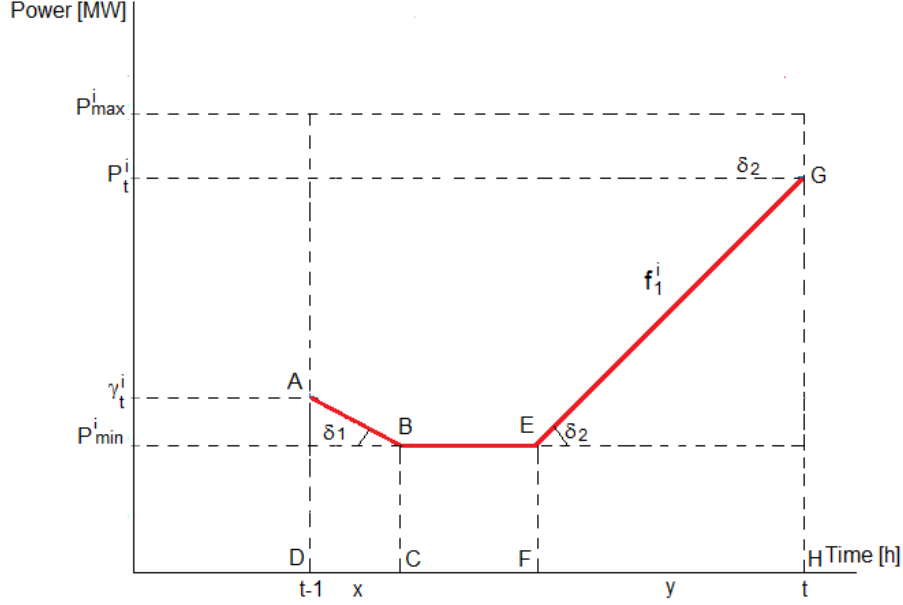
Figure 4.17: Lower bounding function of the energy e_t^i when the minimum power is reached.

The area of rectangle $BEFC$ can be easily determined considering that the value of the time duration BE is given by $BE = 1 - (x + y)$:

$$A_{BEFC} = \overline{p}_{min}^i [1 - (x + y)] \tag{4.41}$$

Substituting the values of x and y into (4.41), the following expression of the area of the rectangle $BEFC$ is obtained

$$A_{BEFC} = \overline{p}_{min}^i \left[\frac{\delta_1 \delta_2 - \gamma_t^i \delta_2 + \overline{p}_{min}^i \delta_2 - p_t^i \delta_1 + \overline{p}_{min}^i \delta_1}{\delta_1 \delta_2} \right] \tag{4.42}$$

The area that represents the energy determined by the power curve $f_1^i(\gamma_t^i, p_t^i)$ is given by the sum of the areas previously determined:

$$f_1^i(\gamma_t^i, p_t^i) = \frac{{p_t^i}^2 \delta_1 + {\gamma_t^i}^2 \delta_2 + {\overline{p}_{min}^i}^2 \delta_1 + {\overline{p}_{min}^i}^2 \delta_2 - 2\delta_1 p_t^i \overline{p}_{min}^i - 2\delta_2 \gamma_t^i \overline{p}_{min}^i + 2\delta_1 \delta_2 \overline{p}_{min}^i}{2\delta_1 \delta_2} \tag{4.43}$$

Determination of the upper bounding function

In order to calculate the expression of the function $f_2^i(\gamma_t^i, p_t^i)$, consider Fig. 4.18, where, for the sake of simplicity, only the curve $f_2^i(\gamma_t^i, p_t^i)$ has been drawn (in the figure, for simplicity, δ_+^i and δ_-^i have been substituted with δ_1 and δ_2). It is easy to observe that the area determined by
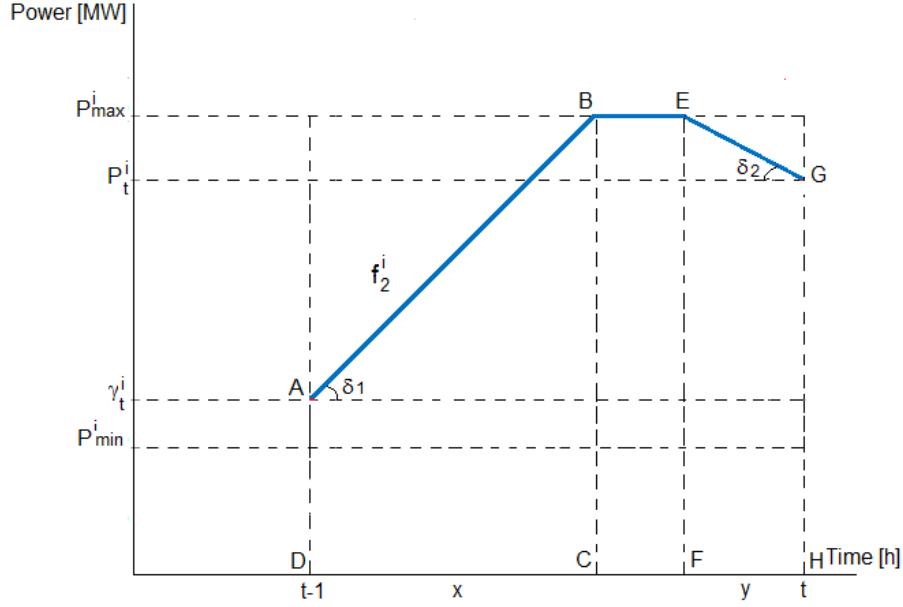
Figure 4.18: Upper bounding function of the energy e_t^i when the maximum power is reached.

the curve $f_2^i(\gamma_t^i, p_t^i)$ consists of the sum of two trapeziums ($ABCD$ and $EGHF$) and a rectangle ($BEFC$).

Since the value of the time duration x is given by $x = \frac{\bar{p}_{max}^i - \gamma_t^i}{\delta_1}$, the area of the trapezium $ABCD$ can be expressed as follows

$$A_{ABCD} = \frac{(\gamma_t^i + \bar{p}_{max}^i) \cdot x}{2} = \frac{\bar{p}_{max}^{i\,2} - \gamma_t^{i\,2}}{2\delta_1} \tag{4.44}$$

Moreover, considering that the value of the time duration y is given by $y = \frac{\bar{p}_{max}^i - p_t^i}{\delta_2}$, the area of the trapezium $EGHF$ can be expressed as follows

$$A_{EGHF} = \frac{(\bar{p}_{max}^i + p_t^i) \cdot y}{2} = \frac{\bar{p}_{max}^{i\,2} - p_t^{i\,2}}{2\delta_2} \tag{4.45}$$

The area of rectangle $BEFC$ can be easily determined considering that the value of the time duration BE is given by $BE = 1 - (x + y)$:

$$A_{BEFC} = \bar{p}_{max}^i [1 - (x + y)] \tag{4.46}$$

Substituting the values of x and y into (4.46), the following expression of the area of the rectangle $BEFC$ is thus obtained

$$A_{BEFC} = \bar{p}_{max}^i \left[\frac{\delta_1\delta_2 + \gamma_t^i\delta_2 - \bar{p}_{max}^i\delta_2 + p_t^i\delta_1 - \bar{p}_{max}^i\delta_1}{\delta_1\delta_2} \right] \tag{4.47}$$

The area that represents the energy determined by the power curve $f_2^i(\gamma_t^i, p_t^i)$ is given by the sum of the areas previously determined:

$$f_2^i(\gamma_t^i, p_t^i) = \frac{-p_t^{i^2}\delta_1 - \gamma_t^{i^2}\delta_2 - \overline{p}_{max}^i{}^2\delta_1 - \overline{p}_{max}^i{}^2\delta_2 + 2\delta_1 p_t^i\overline{p}_{max}^i + 2\delta_2\gamma_t^i\overline{p}_{max}^i + 2\delta_1\delta_2\overline{p}_{max}^i}{2\delta_1\delta_2} \qquad (4.48)$$

A special case: bounding functions when the unit is off

When the unit i is off (e.g., $u_t^i = 0$), we should have that the total energy produced is equal to zero (e.g., $e_t^i = 0$). In order to obtain this result, the functions (4.43) e (4.48) must be written as follows, introducing the variable u_t^i:

$$f_1^i(\gamma_t^i, p_t^i) = \frac{p_t^{i^2}\delta_1 + \gamma_t^{i^2}\delta_2 + \overline{p}_{min}^i{}^2\delta_1 u_t^i + \overline{p}_{min}^i{}^2\delta_2 u_t^i - 2\delta_1 p_t^i\overline{p}_{min}^i - 2\delta_2\gamma_t^i\overline{p}_{min}^i + 2\delta_1\delta_2\overline{p}_{min}^i u_t^i}{2\delta_1\delta_2} \qquad (4.49)$$

$$f_2^i(\gamma_t^i, p_t^i) = \frac{-p_t^{i^2}\delta_1 - \gamma_t^{i^2}\delta_2 - \overline{p}_{max}^i{}^2\delta_1 u_t^i - \overline{p}_{max}^i{}^2\delta_2 u_t^i + 2\delta_1 p_t^i\overline{p}_{max}^i + 2\delta_2\gamma_t^i\overline{p}_{max}^i + 2\delta_1\delta_2\overline{p}_{max}^i u_t^i}{2\delta_1\delta_2} \qquad (4.50)$$

The constant terms of the constraints have been multiplied for the variable u_t^i, in order to consider them only when the unit is on, that is to say $u_t^i = 1$.

4.3 Results and discussion

In this section we describe and discuss the main results obtained with the new continuous models presented previously.

4.3.1 Simple continuous model

In order to analyze the behavior of the simple continuous model, different simulations over realistic instances have been made. The energy-based model described in section 4.1.1 (table (4.1)) and the simple continuous power-based model have been implemented in a C++ programming language code, and they have been solved with the CPLEX 11.0 commercial solver, using the perspective-cuts algorithm presented in [FG06]. A typical realistic instance consisting of 2 thermal units has been used as input to the two models. The results obtained in the simulation phase are shown in the figures 4.19 and 4.20. In the pictures, the blue and the red lines indicate the power produced by each thermal unit.

It is thus possible to observe the following interesting aspects:

- Fig. 4.19 shows that in a typical energy-based model power is constant in each time period and follows a step function; this is due to the basic assumptions of the model itself, as previously described in the initial part of this chapter;
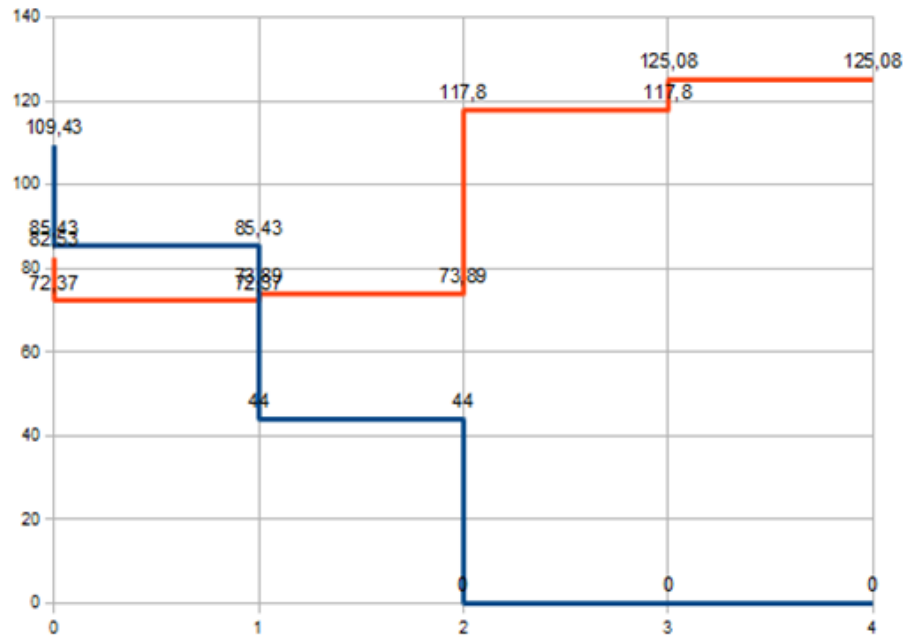
Figure 4.19: Standard energy-based model: simulation results.
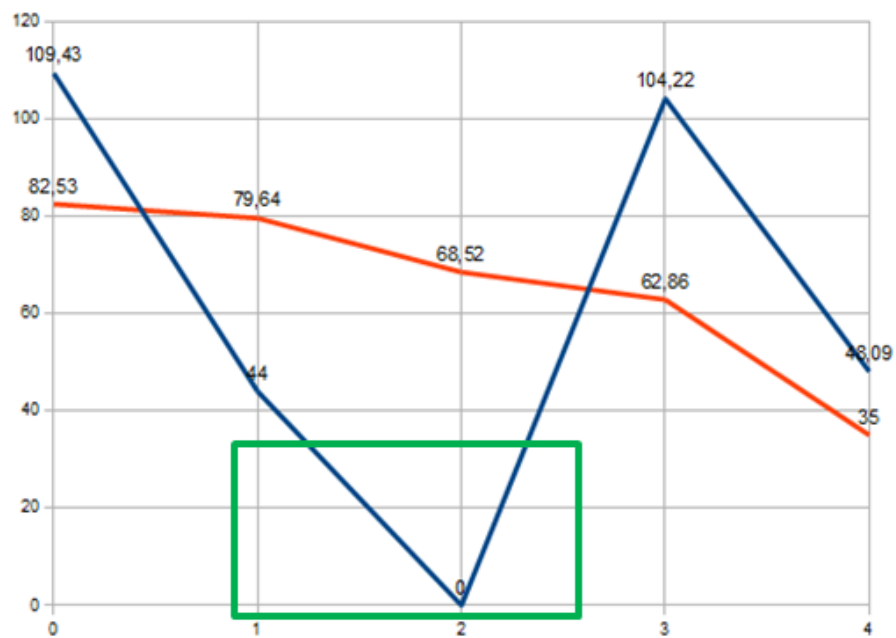

Figure 4.20: Simple continuous power-based model: simulation results.

- Fig. 4.20 shows that the simple continuous power based model is completely different from an energy-based model, because it models the operating behavior of the units from a realistic point of view. Furthermore, the figure demonstrates that the model has been correctly formulated, since it respects all the assumptions which is based on, that is to say, that all the generating units are always ramping linearly during each time period (the power output increases - or decreases - uniformly from p_{t-1}^i to p_t^i during all the time period t; if $p_{t-1}^i = p_t^i$, then the unit is not ramping);

- the simple continuous formulation presents some drawbacks, because, in some cases, the assumption that $\overline{u}^i = \overline{l}^i = \overline{p}_{min}^i$ it is not always verified, as shown in the green box of picture (4.20). In fact, a thermal unit does not always reaches $\overline{p}_{min}^i$ as its minimum power, but in some cases its power reaches 0 when it is shut down. For this reason, the simple continuous model, as it is formulated, does not cover this situation.

The issues previously mentioned motivate the necessity to formulate a more accurate power-based model, as described in the section 4.2.2.

4.3.2   Semi-continuous model

In order to analyze the behavior of the semi-continuous model, different simulations over realistic instances have been made. The semi-continuous power-based model described in section 4.2.2 has been implemented in a C++ programming language code, and it has been solved with the CPLEX 11.0 commercial solver, over a machine with standard computational characteristics. A typical realistic instance consisting of 2 thermal units has been used as input to the model. The results obtained in the simulation phase are shown in Fig. 4.21. In the picture, the blue and the red lines indicate the power produced by each thermal unit.

It is thus possible to observe the following interesting aspects:

- Fig. 4.21 shows that the semi-continuous power based formulation properly models the operating behavior of the units from a realistic point of view, since the cases in which the unit changes its status are correctly managed by using the auxiliary variable γ_t^i. Furthermore, the figure demonstrates that the model has been correctly formulated, since it respects the main assumption which is based on, that is to say, that all the generating units are always ramping linearly during each time period;

- however, it could be possible that the model forces the power trajectory to reach the maximum power output of the unit at the end of the current time period using a lower ramp rate than required, as shown in the green box of the picture (4.21);

- furthermore, even if the semi-continuous model realistically reflects the technical behavior of the generating units, it does not take into account the case when power trajectories are characterized by different ramp rates into the same time period.

These issues motivate the necessity to formulate a more accurate power-based model, that is an extension of the semi-continuous model, and that considers also the aspects mentioned above, as described in section 4.2.3.
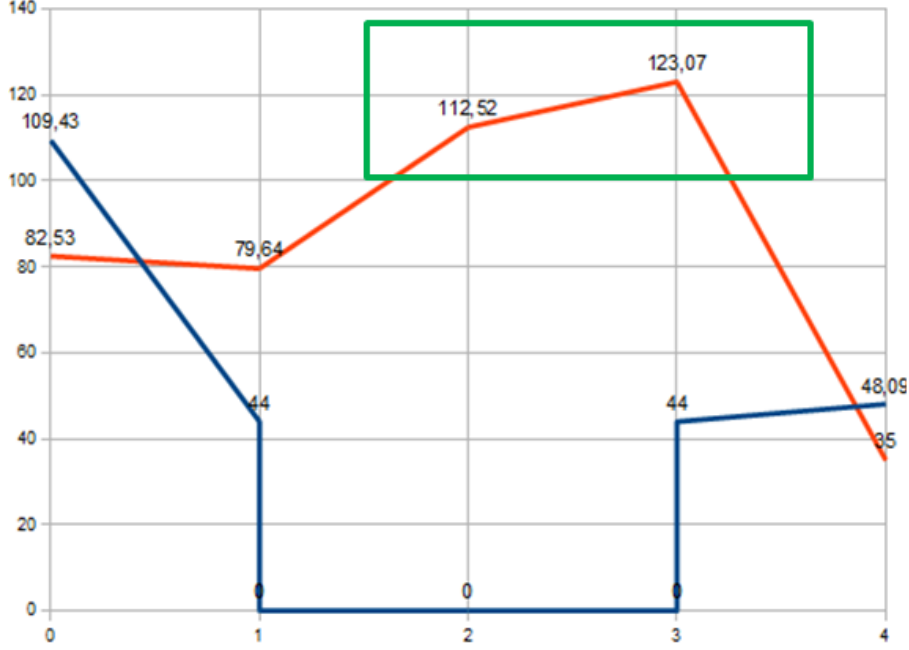
Figure 4.21: Semi-continuous power-based model: simulation results.

4.3.3 Two-sloped continuous model

The formulation of the two-sloped continuous model, previously described, presents some important aspects that make it a very interesting model from a mathematical point of view. This important results demonstrate that the model has been correctly formulated. This formulation is suitable to be easily solved by a MILP available commercial solver like CPLEX, due to its mathematical characteristics related with the convexity of the energy bounding functions. In fact, it is possible to notice that the bounding functions $f_1^i(\gamma_t^i, p_t^i)$ and $f_2^i(\gamma_t^i, p_t^i)$ of the energy e_t^i previously determined, represent respectively convex and concave functions, as expected.

Proposition 6 *The function $f_1^i(\gamma_t^i, p_t^i)$ is convex.*

Proof. In order to study the convexity of the function $f_1^i(\gamma_t^i, p_t^i)$, expressed by the (4.49), the first and second derivative functions have been calculated. For the sake of simplicity, the constant factor $\frac{1}{\delta_1 \delta_2}$ has been neglected.

The first derivative function, determined according to γ_t^i is expressed as follows

$$2\gamma_t^i \delta_2 - 2\delta_2 \bar{p}_{min}^i \tag{4.51}$$

which, derived again, is equal to $2\delta_2$.

The first derivative function, determined according to p_t^i is expressed as follows

$$2p_t^i \delta_1 - 2\delta_1 \bar{p}_{min}^i \tag{4.52}$$

which, derived again, is equal to $2\delta_1$.

The second derivative function, determined according to γ_t^i and p_t^i, is equal to zero.

The Hessian matrix of the function is expressed as follows

$$\mathcal{H}(f_1^i(\gamma_t^i, p_t^i)) = \begin{pmatrix} 2\delta_2 & 0 & 0 \\ 0 & 2\delta_1 & 0 \\ 0 & 0 & 0 \end{pmatrix}$$

The determinant of $\mathcal{H}(f_1^i(\gamma_t^i, p_t^i))$ is equal to 0. The eigenvalues of the matrix are $\lambda_1 = 2\delta_1$, $\lambda_2 = 2\delta_2$, $\lambda_3 = 0$, that are not negative. For this reason, the Hessian matrix $\mathcal{H}(f_1^i(\gamma_t^i, p_t^i))$ is positive semidefinite, so it is possible to affirm that the function $f_1^i(\gamma_t^i, p_t^i)$ is convex. ∎

Proposition 7 *The function $f_2^i(\gamma_t^i, p_t^i)$ is concave.*

Proof. In order to study the convexity of the function $f_2^i(\gamma_t^i, p_t^i)$, expressed by (4.50), the first and second derivative functions have been calculated. For the sake of simplicity, the constant factor $\frac{1}{\delta_1 \delta_2}$ has been neglected.

The first derivative function, calculated according to γ_t^i is expressed as follows

$$- 2\gamma_t^i \delta_2 + 2\delta_2 \bar{p}_{max}^i \tag{4.53}$$

which, derived again, is equal to $-2\delta_2$.

The first derivative function, calculated according to p_t^i is expressed as follows

$$- 2p_t^i \delta_1 + 2\delta_1 \bar{p}_{max}^i \tag{4.54}$$

which, derived again, is equal to $-2\delta_1$.

The second derivative function, calculated according to γ_t^i and p_t^i, is equal to zero.

The Hessian matrix of the function is expressed as follows

$$\mathcal{H}(f_2^i(\gamma_t^i, p_t^i)) = \begin{pmatrix} -2\delta_2 & 0 & 0 \\ 0 & -2\delta_1 & 0 \\ 0 & 0 & 0 \end{pmatrix}$$

The determinant of $\mathcal{H}(f_2^i(\gamma_t^i, p_t^i))$ is equal to 0. The eigenvalues of the matrix are $\lambda_1 = -2\delta_1$, $\lambda_2 = -2\delta_2$, $\lambda_3 = 0$, which are less or equal to zero. For this reason, the Hessian matrix $\mathcal{H}(f_2^i(\gamma_t^i, p_t^i))$ is negative semidefinite, so it is possible to affirm that the function $f_2^i(\gamma_t^i, p_t^i)$ is concave. ∎

4.4   Conclusions

In this chapter, new power-based continuous models for the UC problem have been proposed, in order to overcome the drawbacks of the energy-based discontinuous models, defining more realistic mathematical formulations than the ones proposed in the literature. In particular, new Mixed-Integer Quadratic Programming (MIQP) models for UC have been proposed, where decision variables represent the power levels instead of energy.

Different types of power-based models have been proposed, like simple continuous, semi-continuous and two-sloped continuous models. The basic assumption of these models is that the unit is always ramping linearly during each time period. This means that the power increases

-or decreases- uniformly from p_{t-1} to p_t during all the period. These assumptions make it possible that these new formulations properly reflect the actual technical and operating behavior of the generating units, in contrast to what happens in the energy-based models presented in the literature.

Simulations results have shown that in the proposed models the trajectories of power p constructed by the model and the energy decisions are surely feasible, since the physical constraints on power are directly modeled. Furthermore, even if these formulations require to use more constraints and more variables, the resulting MIQP problems can be easily solved at optimality with commercial solvers, like CPLEX, exploiting their mathematical characteristics.

As far as future work is concerned, it could be very interesting to compare the solutions obtained with an energy-based discontinuous UC model integrated with the RED formulation (presented in chapter 5) and the new continuous power-based models proposed in our research activities, in order to demonstrate that the continuous models better reflect the real behavior of the generating units, since they are based on novel assumptions that have been neglected in the literature so far.

Chapter 5

Unit Commitment models integrated with Economic Dispatch

As described in the previous chapters, electrical energy production is a complex activity, which requires to co-ordinate the operations of many geographically distributed generating units in order to satisfy a continuously varying power demand. Furthermore, the introduction of deregulated energy markets has deeply changed the form of the problem, introducing the trading of power energy in the day-ahead market between several independent and competing generation companies (Gencos). Some years ago there was a single centralized system coordinating all the generating units, now we have a distributed decision process: each Genco offers specific quantities of energy at some definite prices for each hour of the next day. An Independent Market Operator (IMO) acts as clearing house to reconcile all the transactions, minimizing the total user cost for the satisfied power demand while taking into account technical and security constraints, mostly regarding the interconnection network. Thus, a Genco must be able to optimize the use of its generating units to be competitive in that market, this requires to solve a sequence of complex optimization problems at various stages of this process.

Gencos have to schedule their generating units based on IMO inputs at the end of the bidding process, in this stage Unit Commitment (UC) problem is applied. As described previously, the objective of the (UC) is to optimally schedule a set of generating units over a given time horizon (typically one day or one week), in order to satisfy a forecast energy demand at minimum total operational cost or at the maximum total profit, satisfying the technical restrictions of the generating units, that depend on their type and characteristics. In the adjustment market Gencos can modify the programs defined in the day-ahead market, performing other transactions of electrical energy, in this stage Economic Dispatch (ED) is applied. The scope of ED is to properly determine the amount of power that each scheduled unit has to produce in order to satisfy the real-time demand, in the short-term period (minutes or hours).

In the day-ahead market UC solves a problem where demand and power are continuous only in the time interval, this means that the power variation is concentrated passing from a time interval to the following (see Chapter 2). Given the UC solution, we know the units that will be committed in the day-after and the energy that each unit must generate in each time interval, but

the power trajectory of each time interval is not defined.

For these reasons, we have defined a novel mathematical formulation for the UC integrated with the ED, called *Reduced Economic Dispatch* (RED), in order to obtain more realistic solutions for this problem. The objective of the RED problem is to refine the UC solution, individuating the power trajectory that each unit must generate in a given time sub-interval belonging to an assigned time interval. RED solves a problem where demand has been processed to be continuous in all time horizon, using a power demand as input instead of energy demand. Units that are committed are known, while the variable to be considered is the power generated in a given time sub-interval, instead of the power-mean-value in a given time interval.

In this chapter we present a sampling technique to reduce energy demand profile in a finer grid; hence we illustrate the detailed formulation of our RED models; finally we present simulation results of the various RED models we have defined and we outline the conclusions.

5.1 Sampling the energy demand profile over a finer time grid

Generally, the actual energy demand profile that the ED problem has to resolve is different from the forecast demand one, which is utilized to solve the UC problem in the day-ahead-market. In the RED model, the actual demand is generated applying a casual perturbation of the load distribution to the forecast demand. This is a simulation technique that will allow us to better compare the accuracy of the different RED models proposed.

In this section, the problem of sampling the energy demand profile and its correct formulation is treated. This will be made considering the following three steps:

1. the subdivision of the energy demand into regular time intervals;

2. the transformation of the energy demand into power demand;

3. the transformation of the power demand into energy demand over a finer time grid (sampling).

In order to define the RED model, the energy demand profile has been divided into regular time intervals, then energy demand has been transformed into power demand which has been processed to sample an energy demand profile over a finer time grid (generally 15 minutes). Finally, the RED problem has been solved considering this energy demand profile, for given input data whose UC solution is known. The algorithm utilized to properly solve the RED problem can be described by the following steps:

1. given input data with i thermal units and j hydro units and given a forecast energy demand profile (d_t) in the time horizon $\mathcal{T}$, the corresponding UC problem is solved;

2. the given forecast energy demand profile (d_t) in a time interval t is divided into Λ demands [1] in the time interval t, applying a quadratic interpolation between d_{t-1} and d_{t+1};

3. each λ energy demand profile is processed into a continuous power demand profile, utilizing a division into K intervals [2];

---

[1] In our simulations, we assume $\Lambda = 2$, if we consider $t = 1$ hour we have two demand profiles in a 30 minutes time horizon.

[2] In our simulations, we assume $K = 30$, if we consider $t = 1$ hour and $\Lambda = 2$ we have power demands in each minute.

4. time interval t is divided into M time sub-intervals [3], so that power demand obtained at the previous step can be divided in order to have a corresponding energy demand for each time sub-interval m;

5. given this energy demand profile, and knowing the characteristics of each unit (unit state and ramping constraints), the RED problem is solved. In that way, we can individuate the power that each (thermal and hydro) unit must generate at the end of each time sub-interval m, assuming a linear variation in m.

The RED problem has been solved considering a finer time grid, since our objective is to determine the power that has to be generated by the units during the time interval t. For this reason, it's necessary to determine an energy demand profile over a finer time grid, where the time sub-interval $m < t$, considering an actual demand profile generated with a casual variation of forecast demand.

The new demand profile is thus determined considering the following steps:

1. division of the energy demand d_t of time interval t into Λ energy demands d_t^λ;

2. transformation of the energy demand d_t^λ into power demand $d_{t,k}^\lambda$ in K time intervals;

3. transformation of the power demand $d_{t,k}^\lambda$ into energy demand $d_{t,m}$ in M time sub-intervals.

5.1.1   Step 1: division of the energy demand over a finer time grid

For each time interval t, the energy demand d_t is divided into Λ demands d_t^λ considering a quadratic interpolation algorithm, with the condition:

$$\sum_\lambda d_t^\lambda = d_t \quad \text{con } 1 \leq \lambda \leq \Lambda \tag{5.1}$$

In particular, given the energy demand profile, in which we assume power to be constant in time interval t, we can use a parabolic function of type $y(x) = ax^2 + bx + c$ which passes through the three points A, B, C as depicted in picture 5.1 (in the case $\Lambda = 2$):

$$
\begin{aligned}
A &: \quad (-1, d_{t-1}) \quad 1 < t < \mathcal{T} & \text{(5.2)} \\
B &: \quad (0, d_t) & \text{(5.3)} \\
C &: \quad (+1, d_{t+1}) & \text{(5.4)} \\
\text{if } t &= 1 \rightarrow d_{t-1} = d_{t,0} & \text{(5.5)} \\
\text{if } t &= \mathcal{T} \rightarrow d_{t+1} = d_t & \text{(5.6)}
\end{aligned}
$$

In this way, powers which are constant in time interval t are associated with the values of the parabolic function corresponding to the central coordinate of the interval, so we have:

$$
\begin{aligned}
a &= \frac{1}{2}(d_{t+1} + d_{t-1}) - d_t & \text{(5.7)} \\
b &= \frac{1}{2}(d_{t+1} - d_{t-1}) & \text{(5.8)} \\
c &= d_t & \text{(5.9)}
\end{aligned}
$$

---

[3]In our simulations, we assume $M = 4$, if we consider $t = 1$ hour we can have a 15 minutes energy demand profile.
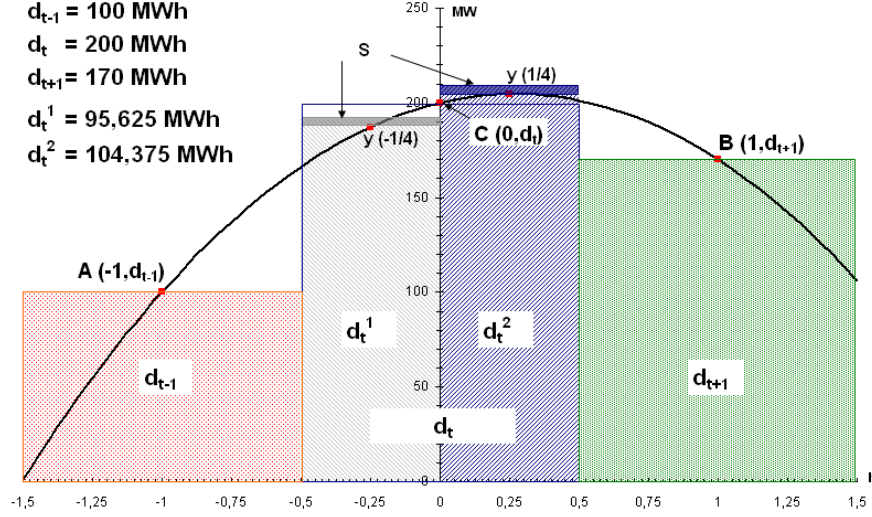
Figure 5.1: Demand quadratical approximation using a parabolic function.

Demand to be divided, in this representation, is related to an energy associated to a power which is constant in the interval $-1/2 < x < 1/2$. The values of the heights of the Λ rectangles in which the demand is divided are equal to the values of the parabolic function corresponding to particular coordinates x. These coordinates can be chosen in an arbitrary way; in our model, we individuate them as the mean point of the basis of the λ rectangle, considering the value $-1/2$.

With these assumptions, the energy demand to be divided can be represented by Λ rectangles with a height equal to $y(x)$ and a basis equal to $1/\Lambda$, i.e.:

$$x \;=\; x_0 + (\lambda - 1)\frac{1}{\Lambda} \qquad \text{con } -\tfrac{1}{2} < x < \tfrac{1}{2} \tag{5.10}$$

$$x_0 \;=\; -\frac{1}{2} + \frac{1}{2\Lambda} \tag{5.11}$$

$$\widetilde{d}_t^{\lambda} \;=\; \frac{y(x)}{\Lambda} \qquad \text{con } 1 \le \lambda \le \Lambda \tag{5.12}$$

For instance, if $\Lambda = 2$ (standard case) we have

$$\widetilde{d}_t^{1} \;=\; \frac{y(-\frac{1}{4})}{\Lambda} \tag{5.13}$$

$$\widetilde{d}_t^{2} \;=\; \frac{y(\frac{1}{4})}{\Lambda} \tag{5.14}$$

To respect the condition $\sum_\lambda d_t^\lambda = d_t$ we calculate the difference S between the sum of the values determined by the parabolic approximation and the demand to be divided. Then, the difference S is divided in a uniform way:

$$S = d_t - \sum_{\lambda} \widetilde{d_t^{\lambda}} \tag{5.15}$$

$$d_t^{\lambda} = \widetilde{d_t^{\lambda}} + S/\Lambda = \frac{y(x) + S}{\Lambda} \tag{5.16}$$

With this formulation the parabolic function always exists even if $d_{t-1} = d_t$, $d_t = d_{t+1}$ and $\Lambda = 1$.

5.1.2 Step 2: transformation of the energy demand into power demand

It's possible to process the energy demand d_t^{λ}, determined at the previous step, into a power demand profile $d_{t,k}^{\lambda}$ considering K intervals. This can be made considering a first order approximation, with two modalities with a different physical meaning, but with an equivalent mathematical formulation:

1. approximation of the demand profile considering trapezoidal shapes;

2. approximation of the demand profile considering rectangles.

Determining the power demand: case of trapezoidal shapes Consider a generic power distribution $d_{t,k}$ [MW] in the time interval of duration $\widehat{f_h} = \frac{f_h}{\Lambda}$ (measured in hours), in which is admitted only a point of variation of the slope at time x (Figure 5.2). The power distribution can be discretized into K intervals of trapezoidal shape so that energy d_t [MWh] can be expressed as follows: [4]

$$d_t = \frac{(d_{t,0} + d_{t,x})}{2} x \frac{f_h}{\Lambda K} + \frac{(d_{t,x} + d_{t,K})}{2} (K - x) \frac{f_h}{\Lambda K} \tag{5.17}$$

Considered

$$d_{t,0} = \sum_i p_0^i \quad i \in \mathcal{P} \quad p_0^i \text{ initial power generated by thermal unit } i \tag{5.18}$$

$$d_{t,x} = d_{t,0} + x\Gamma^+ \tag{5.19}$$

$$d_{t,K} = d_{t,x} + (K - x)\Gamma^- = d_{t,0} + x\Gamma^+ + (K - x)\Gamma^- \tag{5.20}$$

By the substitution of the previous equations in (5.17), we obtain the generic expression from which it's possible to calculate the values Γ^- and Γ^+, given x, d_t and the initial power condition $d_{t,0}$:

$$\Gamma^- \left(x^2 - 2Kx + K^2\right) - \Gamma^+ \left(x^2 - 2Kx\right) + 2K \left(d_{t,0} - d_t \frac{\Lambda}{f_h}\right) = 0 \tag{5.21}$$

---

[4]For the sake of simplicity in the notation we consider d_t instead of the generic demand d_t^{λ} to which the algorithm is actually applied.
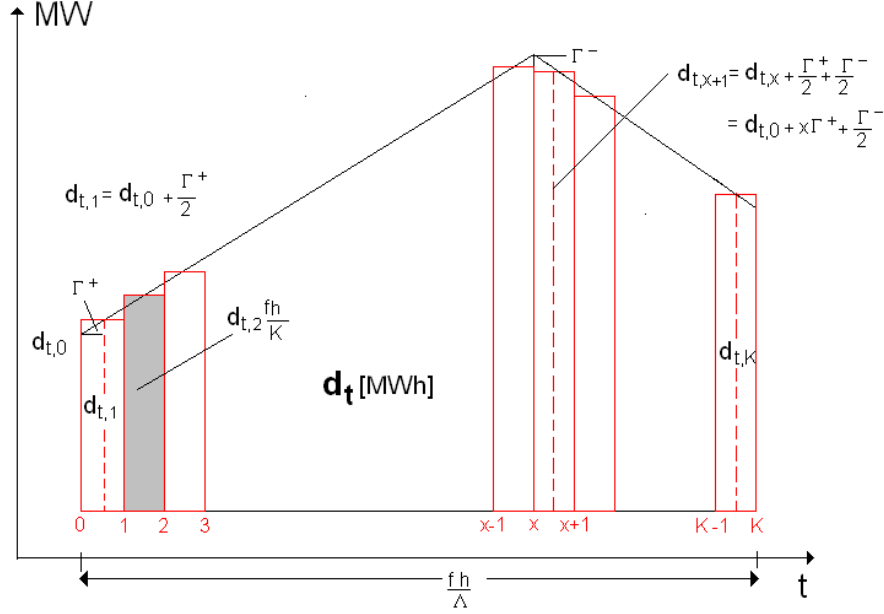
Figure 5.2: Power distribution using trapezoidal intervals.

Determining the power demand: case of rectangles   Consider a generic power distribution $d_{t,k}$ [MW] in the time interval of duration $\widehat{f_h} = \frac{f_h}{\Lambda}$ (measured in hours), in which only a point of variation of the slope is admitted in time x (Figure 5.3). The power distribution can be discretized into K intervals with rectangular shape so that the energy d_t [MWh] can be expressed as follows:
[5]
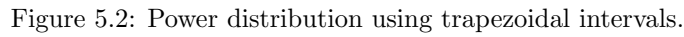
$$d_t = \sum_{k=1}^{K} d_{t,k} \frac{f_h}{\Lambda K} \quad t \in \mathcal{T} \tag{5.22}$$

Considering the case shown in the picture, generally we can have two time intervals:

$$d_t^+ = \sum_{k=1}^{x} d_{t,k} \frac{f_h}{\Lambda K} \qquad \text{time interval to the left of } x \tag{5.23}$$

$$d_t^- = \sum_{k=1}^{K-x} d_{t,x+k} \frac{f_h}{\Lambda K} \qquad \text{time interval to the right of } x \tag{5.24}$$

$$d_t = d_t^+ + d_t^- \tag{5.25}$$

---

[5]For the sake of simplicity in the notation we consider d_t instead of the generic demand d_t^λ, to which the algorithm is actually applied.

Figure 5.3: Power distribution using centered intervals.

Considered

$$d_{t,0} = \sum_i p_0^i \quad i \in \mathcal{P} \; p_0^i \text{ initial power generated by thermal unit } i \tag{5.26}$$

$$d_{t,1} = d_{t,0} + \frac{\Gamma^+}{2} \tag{5.27}$$

$$d_{t,x} = d_{t,1} + (x-1)\Gamma^+ = d_0 + x\Gamma^+ - \frac{\Gamma^+}{2} \tag{5.28}$$

$$d_{t,x+1} = d_{t,x} + \frac{\Gamma^+}{2} + \frac{\Gamma^-}{2} = d_{t,0} + x\Gamma^+ + \frac{\Gamma^-}{2} \tag{5.29}$$

By the substitution of the previous equations respectively in (5.23) and in (5.24), we have:

$$d_t^+ = \frac{f_h}{\Lambda K}\left[d_{t,1}x + \Gamma^+ \sum_{k=1}^{x-1}(x-k)\right] = \frac{f_h}{\Lambda K}\left[d_{t,0}x + \frac{\Gamma^+}{2}x^2\right] \tag{5.30}$$

$$d_t^- = \frac{f_h}{\Lambda K}\left[d_{t,x+1}(K-x) + \Gamma^- \sum_{k=1}^{K-x-1}(K-x-n)\right] = \tag{5.31}$$

$$= \frac{f_h}{\Lambda K}\left[d_{t,x+1}(K-x) + \frac{\Gamma^-}{2}\left[(K-x)^2 - (K-x)\right]\right] \tag{5.32}$$

By the substitution of the previous expressions in the balance condition (5.25), we obtain the generic expression by which it's possible to calculate the values Γ^- and Γ^+, given x, d_t and the

initial condition $d_{t,0}$:

$$\Gamma^- \left(x^2 - 2Kx + K^2\right) - \Gamma^+ \left(x^2 - 2Kx\right) + 2K \left(d_{t,0} - d_t \frac{\Lambda}{f_h}\right) = 0 \qquad (5.33)$$

Note that (5.33) is equal to (5.21).

Analysis of the possible profiles of power demand   As we explained above, an energy demand profile can be divided in a generic way by (5.21) or (5.33), regardless to the type of processing chosen (with trapezoidal shapes or rectangles), given:

- a possible point of variation of the slope x;
- the energy demand to be satisfied d_t;
- the initial power condition $d_{t,0}$.

To analyze the possible demand profiles we define:

$$\delta = \frac{\Gamma^-}{\Gamma^+}$$

By the substitution of δ in (5.21) or (5.33) we obtain the definitive expression

$$\Gamma^+ \left[(\delta - 1)\left(x^2 - 2Kx\right) + K^2\delta\right] + 2K\left(d_{t,0} - d_t\frac{\Lambda}{f_h}\right) = 0 \qquad (5.34)$$

Chosen arbitrarily a coordinate of variation of slope x and a value of δ, we can have

$$\Gamma^+ = 2K \frac{\left(d_0 - d_t\frac{\Lambda}{f_h}\right)}{(\delta - 1)\left(x^2 - 2Kx\right) + K^2\delta} = 0 \qquad (5.35)$$

For both formulations (with trapezoidal shapes or rectangles), considering δ, we obtain the cases shown in Fig. 5.4 and 5.5 and explained below:

1. $\delta = 1 \to \Gamma^- = \Gamma^+$: increasing/decreasing power demand profile slope:

$$\Gamma^+ = \frac{2}{K}\left(d_t\frac{\Lambda}{f_h} - d_{t,0}\right)$$

   (a) If $d_t\frac{\Lambda}{f_h} - d_{t,0} > 0 \to \Gamma^+ > 0$ increasing power demand profile slope (Figure 5.6)

   (b) If $d_t\frac{\Lambda}{f_h} - d_{t,0} < 0 \to \Gamma^+ < 0$ decreasing power demand profile slope (Figure 5.7)

2. $\delta = 0 \to \Gamma^- = 0$: increasing/decreasing and then constant power demand profile slope

$$\Gamma^+ = 2K\frac{d_t\frac{\Lambda}{f_h} - d_{t,0}}{(2Kx - x^2)}$$

   The sign of Γ^+ depends only on $d_t\frac{\Lambda}{f_h} - d_{t,0}$ because denominator is always positive for $0 < x < K$
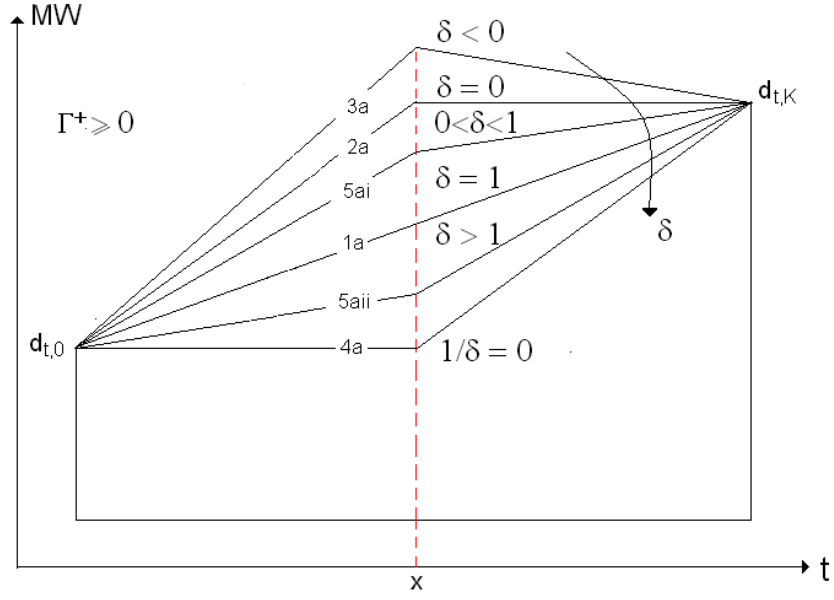
Figure 5.4: Representation of cases when $\Gamma^+ \geq 0$.
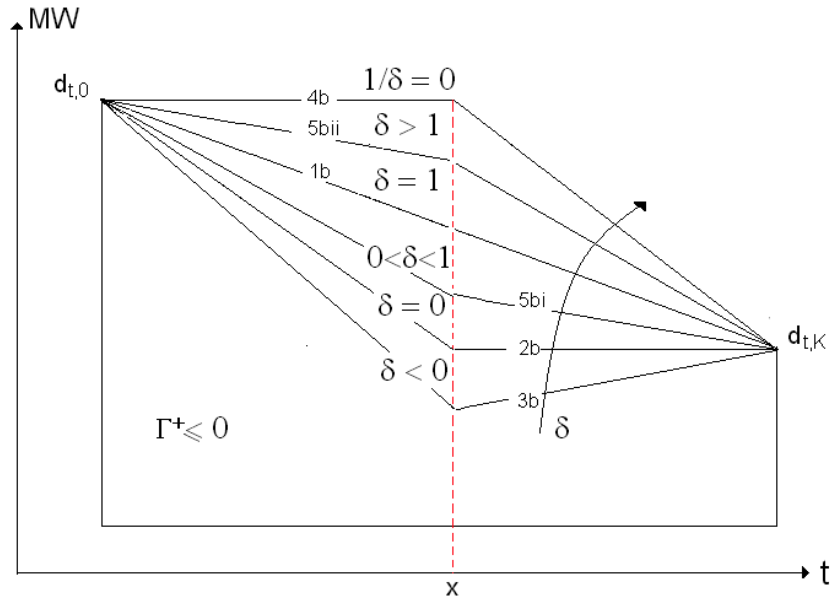
Figure 5.5: Representation of cases when $\Gamma^+ \leq 0$.

(a) if $d_t \frac{\Lambda}{f_h} - d_{t,0} > 0 \rightarrow \Gamma^+ > 0$ increasing and then constant power demand profile slope; (Figure 5.8)

(b) if $d_t \frac{\Lambda}{f_h} - d_{t,0} < 0 \rightarrow \Gamma^+ < 0$ decreasing and then constant power demand profile slope; (Figure 5.9)

3. $\delta < 0$: increasing (decreasing) and then decreasing (increasing) power demand profile slope:

   (a) $\delta < 0 \rightarrow \Gamma^+ > 0; \Gamma^- < 0$ increasing and then decreasing power demand profile slope (Figure 5.10);

   (b) $\delta < 0 \rightarrow \Gamma^+ < 0; \Gamma^- > 0$ decreasing and then increasing power demand profile slope (Figure 5.11);

4. $\frac{1}{\delta} = 0 \rightarrow \delta = \infty \rightarrow \Gamma^+ = 0$: constant and then increasing (or decreasing) power demand profile slope

$$\Gamma^- = 2K \frac{d_t \frac{\Lambda}{f_h} - d_{t,0}}{(x - K)^2}$$

   The sign of Γ^- depends only on $d_t \frac{\Lambda}{f_h} - d_{t,0}$ since denominator is always positive.

   (a) if $d_t \frac{\Lambda}{f_h} - d_{t,0} > 0 \rightarrow \Gamma^- > 0$ constant and then increasing power demand profile slope (Figure 5.12);

   (b) if $d_t \frac{\Lambda}{f_h} - d_{t,0} < 0 \rightarrow \Gamma^- < 0$ constant and then decreasing power demand profile slope (Figure 5.13);

5. $0 < \delta < 1$ o $\delta > 1$: increasing (or decreasing) power demand profile with two slopes

   (a) If $d_t \frac{\Lambda}{f_h} - d_{t,0} > 0$

      i. $0 < \delta < 1 \rightarrow \Gamma^+ > 0; \Gamma^+ > \Gamma^-$ increasing power demand profile slope with decreasing slope in the second part (Figure 5.14);

      ii. $\delta > 1 \rightarrow \Gamma^+ > 0; \Gamma^+ < \Gamma^-$ increasing power demand profile slope with increasing slope in the second part (Figure 5.15);

   (b) If $d_t \frac{\Lambda}{f_h} - d_{t,0} < 0$

      i. $0 < \delta < 1 \rightarrow \Gamma^+ < 0; \Gamma^+ < \Gamma^-$ decreasing power demand profile slope with decreasing slope in the second part (Figure 5.16);

      ii. $\delta > 1 \rightarrow \Gamma^+ < 0; \Gamma^+ > \Gamma^-$ decreasing power demand profile slope with increasing slope in the second part (Figure 5.17);

5.1.3 Step 3: transformation of the power demand into energy demand over a finer time grid

As explained above, RED problem works on a finer time grid, characterized by a time sub-interval m. Summarizing:

- a time interval t has a duration f_h (measured as a fraction of hour);
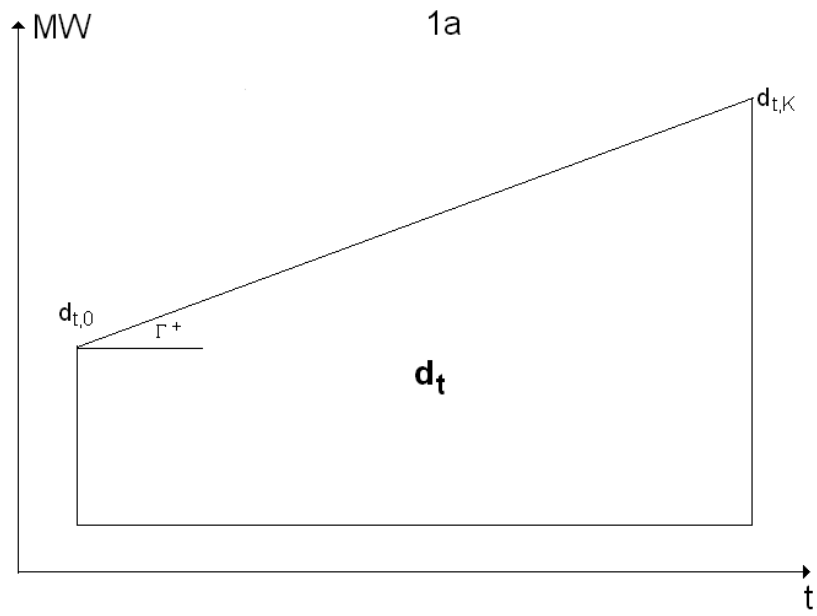
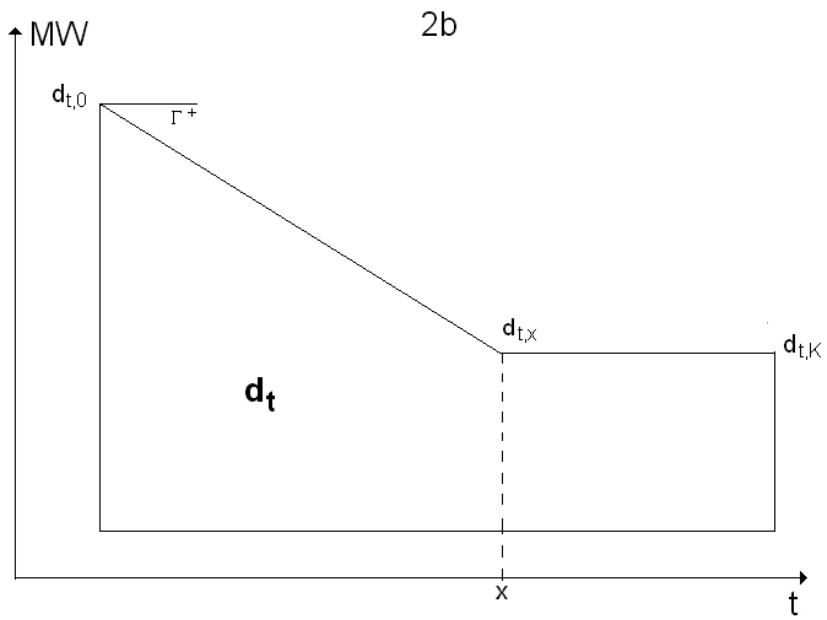Figure 5.6: Case 1a.
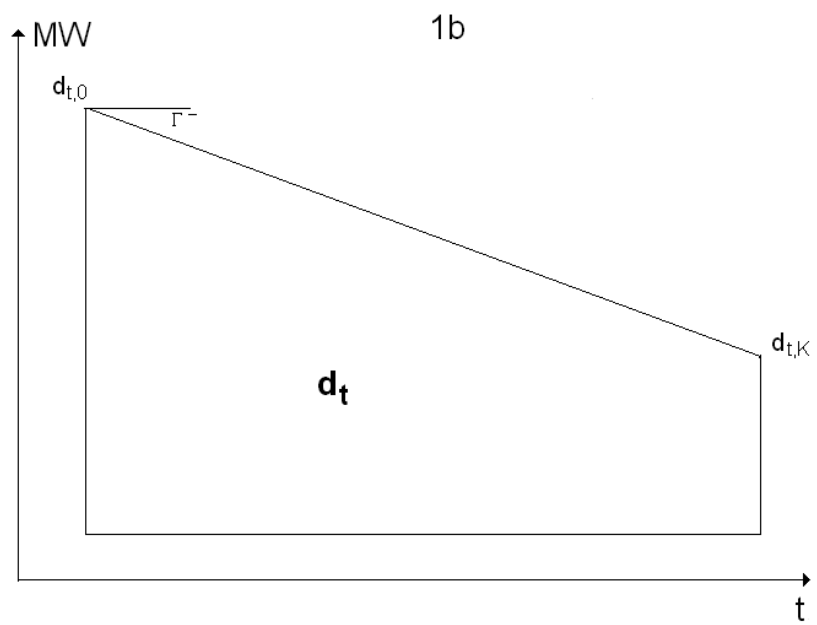
Figure 5.7: Case 1b.
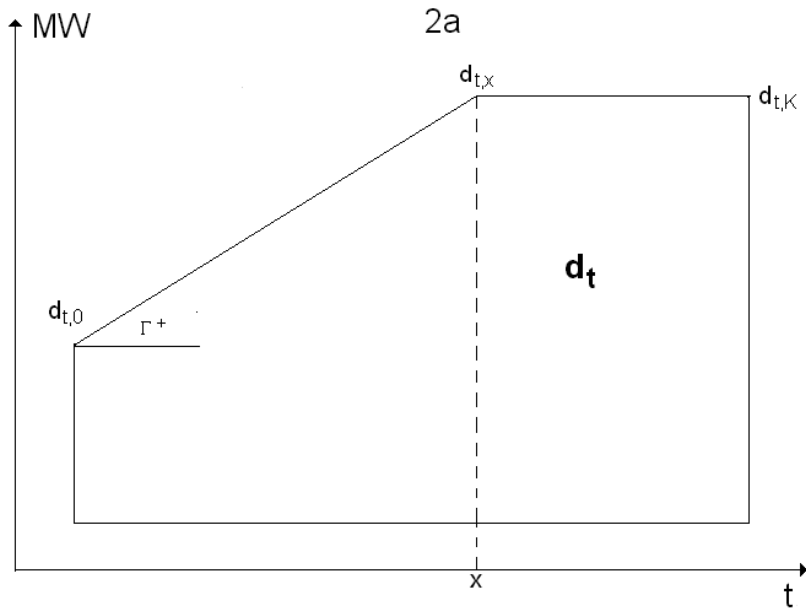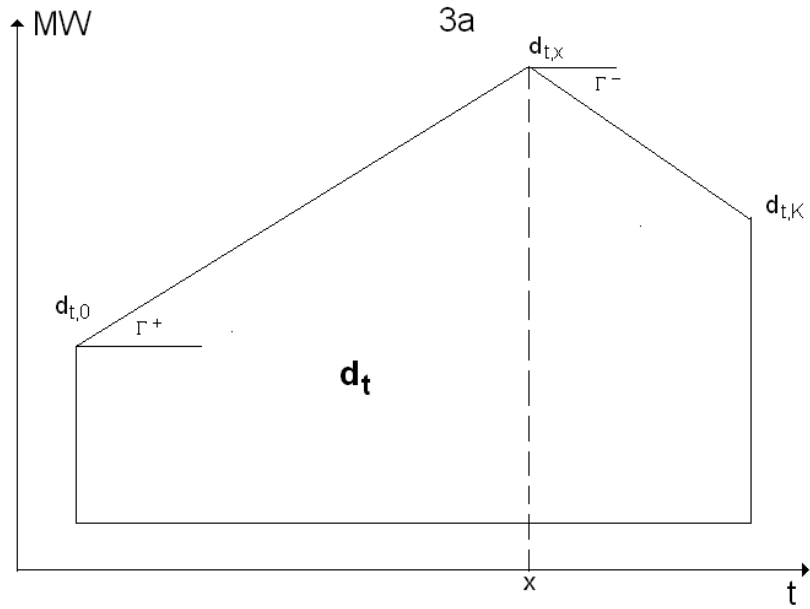
Figure 5.8: Case 2a.
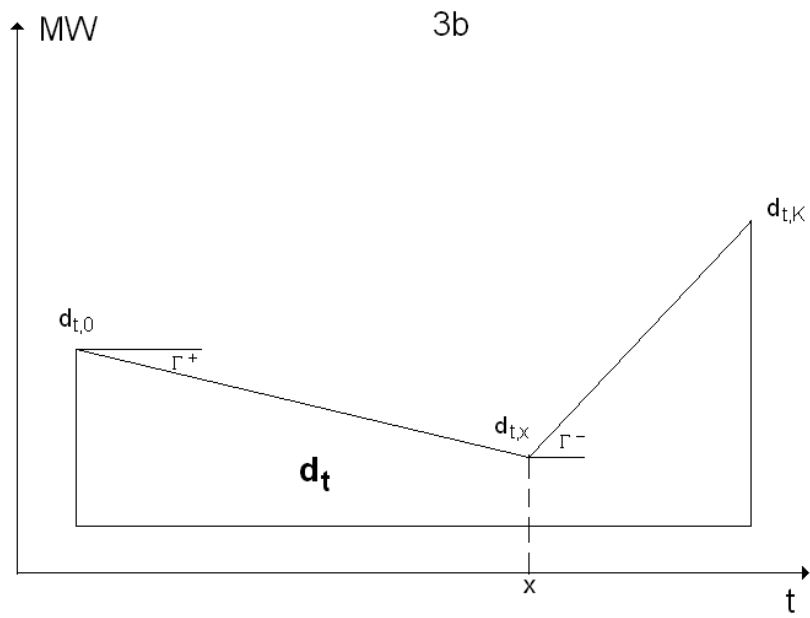

Figure 5.9: Case 2b.

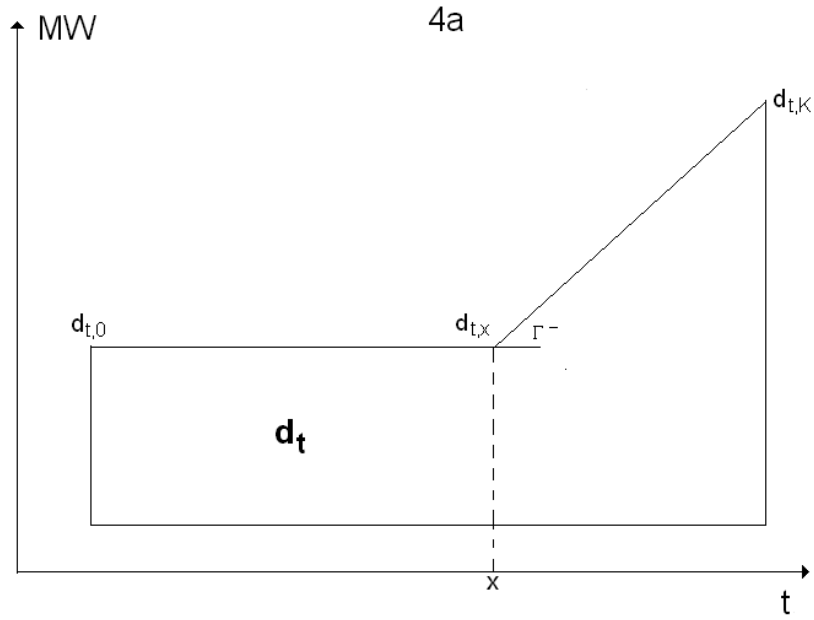Figure 5.10: Case 3a.

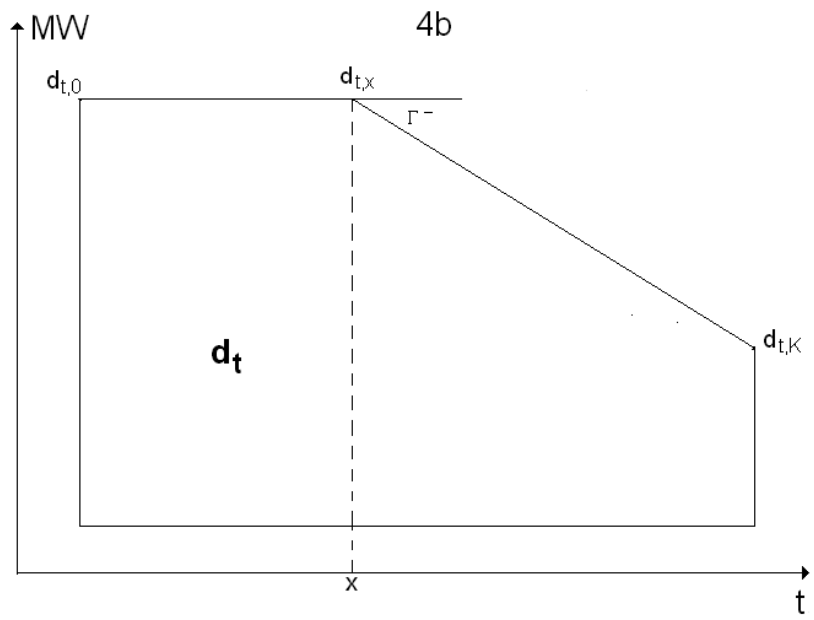Figure 5.11: Case 3b.

Figure 5.12: Case 4a.
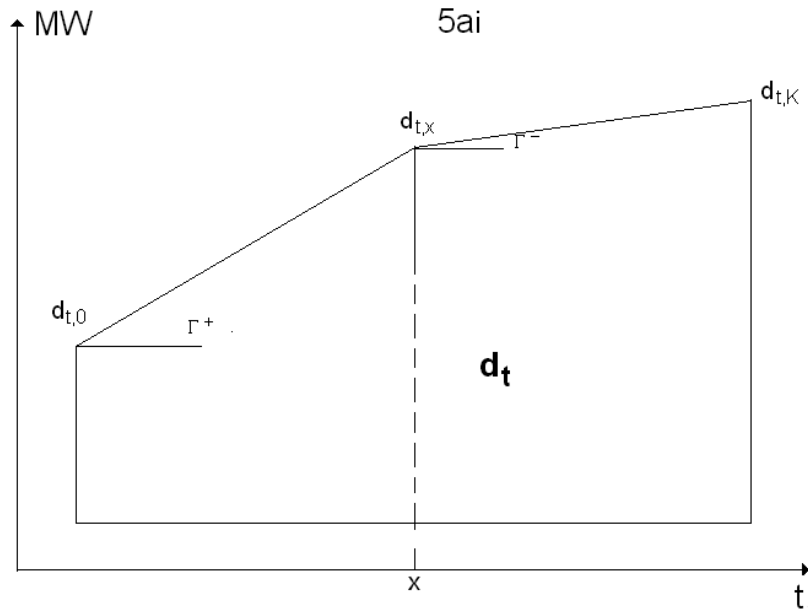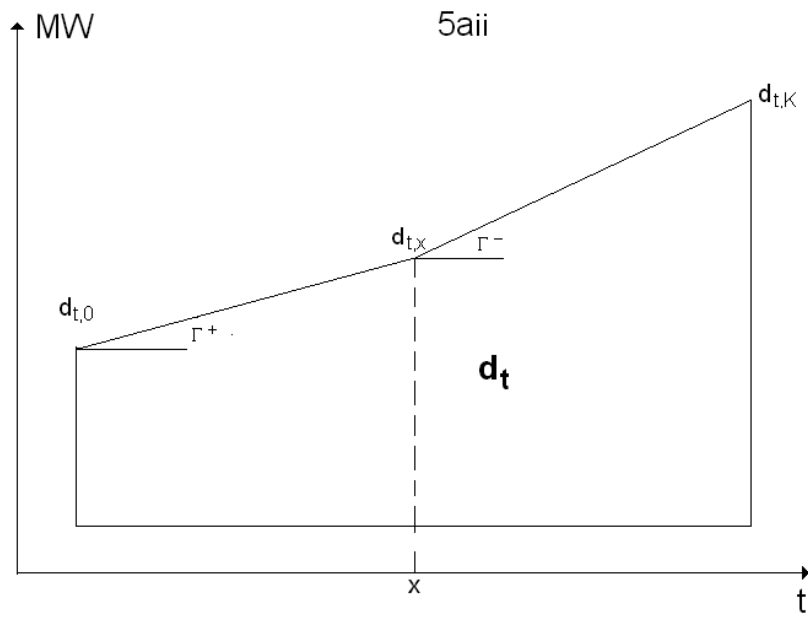

Figure 5.13: Case 4b.
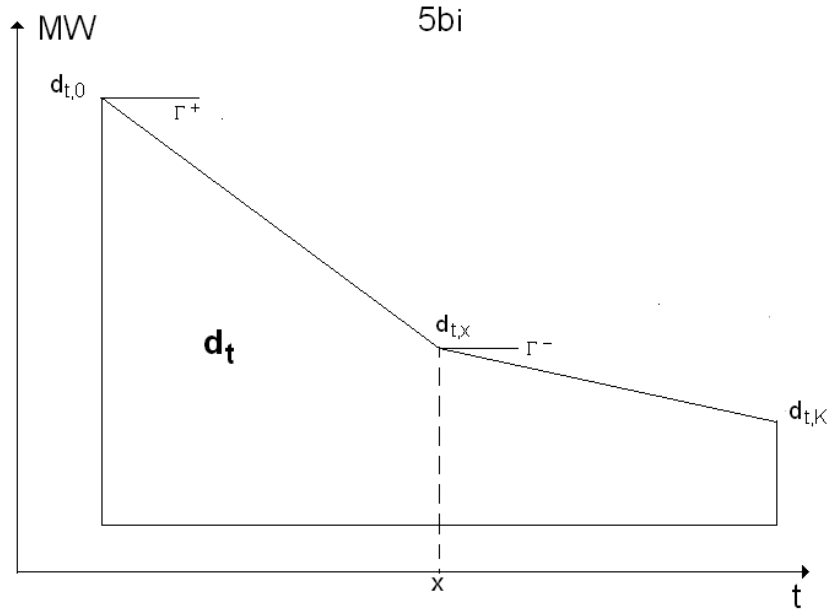
Figure 5.14: Case 5ai.

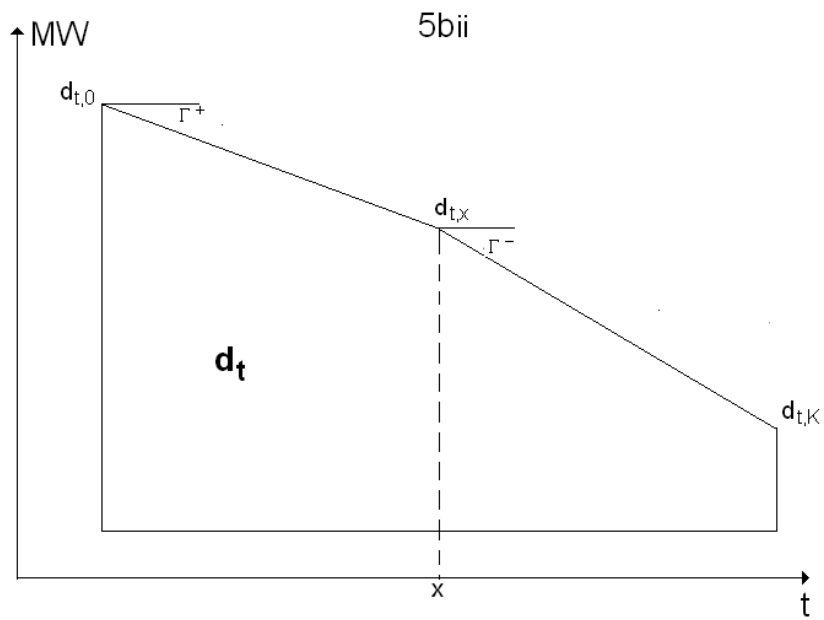Figure 5.15: Case 5aii.

Figure 5.16: Case 5bi.

Figure 5.17: Case 5bii.

- at step 1, each time interval t is divided into Λ sub-intervals of duration $\frac{f_h}{\Lambda}$ (measured as a fraction of hour) to which an energy demand d_t^λ is associated;

- at step 2, each time interval λ is divided into K sub-intervals of duration $\frac{f_h}{\Lambda K}$ (measured as a fraction of hour) to which a power demand $d_{t,k}^\lambda$ is associated;

- at step 3, each time interval t is divided into M time sub-intervals of duration $\frac{f_h}{M}$ (measured as a fraction of hour) to which an energy demand $\overline{d}_{t,m}$ is associated. The m time sub-interval has a duration of $\frac{f_h}{M}\Lambda K$, expressed as a number of k intervals.

In order to determine the energy demand $\overline{d}_{t,m}$ at time m it's necessary to consider the $R = \frac{f_h}{M}\Lambda K$ power demand $d_{t,k}^\lambda$ into which the demand d_t^λ has been divided. According to the different method adopted (with trapezoidal shapes or with rectangles) we obtain the following formulations:

$$\overline{d}_{t,m} \quad = \quad \sum_{k=(m-1)R+1}^{mR} \overline{d}_{t,k}\frac{f_h}{\Lambda K} \quad 1 \le k \le K, \quad 1 \le m \le M \tag{5.36}$$

$$\overline{d}_{t,m} \quad = \quad \sum_{k=(m-1)R+1}^{mR} \frac{d_{t,k-1}+d_{t,k}}{2}\frac{f_h}{\Lambda K} \quad 1 \le k \le K, \quad 1 \le m \le M \tag{5.37}$$

5.2 Reduced Economic Dispatch problem for thermal units with ramping constraints

In this section we will explain the *Reduced Economic Dispatch* (RED) problem formulation for thermal units considering ramping constraints. Given the solution of the UC problem, we know the units that are on in each time interval t and the mean values of powers to be generated by each unit in t.

Consider a set $\mathcal{P}$ of thermal units in $\mathcal{T} = \{1, \ldots, T\}$, set of time periods which define the time horizon. We indicate with d_t the energy demand to be satisfied in each time interval t. $\mathcal{M} = \{1, \ldots, M\}$ is the set of time intervals into which time interval t is discretized. [6] We denote with $\overline{d}_{t,m}$ the energy demand to be satisfied in each time sub-interval m.

With these assumptions, it's possible to formulate the RED problem considering analogous characteristics of the UC problem. In fact, RED problem and UC problem are similar, we can think to RED problem as an *on-line* UC, since in each time sub-interval m a smaller problem is solved, knowing the status of the units. In the time horizon T, $M \times T$ problems are solved, considering the complete RED formulation.

In order to make our simulations to compare the different formulations of the RED problem, we have implemented an object called '*simulator*' in C++ programing language. This object allows to compare the flexibility, efficiency and effectiveness of UC solutions in the adaptation to actual electricity demand (load) in an electrical system, real time. We developed 4 types of simulators, as described below:

- *greedy continuous* simulator;

- *greedy discontinuous* simulator;

---

[6] Usually $M = 4$, since $t = 1$ hour and t is divided into quarters of hour.

- *not greedy continuous* simulator;

- *not greedy discontinuous* simulator.

The *greedy* type simulator is *greedy* (according to the meaning of this word in Operations Research) since the actual demand (load) is known in each time interval, but the same is not possible for demands related to the future. As far as future is concerned, only forecast demand is known.

The *not greedy* type simulator is *not greedy* since it considers a predictive part that allows to know some aspect of the future (such as load).

The continuity or discontinuity aspect of the model is related to the way of considering power and consequently system wide constraints. The model (simulator) is defined continuous if the power is continuous by passing from a time sub-interval m to the following, but it is not necessarily derivable. The model (simulator) is defined discontinuous if the power is constant in each time sub-interval m and it is discontinuous passing from a time sub-interval m to the following.

5.2.1   Objective Function

As previously explained in Chapter 2 (section 2.1.1), the objective function of the UC is defined as follows:

$$\sum_{i \in \mathcal{P}} c^i(p^i, u^i) = \sum_{i \in \mathcal{P}} \left(s^i(u^i) + \sum_{t \in \mathcal{T}} \left(a_t^i(p_t^i)^2 + b_t^i p_t^i + c_t^i u_t^i \right) \right) \tag{5.38}$$

This objective function is posed in classical form, representing the total power production cost to be minimized. It's possible to consider different objective functions, in order to maximize the expected value of electricity market profit or taking into account environmental impacts. We have chosen to consider the classical form for two main reasons: to pose the accent on the peculiarity of the proposed model and to better compare results with standard UC formulation.

Status variables u_t^i (with $i \in \mathcal{P}$ and $t \in \mathcal{T}$) indicate if the thermal unit i is on (value 1) or if it is off (value 0) in time period t. Variables p_t^i (with $i \in \mathcal{P}$ and $t \in \mathcal{T}$) represent power generated by the thermal unit i at the end of the time period t and they are expressed in MW. Coefficients a_t^i, b_t^i, c_t^i represent respectively the quadratic, linear and constant term of the cost function of the thermal unit i in period t. In RED problem, cost coefficients are expressed as follows:

$$\hat{a}_{t,m}^i = a_{t,m}^i f_m \tag{5.39}$$

$$\hat{b}_{t,m}^i = b_{t,m}^i f_m \tag{5.40}$$

$$\hat{c}_{t,m}^i = c_{t,m}^i f_m \tag{5.41}$$

with $f_m = \frac{f_h}{M}$ where f_h is the duration of time interval t and f_m is the duration of time sub-interval m.

In RED, variables u_t^i are fixed, knowing the UC solution. If we consider the discretization of time interval t into m time sub-intervals, as explained above, the power variables are expressed as follows:

$$p_{t,m}^i \quad i \in \mathcal{P} \quad t \in \mathcal{T} \quad 1 \le m \le M \tag{5.42}$$

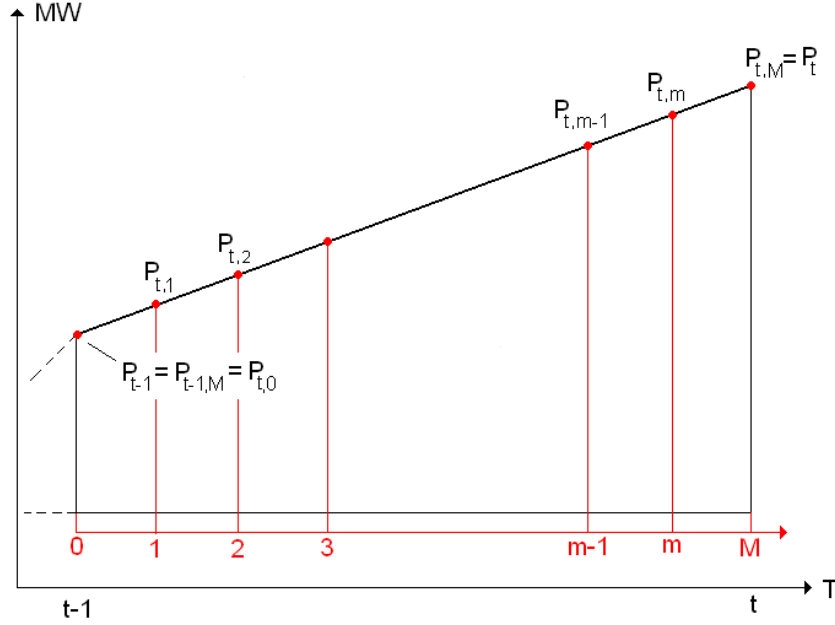In picture 5.18 a representation of power variables considered in the RED problem is given.

Figure 5.18: Correspondence between UC and RED power variables.

In our model, we considered 3 types of *slack variables* θ (expressed in MWh) which are used to relax the system wide constraints on energy balance, as described below:

- *slack variables* $\theta^+_{\bar{t},m}$ and $\theta^-_{\bar{t},m}$ are related to slacks obtainted in the time sub-interval m for the current hour $\bar{t}$;

- *slack variables* $\theta^{+,suc}_{t,m}$ and $\theta^{-,suc}_{t,m}$ are related to slacks obtained in the following hours (hours that follow the current hour $\bar{t}$); these *slack variables* exist only if we consider *not greedy* simulators (both continuous and discontinuous), since these simulators are taken into account when a prediction over the energy demand is required;

- *slack variables* $\theta^{+,res}_{\bar{t},m}$ and $\theta^{-,res}_{\bar{t},m}$ are related to slacks obtainted in the remaining part of the current hour $\bar{t}$; these *slack variables* exist only if we consider *not greedy* simulators (both continuous and discontinuous).

With these assumptions, the objective function for the generic RED problem considering the $\bar{t},m$ time interval will read

$$f(p^i_{\bar{t},m},\theta^+_{\bar{t},m},\theta^-_{\bar{t},m}) + f(p^i_{\bar{t},M},\theta^{+,res}_{\bar{t},m},\theta^{-,res}_{\bar{t},m}) + f(p^i_t,\theta^{+,suc}_{t,m},\theta^{-,suc}_{t,m}) \qquad (5.43)$$

which is equal to

$$f(p^i_{\bar{t},m}) + f(p^i_{\bar{t},M}) + f(p^i_t) + f(\theta^+_{\bar{t},m},\theta^-_{\bar{t},m},\theta^{+,res}_{\bar{t},m},\theta^{-,res}_{\bar{t},m},\theta^{+,suc}_{t,m},\theta^{-,suc}_{t,m}) \qquad (5.44)$$

with $\bar{t} \leq t + 1 \leq T$. The terms concerning the remaining part of the current hour are considered in the part $f(p_t^i)$ since we have $p_{\bar{t},M}^i = p_{\bar{t}}^i$. So the objective function becomes:

$$f(p_{\bar{t},m}^i) + f(p_t^i) + f(\theta_{\bar{t},m}^+, \theta_{\bar{t},m}^-, \theta_{\bar{t},m}^{+,res}, \theta_{\bar{t},m}^{-,res}, \theta_{t,m}^{+,suc}, \theta_{t,m}^{-,suc}) \tag{5.45}$$

with $\bar{t} \leq t + 1 \leq T$.

The objective function of the generic RED problem consists of three parts:

1. $f(p_{\bar{t},m}^i)$ is the objective function for the m time interval in the current hour $\bar{t}$ and it is expressed as follows:

   - *Continuous case*

   $$\sum_{i \in \mathcal{P}} c^i(p^i) = \sum_{i \in \mathcal{P}} \left(\hat{a}_{\bar{t},m}^i \frac{\left(p_{\bar{t},m-1}^i + p_{\bar{t},m}^i\right)^2}{3} + \hat{b}_{\bar{t},m}^i \frac{\left(p_{\bar{t},m-1}^i + p_{\bar{t},m}^i\right)}{2} + \hat{c}_{\bar{t},m}^i u_{\bar{t}}^i \right) \tag{5.46}$$

   - *Discontinuous case*

   $$\sum_{i \in \mathcal{P}} c^i(p^i) = \sum_{i \in \mathcal{P}} \left(\hat{a}_{\bar{t},m}^i (p_{\bar{t},m}^i)^2 + \hat{b}_{\bar{t},m}^i + p_{\bar{t},m}^i + \hat{c}_{\bar{t},m}^i u_{\bar{t}}^i \right) \tag{5.47}$$

2. $f(p_t^i)$ is the objective function of the UC problem for $\bar{t} \leq t \leq T$ (considering also $\bar{t}$) and it is expressed as follows:

   $$\sum_{i \in \mathcal{P}} c^i(p^i, u^i) = \sum_{i \in \mathcal{P}} \left(s^i(u^i) + \sum_{t \in \mathcal{T}} \left(a_t^i(p_t^i)^2 + b_t^i p_t^i + c_t^i u_t^i \right) \right) \tag{5.48}$$

3. $f(\theta_{\bar{t},m}^+, \theta_{\bar{t},m}^-, \theta_{\bar{t},m}^{+,res}, \theta_{\bar{t},m}^{-,res}, \theta_{t,m}^{+,suc}, \theta_{t,m}^{-,suc})$ is the objective function of slack variables.

As far as point 1 is concerned, given the time interval t, the demand variation is expressed as follows

$$p(s) = p_{t-1}^i + \alpha s \tag{5.49}$$

with $0 < s < f_m$ and $\alpha = \frac{p_t - p_{t-1}}{f_m}$.

The objective function can be obtained by the integral

$$\int_0^{f_m} a\left[p(s)\right]^2 + bp(s) + c \, ds \tag{5.50}$$

which is composed by three parts:

- part considering c^i

$$c^i f_m \tag{5.51}$$

- part considering b^i, the primitive is

$$b^i \left(p_{t-1}^i s + \alpha \frac{s^2}{2}\right) \tag{5.52}$$

so the integral is

$$b^i(p_{t-1}^i f_m + \frac{1}{2}\alpha f_m^2) = b^i f_m(p_{t-1}^i + \alpha \frac{f_m}{2}) \tag{5.53}$$

which, by substituting the value of α, becomes

$$b^i f_m(p_{t-1}^i + \frac{p_t^i - p_{t-1}^i}{2}) = b^i f_m \frac{p_{t-1}^i + p_t^i}{2} \tag{5.54}$$

- part considering a^i, the primitive is

$$a^i(p_{t-1}^i)^2 s + \alpha p_{t-1}^i s^2 + \alpha^2 \frac{s^3}{3} \tag{5.55}$$

so the integral is

$$a^i(p_{t-1}^i)^2 f_m + \alpha p_{t-1}^i f_m^2 + \alpha^2 \frac{f_m^3}{3} \tag{5.56}$$

which, by substituting the value of α, is equal to the following expression

$$a^i f_m \frac{(p_t^{i\,2} + (p_{t-1}^i)^2 + p_{t-1}^i p_t^i)}{3} \tag{5.57}$$

5.2.2 Constraints of the RED model

We can assume, without loss of generality, that $\hat{a}_{t,m}^i$, $\hat{b}_{t,m}^i$, $\hat{c}_{t,m}^i$ are constant for $1 \leq m \leq M$, since t is constant in this time interval. We have two types of RED constraints:

- *local constraints for thermal units*;

- *system wide constraints.*

We consider also a *continuity constraint* for power variables passing from a time interval t into the following.

Local constraints for thermal units

These constraints represent technical restrictions for thermal units, they are:

- *power limit constraints*;

- *ramping constraints.*

Power limit constraints imply that power must be limited between a minimum and maximum power as shown below:

$$\bar{p}_{min}^i u_t^i \leq p_{t,m}^i \leq \bar{p}_{max}^i u_t^i \quad t \in \mathcal{T} \quad m \in \mathcal{M} \quad u_t^i \in \{1\} \tag{5.58}$$

where $\bar{p}_{max}^i$ and $\bar{p}_{min}^i$ are respectively the maximum and minimum power generated when the thermal unit i operates in a steady state and they are expressed in MW. These constraints are considered only for $u_t^i = 1$ in RED, since we know that if $u_t^i = 0$ the thermal unit i is off and $p_{t,m}^i = 0 \quad \forall m$.

As far as not greedy RED simulations are concerned, power limit constraints are expressed as follows:

- *Power limit constraints for thermal units considering time sub-intervals m*

$$\overline{p}^i_{min} \le p^i_{\overline{t},m} \le \overline{p}^i_{max} \tag{5.59}$$

- *Power limit constraints for thermal units considering remaining parts of the current hour $\overline{t}$*

$$\overline{p}^i_{min} \le p^i_{\overline{t},M} \le \overline{p}^i_{max} \tag{5.60}$$

- *Power limit constraints for thermal units considering the following hours*

$$\overline{p}^i_{min} \le p^t_i \le \overline{p}^i_{max} \qquad \overline{t}+1 \le t \le T \tag{5.61}$$

Ramping constraints   limit the maximum increase or decrease in power generated from a time period to the following and reflect the thermal and mechanical inertia of thermal units. These constraints require that the maximum increase of power generated from a time period to the following is limited to $\Delta^i_+ > 0$ (Δ^i_+ is called *maximum ramp-up rate* and it is expressed in MW/h), and, analogously, the maximum decrease of power generated from time period t to the following is limited to $\Delta^i_- > 0$ (Δ^i_- is called *maximum ramp-down rate* and it is expressed in MW/h).

This definition can be applied only if the thermal unit is on in both periods t and $t+1$.

For RED problem, it's necessary to modify the *ramp rates* considering the discretization of time interval t into M time sub-intervals, so the *ramp rate* between $m-1$ and m is expressed as

$$\frac{\Delta^i}{M}$$

With these assumptions, ramping constraints in RED problem are expressed as follows, the terms $\overline{\bullet}$ are known form the solution at time $m-1$:

- *Ramp-up constraints*

$$\text{for } m=1 \quad p^i_{t,m} \quad \le \quad \overline{p}^i_{t-1,M} + \overline{u}^i_{t-1}\frac{\Delta^i_+}{M} + (1-\overline{u}^i_{t-1})\overline{l}^i \tag{5.62}$$

$$\text{for } m>1 \quad p^i_{t,m} \quad \le \overline{p}^i_{t,m-1} + \overline{u}^i_{t-1}\frac{\Delta^i_+}{M} \tag{5.63}$$

- *Ramp-down constraints*

$$\forall m \quad \overline{p}^i_{t,m-1} \quad \le \quad p^i_{t,m} + \overline{u}^i_t\frac{\Delta^i_-}{M} + (1-\overline{u}^i_t)\overline{u}^i \tag{5.64}$$

for

$$t \in \mathcal{T} \quad m \in \mathcal{M} \quad i \in \mathcal{P} \quad \overline{u}^i_t \in \{1\}$$

Ramping constraints are considered only if $u^i_t = 1$ in RED, since it's known that if $u^i_t = 0$ the thermal unit i is off and $p^i_{t,m} = 0 \quad \forall m$.

As far as not greedy RED simulations are concerned, ramping constraints are expressed as follows:

- *Ramping constraints for thermal units considering time sub-intervals m* Variables u_t^i are known from the UC solution. Ramping constraints are considered only if $u_{\bar{t}}^i \neq 0$.

  – *Ramp-up constraints*

  1. for $m = 1$

$$p_{\bar{t},m}^i \leq p_{\bar{t}-1,M}^i + u_{\bar{t}-1}^i \frac{\Delta_+^i}{M} + (1 - u_{\bar{t}-1}^i)\bar{l}^i \tag{5.65}$$

  2. for $m > 1$

$$p_{\bar{t},m}^i \leq p_{\bar{t},m-1}^i + \frac{\Delta_+^i}{M} \tag{5.66}$$

  – *Ramp-down constraints*

$$p_{\bar{t},m-1}^i \leq p_{\bar{t},m}^i + \frac{\Delta_-^i}{M} \qquad \forall m \tag{5.67}$$

  The values of $p_{\bar{t},m-1}^i$ are known from the initial conditions at time $t = 0$ or from the $m - 1$ RED problem results.

- *Ramping constraints for thermal units considering remaining parts of the current hour $\bar{t}$* In order to write ramping constraints we consider power variables in the same time interval $\bar{t}$. Ramping constraints are considered only if $u_{\bar{t}}^i \neq 0$.

  – *Ramp-up constraints*

$$p_{\bar{t},M}^i \leq p_{\bar{t},m}^i + \Delta_+^i \frac{(M - m)}{M} \tag{5.68}$$

  – *Ramp-down constraints*

$$p_{\bar{t},m}^i \leq p_{\bar{t},M}^i + \Delta_-^i \frac{(M - m)}{M} \tag{5.69}$$

- *Ramping constraints for thermal units considering the following hours* Ramping constraints are considered only if $u_t^i \neq 0$. We have:

  – *Ramp-up constraints*

$$p_t^i \leq p_{t-1}^i + u_{t-1}^i \Delta_+^i + (1 - u_{t-1}^i)\bar{l}^i \qquad \bar{t} + 1 \leq t \leq T \tag{5.70}$$

  1. $u_t^i = 1$

$$\begin{aligned} u_{t-1}^i = 0 &\quad \rightarrow p_t^i \leq \bar{l}^i \\ u_{t-1}^i = 1 &\quad \rightarrow p_t^i - p_{t-1}^i \leq \Delta_+^i \end{aligned} \tag{5.71}$$

  2. $u_t^i = 0$

$$u_{t-1}^i = 0 \rightarrow 0 \leq \bar{l}^i \qquad \text{always satisfied} \tag{5.72}$$

$$u_{t-1}^i = 1 \rightarrow p_{t-1}^i \leq \Delta_+^i \quad \text{always satisfied} \tag{5.73}$$

– *Ramp-down constraints*

$$p_{t-1}^i \leq p_t^i + u_t^i \Delta_-^i + (1 - u_t^i)\overline{u}^i \qquad \overline{t} + 1 \leq t \leq T \tag{5.74}$$

1. $u_t^i = 1$

$$\begin{aligned} u_{t-1}^i = 0 \quad &\rightarrow p_t^i \geq -\Delta_-^i \quad \text{always satisfied} \\ u_{t-1}^i = 1 \quad &\rightarrow p_{t-1}^i - p_t^i \leq \Delta_-^i \end{aligned} \tag{5.75}$$

2. $u_t^i = 0$

$$\begin{aligned} u_{t-1}^i = 0 \quad &\rightarrow 0 \geq -\Delta_-^i \text{always satisfied} \\ u_{t-1}^i = 1 \quad &\rightarrow p_{t-1}^i \leq \overline{u}^i \end{aligned} \tag{5.76}$$

System wide constraints

System wide constraints are necessary to respect the balance condition between the energy demand at time m and the energy generated by each unit at time m. For each time period $t \in \mathcal{T}$ of duration f_h (measured as a fraction of hour) the forecast energy demand d_t (MWh) can be divided into M time subintervals, as indicated in section 5.1.3 , so that we can obtain a constant energy demand $\overline{d}_{t,m}$ in the time sub-interval m .

The energy demand at time sub-interval m must be balanced by the generated energy, that is equal to the sum of the energies generated by the thermal units i in the time sub-interval m, with the assumption that power $p_{t,m}$ at time (t,m) must satisfy ramping constraints.

As far as RED simulations are concerned, system wide constraints are expressed as follows:

• *System wide constraints for thermal units considering time sub-intervals m*

– *Continuous case*

$$\sum_{i \in \mathcal{P}} \frac{1}{2} \frac{\left(p_{\overline{t},m-1}^i + p_{\overline{t},m}^i\right)}{M} + \theta_{\overline{t},m}^+ + \theta_{\overline{t},m}^- = d_{\overline{t},m} \tag{5.77}$$

– *Discontinuous case*

$$\sum_{i \in \mathcal{P}} \frac{1}{M} p_{\overline{t},m}^i + \theta_{\overline{t},m}^+ + \theta_{\overline{t},m}^- = d_{\overline{t},m} \tag{5.78}$$

with $1 \leq m \leq M$

$\overline{t}$ indicates the current hour

m indicates the current quarter of the current hour $\overline{t}$

M indicates the number of the time sub-intervals m in the current hour $\overline{t}$, so $\frac{1}{M}$ represents a fraction of the current hour $\overline{t}$, in our case $M = 4$

$\theta_{\overline{t},m}^+ \geq 0$ and $\theta_{\overline{t},m}^- \leq 0$ are slack variables in order to relax the system wide constraints for energy balance.

• *System wide constraints for thermal units considering remaining parts of the current hour $\overline{t}$*
  We have remaining parts of the current hour $\overline{t}$ only if $m < M$ and $u_{\overline{t}}^i \neq 0$

    – *Continuous Case*

$$\sum_{i \in \mathcal{P}} \frac{1}{2} \left(p_{\bar{t},m}^i + p_{\bar{t},M}^i \right) \frac{(M-m)}{M} + \theta_{\bar{t},m}^{+,res} + \theta_{\bar{t},m}^{-,res} = d_{\bar{t},m} - \sum_{\bar{k}=1}^{m} D_{\bar{t},\bar{k}} \qquad (5.79)$$

    – *Discontinuous Case*

$$\sum_{i \in \mathcal{P}} p_{\bar{t},m}^i \frac{(M-m)}{M} + \theta_{\bar{t},m}^{+,res} + \theta_{\bar{t},m}^{-,res} = d_{\bar{t},m} - \sum_{\bar{k}=1}^{m} D_{\bar{t},\bar{k}} \qquad (5.80)$$

$d_{\bar{t},m}$ indicates the actual energy demand in the time interval $\bar{t}-1, \bar{t}$

$D_{\bar{t},\bar{k}}$ indicates the actual energy demand in the current time interval k with $1 \le k \le M$

$p_{\bar{t},M}^i = p_{\bar{t}}^i$ indicates the power at the end of the hour $\bar{t}$

$\theta_{\bar{t},m}^{+,res} \ge 0$ and $\theta_{\bar{t},m}^{-,res} \le 0$ are slack variables in order to relax the system wide constraints for energy balance.

$\frac{(M-m)}{M}$ indicates the remaining part of the current time interval

- *System wide constraints for thermal units considering the following hours*

    – *Continuous Case*

$$\sum_{i \in \mathcal{P}} \frac{1}{2} \left(p_{t-1}^i + p_t^i \right) + \theta_t^{-,suc} + \theta_t^{-,suc} = d_{\bar{t}} \qquad \bar{t}+1 \le t \le \mathcal{T} \qquad (5.81)$$

    – *Discontinuous Case*

$$\sum_{i \in \mathcal{P}} p_t^i + \theta_t^{-,suc} + \theta_t^{-,suc} = d_{\bar{t}} \qquad \bar{t}+1 \le t \le \mathcal{T} \qquad (5.82)$$

$\theta_t^{+,suc} \ge 0$ and $\theta_t^{-,suc} \le 0$ are slack variables in order to relax the system wide constraints for energy balance. Variables u_t^i are known from the UC solution.

Continuity constraints

    Continuity constraints are necessary in order to have a continuous power in time period $\mathcal{T}$, as shown in picture 5.18. Considering that power and ramping constraints exist only if $u_t^i = 1$, we have the following assumptions:

- For $u_t^i = 1$

$$
\begin{aligned}
p_{1,0}^i &= P_0^i \quad i \in P \ \ t = 1 & (5.83) \\
p_{t-1,M}^i &= p_{t,0}^i \quad i \in P \ \ t > 1 & (5.84)
\end{aligned}
$$

- For $u_t^i = 0$:

$$p_{t,M}^i = 0 \quad i \in P \ \ t > 1 \qquad (5.85)$$

The (5.83) is necessary to the ramp up constraint at time $t = 1$ where the value of power $p_{1,0}^i$ is considered. The (5.84) is the condition of coincidence between $m = M$ at time t and $m = 0$ at time $t + 1$, necessary to ramp-up/down constraints. The (5.85) is necessary to ramp-up/down constraints, in fact, for $u_{t+1}^i = 1$ and $m = 1$ we have $p_{t+1,0}^i = p_{t,M}^i$, if the thermal unit i is off at time t then $p_{t,M}^i = 0 \rightarrow p_{t+1,0}^i = 0$.

As far as not greedy RED simulations are concerned, variables p_t^i are subject to the following continuity constraints:

$$p_{\bar{t},M}^i = p_{\bar{t}}^i \tag{5.86}$$

The constraints on the UC solution are expressed as follows:

$$u_t^i = 0 \rightarrow p_t^i = 0 \tag{5.87}$$

5.3   Results and discussion

In order to test our simulators, we considered 4 input data instances, (2 instances with 10 thermal units and 2 instances with 20 thermal units). The UC problem was solved for each input data instance. The actual demand profile is assumed to be identical to the forecast demand profile, used to solve the UC problem. For each simulator type, tests have been made considering the 4 input data instances mentioned above. To process the actual demand profile into energy demand profile we used a piece-wise approximation, as described in section 5.1. In particular, the actual demand profile has been obtained setting *ad hoc* parameters involving the slope discretization type in order to make this profile as smooth as possible. These parameters settings are the same for all simulations regardless to the instance since the demand profile characteristics are similar: lower power demand in times $3 - 4$ and higher power demand in times $12 - 13$.

Table 5.1) and Table 5.2) summarize the results that we have obtained in our simulations. The tables present the following columns:

- **ID** (column 1): represents the simulation ID;

- **Thermal units number** (column 2): represents the thermal units number considered in the simulation;

- **Simulator type** (column 3): represents the simulator type (greedy, not greedy, continuous, discontinuous);

- **Number of** $\theta_{\bar{t},m}^+$ (column 4): represents the number of positive *slack variables* in the time sub-interval m;

- **Number of** $\theta_{\bar{t},m}^-$ (column 5): represents the number of negative *slack variables* in the time sub-interval m;

- **Total number of** $\theta_{\bar{t},m}^+$ **and** $\theta_{\bar{t},m}^-$ (column 6): represents the total number of *slack variables* in the time sub-interval m;

- **Total value of** $\theta_{\bar{t},m}^+$ **and** $\theta_{\bar{t},m}^-$ (column 7): represents the total value of *slack variables* in the time sub-interval m expressed in $[MWh]$;

- **Number of** $\theta_{t,m}^{+,suc}$ (column 8): represents the number of positive *slack variables* in the following hours (the hours that follow the current hour $\bar{t}$ considered);

- **Number of** $\theta_{t,m}^{-,suc}$ (column 9): represents the number of negative *slack variables* in the following hours (the hours that follow the current hour $\bar{t}$ considered);

- **Total number of** $\theta_{t,m}^{+,suc}$ **and** $\theta_{t,m}^{-,suc}$ (column 10): represents the total number of *slack variables* in the following hours (the hours that follow the current hour $\bar{t}$ considered);

- **Total value of** $\theta_{t,m}^{+,suc}$ **and** $\theta_{t,m}^{-,suc}$ (column 11): represents the total value of *slack variables* in the following hours (the hours that follow the current hour $\bar{t}$ considered) expressed in $[MWh]$;

- **Number of** $\theta_{\bar{t},m}^{+,res}$ (column 12): represents the number of positive *slack variables* in the remaining part of the current hour $\bar{t}$;

- **Number of** $\theta_{\bar{t},m}^{-,res}$ (column 13): represents the number of negative *slack variables* in the remaining part of the current hour $\bar{t}$;

- **Total number of** $\theta_{\bar{t},m}^{+,res}$ **and** $\theta_{\bar{t},m}^{-,res}$ (column 14): represents the total number of *slack variables* in the remaining part of the current hour $\bar{t}$;

- **Total value of** $\theta_{\bar{t},m}^{+,res}$ **and** $\theta_{\bar{t},m}^{-,res}$ (column 15): represents the total value of *slack variables* in the remaining part of the current hour $\bar{t}$ expressed in $[MWh]$.

If we analyze tables 5.1 and 5.2 we observe that:

- *greedy* simulators (both continuous and discontinuous) present only *slack variables* for time sub-interval m;

- generally, *greedy discontinuous* simulators are more efficient than *greedy continuous* simulators, since they present a lower number of *slack variables* in a lower value;

- in *not greedy discontinuous* simulators slacks over balance constraints for the following hours are equal to zero, that's why constraints have been already satisfied by the UC problem solution; this means that *slack variables* number and values are lower than these present in *greedy continuous* simulators;

- generally, *not greedy discontinuous* simulators work better than the *continuous* ones, since they consider UC discontinuous solution from a power point of view. *Not greedy* simulators are more efficient than the *greedy* ones, since they present a predictive part which allows to reduce the number of *slack variables* and to satisfy constraints in RED problems.

To analyze the difference between the performances of the simulators developed, we carried on a statistical results analysis. The term 'performances' stands for the 'good behavior' of the model in the adaptation to the load profile and it is not related with the computational efficiency of the model itself. In particular, we studied the statistical correlation between the actual demand profile and the demand profile obtained with the simulators (considering simulation 3). Table 5.3 summarizes the results obtained. We analyze the result looking at the ability of the simulator in following the input demand profile: less slack variables different from zero value mean a lower

number of not satisfied constraints, hence the model that has this behavior and the higher correlation of the output profile with the demand profile is to be preferred. If we analyze table 5.3, we notice that *not greedy discontinuous* simulators present the greatest value of correlation, while the standard deviation is the lowest.

ID	Units	Type	No $\theta_{\bar{t},m}^+$	No $\theta_{\bar{t},m}^-$	Tot No $\theta_{\bar{t},m}^+, \theta_{\bar{t},m}^-$	Tot Val $\theta_{\bar{t},m}^+, \theta_{\bar{t},m}^-$	No $\theta_{t,m}^{+,suc}$	No $\theta_{t,m}^{-,suc}$
1	10		19	3	22	223.70	-	-
2	10	Greedy	27	4	31	258.16	-	-
3	20	Cont.	23	0	23	82.61	-	-
4	20		30	2	32	232.27	-	-
1	10		14	1	15	148.86	-	-
2	10	Greedy	22	3	25	222.35	-	-
3	20	Discont.	18	1	19	70.46	-	-
4	20		17	2	19	150.07	-	-
1	10	Not	34	28	62	259.00	200	119
2	10	Greedy	40	29	69	130.42	336	191
3	20	Cont.	39	31	70	205.41	380	227
4	20		38	31	69	259.95	334	217
1	10	Not	12	1	13	124.2	0	0
2	10	Greedy	18	3	21	112.4	0	0
3	20	Discont.	12	0	12	46.27	0	0
4	20		13	2	15	128.68	0	0

Table 5.1: Results obtained in simulations - table 1.

ID	Units	Type	Tot No $\theta_{t,m}^{+,suc}, \theta_{t,m}^{-,suc}$	Tot Val $\theta_{t,m}^{+,suc}, \theta_{t,m}^{-,suc}$	No $\theta_{\bar{t},m}^{+,res}$	No $\theta_{\bar{t},m}^{-,res}$	Tot No $\theta_{\bar{t},m}^{+,res}, \theta_{\bar{t},m}^{-,res}$	Tot Val $\theta_{\bar{t},m}^{+,res}, \theta_{\bar{t},m}^{-,res}$
1	10		-	−	-	-	-	−
2	10	Greedy	-	−	-	-	-	−
3	20	Cont.	-	−	-	-	-	−
4	20		-	−	-	-	-	−
1	10		-	−	-	-	-	−
2	10	Greedy	-	−	-	-	-	−
3	20	Discont.	-	−	-	-	-	−
4	20		-	−	-	-	-	−
1	10	Not	319	4678	17	6	23	308.23
2	10	Greedy	527	2098.31	18	7	25	153.84
3	20	Cont.	607	10879.41	15	8	23	185.37
4	20		551	5347.7	19	7	26	263.04
1	10	Not	0	0	6	0	6	24.83
2	10	Greedy	0	0	4	0	4	34.43
3	20	Discont.	0	0	4	0	4	19.48
4	20		0	0	6	0	6	29.42

Table 5.2: Results obtained in simulations - table 2.

Simulator Type	Correlation	Standard Deviation	$\%Pdem_{min}$	$\%Pdem_{max}$
Greedy Disc.	99.89	19.12	1.76	0.81
Not Greedy Disc.	99.92	22.49	1.56	0.72

Table 5.3: Statistical analysis of the simulations results.

5.3.1 RED Greedy model

As far as greedy simulations are concerned (both continuous and discontinuous) they present difficulties in the adaptation to the actual demand profile, since the predictive part is totally absent. Greedy continuous simulator presents more difficulties than the greedy discontinuous one, since the UC problem is discontinuous as far as power is concerned. In fact, in UC power is not continuous, since we have a discontinuity in the power between a time interval and the following.

Both greedy and not greedy simulators present some difficulties at time $t = 1$ since there's a marked difference between p_0^i and the demand to be satisfied; this is a structural characteristic of the input data instances utilized in simulations. However, these difficulties can be partially overcome if we consider 'ad hoc' load profiles in our simulations, for instance, profiles without marked asperities, as we can observe in simulation 3.

The images depicted below represent the behavior of greedy (both continuous and discontinuous) simulators for each test that has been made. In figures which represent power demand profile, black line indicates actual demand profile while green line indicates forecast demand profile.

5.3.2   RED Not-Greedy model

As far as not greedy discontinuous simulations are concerned they present a better behavior than greedy simulators (both continuous and discontinuous) in the adaptation to the actual demand profile, since the predictive part allows to know some future aspects (like loads in the following hours). In particular, since UC problem is discontinuous as far as power is concerned, not greedy discontinuous simulators implement global constraints for the following hours (not greedy component) as UC problem does. This comes up to our expectations and it results the best simulator among the 4 developed. As we can see, not greedy continuous simulations present the worst behavior due just to continuous global constraints for the following hours.

The images depicted below represent the behavior of not greedy (both continuous and discontinuous) simulators for each test that has been made. In figures which represent power demand profile, black lines indicate actual demand profile while green lines indicate forecast demand profile.

5.4   Conclusions

In this chapter a new model, called '*Reduced Economic Dispatch*' (RED), has been presented. The objective of this model is to refine the UC solution, individuating the power that each unit must generate in a given time sub-interval of an assigned time interval. The various simulators that have been developed, based on this new model, are effective to compare the flexibility, the efficiency and the effectiveness of different UC solutions in the adaptation to the actual electricity demand (load) in a real time electrical system. In the simulation phase, we observed that the best simulator, among the four developed, is the *not greedy discontinuous* one, because it gives the better results, since the lowest number of slack variables is obtained. It came up to our expectations, since, as explained previously, the UC is discontinuous from a power point of view. Besides, simulations results show that it is very important to correctly set the parameters which determine the transformation of the power-demand profile used in the UC problem into the energy-demand profile used in the simulator. These parameters have to take into account the characteristics of the power-demand profile in order to avoid marked asperities of the load. In these cases, simulators generally work properly since they consider the status of the units obtained in the solution of the UC.

As far as future work is concerned, it could be very interesting to use the simulator developed in order to analyze the differences between the various UC formulations, in terms of the quality of the solution obtained, considering more input data instances with more generating units. Besides, simulations could be made considering also hydro units and more different load profiles. In order to study these differences, it could be necessary to perform several simulations on real time problems. The aim of these simulations is to compare the flexibility, the efficiency and the effectiveness of the UC solutions in the adaptation to the actual load. The formulations that could be taken into account in this analysis could be represented by the models for UC with spinning reserve constraints and by the robust models which are based on Robust Optimization considerations.

As far as spinning reserve UC models are concerned, Spinning Reserve constraints are taken into account in the formulation. Energy operators in the electricity market are required to store an energy reserve for different reasons, such as load peaks, units' failures or bad power scheduling. This reserve is defined operating reserve and consists of a Spinning Reserve and a Non-spinning Reserve. Spinning Reserve is defined as the available additional synchronized electricity to satisfy demand immediately. Non-spinning Reserve is not connected to the system but it can be useful to satisfy the load for about ten minutes. The Spinning Reserve quantity is estimated by technicians;

in most of UC applications, Spinning Reserve requirement is assumed deterministic. For example, in some applications, it is considered as a percentage of the load peak. Energy operators store Spinning Reserve in case of unexpected problems, however storing too much reserve is costly and so extra quantities of Spinning Reserve must be avoided.

Since only small quantities of energy can be stored, the electricity production has to follow the demand exactly and real-time. However, this is very difficult, since, even if demand forecasts are developed, demand that must be satisfied effectively (load) is different from forecast demand. That's why uncertainty of the load level must be considered in order to obtain a more realistic model for UC. A new approach that considers Robust Optimization can represent a useful way to formulate such model for UC, so that it's possible to manage load variations in a flexible way. Robust Optimization is an approach for optimization under input data uncertainty. It does not rely on a stochastic model to model the distribution of data. Despite of immunize solution from stochastic uncertainty in a probabilistic sense, according to Robust Optimization approach, decisions maker chooses the worst feasible solutions in a given uncertainty set, then these solutions are minimized considering uncertain parameters. In that way, solutions that are insensitive to uncertain parameters variations and models more useful from a computational point of view are obtained [Nai08].

In a future work, the main differences, expressed in terms of solution, between the spinning reserve and the robust UC models will be analyzed, considering the simulator model presented in this chapter, useful to make simulations on real time Reduced Economic Dispatch (RED) problems. Our final objective will be to show the main differences between the robust model and the spinning reserve model. The first difference is that the robust model guarantees the ramping constraints feasibility both in the case of an increasing load and in the case of a decreasing load. Furthermore, the robust model considers thermal and hydro units in the same way, while spinning reserve model is asymmetrical from this point of view. In fact, the spinning reserve model works well only if we have increasing load peak, while if we have decreasing load peaks the model presents several difficulties; the robust model instead is more flexible in the adaptation to the load profile.

(a) *Power distribution for continuous greedy simulators in sim 1.*

(b) *Power demand profile for continuous greedy simulators in sim 1.*
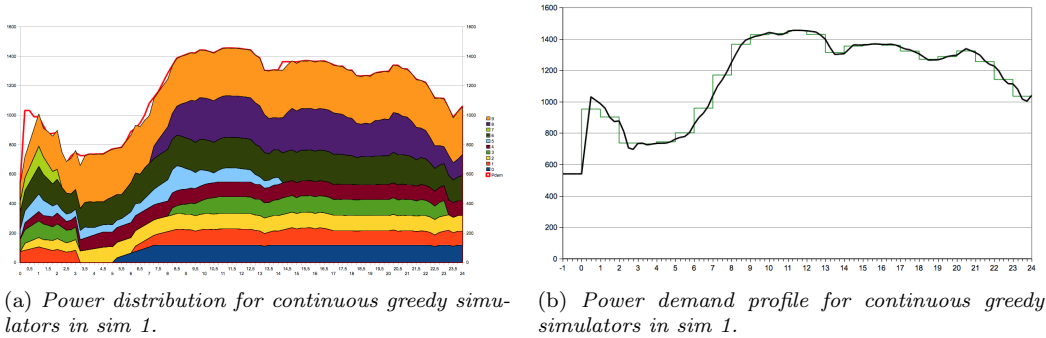
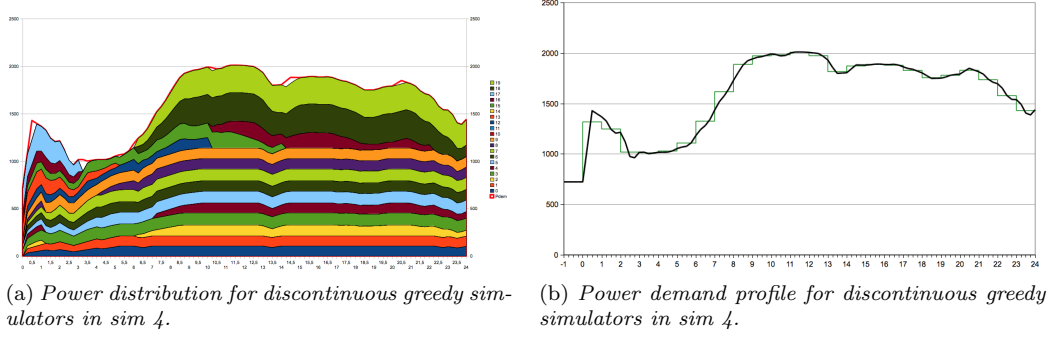Figure 5.19: Greedy continuous simulation results - sim 1.

(a) *Power distribution for discontinuous greedy simulators in sim 1.*

(b) *Power demand profile for discontinuous greedy simulators in sim 1.*
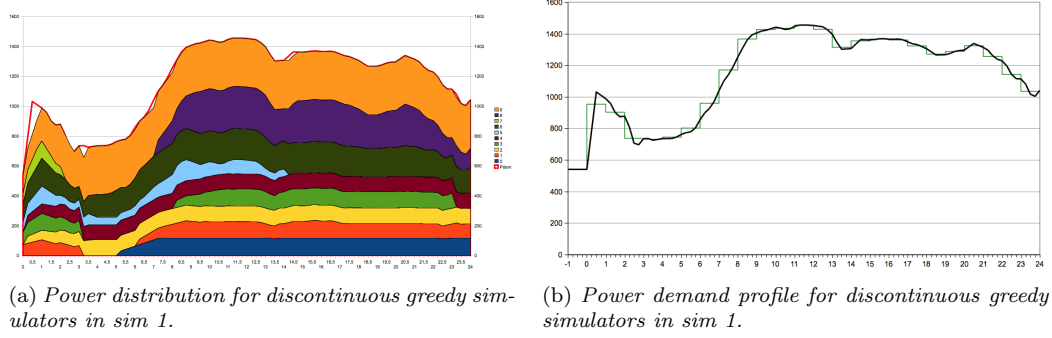
Figure 5.20: Greedy discontinuous simulation results - sim 1.

(a) *Power distribution for continuous greedy simulators in sim 2.*

(b) *Power demand profile for continuous greedy simulators in sim 2.*
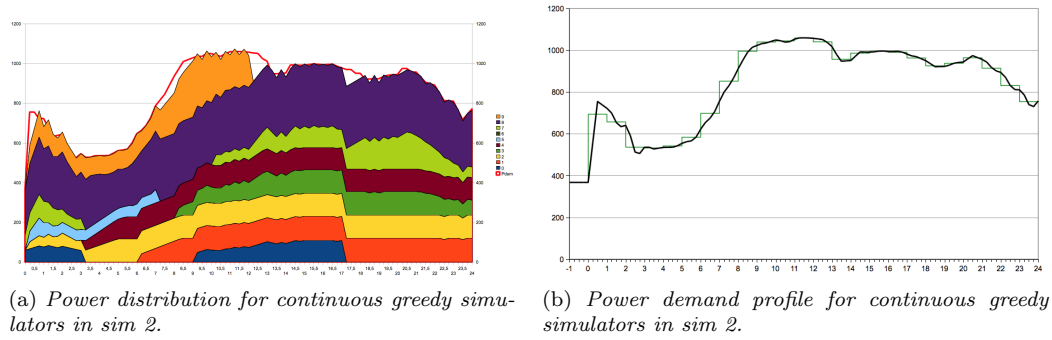
Figure 5.21: Greedy continuous simulation results - sim 2.

(a) *Power distribution for discontinuous greedy simulators in sim 2.*

(b) *Power demand profile for discontinuous greedy simulators in sim 2.*
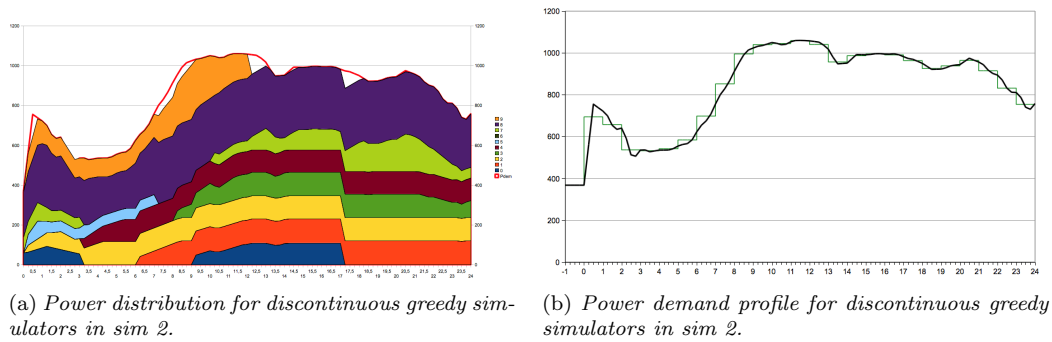
Figure 5.22: Greedy discontinuous simulation results - sim 2.
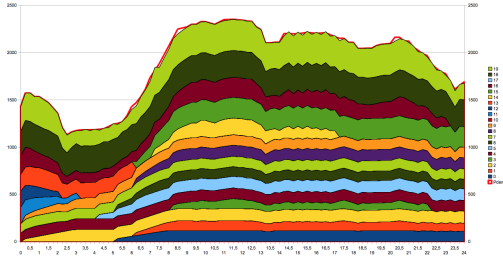
(a) *Power distribution for continuous greedy simulators in sim 3.*
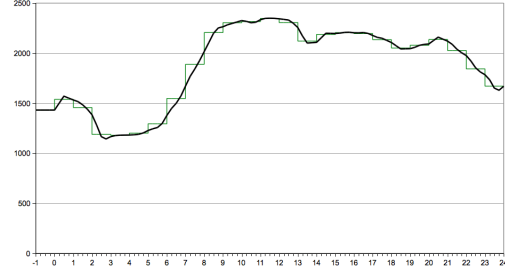
(b) *Power demand profile for continuous greedy simulators in sim 3.*

Figure 5.23: Greedy continuous simulation results - sim 3.
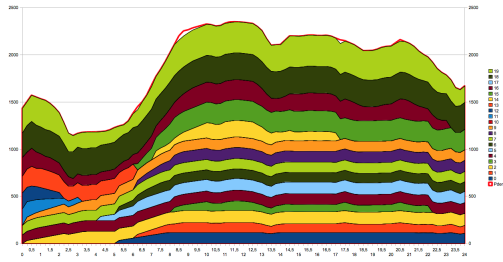
(a) *Power distribution for discontinuous greedy simulators in sim 3.*
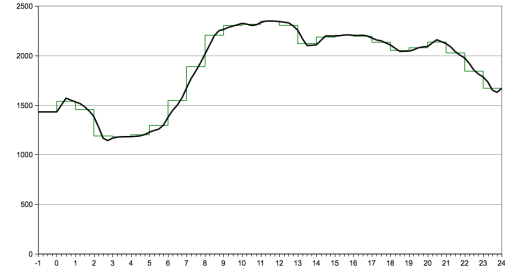
(b) *Power demand profile for discontinuous greedy simulators in sim 3.*

Figure 5.24: Greedy discontinuous simulation results - sim 3.
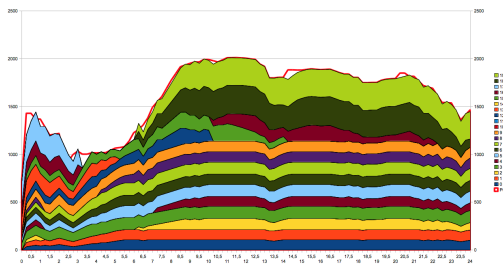
(a) *Power distribution for continuous greedy simulators in sim 4.*
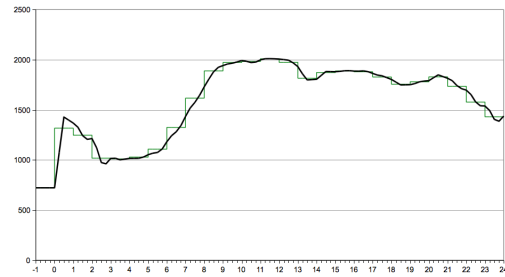
(b) *Power demand profile for continuous greedy simulators in sim 4.*

Figure 5.25: Greedy continuous simulation results - sim 4.

(a) *Power distribution for discontinuous greedy sim-*
ulators in sim 4.

(b) *Power demand profile for discontinuous greedy*
simulators in sim 4.

Figure 5.26: Greedy discontinuous simulation results - sim 4.

(a) *Power distribution for continuous not greedy*
simulators in sim 1.

(b) *Power demand profile for continuous not greedy*
simulators in sim 1.
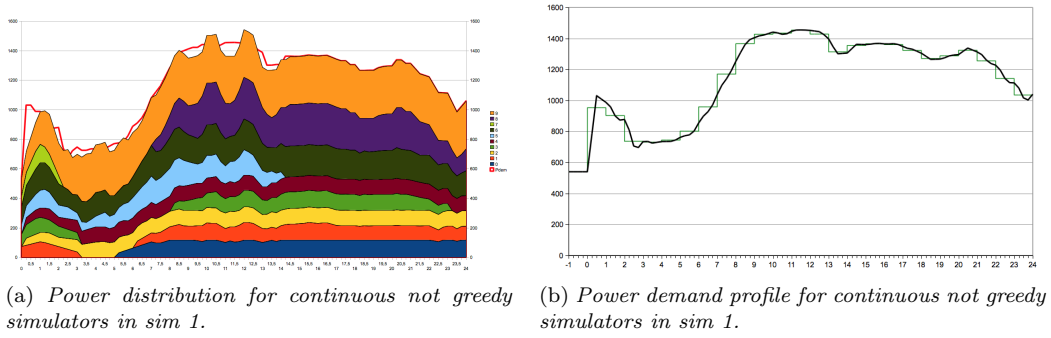
Figure 5.27: Not-Greedy continuous simulation results - sim 1.

(a) *Power distribution for discontinuous not greedy*
simulators in sim 1.

(b) *Power demand profile for discontinuous not*
greedy simulators in sim 1.
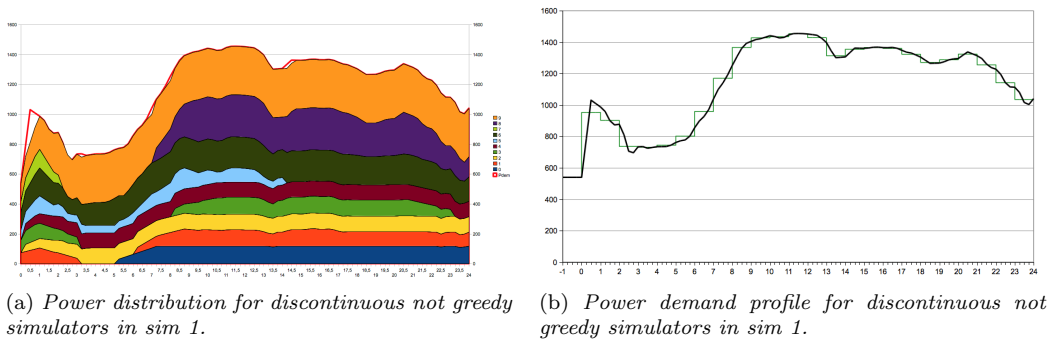
Figure 5.28: Not-Greedy discontinuous simulation results - sim 1.

(a) *Power distribution for continuous not greedy simulators in sim 2.*

(b) *Power demand profile for continuous not greedy simulators in sim 2.*
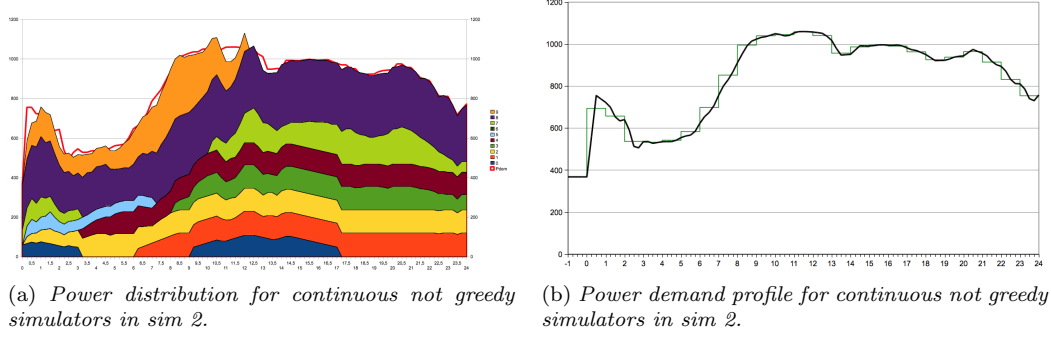
Figure 5.29: Not-Greedy continuous simulation results - sim 2.

(a) *Power distribution for discontinuous not greedy simulators in sim 2.*

(b) *Power demand profile for discontinuous not greedy simulators in sim 2.*
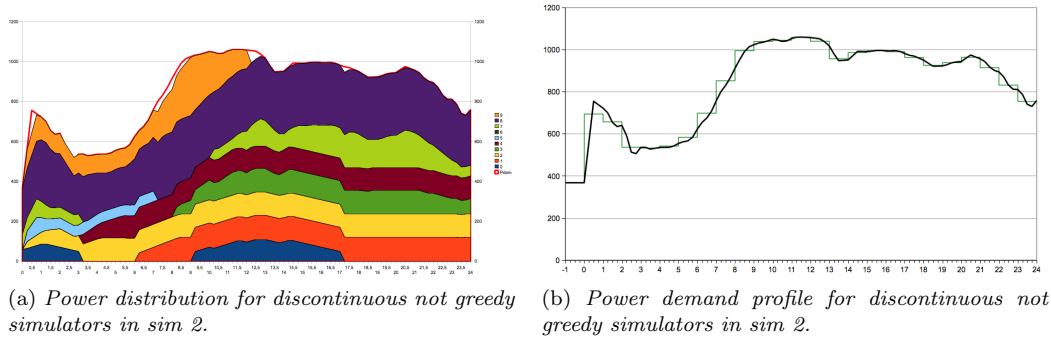
Figure 5.30: Not-Greedy discontinuous simulation results - sim 2.

(a) *Power distribution for continuous not greedy simulators in sim 3.*

(b) *Power demand profile for continuous not greedy simulators in sim 3.*
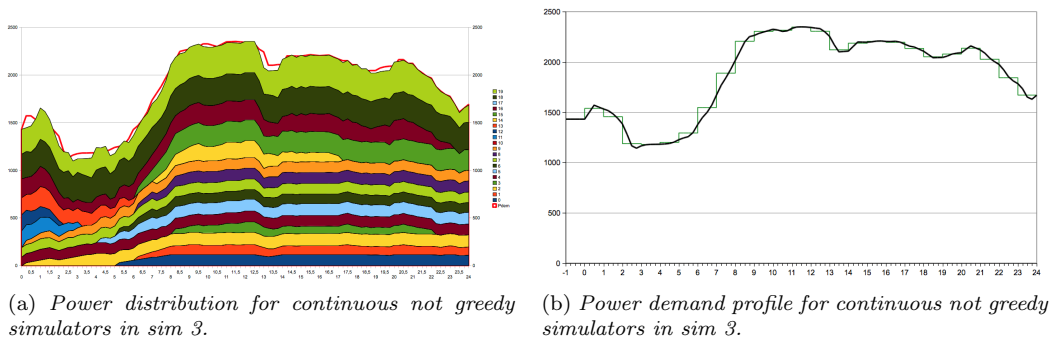
Figure 5.31: Not-Greedy continuous simulation results - sim 3.

(a) *Power distribution for discontinuous not greedy simulators in sim 3.*

(b) *Power demand profile for discontinuous not greedy simulators in sim 3.*
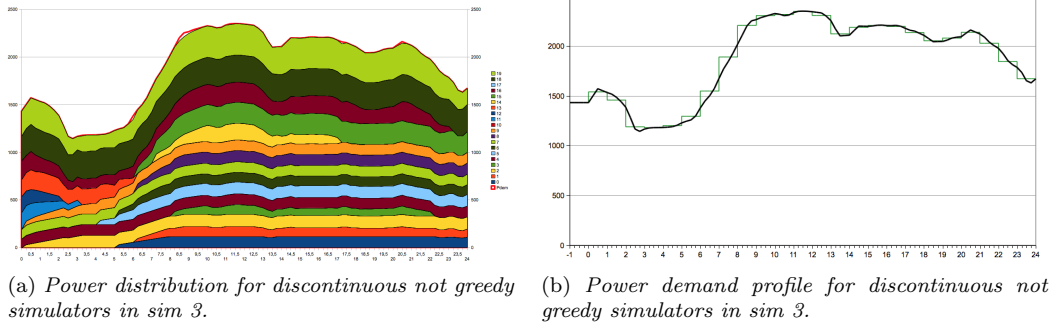
Figure 5.32: Not-Greedy discontinuous simulation results - sim 3.

(a) *Power distribution for continuous not greedy simulators in sim 4.*

(b) *Power demand profile for continuous not greedy simulators in sim 4.*
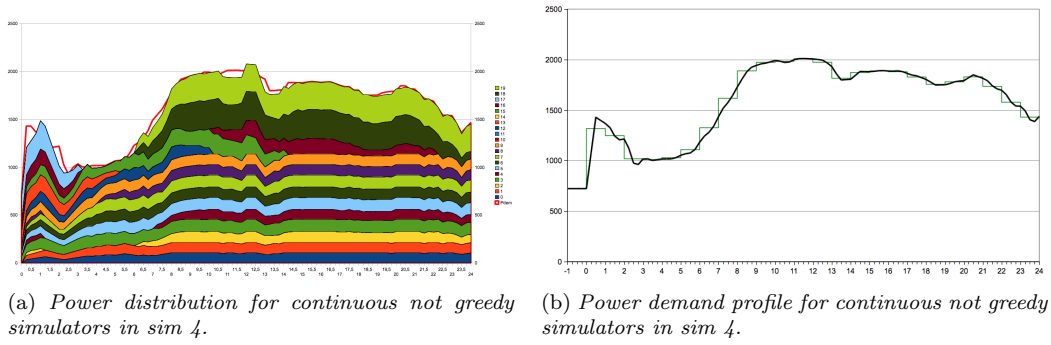
Figure 5.33: Not-Greedy continuous simulation results - sim 4.

(a) *Power distribution for discontinuous not greedy simulators in sim 4.*

(b) *Power demand profile for discontinuous not greedy simulators in sim 4.*
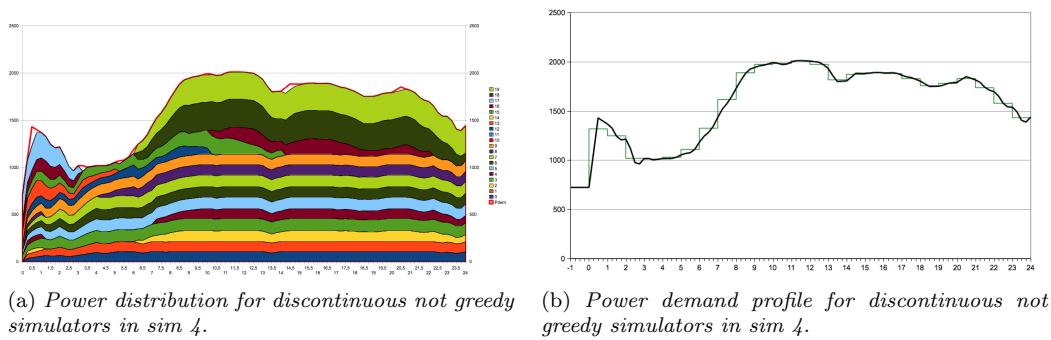
Figure 5.34: Not-Greedy discontinuous simulation results - sim 4.

Part III

Towards an integration of wind energy sources into electrical systems

Chapter 6

Improved Unit Commitment models in presence of wind energy sources *

Conventional electrical systems are highly fossil fuel dependent, being the major contributors to greenhouse gas emissions and depletion of global fossil fuel resources which are characterized by more volatile prices [EIA04]. Several world countries actively support the growing use of renewable energy sources, such as wind, in order to meet Kyoto Protocol targets for reducing greenhouse gas emissions, provide energy security and promote economic development [Hel05]. Wind energy contributes to this target with a significant percentage. In particular, wind has been the most exploited renewable energy source in the United States and in Europe in the past decade [WWE11]. In order to promote the use of renewable energy sources, the European Union Parliament adopted the 'Renewables Directive' in 2001. This directive obliges all the member states to produce a certain amount of electricity from renewable energy sources [Com97] [Par01].

By the end of 2004, 2% of the European Union's electricity was produced by wind turbines; this percentage reached about 6% at the end of 2010 [Sta04]. In some world and European countries wind is an important part of the electricity supply, for instance, in Europe, countries like Spain, Germany and Denmark already produce over 20% of their electricity utilizing wind sources [dEn03] [dPdERA05] [End05] [Aut04]. The amount of electricity produced from wind in Europe will increase in the next years, especially in most of the northern European countries. Also the United States is currently characterized by a strong growth in wind energy production [SDPM04]. Figures (6.1) and (6.2) show how wind energy represents a high portion of world electricity.

In this chapter we present the state of the art on the integration of wind energy sources into conventional electrical systems; hence we illustrate the basic idea of our model and its detailed formulation; thus we set-up a suitable dataset based on realistic data (based on the Italian electrical system); finally we present the simulation results and outline the conclusions.

---

*Part of the material presented in this chapter is based on the following publication *A. Naimo. A novel model for power Unit Commitment in presence of wind energy sources. Technical Report R. 12-14, IASI-CNR, 10/2012.*
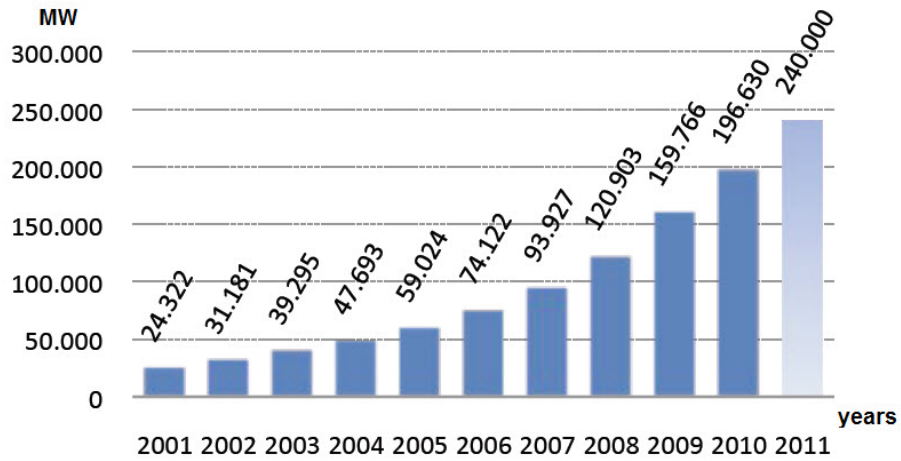
Figure 6.1: World Total Wind Installed Capacity (source: WWEA - World Wind Energy Report 2010).
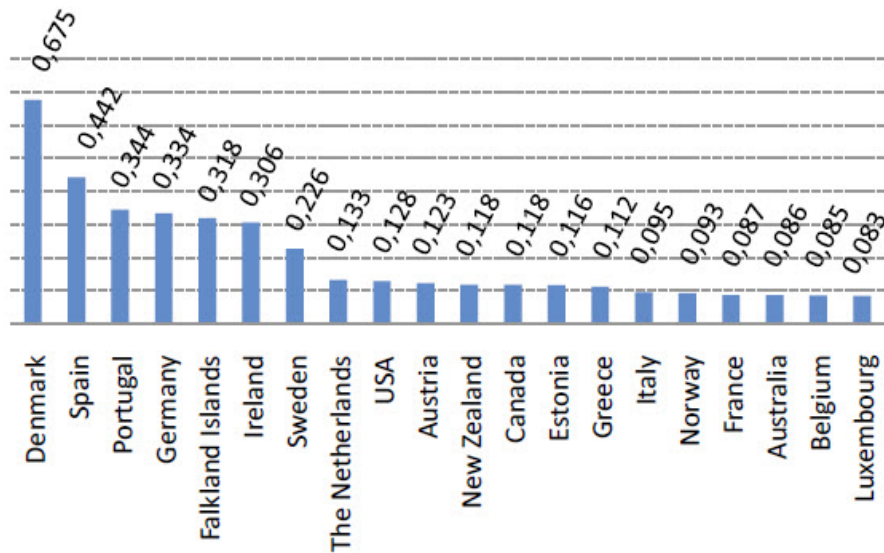
Figure 6.2: Wind Capacity per capita [KW/cap] in some world countries (source: WWEA - World Wind Energy Report 2010).

6.1   State of the art on use of wind into electrical systems

The integration of wind energy into the electrical systems is complex and significantly challenging, especially when large amounts of variable wind generation are introduced [BDO04]. Even if there exist positive aspects related with the utilization of wind energy, there is a current debate on the advantages and disadvantages associated with this type of energy source; some researchers are convinced that the use of wind energy sources leads to high operational costs and influences the stability of the system, resulting in increased prices [Eth06]. When wind power plants are connected to the electrical network, it is necessary to improve transmission lines, in order to avoid grid stability problems, needing additional operational costs. Furthermore, when the uncertainty associated with the electricity produced by wind energy sources becomes greater than the uncertainty of the demand, it is no longer possible to maintain the same power system reliability with the conventional power plant scheduling techniques.

Moreover, the ongoing integration and deregulation of electricity markets in Europe and in the world requires that part of the electricity production is traded daily on power pools where producers state how much electricity they will provide up to 36 hours in advance. This market structure induces additional costs for wind power producers due to the greater unpredictability of wind power at these time horizons. These issues motivate the importance of wind power forecasting techniques that are fundamental to provide accurate forecasts on wind production. Furthermore, power system operators, producers, and energy authorities must know the wind power plants costs, like it happens for conventional generating units, in order to make correct investments and decisions. Evaluating the costs associated with the utilization of wind energy sources is not trivial, since they depend on many factors like the availability of fuels and the capacities of the existing power plants and transmission lines. Finally, wind power plants influence the operational costs of the whole power system, especially if large amounts of wind power are installed.

However, according to some researchers, the development of wind generation should by widely supported in order to avoid the depletion of fossil fuel resources, and to save fuel costs by deallocating conventional generating units, consequently reducing gas emissions [Bro06]. For these reasons, even if the integration of wind energy sources into conventional electrical system is growing in importance, due to its economical and environmental development benefits, particular attention must be devoted to the related practical operational aspects.

As described in the previous chapters, in any power system, power plants should adapt their production to the variations of load, ensuring their output during planned and unplanned outages. As far as this aspect is concerned, conventional power systems that own thermal power plants do not present difficulties in their scheduling dispatch, since daily loads are easily predictable. Statistical distributions are often taken into account to manage the uncertainty in the load and in the variable costs of each power plant. For this reason, stochastic optimization techniques [KW94] are generally used by utilities to schedule power plants in order to minimize the total variable operational and maintenance costs. Furthermore, when power systems with significant amounts of hydro and wind power are considered, the uncertainty in the power production is greater, because the output of wind and hydro generators depends on the varying weather conditions [NGH+04]. Stochastic optimization techniques are also used in such types of systems, since the probability that hydro and wind power plants will not be able to produce electricity at a given time in the future is greater, with respect to thermal power plants.

In order to overcome the drawbacks of the statistical approaches, Gardiner *et al.* [GHSHG03] and DETI [otETD07] presented a simpler approach to operate a power system with wind generation, called '*fuel-saver*' approach. According to the '*fuel-saver*' system operation approach, the

utilities vary the output of their conventional power plants in order to compensate the uncertain output of the wind power plants, resulting in greater fuel and operational costs. In particular, this approach assumes that '*the conventional generation that would run if there was no wind generation on the system will also run when wind generation is connected*'. As the output of wind generation is increased, the output of the conventional generators will be reduced accordingly, but no conventional generation will be shut down [Den07]. This method consists of three steps. At first step, wind generation is not considered in the power scheduling and the UC decisions are made ignoring any installed wind capacity. At second step, once the commitment decision has been made, the wind generation is taken into account. At third step, if wind generation is available, it is used and the conventional plants which have been previously dispatched are de-loaded at their minimum power (but not switched off) to take into account wind generation. If wind production reaches a level such that no more conventional generation can be de-loaded, then any further wind production is curtailed.

Even if this approach is simple, it presents several drawbacks. In fact, it assumes that wind generation has a capacity equal to zero and it is available at real time. Furthermore, this strategy ignores forecasting and reliability issues of wind production and it results in an over commitment of conventional units, making these units running at much lower levels of efficiency than under the approach adopting wind power forecasts. For this reason, the fuel-saver approach results in large amounts of wind energy curtailment, of up to 30% of the annual output at high levels of installed wind power [Den07], and it is a highly inefficient method since the costs of wind generation exceed the benefits at all levels of installed wind generation.

The integration of wind energy sources into conventional electrical system is becoming fundamental due to all the benefits that it leads, nevertheless, this integration must be carried out with particular attention and accuracy, taking into account all the aspects that could conflict with the operational characteristics of the already existing conventional electrical systems.

The large integration of wind energy resources into electrical systems poses important challenges to the power operators in the scheduling of the production and in the management of the network. This leads to the necessity to modify the current industry procedures, such as the UC and the ED, to take into account large amounts of wind power production. Even if an exhaustive literature exists on the general UC problem, devoted on how improve its mathematical formulation and its solution algorithm [Pad04], the research that considers the UC problem in presence of wind energy resources is limited. Some researchers have focused their attention on the improvement of the Security-Constrained Unit Commitment (SCUC) formulation, taking into account wind energy resources, while others have developed novel methods for solving the UC problem. Bart *et al.* presented the first stage of the WILMAR model (Wind Power Integration in the Liberalised Electricity Markets) [WIL05]; later, a more refined UC algorithm based on MILP approaches has been introduced in WILMAR. Tuohy *et al.* [TMDM09] studied the effects of stochastic wind on UC using the WILMAR model and extending their previous studies in [TDM07] and [TMM08]. Ummels *et al.* analyzed the impacts of wind on the UC in the Dutch system, utilizing an ARMA model to consider the forecasting error [UGP+07]. Bouffard and Galiana [BG08] developed a stochastic UC model to take into account wind power generation and system security. Ruiz *et al.* [RPS09] used a stochastic framework, already presented in [RPZ+09], to consider the uncertainty and the variability of wind power in the UC problem. Wang *et al.* [WS08] presented a SCUC algorithm that considers also wind generation, capturing the uncertainty of wind in a number of scenarios.

When we consider a UC problem in presence of wind power plants, it is fundamental to study how the characteristics of the solution are influenced by the introduction or the substitution of

power plants in the set of the available generating units. In particular, it is necessary to:

- analyze how the UC solution is affected by the substitution of conventional generating units with wind turbines and vice versa, within a given set of available generators, in terms of adaptation to the given demand profile;

- analyze how the UC solution is affected by the introduction of new generating units (conventional and wind power plants), within a given set of available generators, in terms of adaptation to the given demand profile;

- determining the best configuration (optimal mix) of available generating units to be utilized, choosing them within a given set of available units, in terms of a fraction of the total energy produced.

In our research activities, a new UC model in presence of wind energy sources has been defined and analyzed, in order to formulate and solve the problem of determining the best configuration (optimal mix) of available thermal, hydro and wind power plants. The proposed model is a generalized form of the UC problem, which takes into account conventional generating units (like thermal and hydro power plants) and wind turbines; we call this model *Generalized Wind Unit Commitment Problem* - (GWUCP). The objective of the new proposed model is to integrate the renewable energy sources, like wind, into a conventional electrical system, taking into account emission considerations and the risk associated with the utilization of wind turbines.

6.2 Basic ideas of the Generalized Wind Unit Commitment Problem

The *Generalized Wind Unit Commitment* - (GWUC) model is based on the concept of subsets of units: it is possible to choose only a part of the available generators, making a dynamic modification of the given set of generating units, in order to determine the best configuration of generators (optimal mix), minimizing the total production cost and satisfying the energy demand. The main difference between this novel model and a classical UC one is that in the classical UC all the available units (conventional and not) are considered committable for each time interval, satisfying the constraints of the model. On the other hand, additional constraints are introduced in the GWUC model, these constraints are taken into account during all the optimization scenario and individuate a subset of units that can be committed: the units that the solution of the model chooses to not belong to these subsets will be never committed. In this way, subset constraints can be used as external requirements, for instance related to regulatory laws, such as limited number of units of a particular type, risk limits associated with not programmable sources, emissions constraints, geographical distribution requirements, reliability and security constraints, transmission constraints. In all these cases we do not know *a priori* which is the single unit that is not committed, hence the classical UC model is not applicable, while the GWUC model could represent a valid approach because, as we will show in the following sections, the additional constraints are general purpose; in this thesis, we have specialized them to geographical distribution requirements, emission control, and risk limit.

The GWUC model is defined as follows. Consider a set of thermal generating units $\mathcal{P}$, a set of hydro generating units $\mathcal{H}$ and a set of wind turbines $\mathcal{W}$. Thermal generating units belonging to the set $\mathcal{P}$ can be grouped into subsets called S_s, with respect to similar technical and operating

characteristics. The same idea can be applied to the case of wind turbines belonging to the set $\mathcal{W}$. These units can be grouped into subsets called E_e, with respect to similar technical and operating characteristics. On the other hand, we assume that hydro generating units belonging to the set $\mathcal{H}$ are not grouped into subsets. In fact, the optimal mix depends on the status of the units, as we will describe in the following sections, and no binary variables are necessary to model the status of hydro units, since these power plants are not subjected to on/off constraints. For this reason, we assume that hydro units are always available in the set $\mathcal{H}$.

Thermal units and wind turbines could be grouped into subsets as depicted in the example of Fig. 6.3. For the issues described above, the representation of the set $\mathcal{H}$ of hydro units is not considered.
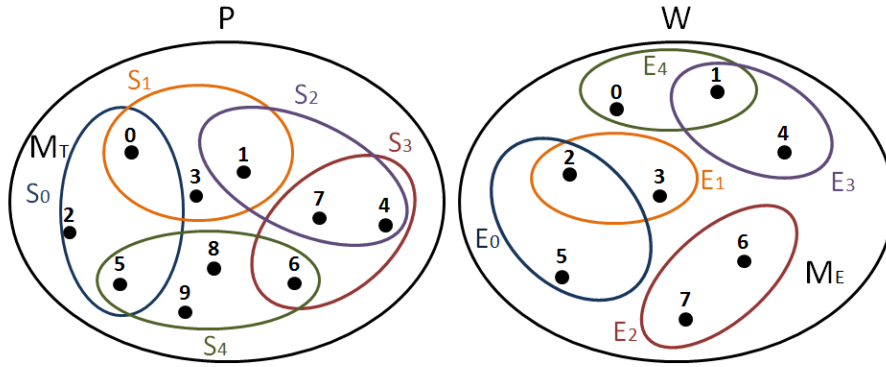
Figure 6.3: Assigned data structure for the GWUC problem.

In this example, thermal units subsets S_s are defined as follows:

$$S_0 = \{0, 2, 5\}$$

$$S_1 = \{0, 1, 3\}$$

$$S_2 = \{1, 4, 7\}$$

$$S_3 = \{4, 6, 7\}$$

$$S_4 = \{5, 6, 8, 9\}$$

Indeed, wind turbines subsets E_e are shown below:

$$E_0 = \{2, 5\}$$

$$E_1 = \{2, 3\}$$

$$E_2 = \{6, 7\}$$

$$E_3 = \{1, 4\}$$

$$E_4 = \{0, 1\}$$

Assigned this data structure for thermal units and wind turbines, the objective of the GWUC model is to analyze all the given subsets S_s and E_e and to determine the optimal mix of thermal, hydro and wind generating units, in order to satisfy the energy demand, minimizing the total production cost and respecting the operating and technical constraints of the generating units.

The optimal mix of generating units M_{OPT} has the following properties:

- it is a subset of the available thermal and wind generating units set, this means that all the available units could be chosen in the optimal mix. In other words, we have:

$$M_{OPT} \subseteq \mathcal{P} \cup \mathcal{W}$$

- generating units which constitutes the optimal mix M_{OPT} belong to subsets S_s and E_e which satisfy certain relationship criteria; this concept is better described in the sections 6.3.7 and 6.3.8.

Given the assigned data structure depicted in Fig. 6.3, an example of optimal mix of thermal and wind units is shown in Fig. 6.4. M_T represents the optimal mix of thermal units, while M_E is the optimal mix of wind turbines.
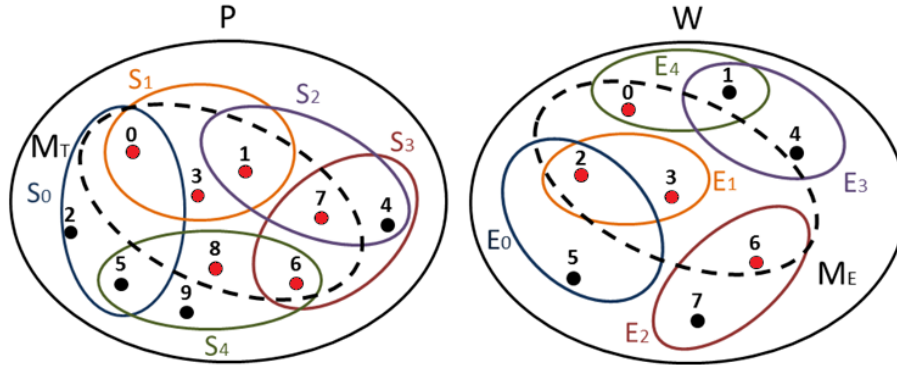
Figure 6.4: Optimal mix of thermal and wind units.

Subsets S_s and E_e have some structural properties, as described below:

- $\bigcup_{s=0}^{n_S-1} S_s = \mathcal{P}$ ($\bigcup_{e=0}^{n_E-1} E_e = \mathcal{W}$) $\rightarrow$ the union of subsets S_s (E_e) is equal to the given set of thermal (wind) units $\mathcal{P}$ ($\mathcal{W}$) (where n_S (n_E) is the number of subsets S_s (E_e) of thermal (wind) units);

- $S_s \cap S_{s'} \neq \varnothing \; \forall s \neq s' \; s, s' = \{0, \dots, n_S - 1\}$ ($E_e \cap E_{e'} \neq \varnothing \; \forall e \neq e' \; e, e' = \{0, \dots, n_E - 1\}$) $\rightarrow$ subsets S_s (E_e) could be not disjoint: a thermal (wind) unit could belong to different subsets S_s (E_e) at the same time, with respect to its technical and operating characteristics.

In the following section, a mathematical model for the GWUC is proposed and described.

6.3 Mathematical formulation of the GWUC

In this section, the mathematical formulation of the GWUC is presented. In particular, the objective function, the variables and the constraints considered for the formulation are shown.

6.3.1 Objective function

As described previously in chapter 1, the objective of the UC decision process is to select the generating units that have to be on or off, the type of fuel that has to be utilized, the power generation level for each unit and the spinning reserve margins. The objective function of the UC problem consists in minimizing the total operational cost, subjected to the system operating constraints. In the case of the GWUC, the objective function includes also the operational costs related with the utilization of wind energy sources, and the penalty terms associated with the maximum and minimum energy deficit or surplus produced by thermal and wind units. In our model, we assume that the objective function has a quadratic form with respect to the power p_t^i produced by the thermal unit i at time period t, as explained in [HRNC01].

Consider a set $\mathcal{P}$ of thermal units, a set $\mathcal{H}$ of hydro cascades, each comprising one or more basin units, and a set $\mathcal{W}$ of wind turbines. $\mathcal{T} = \{1, \ldots, n\}$ is the set of time periods defining the time horizon (the time period "0" will be used to indicate the initial conditions of the power system). Introducing status and power production variables of the thermal units, u_t^i (binary variable) and p_t^i (continuous variable), respectively, with $i \in \mathcal{P}$, $t \in \mathcal{T}$, and introducing status, start-up, shut-down variables of the wind units, x_t^w, y_t^w, z_t^w (binary variables), respectively, with $w \in \mathcal{W}$, $t \in \mathcal{T}$, the objective function of the UC, representing the total power production cost to be minimized, has the following form

$$
\begin{aligned}
&\sum_{i \in \mathcal{P}} \left(s^i(u^i) + \sum_{t \in \mathcal{T}} \left(a_t^i (p_t^i)^2 + b_t^i p_t^i + c_t^i u_t^i \right) \right) \\
&+ \sum_{w \in \mathcal{W}} \sum_{t \in \mathcal{T}} (e_t^w x_t^w + f_t^w y_t^w + g_t^w z_t^w) \\
&+ M\theta_{up} + M\theta_{down}
\end{aligned}
\tag{6.1}
$$

where

- $s^i(u^i)$ is the start-up costs function of unit i, possibly time-dependent;

- a_t^i is the quadratic term of power cost function of thermal unit i at period t, expressed in €/MW^2;

- b_t^i is the linear term of power cost function of thermal unit i at period t, expressed in €/MW;

- c_t^i is the constant term of power cost function of thermal unit i at period t, expressed in €;

- e_t^w is the power production cost of wind turbine w at period t, expressed in €;

- f_t^w is the start-up cost of wind turbine w at period t, expressed in €;

- g_t^w is the shut-down cost of wind turbine w at period t, expressed in €;

- M is a sufficiently high constant value (big M) for slack variables θ_{down} and θ_{up}, expressed in MWh;

- θ_{down} is a slack variable that represents the minimum energy deficit (negative) or surplus (positive) produced by thermal and wind units, required to satisfy the exchange constraints for $\overline{d}_{min}$, expressed in MWh;

- θ_{up} is a slack variable that represents the maximum energy deficit (negative) or surplus (positive) produced by thermal and wind units, required to satisfy the exchange constraints for $\overline{d}_{max}$, expressed in MWh.

As shown previously in chapter 1, power plants are subjected to technical constraints, depending on their type and characteristics. The constraints of GWUC can be grouped in four categories:

- operating constraints for thermal units;

- operating constraints for hydro units;

- operating constraints for wind turbines;

- power balance constraints.

6.3.2   Operating constraints for thermal units

The operating requirements of thermal generating units are usually expressed by inequality constraints, which are used to model the technical characteristics of the units. As far as minimum up and down time constraints, unit generation capability limits and ramp rate constraints, we considered the constraints presented in chapter 2, section 2.1.2, which are the typical thermal requirements of the classical UC problem. Nevertheless, in order to properly model the concept of subsets and optimal mix, new additional constraints are required. In particular, we introduce a binary variable, called v_{th}, which indicates if a thermal unit belongs to the optimal mix (value 1) or not (value 0). As far as thermal units are concerned, a thermal unit i should belong to the optimal mix M_{OPT} in order to be utilized. In other terms $u_t^i \to v_{th}^i$. A thermal unit i belongs to the optimal mix M_{OPT} if all the other constraints on v_{th}^i are satisfied. Constraints on u_t^i and v_{th}^i variables are thus defined as follows

$$u_t^i - v_{th}^i \leq 0 \quad t \in \mathcal{T} \tag{6.2}$$

The constraints presented above represent the following logical implication

$$u_t^i \to v_{th}^i$$

according to the truth table depicted below

If a thermal unit i does not belong to the optimal mix M_{OPT} ($v_{th}^i = 0$), it can't be turned on ($u_t^i = 0$) (first row of the truth table).

A thermal unit i belongs to the optimal mix M_{OPT} ($v_{th}^i = 1$), but it is turned off ($u_t^i = 0$) (second row of the truth table).

If a thermal unit i does not belong to the optimal mix M_{OPT} ($v_{th}^i = 0$), it can't be turned on (it must be necessarily $u_t^i = 0$) (third row of the truth table).

A thermal unit i belongs to the optimal mix M_{OPT} ($v_{th}^i = 1$) and it is turned on ($u_t^i = 1$) (fourth row of the truth table).

u_t^i	v_{th}^i	
0	0	T
0	1	T
1	0	F
1	1	T

6.3.3   Operating constraints for hydro units

As it happens for the thermal generating units, the operating requirements of hydro generating units are usually expressed by inequality constraints, which are used to model the technical characteristics of the generators themselves. As far as constraints on discharged water, on reservoir volume and hydro balance constraints, we considered the constraints presented in chapter 2, section 2.1.3, which are the typical hydro requirements of the classical UC problem. We did not require additional constraints, since we made the assumption that hydro units are not grouped into subset and for this reason other binary variables such as v_{th} are not needed.

6.3.4   Operating constraints for wind turbines

In order to represent the technical restrictions of wind turbines, new constraints to model the operating characteristics of this type of generating units are required. As it happens for thermal units, minimum up and down time constraints, and unit generation capability limits are required. Furthermore, in order to properly model the concept of subsets and optimal mix, new additional constraints are needed. In particular, we introduce a binary variable, called v_{wind}, which indicates if a wind unit belongs to the optimal mix (value 1) or not (value 0). As far as wind units are concerned, a wind unit w should belong to the optimal mix M_{OPT} in order to be utilized. In other terms $x_t^w \to v_{wind}^w$. A wind unit w belongs to the optimal mix M_{OPT} if all the other constraints on v_{wind}^w are satisfied. Constraints on x_t^w and v_{wind}^w variables are thus defined as follows

$$x_t^w - v_{wind}^w \le 0 \quad t \in \mathcal{T} \tag{6.3}$$

The constraints presented above represent the following logical implication

$$x_t^w \to v_{wind}^w$$

whose meaning is analogous to that explained above in section 6.3.2, regarding thermal units.

Moreover, other constraints which are related to wind power output forecasts and curtailment are needed. In the following sections, these operating constraints for wind turbines are presented.

Minimum up and down time constraints

These constraints are related with wind turbines start-up and shut-down and are useful to determine if a wind turbine is going to be turned on or off at time t. In general, these transition phases can represent additional costs related to wind power plants maintenance.

$$x_t^w - x_{t-1}^w - y_t^w \le 0 \quad t \in \mathcal{T} \tag{6.4}$$

$$y_t^w \ge 0 \quad t \in \mathcal{T} \tag{6.5}$$

$$x_{t+1}^w - x_t^w - z_t^w \leq 0 \quad t \in \mathcal{T} \tag{6.6}$$

$$z_t^w \geq 0 \quad t \in \mathcal{T} \tag{6.7}$$

In the previous expressions:

- x_t^w is the status of the wind turbine w at time t (0/1);

- y_t^w is the start-up variable for wind turbine w at time t (0/1);

- z_t^w is the shut-down variable for wind turbine w at time t (0/1).

Unit generation capability limits

The power output $p_{W,t}^w$ of a wind turbine must vary between a minimum and a maximum power, as expressed below:

$$\overline{p}_{W,min}^w x_t^w \leq p_{W,t}^w \leq \overline{p}_{W,t}^w x_t^w \qquad t \in \mathcal{T} \tag{6.8}$$

where

- $\overline{p}_{W,min}$ is the minimum power output of wind turbine w, expressed in MW;

- $\overline{p}_{W,max}$ is the maximum power output of wind turbine w, expressed in MW;

- $\overline{p}_{W,t}^w$ is the forecast power output of wind turbine w, at time t, expressed in MW.

The upper bound on power is determined by the forecast power output of the wind turbine, assuming that it represents the maximum power output produced by the generating unit.

Constraints on forecasts and curtailment

In wind production, in a given time period t, part of the power produced by the wind turbine w ($p_{W,t}^w$) is actually utilized to satisfy the required demand, while the remaining part is curtailed ($c_{W,t}^w$); the sum of these quantities (power actually utilized and curtailment) must balance the forecast power output, as expressed by the following constraint

$$p_{W,t}^w + c_{W,t}^w - \overline{p}_{W,t}^w x_t^w = 0 \qquad t \in \mathcal{T} \tag{6.9}$$

Furthermore, the power curtailed must not be greater than the forecast power output, as expressed by the following constraint

$$c_{W,t}^w - \overline{p}_{W,t}^w x_t^w \leq 0 \qquad t \in \mathcal{T} \tag{6.10}$$

and it must not be greater than the maximum power output of the wind turbine w at time t, as described below

$$c_{W,t}^w \leq \overline{p}_{W,max} \qquad t \in \mathcal{T} \tag{6.11}$$

6.3.5   Power balance constraints

Global constraints represent the fundamental constraints for the UC problem: at each time period $t \in \mathcal{T}$ forecast energy demand to be satisfied must be balanced by the output energy produced by thermal, hydro and wind power plants. In the real world, the demand to be satisfied is the result of the trading in the day-ahead-market and in the intra-day market, we have already discussed about this aspect in the previous chapter when we formulated the Reduced Economic Dispatch model. In this dissertation we focus on stressing the novel aspects of the formulation of GWUC model (such as subset constraints and wind constraints) instead of well-known balance constraints. Uncertainty aspects related with forecast energy demand are deeply investigated in [Nai08] where Robust Optimization models for UC are proposed.

As we have seen in the previous chapter it's possible to formulate a power-based UC model, nevertheless for sake of clarity and without loss of generality, in this formulation we assume that power is constant in each time interval t (which is equal to one hour), so that energy and power produced at time t are equivalent from a numerical point of view.

Let $\bar{d}_t$ be the forecast demand to be satisfied (measured in MWh) in each time period $t \in \mathcal{T}$, and let α^j be the *power-to-discharged-water efficiency* coefficient (measured in MWh/m^3) which represents the efficiency of hydro unit j (q_t^j represents the discharged water of hydro unit j at time period t and it is measured in m^3).

Global constraints are expressed as follows:

$$\sum_{i \in \mathcal{P}} p_t^i + \sum_{h \in \mathcal{H}} \sum_{j \in \mathcal{H}(h)} \alpha^j q_t^j$$
$$+ \sum_{w \in \mathcal{W}} p_{W,t}^w = \bar{d}_t \ t \in \mathcal{T} \tag{6.12}$$

6.3.6   Exchange constraints for thermal and wind power plants

A thermal power plant (wind turbine) can be substituted by a wind turbine (thermal power plant). The total output power produced by thermal and wind power plants which belong to the optimal mix must be greater than a given minimum value and must be less than a given maximum value. There can be different reasons why a conventional unit could or should be replaced by a wind turbine and vice versa: unit scheduled or not scheduled maintenance, mid/long-term replacement plan, regulatory laws such as incentive compensation.

The exchange constraints for thermal and wind power plants are expressed as follows

$$\sum_{i \in \mathcal{P}} \bar{p}_{max}^i v_{th}^i + \sum_{w \in \mathcal{W}} \bar{p}_{W,max}^w v_{wind}^w - \theta_{up} \leq \bar{d}_{max} \tag{6.13}$$

$$\sum_{i \in \mathcal{P}} \bar{p}_{min}^i v_{th}^i + \theta_{down} \geq \bar{d}_{min} \tag{6.14}$$

where

- $\bar{d}_{min}$ is the minimum energy demand that has to be satisfied by the system in security and it is expressed in MWh;

- $\overline{d}_{max}$ is the maximum energy demand that has to be satisfied by the system in security and it is expressed in MWh.

Variables v_{th}^i and v_{wind}^w do not depend on time period t, but only on the units i and w, because the optimal mix must be valid for all the planning horizon $\mathcal{T}$. When the constraint with $\overline{d}_{min}$ is considered, we assume that $\overline{p}_{W,min}^w = 0$ since in this case the risk associated with the utilization of wind energy sources is equal to zero.

$\overline{d}_{min}$ and $\overline{d}_{max}$ do not represent the minimum and maximum demand of the profile curve, but they refer to a lower bound and an upper bound for the production system. In other words, they are useful to dimension the minimum and maximum capacity of the production system. In general, this is necessary in order to guarantee some required parameters like primary, secondary and tertiary reserves and in order to make the system more tolerant to eventual failures.

It is very difficult to satisfy the relationship constraints for thermal and wind power plants, since thermal and wind power plants are not comparable in terms of power output.

For these reasons, we introduce slack variables in order to relax these constraints. A very high cost in the objective function (big M) is associated to these slack variables. In particular, θ_{up} represents a power surplus over $\overline{d}_{max}$ that system can produce. Even if it is an acceptable situation from an operating and a security point of view, it leads to high costs which are considered in the objective function. θ_{down} represents a power deficit which must be overcome buying energy from external sources; this could be a dangerous scenario from a system security point of view and it could lead to high costs which should be considered in the objective function. The big M value should be big enough to penalize the slack variables utilization. It could be assumed equal to the highest cost of the available thermal units.

6.3.7 Constraints on thermal generating units subsets

The main assumption of the GWUC model is that the thermal and wind units are grouped into different subsets according to the geographical site where they are located and to their operating characteristics such as the type of fuel utilized, and the CO_2 emissions rate (for thermal units only). Based on these assumptions, the first constraint introduced is related to the number of thermal units belonging to the optimal mix. In particular, the number of thermal units belonging to subset S_s and to the optimal mix must be less or equal than an assigned number $\overline{n}_S^{max}$ for the given subset S_s:

$$\sum_{i \in \mathcal{P}} \overline{\chi}_s^i v_{th}^i \leq \overline{n}_S^{max}$$
$$s = \{0, \dots, n_S - 1\} \tag{6.15}$$
$$\overline{n}_S^{max} \leq |S_s|$$

The term n_S represents the number of subsets S_s of thermal generating units. The term $\overline{\chi}_s^i$ is equal to 1 if the thermal unit i belongs to the subset S_s, it is equal to 0 otherwise. All the terms $\overline{\chi}_s^i$ for all the thermal units i available constitute the Q matrix which describes the topology of the given subset S_s. An example which describes how the Q matrix is utilized is presented in section 6.3.9. Based on what described above, it is easy to observe that the quantity $\sum_{i \in \mathcal{P}} \overline{\chi}_s^i v_{th}^i$ represents the number of thermal units of subset S_s which also belong to thermal optimal mix M_T. The following property holds:

$$\sum_{i \in \mathcal{P}} \overline{\chi}_s^i v_{th}^i \leq |S_s| \tag{6.16}$$

The costs of thermal units belonging to subset S_s and to the optimal mix must be less or equal than an assigned cost of the units $\overline{c}_S^{max}$ for the given subset S_s:

$$\sum_{i \in \mathcal{P}} \overline{\chi}_s^i v_{th}^i \gamma^i \leq \overline{c}_S^{max} \qquad s = \{0, \ldots, n_S - 1\} \tag{6.17}$$

The term γ^i represents the cost associated to the thermal unit i. In our model, this cost has been determined considering the specific value of the CO_2 emissions of the generating unit i. We have decided to limit this type of cost in order to lead the model to choose for the optimal mix the units that posses the lowest value of emissions, e.g., the units that are more 'virtuous' from this point of view, regardless the absolute value of CO_2 that they will emit after producing a certain amount of energy. This aspect differentiates the GWUC model with subset constraints from a classical UC model with 'emission control', where the emissions are considered as a cost in the objective function.

6.3.8 Constraints on wind turbines subsets

As far as wind units are concerned, the same assumptions on subsets are made. In particular, these units are grouped into different subsets according to the geographical site where they are located and to their operating characteristics. Based on these assumptions, the first constraint introduced is related to the number of wind units belonging to the optimal mix. In particular, the number of wind turbines belonging to subset E_e and to the optimal mix must be less or equal than an assigned number $\overline{n}_E^{max}$ for the given subset E_e:

$$\begin{aligned} &\sum_{w \in \mathcal{W}} \overline{r}_e^w v_{wind}^w \leq \overline{n}_E^{max} \\ &e = \{0, \ldots, n_E - 1\} \\ &\overline{n}_E^{max} \leq |E_e| \end{aligned} \tag{6.18}$$

The term n_E represents the number of subsets E_e of wind generating units. The term $\overline{r}_e^w$ is equal to 1 if the wind unit w belongs to the subset E_e, it is equal to 0 otherwise. All the terms $\overline{r}_e^w$ for all the wind units w available constitute the R matrix which describes the topology of the given subset E_e. An example which describes how the R matrix is utilized is presented in section 6.3.9. Based on what described above, it is easy to observe that the quantity $\sum_{w \in \mathcal{W}} \overline{r}_e^w v_{wind}^w$ represents the number of wind units of subset E_e which also belong to thermal optimal mix M_E. The following property holds:

$$\sum_{w \in \mathcal{W}} \overline{r}_e^w v_{wind}^w \leq |E_e| \tag{6.19}$$

The costs of wind turbines belonging to subset E_e and to the optimal mix must be less or equal than an assigned cost of the units $\overline{c}_E^{max}$ for the given subset E_e:

$$\sum_{w \in \mathcal{W}} \overline{r}_e^w v_{wind}^w \beta^w \leq \overline{c}_E^{max} \qquad s = \{0, \ldots, n_E - 1\} \tag{6.20}$$

The term β^w represents the cost associated to the wind unit w.

6.3.9 An example of thermal and wind power plants subsets

Consider the example depicted in Fig. 6.5 (in this case, subsets are disjoint, in order to simplify the example).
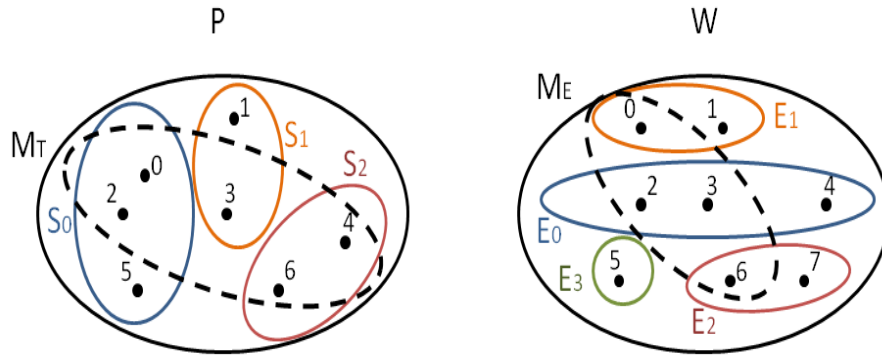
Figure 6.5: Thermal and wind power plants optimal mix.

In this example, subsets S_s of thermal units are defined as follows:

$$S_0 = \{0, 2, 5\}$$

$$S_1 = \{1, 3\}$$

$$S_2 = \{4, 6\}$$

Subsets E_e of wind turbines are defined as follows:

$$E_0 = \{2, 3, 4\}$$

$$E_1 = \{0, 1\}$$

$$E_2 = \{6, 7\}$$

$$E_3 = \{5\}$$

Q matrix is given by

$$\begin{pmatrix} 1 & 0 & 1 & 0 & 0 & 1 & 0 \\ 0 & 1 & 0 & 1 & 0 & 0 & 0 \\ 0 & 0 & 0 & 0 & 1 & 0 & 1 \end{pmatrix}$$

R matrix is given by

$$
\begin{pmatrix}
0 & 0 & 1 & 1 & 1 & 0 & 0 & 0 \\
1 & 1 & 0 & 0 & 0 & 0 & 0 & 0 \\
0 & 0 & 0 & 0 & 0 & 0 & 1 & 1 \\
0 & 0 & 0 & 0 & 0 & 1 & 0 & 0
\end{pmatrix}
$$

If we suppose that the thermal optimal mix is given by (variables v_{th}^i)

$$
\begin{pmatrix}
1 \\
0 \\
1 \\
1 \\
1 \\
0 \\
1
\end{pmatrix}
$$

and that the wind optimal mix is given by (variables v_{wind}^w)

$$
\begin{pmatrix}
1 \\
0 \\
1 \\
1 \\
0 \\
0 \\
1 \\
0
\end{pmatrix}
$$

we obtain the following result

- 2 thermal units of subset S_0 belong to optimal mix;

- 1 thermal unit of subset S_1 belongs to optimal mix;

- 2 thermal units of subset S_2 belong to optimal mix;

- 2 thermal units of subset E_0 belong to optimal mix;

- 1 wind turbine of subset E_1 belongs to optimal mix;

- 1 wind turbine of subset E_2 belongs to optimal mix;

- 0 wind turbines of subset E_3 belong to optimal mix.

6.3.10 Risk constraints correlated to the use of wind turbines

In order to complete the formulation described above, it is very useful to investigate the possibility of introducing a measure of the expected risk, expressed in probability terms, correlated to the utilization of wind power plants in an electrical system. The probability risk Pb_t^w is the probability associated to the happening of a given event, which, in our case, is represented by the deficit of a part of energy (the power $p_{W,t}^w$ produced in 1 hour is numerically equal to the energy) that wind turbines $w \in \mathcal{W}$ have not produced in the time interval t with respect to the total energy demand to satisfy ($\bar{d}_t$).

For each wind unit $w \in \mathcal{W}$ and each time interval $t \in \mathcal{T}$ we have

$$Pb_t^w = r_t^w \cdot \frac{p_{W,t}^w}{\bar{d}_t} \tag{6.21}$$

where

- r_t^w is the '*risk coefficient*' which is calculated as follows

$$r_t^w = \left(1 + log\left(1 + \frac{\epsilon_t^w}{\overline{p}_{W,t}^w}\right)\right)$$

- $\frac{p_{W,t}^w}{\bar{d}_t}$ is the amount of wind energy with respect to the total demand, which represents the usage of wind energy.
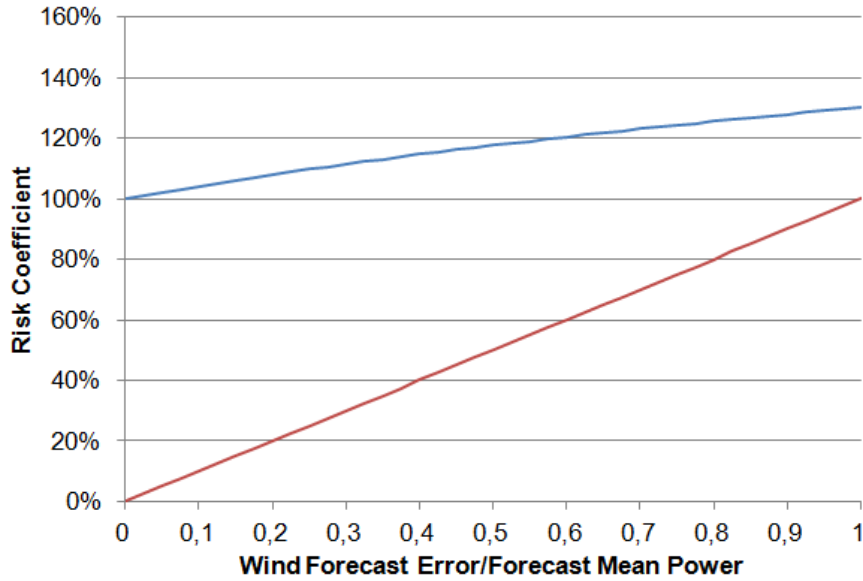
Figure 6.6: Risk coefficient and wind forecast.

Based on these calculations, the risk coefficient takes into account the wind forecast error ϵ_t^w (for each time interval t and each wind turbine w) with respect to the average forecast power

$\overline{p}_{W,t}^w$. The risk is calculated as the amount of the real wind power used $p_{W,t}^w$ (e.g., that has been calculated by the UC model) actually associated with the risk coefficient. The shape of the risk coefficient is depicted in Fig. 6.6. The risk coefficient could be calculated as the simple percentage of the forecast error with respect to the forecast wind power, e.g.:

$$r_t^w = \frac{\epsilon_t^w}{\overline{p}_{W,t}^w}$$

This way, when the forecast error is zero, the risk will be zero regardless of the amount of wind energy used to satisfy the demand. Moreover, when the forecast error is equal to wind nominal power output, the risk coefficient will be equal to 1, and the risk will be only correlated with the amount of wind energy used. These scenarios are not realistic from a practical point of view. Using a logarithmic form allows us to obtain a partially smoother curve of the risk coefficient making it move in a limited range: when the forecast error is zero, the risk coefficient will be equal to 1, and the risk overall will be only correlated to the amount of wind energy used; on the other hand, when the forecast error is greater than zero, the risk coefficient has only the ability to amplify the risk.

The risk probability for each Pb_t^w could be bounded as follows

$$Pb_t^w \leq \overline{Pb}_t^w$$

where $\overline{Pb}_t^w$ is a constant given in input, expressed in probability terms, which represents an upper limit on the risk allowed by the system.

It is possible to determine a global risk associated to the planning horizon $\mathcal{T}$ for all the wind turbines $w \in \mathcal{W}$, as follows

$$Pb = \sum_{t,w \in \mathcal{T}, \mathcal{W}} r_t^w \cdot \frac{p_{W,t}^w}{\overline{d}_t} \tag{6.22}$$

and it could be bounded as follows

$$Pb \leq \overline{Pb}_{max}$$

6.4 How to generate realistic input data for the GWUC

As described in the previous sections, the GWUC has been defined and implemented taking into account risk and subset constraints which are related to emissions considerations. In order to analyze the performances of the new model, we have to set a suitable and realistic instance as input of the UC problem. This instance should have at least three types of generating units, such as conventional thermal, hydro, and wind units. Each type of unit should be different with respect to the class of power, the ramp-rate limits, the type of fuel utilized, the emission rate, the geographical area, the reservoir limits, and wind forecast speed and wind forecast error. In order to set this instance, we have considered the following steps:

- studying the topology of the Italian energy production system, in terms of type and number of units utilized, taking into account the statistical data reported by Terna S.p.A. [ST10];

- performing an accurate analysis of this data in order to realize a data instance which realistically represents the topology of the Italian electrical system, with dimensions scaled about 1:5 with respect to the real system power capacity.

Unit Type	Inst. Power (MW)	%
Thermal	75704	71.08%
Hydro	21520	20.21%
Renewable - Solar	3469	3.26%
Renewable - Wind	5814	5.46%
Total	106507	100.00%

Table 6.1: Total power production per type of unit.

Area	Inst. Power (MW)	%
North	52428	49.23%
Central area	15391	14.45%
South+Islands	38669	36.31%
Total	106488	100.00%

Table 6.2: Total power production per geographical area.

6.4.1 Analysis of the Italian energy production system

In order to set the data instance, we have first analyzed the topology of the Italian electrical system, taking into account the aspects described below regarding thermal, hydro, and wind units, based on 2010 Terna's statistics. In our analysis, we have neglected the other renewable energy sources, to focus our attention on the analysis of the behavior of wind units in a realistic electrical system. The following aspects have thus been taken into account:

- the total power production (expressed in MW) generated by each type of unit (thermal, hydro and renewable) (table 6.1);

- the total power production (expressed in MW) generated by each geographical area (northern, southern and central geographical area) (table 6.2).

Thermal units

As far as thermal units are concerned, they have been classified with respect to their:

- class of power (table 6.3);

- geographical area (table 6.4);

- type of fuel used (table 6.5).

To reduce the number of generating units considered in our instance, we assumed to neglect the thermal units with a power less than 25 MW, thus, we consider the repartition of the classes of power depicted in table 6.6.

Class Type (MW)	# Units	%	Inst. Power (MW)	%	Average Power (MW)
≥ 500	33	1.90%	23581	34%	714
200-500	86	4.95%	29644	43%	344
100200	41	2.36%	7532	11%	183
50100	53	3.05%	3944	6%	74
2550	35	2.02%	1349	2%	38
≤ 25	1488	85.71%	2928	4%	2
Total	1736	100.00%	68978	100%	40

Table 6.3: Thermal power production per class of power.

Area	# Units	%	Inst. Power (MW)	%
North	1626	63.24%	35122	46.39%
Central area	429	16.69%	13236	17.48%
South+Islands	516	20.07%	27345	36.12%
Total	2571	100.00%	75703	100.00%

Table 6.4: Thermal power production per geographical area.

Fuel Type	# Units	%	Inst. Power (MW)	%	Average Power (MW)
Other Fuels(NGL/Coal/etc)	915	36.60%	1762	2%	1.9
Natural Gas	998	39.92%	32950	45%	33.0
Crude Oil	296	11.84%	8180	11%	27.6
Two Fuels (Oil+Gas)	244	9.76%	25400	34%	104.1
Three Fuels (Oil+Gas+Others)	47	1.88%	5600	8%	119.1
Total	2500	100.00%	73892	100%	29.6

Table 6.5: Thermal power production per fuel type.

Class Type (MW)	# Units	%	Inst. Power (MW)	%	Average Power (MW)
≥ 500	33	13.31%	23581	36%	714
200-500	86	34.68%	29644	45%	344
100-200	41	16.53%	7532	11%	183
50-100	53	21.37%	3944	6%	74
25-50	35	14.11%	1349	2%	38
Total	248	100.00%	68978	100%	278

Table 6.6: Thermal power production per class of power (thermal units with power $< 25MW$ have been neglected).

Hydro units

As far as hydro units are concerned, they have been classified with respect to their:

- class of power (table 6.7);

- geographical area (table 6.8).

To reduce the number of generating units considered in our instance, we assumed to neglect the hydro units with a power less than 10 MW, thus, we consider the repartition of the classes of power depicted in table 6.9.

Class Type (MW)	# Units	%	Inst. Power (MW)	%	Average Power (MW)
≥ 200	17	0.62%	8251	38%	485
100-200	25	0.91%	3368	15%	134
50-100	29	1.06%	1964	9%	67
30-50	62	2.27%	2439	11%	39
20-30	55	2.01%	1402	6%	25
10-20	121	4.42%	1733	8%	14
5-10	135	4.93%	958	4%	7
1-5	565	20.65%	1252	6%	2
≤ 1	1727	63.12%	523	2%	1
Total	2736	100.00%	21890	100%	8

Table 6.7: Hydro power production per class of power.

Area	# Units	%	Inst. Power (MW)	%
North	2190	80.04%	15636	72.66%
Central area	339	12.39%	1460	6.78%
South+Islands	207	7.57%	4423	20.55%
Total	2736	100.00%	21519	100.00%

Table 6.8: Hydro power production per geographical area.

Class Type (MW)	# Units	%	Inst. Power (MW)	%	Average Power (MW)
≥ 200	17	5.50%	8251	43%	485
100-200	25	8.09%	3368	18%	134
50-100	29	9.39%	1964	10%	67
30-50	62	20.06%	2439	13%	39
20-30	55	17.80%	1402	7%	25
10-20	121	39.16%	1733	9%	14
Total	309	100.00%	19157	100%	62

Table 6.9: Hydro power production per class of power (hydro units with power $< 10MW$ have been neglected).

Wind units

As far as wind units are concerned, they have been classified with respect to their geographical area and sub-area (in this case, sub-areas are represented by the Italian regions). This classification is very useful since wind units cannot be considered as stand-alone units to be given in input to the UC problem, but they should be grouped into a single '*wind farm*', in order to obtain a data instance characterized by a lower dimension. Without loss of generality it is possible to consider a wind farm as a single unit assuming that all the wind turbines that compose this wind farm are subjected to the same behavior. This is an acceptable simplification if the wind farm considered as a single unit is relative small and it is not so widespread over a given geographical area. For these reasons, as we will also see in the next section, we will consider the distributions depicted in tables 6.10 and 6.11.

Area	# Units	%	Inst. Power (MW)	%
North	49	10.06%	56	0.96%
Central area	28	5.75%	56	0.96%
South+Islands	410	84.19%	5702	98.07%
Total	487	100.00%	5814	100.00%

Table 6.10: Wind power production per geographical area.

Sub-Area (Region)	# Units	Inst. Power (MW)
Piemonte	7	14
Valle D'Aosta	1	0
Lombardia	1	0
Trentino Alto Adige	5	3
Veneto	5	2
Friuli Venezia Giulia	0	0
Liguria	15	19
Emilia Romagna	15	18
Toscana	17	45
Umbria	1	2
Marche	3	0
Lazio	7	9
Abruzzi	25	218
Molise	23	367
Campania	76	803
Puglia	134	1288
Basilicata	28	280
Calabria	31	672
Sicilia	62	1436
Sardegna	31	639
Total	487	5815

Table 6.11: Wind power production per geographical sub-area.

6.4.2 Generating a scaled instance for the GWUC problem

Our objective is to realize an instance scaled about 1:5 with respect to the Italian electrical system, which takes into account with a good approximation the analyses of the data previously performed considering the Terna's statistics. For this reason, we have considered some basic assumptions for each type of units, described in the following sections.

Thermal units

Regarding thermal units, we have considered 65 units. We have used one of the instances considered in the simulation phase performed for the analysis of the new UC models described in chapters 5 and 4. Then, we have adjusted some parameters in order to respect the statistics we have seen above. In particular, the following sections explain how this adjustment has been made.

Maximum and minimum power output   We have assigned a class of power to each unit, based on the percentage distribution indicated in table 6.6. For each class of power, we have generated a random number, bounded between the extremal values of the class and rounded to 5 MW; this value has been assumed as the maximum power (i.e., for class $200 - 500$ a suitable maximum power could be 350 MW). Minimum power has been generated as a random percentage bounded between $20\% - 50\%$ of the maximum power. In this way, we have obtained the distribution depicted in table 6.12, that well reflects the real set of data previuosly described.

Class Type (MW)	# Units	%	Inst. Power (MW)	%	Average Power (MW)
≥ 500	8	12.31%	4770	30%	596
200-500	22	33.85%	8100	52%	368
100-200	10	15.38%	1520	10%	152
50-100	15	23.08%	985	6%	66
25-50	10	15.38%	355	2%	35
Total	65	100.00%	157308	100%	242

Table 6.12: Thermal power production per class of power: scaled instance.

Fuel cost coefficient   We have assigned a fuel type class to each unit, based on the percentage distribution indicated in table 6.3. We have used a pseudo-random algorithm to assign higher costs to the smallest units and higher costs to oil-fuel based units. In this way, we have obtained the distribution depicted in table 6.13. This distribution well reflects the percentage values of the real set of data, and it widely overestimates the average power, because in the real world there exist more units than in the scaled instance.

Fuel Type	# Units	%	Inst. Power (MW)	%	Average Power (MW)
Other Fuels (NGL/Coal/etc)	15	23.08%	715	5%	48
Natural Gas	26	40.00%	6135	39%	236
Crude Oil	10	15.38%	2500	16%	250
Two Fuels (Oil+Gas)	13	20.00%	5920	38%	455
Three Fuels (Oil+Gas+Others)	1	1.54%	460	3%	460
Total	65	100.00%	15730	100%	242

Table 6.13: Thermal power production per fuel type: scaled instance.

Geographical distribution   We have assigned a geographical label to each unit, based on the percentage distribution indicated in table 6.4, reflecting the number of the units and the nominal power for each area. In this way, we have obtained the distribution depicted in table 6.14.

Emission rate   The different types of fuels (oil, gas, etc) have been classified with respect to the emissions of CO_2 produced (g CO_2/KWh); we obtained this classification analyzing the data reported by IEA [IEA12], which is briefly resumed in table 6.15. Based on this data, we have aggregated the values and extrapolated an average value for each class of fuel considered, reported in table 6.16. In the real world each power unit has its own specific emission rate, hence, in order to generalize our approximation, we have calculated a corrective coefficient assuming a dependence of the emission rate with respect to the installed power (expressed in MW). According to our assumption, the emission rate is higher for smaller power units. The emission coefficient, called

Area	# Units	%	Inst. Power (MW)	%
North	36	55.38%	7730	49.14%
Central area	11	16.92%	2675	17.01%
South+Islands	18	27.69%	5325	33.85%
Total	65	100.00%	15730	100.00%

Table 6.14: Thermal power production per geographical area: scaled instance.

K^i, is related with each thermal unit i and it has been calculated as follows

$$K^i = 1 - log(\frac{\overline{p}^i_{max}}{\overline{p}})$$
(6.23)

where $\overline{p}^i_{max}$ is the maximum power of the unit i of the scaled instance, and $\overline{p}$ is the average power calculated taking into account all the units of the scaled instance. In this way, the generating units that present a higher power are associated with a lower CO_2 coefficient and vice versa, since, from a practical point of view, the units with smaller dimensions are usually characterized by greater emissions; this concept is depicted in the Fig. 6.7.
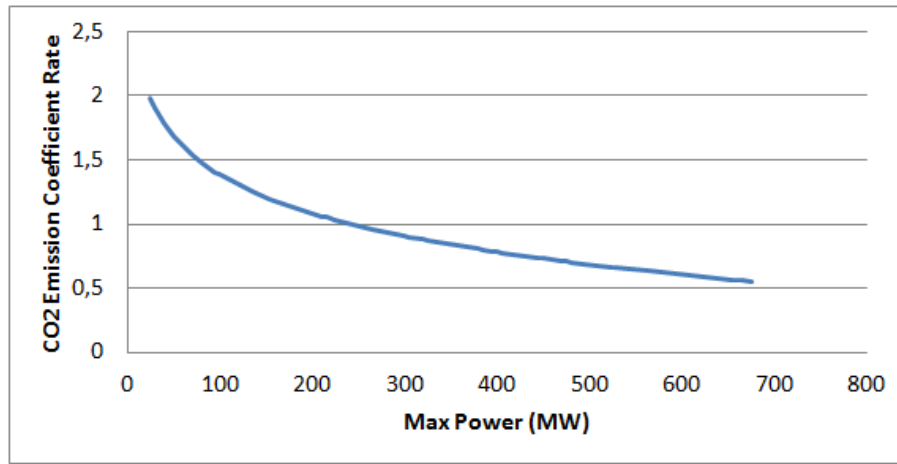
Figure 6.7: CO_2 emissions coefficient.

The distribution of the average-emission coefficient is depicted in table 6.17.

Fuel Class	Fuel Type	Emission: gCO_2/kWh
Other Fuels (NGL/Coal/etc)	Anthracite	835
Other Fuels (NGL/Coal/etc)	Coking coal	715
Other Fuels (NGL/Coal/etc)	Other bituminous coal	830
Other Fuels (NGL/Coal/etc)	Sub-bituminous coal	920
Other Fuels (NGL/Coal/etc)	Lignite	940
Other Fuels (NGL/Coal/etc)	Natural gas liquids	500
Other Fuels (NGL/Coal/etc)	Liquefied petroleum gases	600
Other Fuels (NGL/Coal/etc)	Petroleum coke	970
Natural Gas	Natural gas	370
Crude Oil	Crude oil	610
Crude Oil	Kerosene	650
Crude Oil	Gas/diesel oil	650
Crude Oil	Fuel oil	620
Not considered	Peat	560
Not considered	Industrial waste	$450 - 1300$
Not considered	Municipal waste (non-renewable)	$450 - 2500$
Not considered	Patent fuel	890
Not considered	Coke oven coke	510
Not considered	BKB/peat briquettes	$500 - 1100$
Not considered	Gas works gas	380
Not considered	Coke oven gas	390
Not considered	Blast furnace gas	2100
Not considered	Oxygen steel furnace gas	1900

Table 6.15: Emission rates (source: IEA statistics).

Fuel Class	Emission: gCO_2/kWh
Other Fuels (NGL/Coal/etc)	788
Natural Gas	370
Crude Oil	632
Two Fuels (Oil+Gas)	501
Three Fuels (Oil+Gas+Others)	597

Table 6.16: Average emission rate values calculated considering IEA statistics.

Fuel Class	Average Emission Rate: gCO_2/kWh	Min Emission Rate	Max Emission Rate
Other Fuels (NGL/Coal/etc)	1372	1108	1564
Natural Gas	434	208	623
Crude Oil	654	464	874
Two Fuels (Oil+Gas)	373	278	498
Three Fuels (Oil+Gas+Others)	430	430	430
Total	671	208	1564

Table 6.17: Average emission rate values calculated considering IEA statistics

Hydro units

Regarding hydro units, we have considered 55 units. We have used one of the instances considered in the simulation phase performed for the analysis of the new UC models described in chapters 5 and 4. Then, we have adjusted some parameters in order to respect the statistics we have seen above. In particular, the following sections explain how this adjustment has been made.

Maximum power output We have assigned a class of power to each unit, based on the percentage distribution indicated in table 6.9. For each class of power we have generated a random number, bounded between the extremal values of the class and rounded to 5 MW, this value has been assumed as the maximum power (i.e. for class $100 - 200$ a suitable maximum power could be 130 MW). In this way, we have obtained the distribution depicted in table 6.18. This distribution is very similar to the real one extrapolated from the Terna's statistics.

Class Type (MW)	# Units	%	Inst. Power (MW)	%	Average Power (MW)
≥ 200	4	7.27%	1445	37.34% 361	
100-200	6	10.91%	895	23.13%	149
50-100	7	12.73%	485	12.53%	69
25-50	16	29.09%	640	16.54%	40
10-25	22	40.00%	405	10.47%	18
Total	55	100.00%	3870	100%	70

Table 6.18: Hydro power production per class of power: scaled instance.

Geographical distribution We have assigned a geographical label to each unit, based on the percentage distribution indicated in table 6.8, reflecting the number of the units and the nominal power for each area. In this way, we have obtained the distribution depicted in table 6.19.

Area	# Units	%	Inst. Power (MW)	%
North	39	70.91%	2800	72.35%
Central area	10	18.18%	370	9.56%
South+Islands	6	10.91%	700	18.09%
Total	55	100.00%	3870	100.00%

Table 6.19: Hydro power production per geographical area: scaled instance.

Wind units

Regarding wind units, we have considered 32 units. We realized the wind data instance respecting the statistics we have seen above. In particular, the following sections explain how this data instance has been defined.

Geographical distribution The 32 units we have considered in our instance represent a 'wind farm'. To determine the wind turbines maximum power output, we have first considered the geographical distribution depicted in table 6.11. Then, for each region, we have scaled the nominal power by a factor of 15%, hence we have subdivided the regions with more than 10 MW of installed

power in n different wind farms. This type of distribution is depicted in table 6.20. For example, the 'Puglia' region has a real nominal installed power of 1288 MW, its scaled nominal power is 194 MW; we have divided this region into 4 wind farms of different nominal power, as described below:

- "'Puglia1"', of 15 MW;

- "'Puglia2"', of 33 MW;

- "'Puglia3"', of 56 MW;

- "'Puglia4"', of 88 MW.

Finally, we have marked each wind farm with the correct geographical area, in order to realize the distribution shown in table 6.10; we have thus obtained the distribution depicted in table 6.21 for the scaled instance.

Production costs To determine the production average costs for each wind farm, we have assumed as main indicators two mean values confirmed in the literature [EWE12]:

1. the cost based on the wind turbine energy output is about 75 €/MWh;

2. the cost based on the wind turbine Operation and Maintenance (OM) activities is about 15 €/MWh.

Estimating the OM costs is a very complex activity and it is beyond the scope of this thesis; nevertheless, without loss of generality, it is possible to assume that:

- OM costs based on installed nominal power strongly depend on the wind farm scale factor: a wind farm with only 1 turbine, and with only 1 MW of installed power, has a very high cost with respect to a wind farm with dozen of turbines;

- OM costs depend on the age of the wind turbine: older turbines are subjected to failures more frequently, and repair services are more expensive.

For these reasons, in our model we consider the following three types of costs, which are properly included in the objective function:

- e_t^w is the power production cost of wind turbine w at period t, expressed in €;

- f_t^w is the start-up cost of wind turbine w at period t, expressed in €;

- g_t^w is the shut-down cost of wind turbine w at period t, expressed in €.

To take into account these considerations, we have formulated a simple model to assign the costs to each wind farm. We have used a pseudo-random algorithm that assign higher costs to smaller wind farms. Fig. 6.8 shows the trend of the costs generated by the pseudo-random algorithm.

Finally, in our model, as input of the wind farms we considered the forecast power generated taking into account the wind speed. In order to produce a realistic average forecast power profile, we have used the synthetic wind data generator proposed in chapter 7.

Area	Wind Farm	Inst. Power (MW)	%
North	Emilia Romagna	3	0.34%
	Liguria	3	0.34%
	Piemonte	3	0.34%
	Trentino A. A.	1	0.11%
	Veneto	1	0.11%
	Total	11	1.26%
Central area	Lazio	2	0.23%
	Toscana	7	0.80%
	Umbria	1	0.11%
	Totale	10	1.15%
South+Islands	Abruzzi1	20	2.29%
	Abruzzi2	12	1.38%
	Basilicata1	10	1.15%
	Basilicata2	30	3.44%
	Calabria1	16	1.83%
	Calabria2	32	3.67%
	Calabria3	54	6.19%
	Campania1	60	6.88%
	Campania2	40	4.59%
	Campania3	20	2.29%
	Molise1	36	4.13%
	Molise2	20	2.29%
	Puglia1	15	1.72%
	Puglia2	33	3.78%
	Puglia3	56	6.42%
	Puglia4	88	10.09%
	Sardegna1	12	1.38%
	Sardegna2	34	3.90%
	Sardegna3	48	5.50%
	Sicilia1	11	1.26%
	Sicilia2	22	2.52%
	Sicilia3	44	5.05%
	Sicilia4	88	10.09%
	Sicilia5	50	5.73%
	Total	851	97.59%
Grand Total		872	100.00%

Table 6.20: Wind farms distribution: scaled instance.

Area	# Units	%	Inst. Power (MW)	%
North	5	15.63%	11	1.26%
Central area	3	9.38%	10	1.15%
South+Islands	24	75.00%	851	97.59%
Total	32	100.00%	872	100.00%

Table 6.21: Wind power production per geographical area: scaled instance.
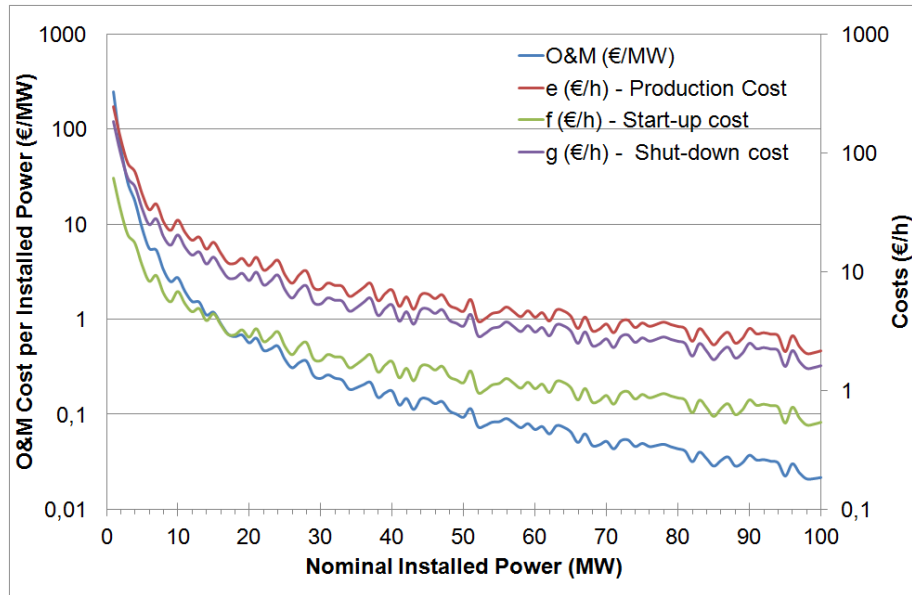
Figure 6.8: Wind farms cost coefficient included in the GWUC objective function.

Load

A typical load, that represents the forecast energy demand, has been extracted from the Terna's statistical data. In particular, we have chosen the actual demand depicted in Fig. 6.9, then this load has been scaled with a 1:5 factor in order to generate the simulated load shown in Fig. 6.10.
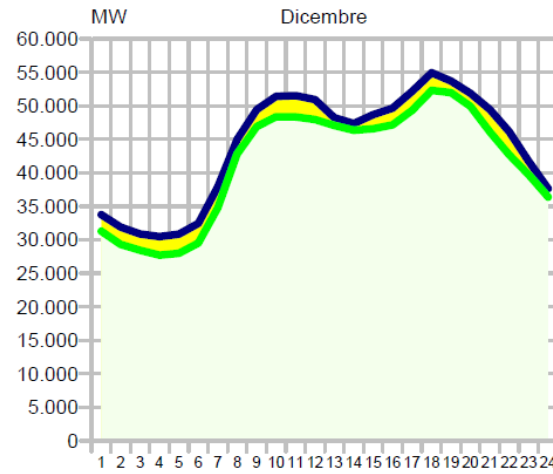
Figure 6.9: Actual load reported in Italy on 15th December 2010.
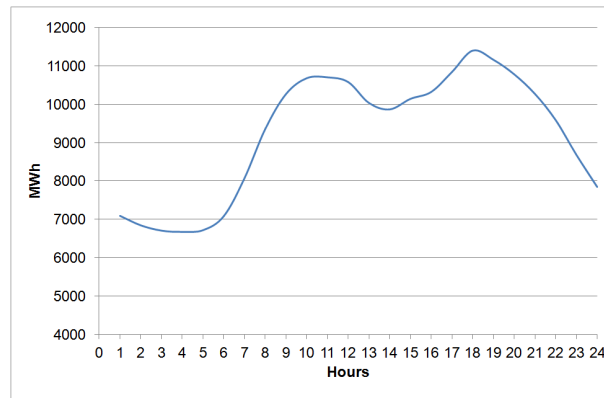
Figure 6.10: Scaled load used in the simulation phase.

Final Instance

The main characteristics of the units chosen in the scaled instance are resumed in table 6.22.

Id	Type	Area	Inst. Power (MW)
0	Hydro	North	280
1	Hydro	North	465
2	Hydro	North	490
3	Hydro	North	210
4	Hydro	North	140
5	Hydro	North	155
6	Hydro	Central area	100
7	Hydro	South+Islands	165
8	Hydro	South+Islands	180
9	Hydro	South+Islands	155
10	Hydro	North	90
11	Hydro	North	55
12	Hydro	North	60
13	Hydro	North	80
14	Hydro	South+Islands	60
15	Hydro	South+Islands	80
16	Hydro	South+Islands	60
17	Hydro	North	40
18	Hydro	North	40
19	Hydro	North	40
20	Hydro	North	40
21	Hydro	North	45
22	Hydro	North	40
23	Hydro	North	40
24	Hydro	North	45
25	Hydro	North	40
26	Hydro	Central area	35
27	Hydro	Central area	40
28	Hydro	Central area	40
29	Hydro	Central area	40
30	Hydro	Central area	35
31	Hydro	North	45
32	Hydro	North	35
33	Hydro	North	15
34	Hydro	North	25
35	Hydro	North	25
36	Hydro	North	15
37	Hydro	North	15
38	Hydro	North	15
39	Hydro	North	20
40	Hydro	North	20
41	Hydro	North	20
42	Hydro	North	25
43	Hydro	North	15
44	Hydro	North	15
45	Hydro	North	20
46	Hydro	Central area	25
47	Hydro	Central area	20
48	Hydro	Central area	25
49	Hydro	Central area	10
50	Hydro	North	20
51	Hydro	North	15
52	Hydro	North	15
53	Hydro	North	15
54	Hydro	North	15

Table 6.22: Scaled instance: hydro units main parameters.

Id	Type	Area	Inst. Power (MW)	Fuel Type	Emission Rate
0	Thermal	North	565	Natural Gas	234
1	Thermal	North	665	Natural Gas	208
2	Thermal	North	595	Natural Gas	225
3	Thermal	North	525	Natural Gas	246
4	Thermal	North	525	Two Fuels	332
5	Thermal	South+Islands	565	Two Fuels	317
6	Thermal	Central area	655	Two Fuels	284
7	Thermal	South+Islands	675	Two Fuels	278
8	Thermal	South+Islands	215	Natural Gas	389
9	Thermal	North	385	Natural Gas	295
10	Thermal	North	210	Natural Gas	393
11	Thermal	North	245	Two Fuels	498
12	Thermal	North	450	Two Fuels	366
13	Thermal	North	480	Two Fuels	352
14	Thermal	North	320	Two Fuels	440
15	Thermal	North	450	Two Fuels	366
16	Thermal	South+Islands	325	Two Fuels	437
17	Thermal	Central area	470	Two Fuels	357
18	Thermal	Central area	495	Two Fuels	345
19	Thermal	Central area	265	Two Fuels	481
20	Thermal	Central area	300	Natural Gas	335
21	Thermal	South+Islands	475	Natural Gas	262
22	Thermal	North	400	Natural Gas	289
23	Thermal	North	405	Natural Gas	287
24	Thermal	South+Islands	460	Three Fuels	430
25	Thermal	South+Islands	225	Crude Oil	652
26	Thermal	South+Islands	395	Crude Oil	498
27	Thermal	South+Islands	305	Crude Oil	568
28	Thermal	South+Islands	445	Crude Oil	465
29	Thermal	South+Islands	380	Crude Oil	508
30	Thermal	North	100	Crude Oil	875
31	Thermal	North	155	Crude Oil	754
32	Thermal	North	135	Crude Oil	792
33	Thermal	North	200	Crude Oil	684
34	Thermal	South+Islands	160	Natural Gas	436
35	Thermal	South+Islands	160	Natural Gas	436
36	Thermal	South+Islands	180	Natural Gas	418
37	Thermal	South+Islands	135	Natural Gas	464
38	Thermal	Central area	135	Natural Gas	464
39	Thermal	Central area	160	Crude Oil	746
40	Thermal	North	65	Natural Gas	581
41	Thermal	North	60	Natural Gas	594
42	Thermal	North	80	Natural Gas	548
43	Thermal	North	65	Natural Gas	581
44	Thermal	North	65	Natural Gas	581
45	Thermal	North	50	Natural Gas	623
46	Thermal	North	55	Natural Gas	608
47	Thermal	North	65	Natural Gas	581
48	Thermal	North	50	Natural Gas	623
49	Thermal	North	70	Natural Gas	569
50	Thermal	South+Islands	60	Other Fuels	1265
51	Thermal	South+Islands	70	Other Fuels	1213
52	Thermal	South+Islands	95	Other Fuels	1108
53	Thermal	Central area	80	Other Fuels	1167
54	Thermal	Central area	55	Other Fuels	1295
55	Thermal	North	35	Other Fuels	1450
56	Thermal	North	40	Other Fuels	1404
57	Thermal	North	30	Other Fuels	1502
58	Thermal	North	50	Other Fuels	1328
59	Thermal	North	45	Other Fuels	1364
60	Thermal	North	40	Other Fuels	1404
61	Thermal	North	25	Other Fuels	1565
62	Thermal	North	30	Other Fuels	1502
63	Thermal	Central area	35	Other Fuels	1450
64	Thermal	Central area	25	Other Fuels	1565

Table 6.23: Scaled instance: thermal units main parameters.

Id	Type	Area	Inst. Power (MW)	Wind Farm
0	Wind	North	3	Piemonte
1	Wind	North	1	Trentino Alto Adige
2	Wind	North	1	Veneto
3	Wind	North	3	Liguria
4	Wind	North	3	Emilia Romagna
5	Wind	Central area	7	Toscana
6	Wind	Central area	1	Umbria
7	Wind	Central area	2	Lazio
8	Wind	South+Islands	20	Abruzzi1
9	Wind	South+Islands	12	Abruzzi2
10	Wind	South+Islands	36	Molise1
11	Wind	South+Islands	20	Molise2
12	Wind	South+Islands	60	Campania1
13	Wind	South+Islands	40	Campania2
14	Wind	South+Islands	20	Campania3
15	Wind	South+Islands	15	Puglia1
16	Wind	South+Islands	33	Puglia2
17	Wind	South+Islands	56	Puglia3
18	Wind	South+Islands	88	Puglia4
19	Wind	South+Islands	10	Basilicata1
20	Wind	South+Islands	30	Basilicata2
21	Wind	South+Islands	16	Calabria1
22	Wind	South+Islands	32	Calabria2
23	Wind	South+Islands	54	Calabria3
24	Wind	South+Islands	11	Sicilia1
25	Wind	South+Islands	22	Sicilia2
26	Wind	South+Islands	44	Sicilia3
27	Wind	South+Islands	88	Sicilia4
28	Wind	South+Islands	50	Sicilia5
29	Wind	South+Islands	12	Sardegna1
30	Wind	South+Islands	34	Sardegna2
31	Wind	South+Islands	48	Sardegna3

Table 6.24: Scaled instance: wind units main parameters.

6.5 Results and discussion

We performed different simulations (about 50) in order to verify with a significant data set the behavior of the model with respect to the risk, the variability of the subsets, the limits on the minimum and maximum capacity of the system, the restrictions on the CO2 emissions used as a cost in the subset constraints. The GWUC model has been implemented in a C++ programming language code, and is has been solved with the CPLEX 11.0 commercial solver, using the perspective-cuts algorithm presented in [FG06]. The results obtained with these simulations are presented in the following sections.

6.5.1 Analysis of the UC models

In order to compare the different types of UC models present in the literature, we analyzed the shape of the objective function with respect to the use of wind energy sources, considering:

- the average use of wind over a 24 hours time horizon (Fig. 6.11);

- the maximum hourly use of wind over a 24 hours time horizon (Fig. 6.12).

Fig. 6.11 and Fig. 6.12 compare four different types of UC models:

1. standard UC: this formulation does not take into account wind generating units;

2. wind UC: this formulation considers also wind generating units that are integrated in the solution of the UC problem, but that are not associated with risk considerations;

3. fuel saver UC: in this formulation the energy demand that has to be satisfied does not take into account the amount of forecast energy that should be produced by wind units;

4. GWUC: as it happens for wind UC, in this formulation wind generating units are integrated in the solution of the UC problem and they are associated with risk considerations, correlated with the forecast error which can be controlled (limited).

Based on the Wind UC model, the graphs depicted in Fig. 6.11 and Fig. 6.12, which show the objective function with respect to the use of wind energy, can be divided in four areas, where the models can be placed in theory. In the first area, we can find the UC models which are characterized by a high objective function and a high risk. This type of model is not interesting at all from a practical point of view. In the second area, we can find the UC models which are characterized by a lower objective function associated with a higher risk. Placed in this area, we can find the fuel saver UC model. In the third area, we can find the UC models which are characterized by a lower objective function associated with a lower risk. Placed in this area, we can find the wind UC model, which is characterized by the lowest objective function without risk control, but integrating wind production scheduling in the solution of the UC problem. In theory, the models belonging to this area should be further investigated, but they are not realizable from a practical point of view, since it is not possible to reduce the objective function reducing at the same time the use of an energy source at a lower cost (in this case wind) and consequently the risk with respect to a conventional energy source. In the extreme side of the fourth area, we can find the standard UC models which are characterized by the highest objective function correlated with a risk and a wind use equal to zero. Within the fourth area, we can find the GWUC model which is characterized by a control of the risk. Thus, this model 'moves' from the standard UC model to the wind UC model and vice versa.
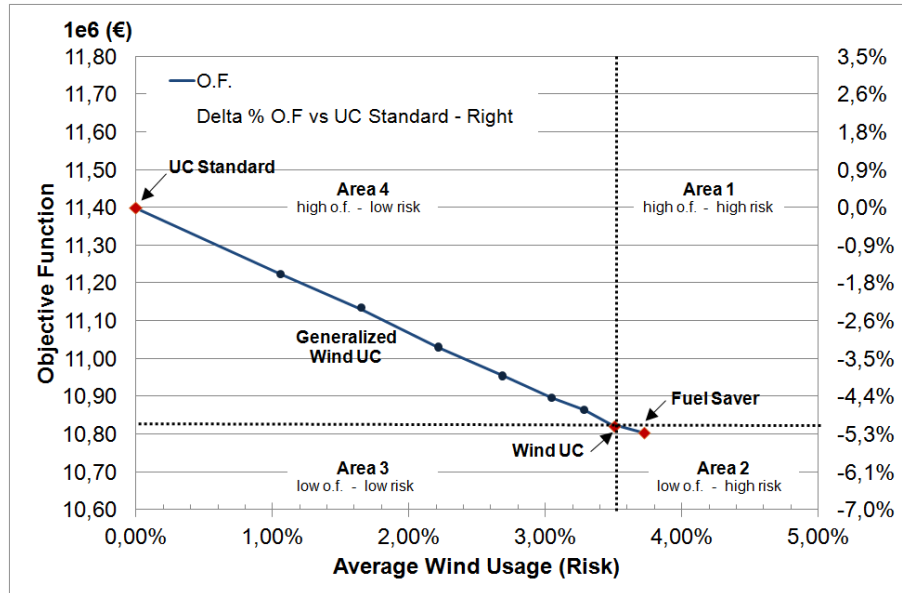
Figure 6.11: Objective function vs average wind usage (risk).
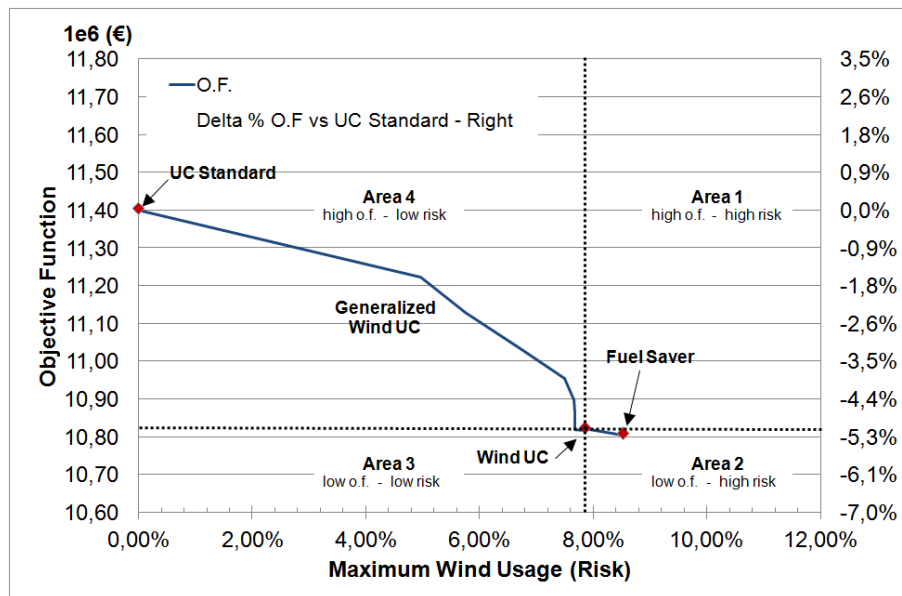
Figure 6.12: Objective function vs maximum wind usage (risk).

6.5.2 Analysis of the risk correlated with the use of wind energy sources

In order to analyze the risk correlated with the use of wind energy sources, we limited the percentage of the global risk Pb, which has been defined as described in section 6.3.10.

Fig. 6.13 shows that the objective function decreases when the use of wind energy increases. The objective function becomes stable when all wind farms are used (in this case, the risk is the highest and the model corresponds to the wind UC one).

The value of the percentage depends on the instance and on the demand that has to be satisfied, for this reason, the result is typical of the instance itself. Fig. 6.14 shows the variation of the use of wind (average and hourly maximum) with respect to the limit imposed on the risk (Pb_{max}).

It is very interesting to observe that the average use tends to increase when the global risk increases (Pb), while the value of the maximum risk (calculated as the maximum value between the risk (Pb_t^w) of each wind unit in a single time interval) rapidly reaches the limit. It is possible to explain this behavior analyzing the data of the instance, since when the risk increases, wind farms with higher dimensions are preferred, in order to un-commit the thermal power plants, determining a higher hourly risk (Pb_t^w).
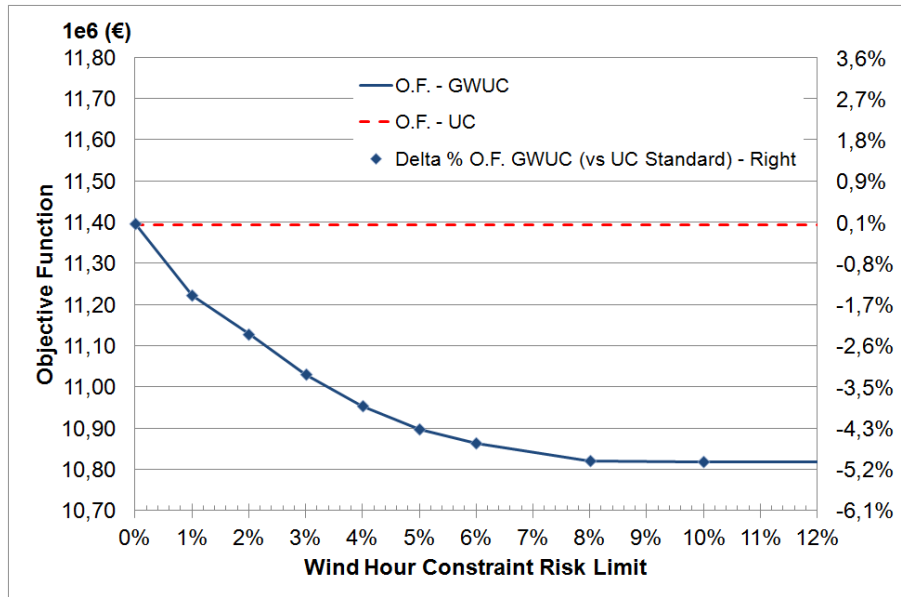
Figure 6.13: Objective function vs wind hour constraint risk limit.
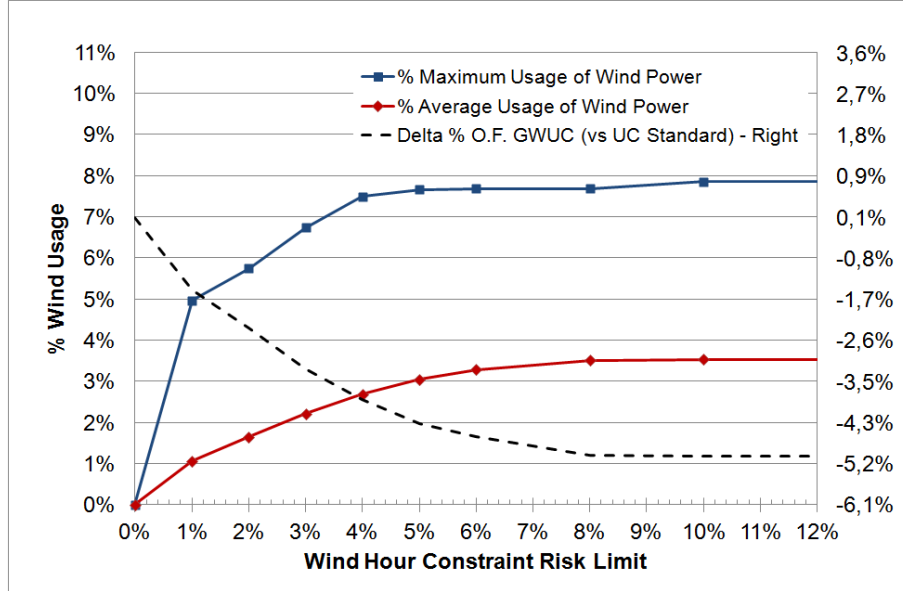
Figure 6.14: Percentage of wind usage vs wind hour constraint risk limit.

6.5.3 Analysis of the influences of the maximum system capacity on the UC solution

The lower bound constraint over the maximum nominal capacity of the system can be applied for market restrictions (for instance, to reduce the monopolistic component), and it influences the exchange constraints between thermal and wind generating units. In general, it imposes a constraint on the use of the generating units (number/type). In a typical instance as the one utilized, the generating units with higher maximum nominal power are associated with lower costs, but also with stronger ramp-up/ramp-down constraints, and consequently they are characterized by a lower flexibility while satisfying the demand. Furthermore, in the UC model that takes into account also hydro generating units, the load variability is satisfied more or less by the variable use of hydro units not subjected to ramp-up/ramp-down constraints. This behavior is easily observable in the graph that shows the hourly production associated with each type of generating unit (thermal, hydro) obtained solving the classical UC problem (Fig. 6.15).

Even if the reduction of the maximum nominal capacity of the system does not affect the feasibility of the solution, it determines a strong increase of the objective function when a certain limit is overcome. This limit is typical of the given instance and depends on the demand to be satisfied; in our case it is about 8000 MW, e.g., 70% of the maximum demand. Furthermore, the reduction of the maximum nominal capacity of the system reduces the number of thermal and wind generating units that belong to the optimal mix. Observing Fig. 6.16 and Fig. 6.17, it is possible to individuate three zones:

1. in the first zone the maximum capacity is greater than 130% of the maximum demand; a reduction of the maximum capacity does not produces effects on the number of units belonging to the optimal mix and on the objective function. This behavior can be explained
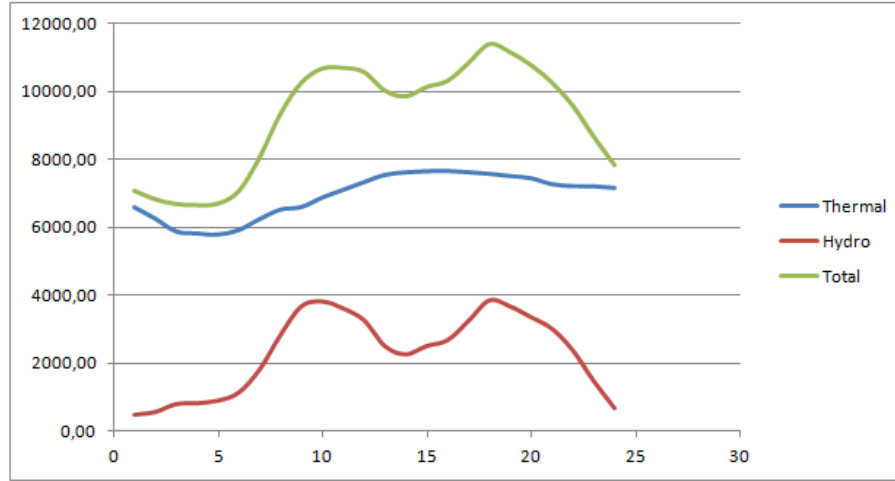
Figure 6.15: Thermal and hydro hourly production.

analyzing the solution in detail: the variability of the available generating units leads the model to choose a different solution, but still optimal;

2. in the second zone the maximum capacity is reduced up to 75% of the maximum demand; in this zone the reduction of the maximum capacity influences thermal production, in fact, a strong reduction of the number of thermal units belonging to the optimal mix is observed; nevertheless wind production is still well employed and consequently the increase of the objective function is limited;

3. in the third zone the reduction of the maximum capacity is greater than 75% of the maximum demand; in this zone it is no longer possible to reduce the number of thermal units, in fact the solution is infeasible otherwise, for this reason, a strong reduction of the use of wind units with a consequent great increase of the objective function is observed.

This type of behavior is visible also in Fig. 6.18 and Fig. 6.19 which show the use of wind energy with respect of the maximum capacity of the system.

At first, imposing constraints on the maximum capacity of the system does not necessarily determines a strong worsening of the solution and consequently an increase in the objective function, nevertheless a significant restriction negatively affects the use of wind generating units. This behavior can be explained considering that the substitution of the thermal power with the wind one is performed with a highly unbalanced rate with respect to the number of units. In fact, if a thermal unit is excluded from the optimal mix in order to satisfy the constraints on the maximum capacity, it should be replaced by an appropriate wind farm, but, normally, this is not available, for this reason the constraints on the maximum capacity will be satisfied more easily reducing the use of wind units when the solution is close to the not feasibility.
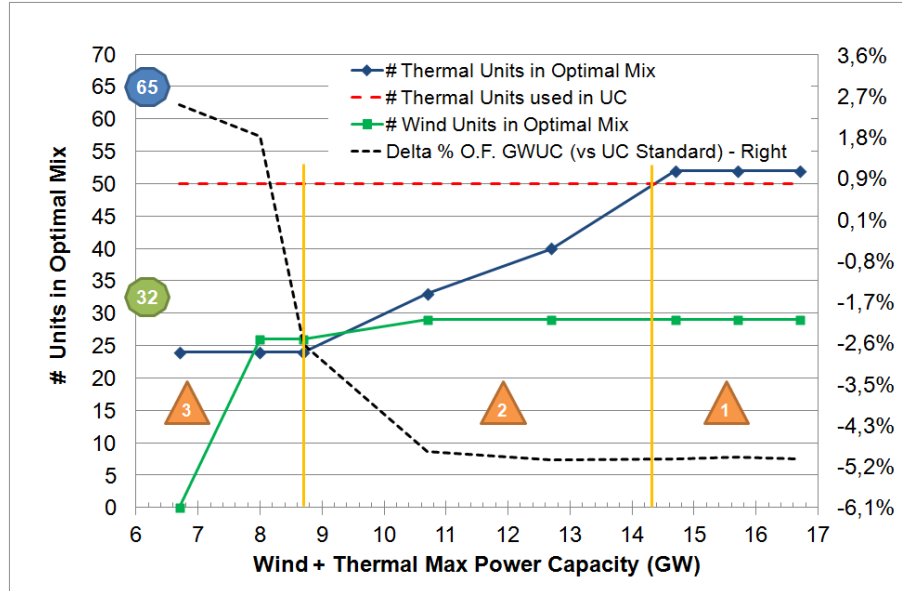
Figure 6.16: Number of units in the optimal mix vs max power capacity.
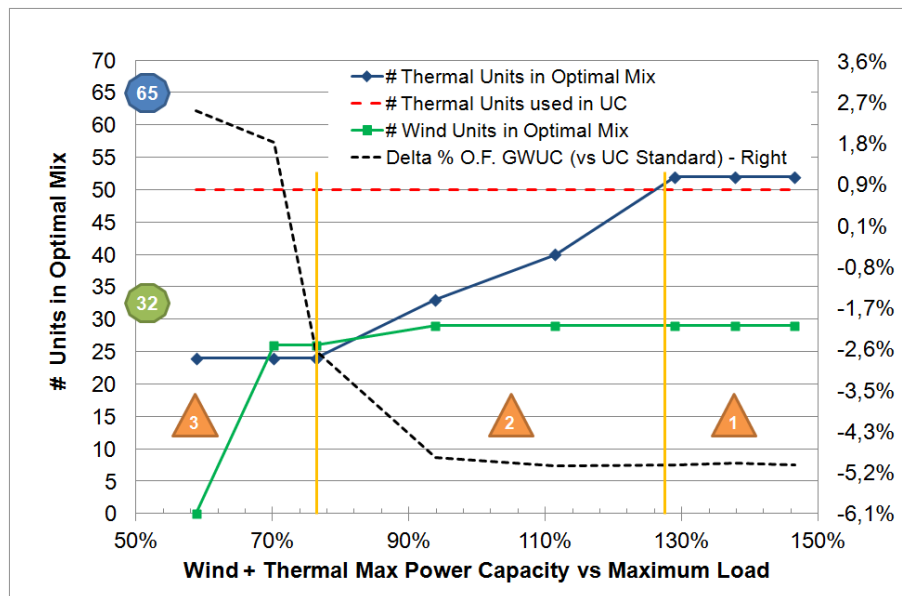
Figure 6.17: Number of units in the optimal mix vs max power capacity/maximum load.
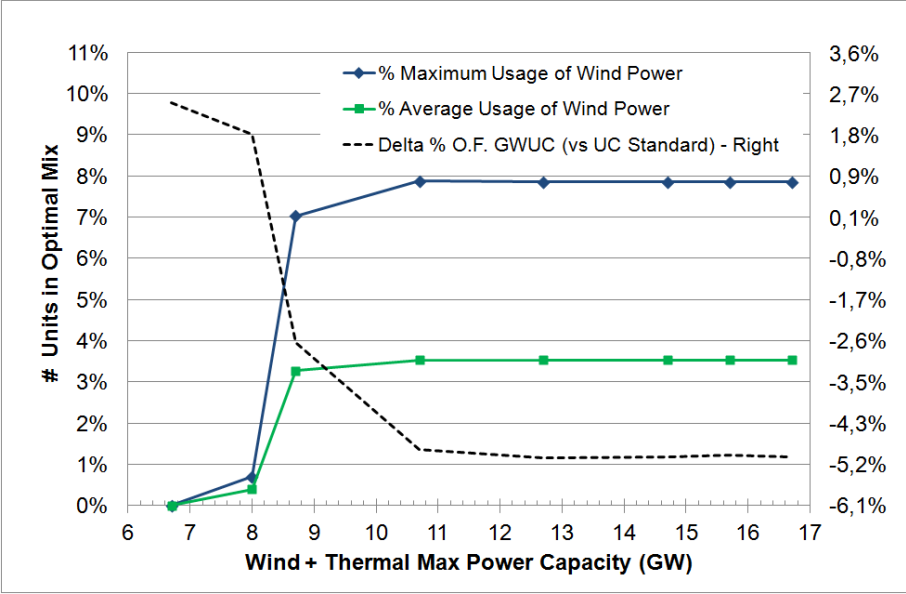
Figure 6.18: Usage of wind power vs max power capacity.
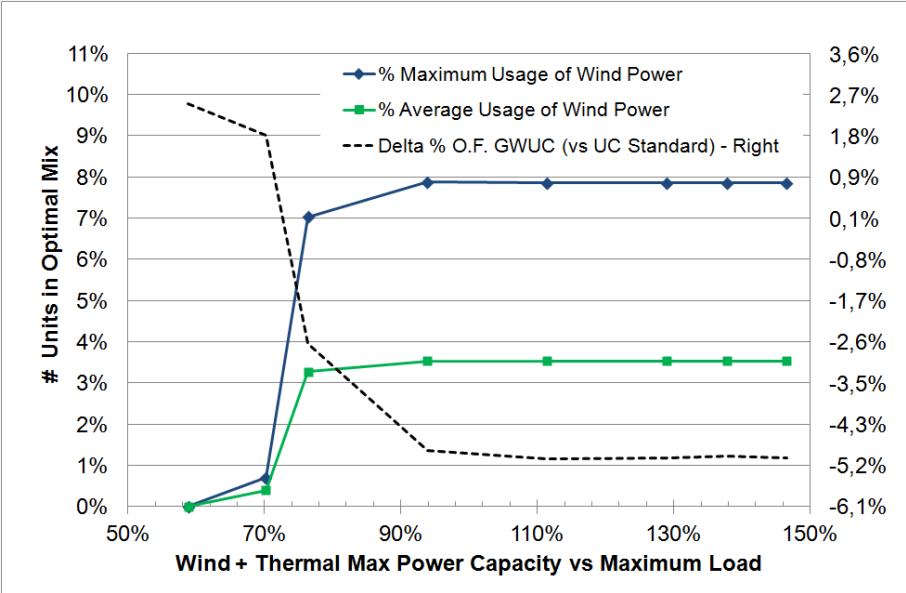
Figure 6.19: Usage of wind power vs max power capacity/maximum load.
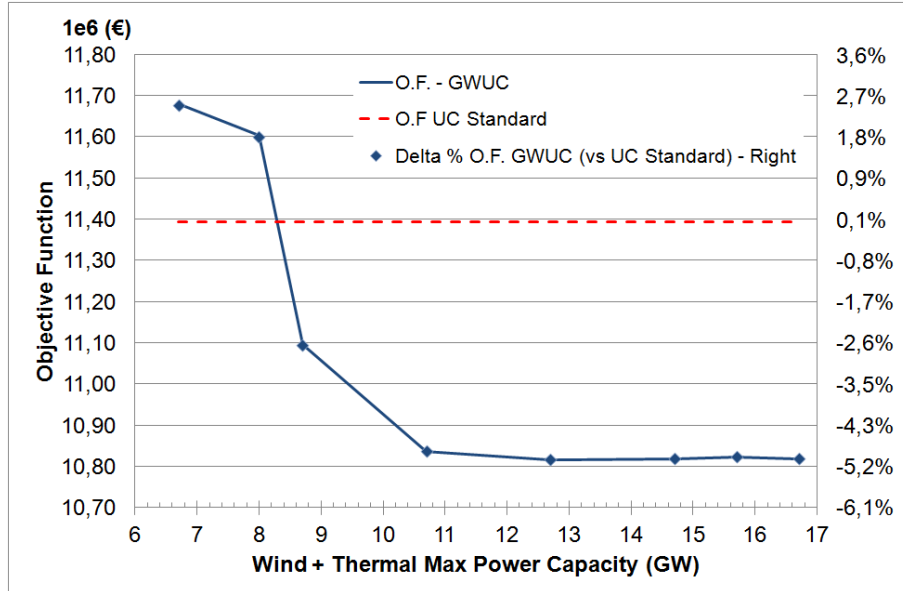
Figure 6.20: Objective function vs max power capacity.
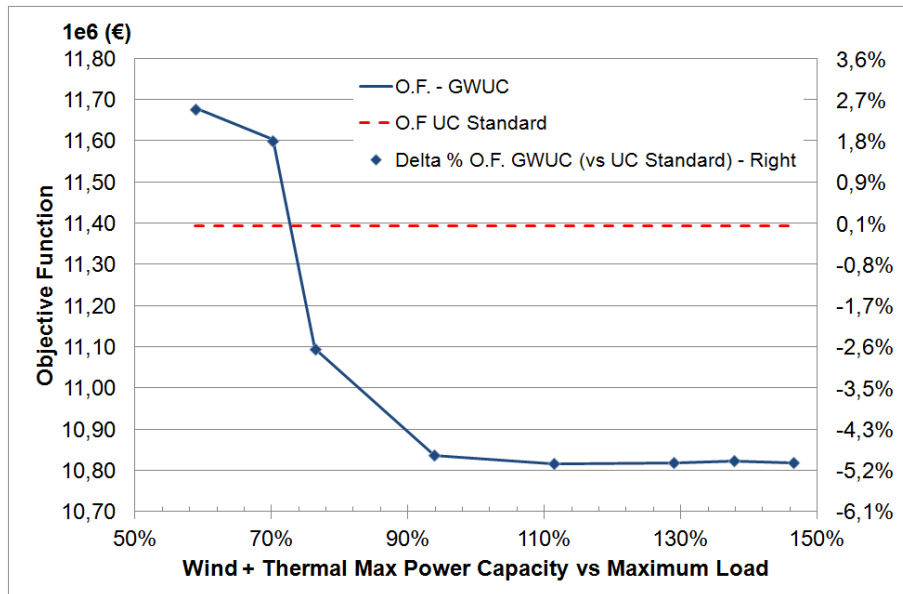
Figure 6.21: Objective function vs max power capacity/maximum load.

6.5.4 Analysis of the influences of the minimum system capacity on the UC solution

The upper bound constraint over the minimum nominal capacity of the system can be applied for market restrictions (for instance, in order to guarantee that certain security requirements are satisfied). This constraint takes into account only the thermal generating units, since only the "known" minimum capacity is considered, when all the thermal units of the assigned instance are on at their minimum power. If the minimum capacity is equal to zero, it actually does not impose any constraint; in theory, it is possible to satisfy the demand without using the thermal units. We analyzed the influence of the increase of the maximum capacity on the UC solution in two different scenarios:

1. no constraints are imposed on the maximum system capacity;

2. specific constraints are applied on the maximum system capacity.

In the first case, it is possible to observe that the increase of the minimum capacity does not influence the number of thermal and wind units belonging to the optimal mix (Fig. 6.22 and Fig. 6.23). This influence is slightly visible only when 100% of the total thermal capacity is required, determining a small increase of the active thermal units. In general, if a higher minimum thermal capacity is required, a higher number of units are started up, even if it is unnecessary to satisfy the demand.

In the second case, a constraint on the maximum capacity has been imposed. This constraint tends to limit the number of units belonging to the optimal mix, for the reasons previously explained. It is possible to observe that in this case an increase of the minimum capacity at first requires a higher number of units, and then it determines a strong reduction of the use of wind units, due to the constraint on the maximum capacity that is now satisfied, with a consequent increase of the objective function (Fig. 6.24 and Fig. 6.25).
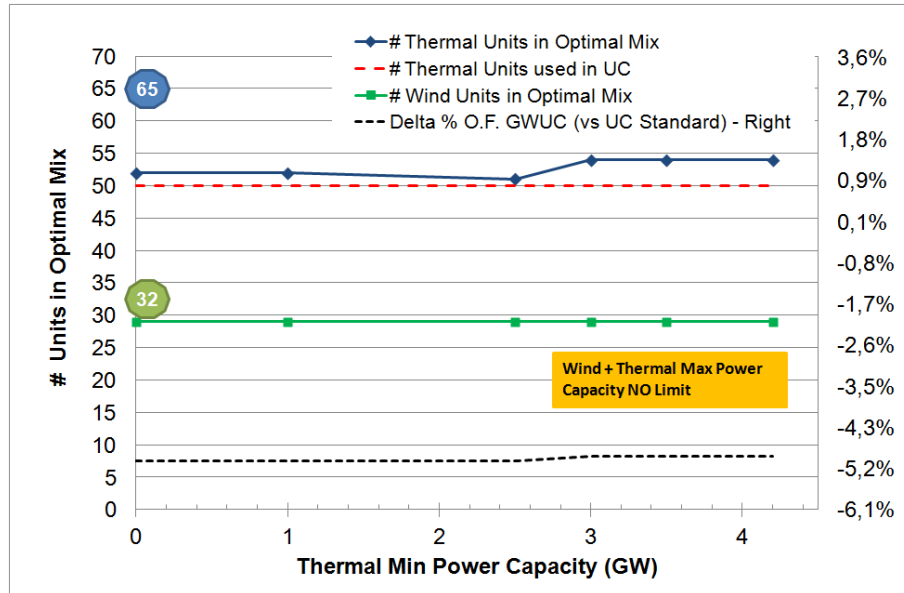
Figure 6.22: Number of units in the optimal mix vs min power capacity.
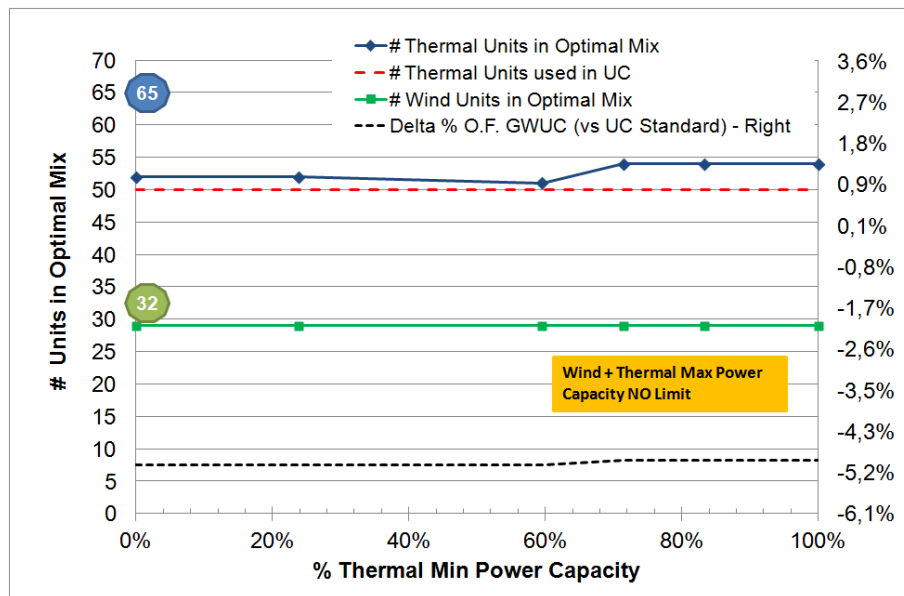
Figure 6.23: Number of units in the optimal mix vs % min power capacity.
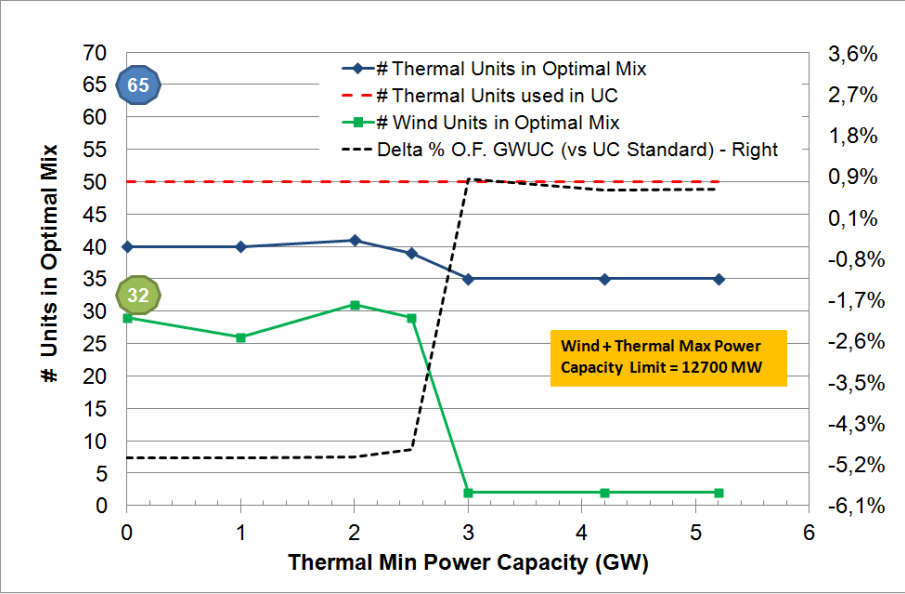
Figure 6.24: Number of units in the optimal mix vs min power capacity (with capacity limit).
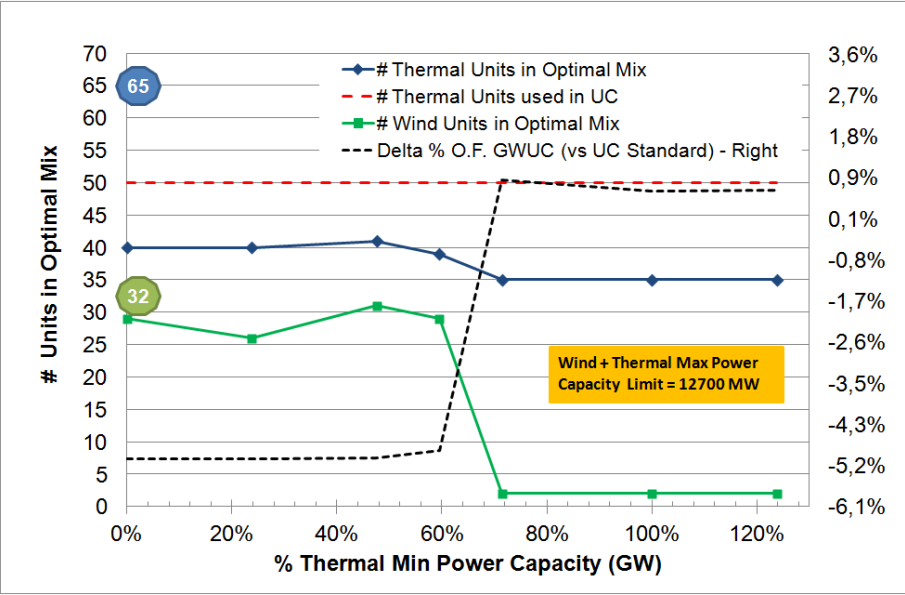
Figure 6.25: Number of units in the optimal mix vs % min power capacity (with capacity limit).

6.5.5 Analysis of the influences of the subset constraints on the UC solution

In order to analyze the influences of the subset constraints on the UC solution, we:

1. studied the influences on the UC solution of the constraints that limit the number of thermal units belonging to assigned subsets, in particular the sets regarding the type of fuel;

2. studied the influences on the UC solution of the constraints that limit the total value that characterizes the rate of CO2 emissions (g of CO2/KWh).

In the first case we performed 6 different simulations, limiting the maximum number of one or more groups of units in the optimal mix, with respect to the fuel used. The objective of these simulations is to verify the effectiveness of the subset constraints in the modification of the optimal mix and how these constraints affect the objective function, making it increase. It is possible to demonstrate the expected result observing Fig. 6.26: if the number of available units in the optimal mix is overall constrained, a consequent reduction of the units utilized is determined. Nevertheless, the increase of the objective function with respect to the not constrained case is not so high (less than 1%); for instance, when a 37% reduction of the units belonging to the optimal mix is obtained, the objective function increases only 0.2%.

Fig. 6.27 shows the constrained sets and the distribution of the optimal mix after the application of the constraints (which are marked with a red hexagon), with respect to the variation of the objective function, represented on the abscissa axis. It is interesting to observe that, for this particular instance, if the constraints are applied on $\frac{3}{5}$ of the subsets a strong reduction of the number of the units belonging to the optimal mix is obtained, but the quality of the solution and the objective function are not affected. Furthermore, the constraints on the subsets of the thermal units do not affect wind units, which are still used, while they influence the distribution of the hourly load between the thermal and the hydro components.

In the second case, we performed 9 simulations, limiting the constraints on the 'cost' of the n-th subset. We considered the geographical subset, while the specific value of the CO_2 emissions has been used to determine the cost of the generating unit i. As explained previously, we have decided to limit this type of cost in order to lead the model to choose for the optimal mix the units that posses the lowest value of emissions, e.g., the units that are more 'virtuous' from this point of view, regardless the absolute value of CO_2 that they will emit after producing a certain amount of energy. This aspect differentiates the GWUC model with subset constraints from a classical UC model with 'emission control', where the emissions are considered as a cost in the objective function. If we analyze Fig. 6.28, it is possible to observe that when the reduction of the CO_2 emission increases, e.g., the constraints become stronger:

- the number of thermal units belonging to the optimal mix decreases; when a reduction of 70% of the value of the specific emission is required, a reduction of 50% of thermal units used is obtained (from 52 to 27);

- the objective function increases, even if this increase is not so high, in fact it is about 1%.

We do not observe a modification of the use of the wind units, since as it happens when the other constraints are considered, the smaller variability of thermal production is absorbed by the hydro component. Fig. 6.29 shows the reduction of the average value of CO_2 emissions of the thermal units belonging to the optimal mix.
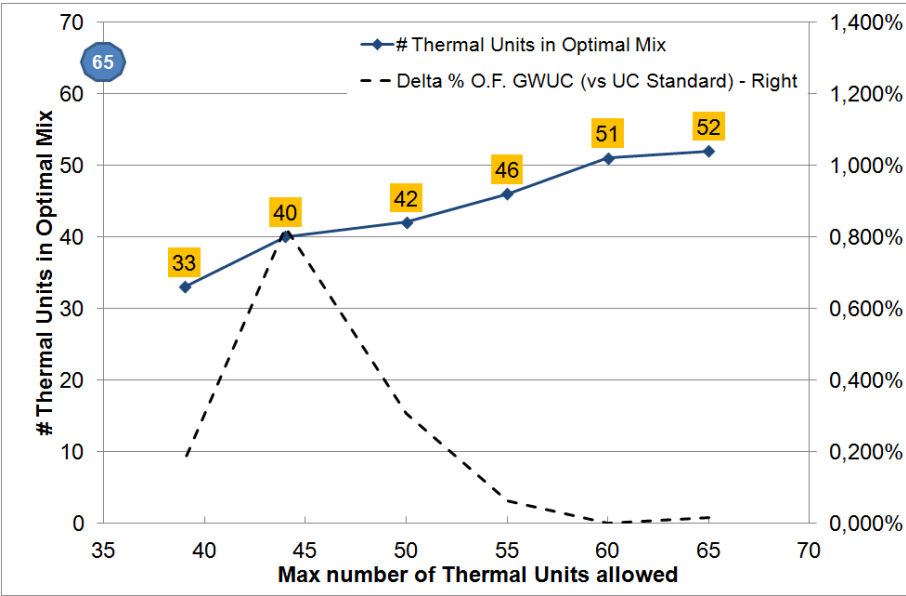
Figure 6.26: Number of thermal units in the optimal mix vs max number of thermal units allowed.
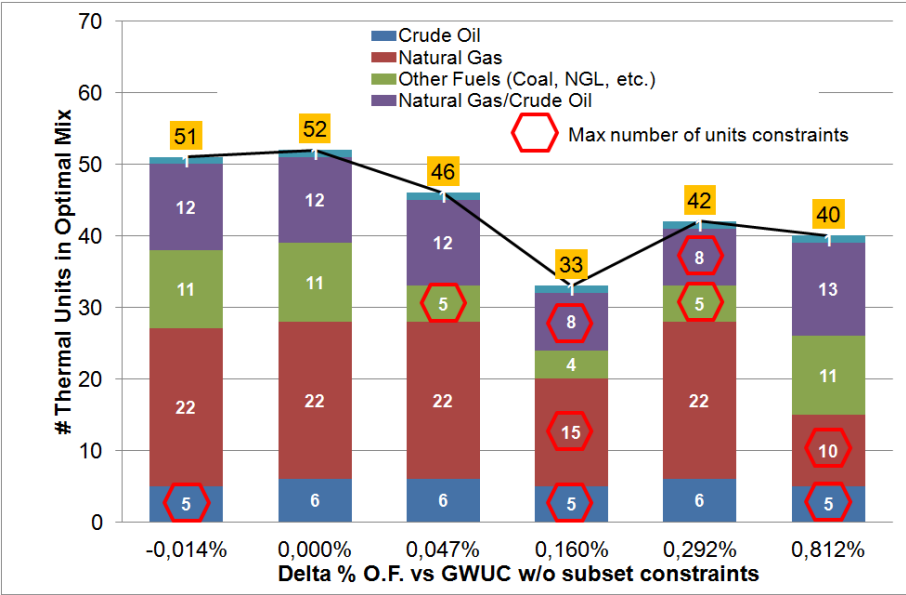
Figure 6.27: Number of thermal units in the optimal mix vs delta % O.F.
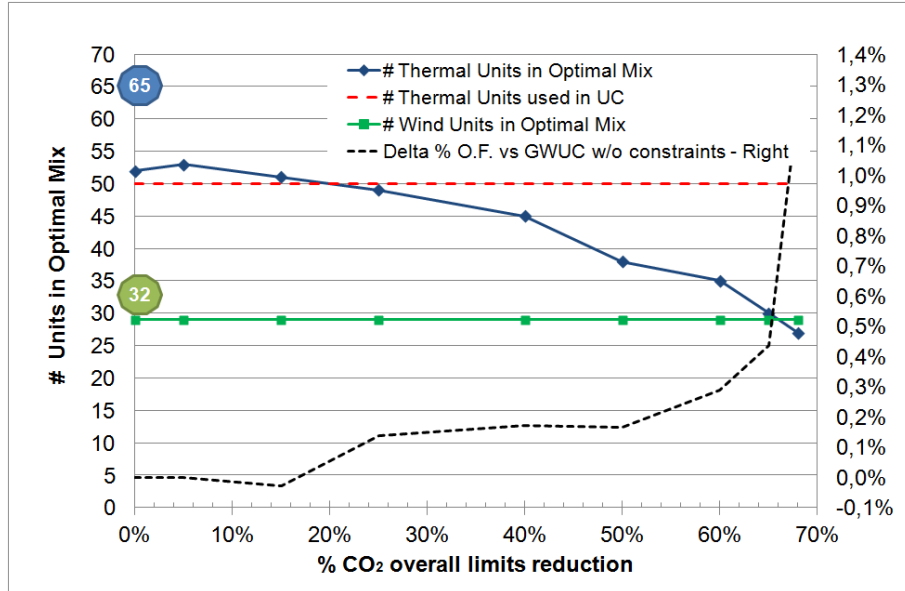
Figure 6.28: Number of units in the optimal mix vs % CO_2 reduction.
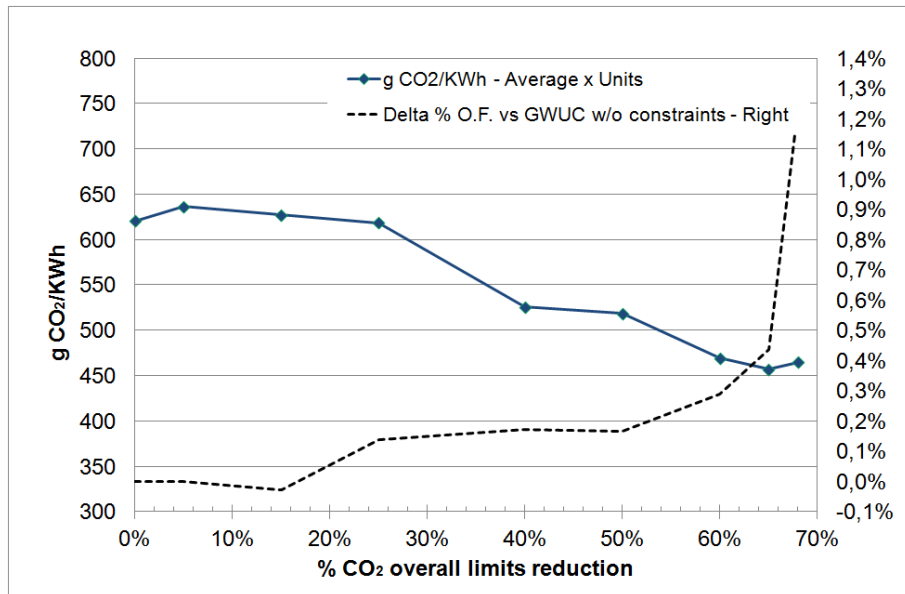
Figure 6.29: g CO_2/KWh vs % CO_2 reduction.

6.6   Conclusions

In this chapter, a new UC model in presence of wind energy sources has been defined and analyzed in order to formulate and solve the problem of determining the best configuration (optimal mix) of available thermal, hydro and wind power plants. The objective of the new proposed model is to integrate renewable energy sources, like wind, in a conventional electrical system. In particular, a generalized form of the UC problem, called *Generalized Wind Unit Commitment Problem* - (GWUC), which takes into account conventional generating units (like thermal and hydro power plants) and wind turbines, has been proposed. The new model allows to analyze how the characteristics of the UC solution are influenced by the introduction or the substitution of power plants in the set of the available generating units. In particular, it has been possible to:

- analyze how the UC solution is affected by the introduction of new generating units (conventional and wind power plants), or by the substitution of conventional generating units with wind turbines and vice versa, within a given set of available generators, in terms of adaptation to the given demand profile;

- determine the best configuration (optimal mix) of available generating units to be utilized, choosing them within a given set of available units, in terms of a fraction of the total energy produced.

The most important results obtained show that, in contrast to the classical UC models and the typical wind UC models, in the GWUC formulation wind generating units are integrated in the solution of the UC problem and furthermore they are also associated with risk considerations, correlated with the forecast error which can be controlled (limited). Moreover, as far as emissions considerations are concerned, the GWUC model chooses for the optimal mix the units that posses the lowest value of emissions, e.g., the units that are more 'virtuous' from this point of view, regardless the absolute value of CO_2 that they will emit after producing a certain amount of energy. This aspect differentiates the GWUC model with subset constraints from a classical UC model with 'emission control', where the emissions are considered as a cost in the objective function.

As far as future work is concerned, it could be very interesting to consider a larger number of subsets of generating units in the GWUC formulation, in order to analyze the behavior of the model in terms of the quality of the solution obtained and in terms of computational times. Furthermore, we could consider a higher number of wind turbines in our model in order to analyze how the solution is influenced by the use of wind sources. Moreover, other additional constraints on wind turbines could be considered in the formulation in order to improve the modeling of the realistic behavior of the wind units, from a practical and an operational point of view. Interconnections, security, and reliability aspects could be also taken into account in order to improve the GWUC formulation; furthermore, the model of the risk correlated with the utilization of wind energy sources could be refined, considering also detailed economical considerations. It could be also very interesting to formulate the GWUC as a power-based continuous model, taking into account the assumptions explained in chapter 4, in order to analyze how the solution obtained is effective for the efficient operation and planning of a real time electrical system. The GWUC could be also modeled taking into account Robust Optimization considerations: it could represent a very interesting aspect since robust optimization techniques could be easily applied to model the risk correlated with the utilization of wind energy sources.

Chapter 7

A novel model to generate synthetic wind data *

The output of wind generation is variable, like other forms of renewable energy sources which are influenced by weather conditions that cannot be controlled by the electrical system operator. Wind generation is also relatively unpredictable, since the amount of wind energy fluctuates as wind speed changes, being a *'non-dispatchable'* source. As discussed in the previous chapters, the objective of power system operators is to supply electricity ensuring that generation meets the demand in all time periods, maintaining the integrity and the reliability of the system at an acceptable operational cost [KS04]. In particular, the reliability associated with a power system is defined as *'the ability to supply adequate electric service on a nearly continuous basis with few interruptions over an extended period of time'* [IoLES04]. Generally, generating units are scheduled to meet the forecast demand and may alter their output levels to follow the load that fluctuates throughout the day. For this reason, the balancing between demand and supply becomes challenging if wind generation is considered, since the output of wind units cannot be directly controlled, but it can only be reduced by the system operators [GHA$^+$06], resulting in increasing operational costs. The operation of conventional systems is thus altered, to take into account the variability of wind generators [GSHG03] [HCP$^+$00]. In particular, conventional generators may be induced to operate at lower levels, increasing the number of start-ups and shut-downs [GHA$^+$06], [Hol04] [Eir04]. Nevertheless, an increase in the ramping and in start-ups and shut-downs can shorten the life of thermal units [LBG97], since they are designed to run at a stable load [Fly03] and are optimized for continuous rather than cyclical operation, ensuring a longer life and a lower risk of failure over a long period. Furthermore, since wind generation is relatively unpredictable and *'non-dispatchable'*, the uncertainty in the electrical system increases as wind capacity utilized grows large, resulting in the requirement of an additional reserve capacity in order to maintain system security [Sod93b]. Thus, when renewable sources, like wind, are considered, forecasts of weather conditions are fundamental.

Since the use of wind energy sources and its integration into power generation systems is assuming increasing importance, new generation models for synthetic wind data are needed, in order to properly generate forecasts of wind speed and power. This data is fundamental in simulations

---

*Part of the material presented in this chapter is based on the following publication *A. Naimo. A new synthetic wind forecast data generation model. Technical Report R. 11-32, IASI-CNR, 12/2011.*

carried out to analyze and improve the performances of wind generating units, individuating the technical parameters of wind turbines that directly affect power production. During our research activities, we developed a new model in order to generate realistic synthetic wind data, which is presented in this chapter. In this model, wind speed is assumed to behave as a Weibull distribution, while wind speed forecast error is simulated using First-Order Auto-Regressive Moving Average - ARMA time-series models. Mathematical Operations Research formulations for the Assignment Problem are used to model wind speed persistence features, which, as shown by simulation results, are essential to properly obtain wind speed and power output forecasts.

In this chapter we present the state of the art on wind speed forecasting techniques; hence we illustrate the basic idea of our synthetic wind data generation model and its detailed formulation; finally we present the simulation results and outline the conclusions.

7.1 The importance of forecasts: wind speed and power prediction models

Wind generation requires complex forecasting techniques which take into account wind speed, wind direction, hub height, geographical conditions, wind farm size, wind turbine technical and operational characteristics and so on. Wind speed and power forecasting techniques are used to support the integration of wind energy sources into the existing power systems. Different research groups and private companies have developed several forecasting systems [GBK03], like WILMAR and ANEMOS European research projects, with the aim to predict how much wind power will be produced in a short-term period, typically up to 48 hours, from a single wind farm or from a region that includes many wind farms.

The WILMAR Project (*Wind Power Integration in Liberalized Electricity Markets*) has been funded by the European Commission [WIL05]. The objective of this project is to quantify the additional costs associated with the integration of large amounts of wind power into European power systems, when wind energy is used to increase the contribution of renewable energy to the power supply, meeting the European stated goals and the Kyoto Protocol emissions targets. This leads to an accurate analysis to reduce as much as possible these additional costs, the costs related with the investments in new thermal power plants, in new transmission lines, and in the improvement of wind power forecasting systems. Furthermore, power market structures are analyzed in order to better exploit wind power resources. In order to carry on this analysis on wind power integration, a suitable planning tool has been developed for the project, taking into account the Nordic and German power systems [PP03]. This tool is able to simulate the operation (hour per hour) of the existing power systems and of the power systems with large amounts of wind power, as they will exist in the near future. Another objective of this project is to estimate the value of potential improvements of wind power prediction tools themselves, developing models to simulate realistic wind speed predictions with a certain accuracy.

The ANEMOS Project (*Advanced Tools for the Management of Electricity Grids with Large-Scale Wind Generation*) has been funded by the ANEMOS Consortium [ANE11]. The objective of this project is to manage at optimality electricity systems with large-scale wind power generation. In order to achieve this goal, new intelligent management tools are developed for the project to study and analyze the variability of wind power. Particular attention is devoted to the integration of wind power forecasts into conventional power systems, taking into account the related uncertainty, in order to trade wind power generation in electricity markets.

The results obtained with these research projects have shown that, in order to operate a power

system with wind generation in a proper way, the short-term (1 to 48 hours) forecasts of wind power production is fundamental. Advanced wind power prediction tools, based on time-series and numerical weather prediction models and designed for power system operators, are being developed and continuously improved.

Nevertheless, no forecast is perfectly accurate and results in some error, that increases and becomes significant as the time horizon lengthens, since wind speed is unpredictable and wind generation forecasts need a large number of factors to be considered [GLKB03]. Usually, only wind speed forecast errors are used to generate synthetic wind data that are useful to carry out simulations over wind generation systems. In fact, it is simpler to work with wind speeds since they have been measured for many more years and in many more locations than wind power and for this reason, it is easier to obtain wind forecasts. Moreover, wind power forecast errors should be normalized taking into account the capacity of each wind farm, while wind speed forecast errors are easily expressed in m/s. Furthermore, wind power is a function of the cube of the wind speed. This non-linearity of the power curve makes it more difficult to simulate correlated time-series of wind power than of wind speed, since correlations between wind power forecasts errors are much more dependent on the wind speed than the correlations between wind speed forecast errors. Moreover, the final step of a wind power prediction system is to convert predicted wind speeds into wind power using a power curve. All wind power measurements, however, do not lie on the power curve since they must be average over a finite time period. Therefore wind power forecast errors will show a greater variance than wind speed forecast errors, making it difficult to identify what the errors depend on. For all these reasons, usually, wind speed forecast errors are considered to properly predict and simulate wind speed and wind power output.

Short-term wind power prediction models have been used by power plant owners and power systems operators for 20 years in order to predict how much wind power will be produced in the short-term (usually up to 48 hours ahead). Wind power prediction models can be classified with respect to the input data they require. The two main types are Time-Series Models and Numerical Weather Prediction-Based Models (NWP-based models), which are represented by physical and statistical models, as shown in Fig. 7.1.

Time-Series models consider only on-line wind speed or wind power measurements and time-series analysis methods to predict wind power production in a short-term period which consists of a few hours.

NWP-based models outperform time series models for forecasts longer than 4 up to 6 hours, and can be classified into physical or statistical models.

Statistical models calculate wind power production directly, ignoring physical considerations. They use NWP output and past measurements of both NWP output and wind power production. Statistical NWP-based models generally outperform physical models, even if they require more input data, but the difference between the two becomes insignificant at longer forecast lengths.

Physical NWP-based models estimate the local wind speed for a wind farm using only the output of a NWP model and then convert it to local wind power production. Some past measurements of NWP output and wind power are required, however, to calculate the model output statistics parameters used to reduce systematic errors.

Generally, wind prediction models use a combination of all three types mentioned above to make the most accurate wind forecasts possible. For instance, more advanced time-series models with the inclusion of statistical models can usually deliver better results, but the errors shown here are still typical for state-of-the-art on wind power prediction systems. The main characteristics of the models used for wind speed and power prediction are described in the following sections.
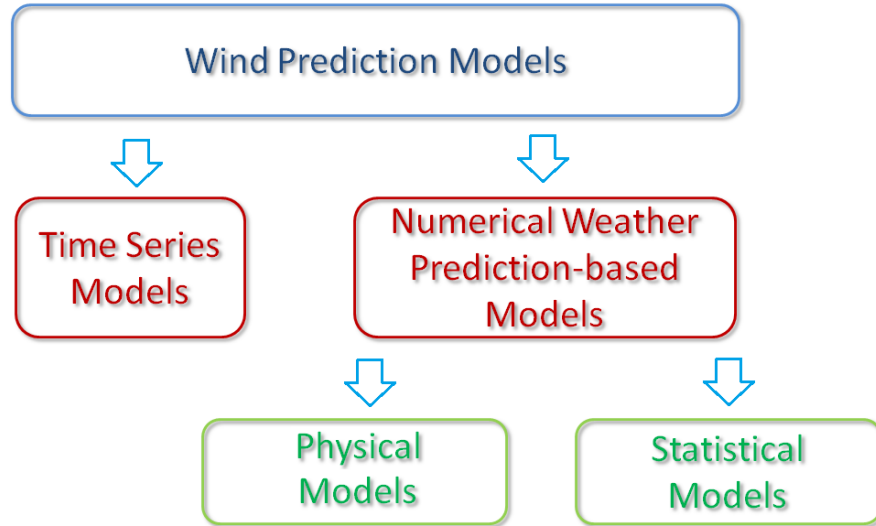
Figure 7.1: Short-term wind speed and power prediction models.

7.1.1   Time-series models

Given a certain wind speed forecast, it is necessary to simulate the associated forecast wind speed error. A realistic measure of this error can be obtained with the *1st-order Auto-Regressive Moving Average* - ARMA - time-series model, as proposed by Soder [Sod93b] [Sod93a] [Sod04]. These models are based on *time-series*, which are sequences of observations; each observation is recorded in a specified time interval. ARMA time-series models have been explained in detail in [DMN03]. There exist different types of time-series models, according to the type of time-series which are based on. Time-series can be discrete, parametric, uni-variate and multi-variate. Discrete time-series are characterized by observations recorded at discrete points in time with a constant time interval between the points. Time-series are parametric if their characteristics are described by constant parameters. Uni-variate time-series are composed of observations of a single variable, while multi-variate time-series are composed of more than one variable. When it is needed to simulate wind speed forecast errors at multiple sites at the same time, the time-series used must be multi-variate. The most appropriate time-series model to use is determined according to the type of time-series wind speed forecast error considered. Time-Series models are the simplest and therefore least expensive type of wind prediction models. They require only the most recent (a few hours) wind speed or wind power measurements from the wind farm or from a few representative wind farms in the region where wind power production has to be forecast. More advanced time-series models require more input data (past wind speed or wind power measurements) [GBK03]. These models use time-series analysis techniques such as recursive least-squares algorithms, auto-regressive models, or artificial neural networks to find trends in the wind speed measurements and then extrapolate these trends a few hours into the future. Many types of time-series models have been investigated, and there is no single best one, since different models result in varying degrees of error for different locations due to the differences in weather conditions and terrain. Time-Series models are the most accurate models up to 4 to 6 hours ahead: this forecast length

is sufficient for some applications, even if it is the most critical for power systems with many thermal power plants, which are not able to vary their production rapidly. This concept is shown in picture (7.2), where it is possible to observe that the forecast error tends to increase when the time horizon considered lengthens.
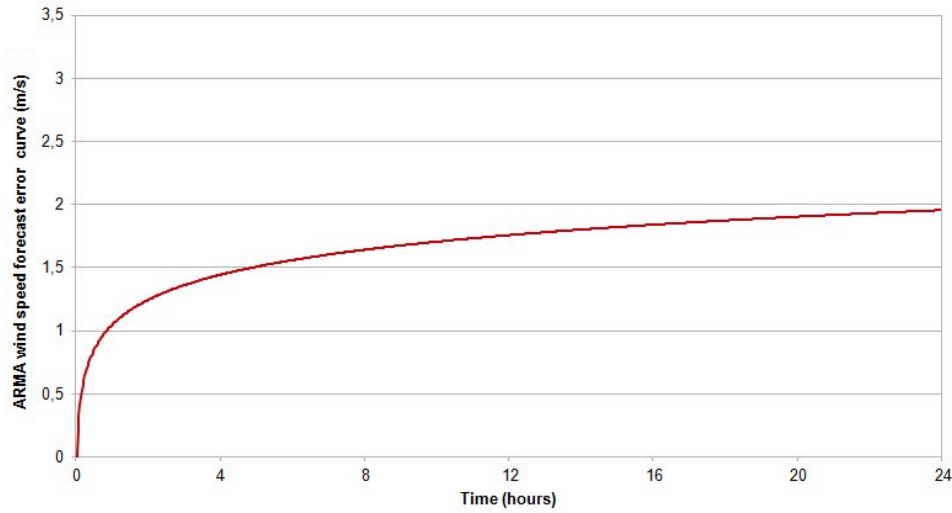
Figure 7.2: Wind speed forecast error curve simulated with time-series models (ARMA).

Uni-variate ARMA time-series models

Soder [Sod93a] first developed a method based on a uni-variate ARMA time-series model to simulate wind speed for the operation planning of a power system by a stochastic optimization approach. The ARMA time-series has been defined as follows:

$$
\begin{align}
X(0) &= 0 \tag{7.1} \\
Z(0) &= 0 \tag{7.2} \\
X(t) &= \alpha X(t-1) + \beta Z(t-1) + Z(t) \tag{7.3}
\end{align}
$$

where $X(t)$ is the wind speed forecast error at time t, α and β are constant parameters, and $Z(t)$ is a random Gaussian variable with average equal to zero and standard deviation σ_Z at time t. The Auto-Regressive parameter α determines to which degree the previous value in the time-series influences the current value. The Moving-Average parameter α determines to which degree the random Gaussian variable of the previous parameter in the time-series influences the current value. A unique set of the three parameters α, β, σ_Z describes an ARMA time-series. Determining the values of the ARMA parameters is fundamental, because if wind speed forecast errors are properly estimated, the power system operational additional cost generated by wind in a given region under certain average weather conditions is correctly individuated. In particular, appropriate ARMA parameters should be properly calculated in order to model also special situations in which extreme weather conditions, such as storms, can result in extreme costs for the operation of the power system, that can be limited if the average forecast errors are

correctly estimated with proper parameters. Furthermore, even the choice of different initial values for α, β, and σ_Z in the minimization algorithms that implement the ARMA model is fundamental, since it can give different results for these parameters themselves because of the presence of local minimums.

The ARMA parameters depend on different factors [Boo05]. The most important are related with the precision of forecast wind speed estimation (this is associated to the simplicity and the accuracy of the prediction system), the terrain complexity of the given site and the average wind speed level where wind turbines are located.

The following table shows the possible values that α, β and σ_z parameters can assume (S.T. means *Simple Terrain*, C.T. means *Complex Terrain*, S.P.S. means *Simple Prediction System*, A.P.S. means *Advanced Prediction System*, $f(\overline{w})$ means that parameters depends on average wind speed $\overline{w}$).

		α	β	σ_z
S.T.	**S.P.S.**	0.98	-0.7	$1.0 \div 2.5 \; f(\overline{w})$
S.T.	**A.P.S.**	> 0.98	$-0.8 \div -0.4 \; f(\overline{w})$	$0.75 \div 1.5 \; f(\overline{w})$
C.T.	**S.P.S.**	0.8	-0.1	$2.5 \div 3 \; f(\overline{w})$
C.T.	**A.P.S.**	0.8	-0.1	$0.50 \div 2.0 \; f(\overline{w})$

Table 7.1: Possible values for the parameters α, β and σ_z.

The most complete study on the value of the parameters considered is [Boo05], where it is suggested that proper values for the parameters are $\alpha = 0.95$, $\beta = -0.6$, $\sigma_z = 0.5$.

Multi-variate ARMA time-series models

In his later studies, Soder [Sod04] developed a multi-variate ARMA time-series model in order to simulate wind speed forecast errors for the simulation of the stochastic optimization operation of power systems. The Soder's idea was to develop a simple and practical model to produce realistic wind speed forecast errors for power system simulation. The model is based on two main assumptions. The first is that the variance of wind speed forecast errors does not depend on the level of wind speed. The second is that the correlation between forecast errors at different sites does not depend on the forecast length. Actually, neither assumption is true, since the correlations increase when the forecast length grows large, but they greatly simplify the model and do not result in significant simulation errors.

Nielsen and Madsen [NM02] also produced a model based on multi-variate ARMA time-series. In particular, they developed a 1st order multi-variate Moving-Average time-series model MA(1). In their work, they found that a Moving-Average model results in about the same simulation accuracy as the more complex Auto-Regressive (AR) and Auto-Regressive Moving-Average (ARMA) models. Nevertheless, in another paper [NNM02], they recommend the use of an ARMA model.

Multi-variate ARMA time-series models can be used to simulate correlated forecast errors at multiple locations. This should not be done for each location separately based on the ARMA time-series model described above because actually, wind speed forecast errors at different locations are correlated with each other. In order to create wind speed forecast errors that are representative of different locations in the power system, various forecast error scenario trees must be created, according to the different locations themselves, so that wind speed is under forecast for wind farms that are near each other. Moreover, the simulated wind speed forecast errors must also be

correlated. If this correlation were not be present, the aggregate simulated wind power error for the given entire region would be near zero, since wind speeds would be over-predicted in some locations and under-predicted in other locations, and these deviations would be uncorrelated. For these reasons, another formulation of the ARMA time-series model, that is represented by the multi-variate ARMA time-series one, is required.

Multi-variate ARMA time-series model is thus created by adding a correlated random variable to each time-series, formulated in the case of two locations as follows (observe that the model can be defined for more than two locations)

$$X_1(0) = 0 \tag{7.4}$$
$$Z_1(0) = 0 \tag{7.5}$$
$$X_1(t) = \alpha_1 X_1(t-1) + \beta_1 Z_1(t-1) + Z_1(t) \tag{7.6}$$
$$X_2(0) = 0 \tag{7.7}$$
$$Z_2(0) = 0 \tag{7.8}$$
$$X_2(t) = \alpha_2 X_2(t-1) + \beta_2 Z_2(t-1) + Z_2(t) \tag{7.9}$$

where Z_1 and Z_2 are correlated random Gaussian variables given by the following expression

$$Z_1(t) = c_{11} Z_a(t) + c_{12} Z_b(t) \tag{7.10}$$
$$Z_2(t) = c_{21} Z_a(t) + c_{22} Z_b(t) \tag{7.11}$$
$$\sigma_{Z_a}^2 = c_{11}^2 + c_{12}^2 \tag{7.12}$$
$$\sigma_{Z_b}^2 = c_{21}^2 + c_{22}^2 \tag{7.13}$$

$Z_a(t)$ and $Z_b(t)$ are independent random Gaussian variables with standard deviations σ_{Z_a} and σ_{Z_b}, both equal to 1.

These standard deviations are related by the 2 by 2 c-matrix. The parameters whose values must be correctly found are $\alpha_1, \alpha_2, \sigma_1, \sigma_2, c_{11}, c_{12}, c_{21}, c_{22}$. It is easier to observe these parameters when the 2-dimensional ARMA model is written in a matrix form, as presented below:

$$\begin{bmatrix} X_1(0) \\ X_2(0) \end{bmatrix} = \begin{bmatrix} 0 \\ 0 \end{bmatrix}$$

$$\begin{bmatrix} Z_1(0) \\ Z_2(0) \end{bmatrix} = \begin{bmatrix} 0 \\ 0 \end{bmatrix}$$

$$\begin{bmatrix} X_1(t) \\ X_2(t) \end{bmatrix} = \begin{bmatrix} \alpha_1 & 0 \\ 0 & \alpha_2 \end{bmatrix} \begin{bmatrix} X_1(t-1) \\ X_2(t-1) \end{bmatrix} + \begin{bmatrix} Z_1(t) \\ Z_2(t) \end{bmatrix} \begin{bmatrix} \beta_1 & 0 \\ 0 & \beta_2 \end{bmatrix} \begin{bmatrix} Z_1(t-1) \\ Z_2(t-1) \end{bmatrix}$$

$$\begin{bmatrix} Z_1(t) \\ Z_2(t) \end{bmatrix} = \begin{bmatrix} c_{11} & c_{12} \\ c_{21} & c_{22} \end{bmatrix} \begin{bmatrix} Z_a(t) \\ Z_b(t) \end{bmatrix}$$

As mentioned above, the model can be extended to include any number of locations. Also in this case, the parameter matrices that describe the time series are always represented by α, β, c. The correct α and β matrices are found using the previous expressions, as done before, while the proper c-matrix is found minimizing the difference between the correlations of the forecast errors and the correlations of the simulated forecast errors at the different locations.

7.1.2   Numerical Weather Prediction Models (NWPs)

Numerical Weather Prediction Models (NWPs) have been studied for decades in order to obtain weather forecasts in several applications [Boo05]. These models use computer simulations of the state of the Earth's atmosphere at a given point in time, in order to make weather forecasts, using physical laws. These physical laws describe how the state variables (represented by pressure, humidity, temperature, wind speed) change over the time period of observation. A set of non-linear partial differential equations, which cannot be solved analytically, is considered, in order to represent the relationship between these state variables. NWPs are used to numerically solve this system of equations at each point of a 3-dimensional grid that covers part or the whole Earth's atmosphere. The most advanced NWPs are run on dedicated super-computers at national weather centers, though even small private companies are currently using these models to obtain weather forecasts, due to the improvement in parallel computing. In fact, NWPs are gradually increasing in importance due to the improvement in the studies about the behavior of the atmosphere and due to the increasing capabilities and speed of computers. Nevertheless, NWPs present some limitations in their accuracy when the state of the atmosphere has to be predicted at very short forecast time horizons (less than about 4 hours), due to the imperfect measurement of the initial state variables that have to be integrated into the model itself. Furthermore, these models are strongly limited when predictions at longer forecast time horizons (more than a few days) are needed, due to the intrinsic nature of weather conditions. Generally, the output of NWPs is used by wind power prediction systems, in order to obtain wind power forecasts. The most important variables output of NWPs that are used are wind speed, wind direction, pressure, and thermal stability. Wind power prediction models can be classified into two main categories: physical and statistical models. The following sections describe the main characteristics of each model.

Physical models

Physical models are usually based on different steps in order to produce wind power forecasts [Boo05].

The first step consists in obtaining the output of the NWP models, which, as mentioned before, attempt to predict the future state of the atmosphere taking into account information about the current state of the atmosphere itself and physical laws that describe the changes of the state variables (pressure, humidity, temperature, wind speed) over a given time horizon.

In the second step, called Local Refinement, the outputs of the NWPs (wind speeds and directions) are translated into the wind speed and direction at the wind farm geographical site where power production has to be forecast, considering the hub height of the wind turbines. The simplest method to obtain these values consists in using the wind speed and direction at the NWPs grid point that is nearest to the given wind farm, considering the vertical level where the lowest forecast errors are obtained. This method can be improved by interpolating wind speed and direction from the four NWPs grid points that circumscribe the wind farm.

The third step, called Model Output Statistics (MOS), is used to reduce the significant systematic errors caused by the resolution of the NWPs as much as possible. In order to obtain this result, a simple linear model is used, taking into account on-line measurements of the NWPs parameters. MOS can be applied before the conversion of wind speed into wind power, after the conversion, or in both of these cases.

The fourth step is based on a physical model that is used to translate the wind speed forecast into a wind power forecast, taking into account either the manufacturer's wind turbines power curve or the actual power curve obtained with the past wind speed and power measurements.
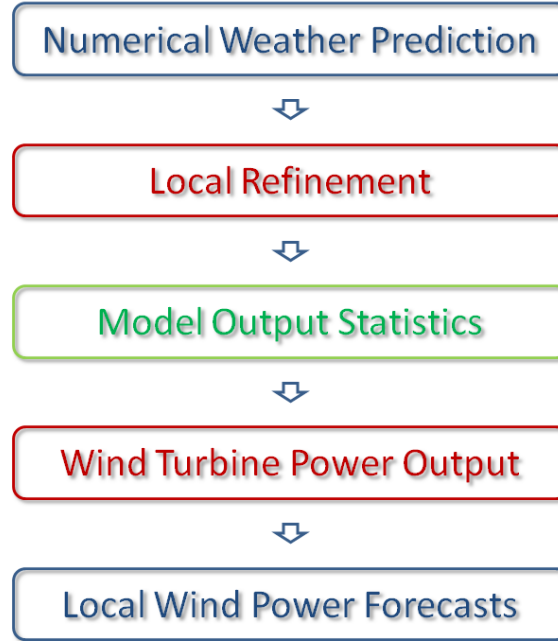
Figure 7.3: Typical steps of a physical NWP-based model.

The steps that physical NWP-based models use to create wind power forecasts are shown in Fig. 7.3.

Statistical models

Statistical models take into account measured wind power output of a wind farm or a geographical region and the corresponding numerical weather predictions to find statistical parameters that describe the relationship between the two [Boo05]. The values of these parameters can change over the time horizon due to the weather conditions, the aging of the wind turbines, and the changes in the terrain site characteristics. For this reason, the parameters are usually updated with algorithms that properly weight the data. With respect to the physical models, the statistical models present the advantage that all physical considerations are implicitly taken into account. This means that all the effects of orography, roughness, and wind turbines are automatically considered. However, the main disadvantage consists in the reduced accuracy at longer forecast time horizons. Moreover, past wind power measurements and NWPs results are needed to find the statistical parameters, and these parameters have to be typically updated in order to obtain accurate forecasts.

7.2 The synthetic wind data generation model

As mentioned above, the integration of wind energy into electrical systems is acquiring global relevance [CSGTXB10] [WWE11]. Knowing the main characteristics of wind is fundamental to
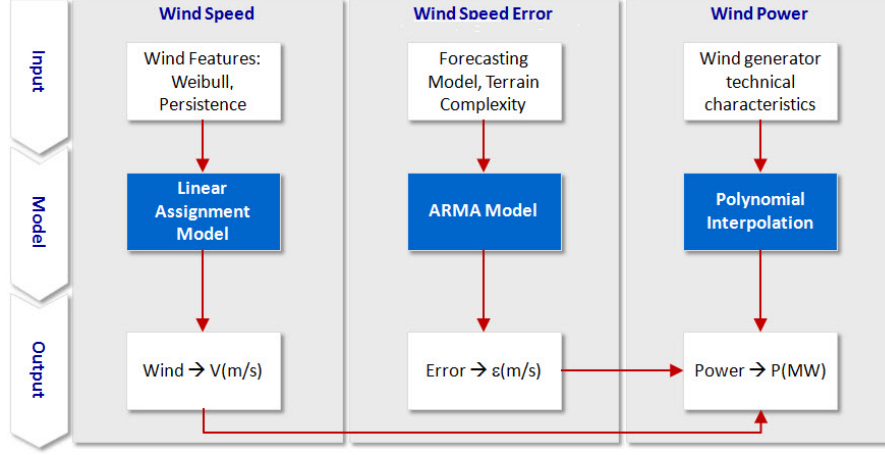
Figure 7.4: Synthetic wind data generation model.

obtain proper wind speed and power output forecasts. Wind persistence is one of the most important factors to be studied to understand the dynamic and intermittent behavior of wind. In order to generate forecasts for wind speed and power, it is also necessary to know how wind speed can be modeled from a statistical point of view. Many authors in the literature show that the statistical distribution of wind speed is modeled with the Two-Parameters Weibull distribution ([CSK78], [Hen77], [JHY76], [SS79], [RdMC89], [RHH94], [GTPdF98], [Gup86], [JHMG78]). A correct estimation of wind speed forecast error is also fundamental. First-Order Auto-Regressive Moving Average - ARMA time-series models - are widely applied to simulate the error associated with wind speed forecasts [Boo05]. Other models to simulate this error exist, such as GARCH models [LKPvdS10], but the comparison of the performances of these different models is beyond the scope of this thesis. The studies carried out for the WILMAR project have shown that the properties of the ARMA well reproduce the behavior of the wind speed forecast error [Boo05]. For these reasons, we have chosen the ARMA model to represent the wind speed forecast error and the Weibull distribution to represent the wind speed in our generation model. The main aim of this study is to define a new model to generate realistic synthetic data for wind speed and power. In this model, wind speed is assumed to behave as a Weibull distribution, while ARMA models are used to estimate wind speed forecast error. The novel approach introduced is represented by the enhanced way to model the wind speed persistence features using a mathematical formulation of the Assignment Problem. The novel generation model proposed in this thesis is compared with a pure random model in which synthetic wind speed is generated applying a casual perturbation to a wind speed fixed curve. The objective of the new generator is to produce realistic data for wind speed and power (Fig. 7.4). The inputs are the Weibull distribution parameters (representing wind speed features), the ARMA model parameters and the wind turbine technical characteristics. The generator is based on three main models. The first is the Optimization model for the Assignment Problem, used to re-sequence wind generated data to fulfill persistence requirements. The second is the ARMA model for wind speed forecast error. The third is the polynomial interpolation algorithm, applied to wind power data to model wind turbine technical characteristics. The main output parameters of the generator are the forecast wind speed, the forecast wind speed error and the forecast wind power.
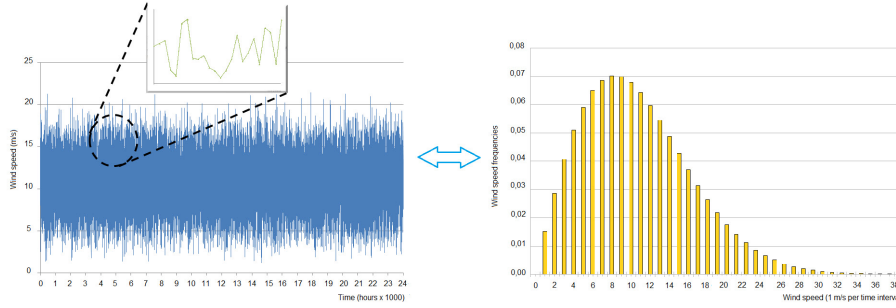
Figure 7.5: Random wind speed data generated with respect to a Weibull distribution.

7.2.1 Synthetic wind speed curve generation

Synthetic wind speed data is typically generated respecting a Weibull distribution [BBL03], that is defined as follows

$$f(v) = \left(\frac{k}{\lambda}\right) \left(\frac{v}{\lambda}\right)^{k-1} exp\left[-\left(\frac{v}{\lambda}\right)^k\right] \tag{7.14}$$

where:

- $f(v)$ is the probability to observe wind speed v;

- k is the *shape parameter*, which is used to determine the shape of the Weibull distribution and usually varies from 1.2 to 2.75 ([CSK78], [Hen77], [JHY76], [SS79], [RdMC89], [RHH94], [GTPdF98], [Gup86], [JHMG78]);

- λ is the *scale parameter*, which represents a scale factor for the Weibull distribution.

It is possible to observe that, even if wind speed seems to have a random behavior, statistical wind speed properties of the Weibull distribution are maintained (Fig. 7.5). Nevertheless, the generated wind speed data does not reflect persistence characteristics of the given average observed wind speed, due to the random generation process itself. This means that the average value of the generated wind speed is constant and the autocorrelation tends to zero as far as the time horizon increases. For this reason, and for the apparent random behavior of wind speed, enhanced models that properly consider wind speed characteristics, such as persistence, are needed.

7.2.2 Modeling wind speed persistence with Assignment Problem formulations

To obtain a proper wind speed forecast, it is necessary to consider that wind speed is distributed respecting the Weibull distribution. Furthermore, wind speed autocorrelation reflects synoptic and seasonal wind speed behavior; this aspect is represented by the persistence feature that is measured as the average duration of wind speed in a given time interval for a certain site. Many models for wind speed persistence have been proposed in the literature [CSGTXB10]. The most applied ones are ARMA, Markov, and Wavelet models [BK09]. Nevertheless, these models do not guarantee at the same time that wind speed autocorrelation reflects synoptic cycles and that wind speed persistence and Weibull statistical characteristics are not altered. In order to overcome some of the
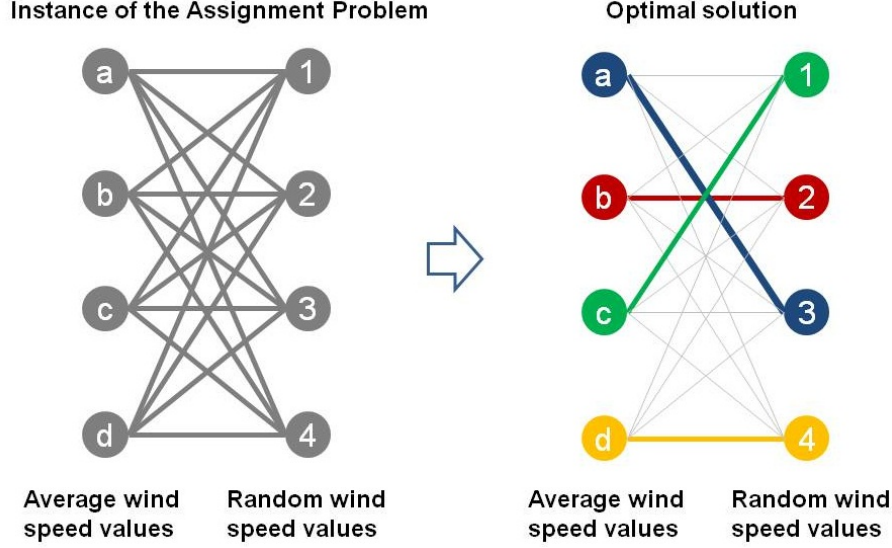
Figure 7.6: An example for the Assignment Problem, used to model wind speed persistence features.

drawbacks of these models, in this work wind speed persistence features are modeled considering mathematical formulations for the Assignment Problem. The Assignment Problem is one of the most studied Optimization problems in the Operations Research literature [BDM09]. Given two disjoint sets of equal size and a cost associated with each element of the cross product of the two sets, it is required to assign exactly one element belonging to the first set to one element belonging to the second set, so that all the elements belonging to the sets have been assigned and the total cost of the assignment is minimized. In our study:

- the elements of the first set are the average wind speed points, which are individuated on an hourly average observed wind speed curve (left part of Fig. 7.6);

- the elements of the second set are the wind speed points generated in a random way, respecting a Weibull distribution, and that have to be sequenced, to consider wind speed persistence features (right part of Fig. 7.6);

- assignment costs are represented by a function of the distances between average observed wind speed points and random wind speed points.

In this study, the Assignment Problem has been solved considering a well known Operations Research algorithm, called Hungarian Algorithm [BDM09]. The correct re-assignment of the random wind speed points to the average wind speed points is obtained solving the Assignment Problem with the Hungarian Algorithm and minimizing the total distance between the random points and the average points. It is fundamental to observe that the Assignment Problem is solved considering the hourly observed average wind speed curve. This could lead to think that an alternative way to model wind speed features could be based only on a casual perturbation of the observed average wind speed, but we will show that this is not the case, comparing this alternative model with the new proposed one.
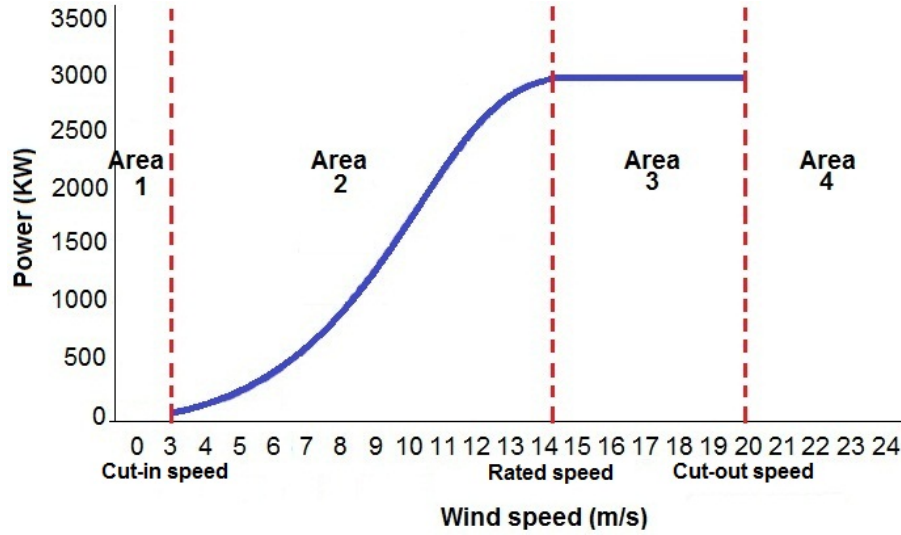
Figure 7.7: Wind turbine power technical curve.

7.2.3 Synthetic wind speed error and wind turbine power curve generation

A realistic measure of the forecast wind speed error can be obtained with ARMA models, as proposed by Soder [Sod93b] [Boo05].These models are based on time-series, which are sequences of observations recorded in specified time intervals. An ARMA time-series is described by the parameters α, β and σ_z [Boo05]. An example of wind speed forecast error curve simulated with the ARMA model is shown in Fig. 7.2. To obtain proper wind power output forecasts, it is necessary to analyze the power technical curve of a wind turbine, shown in the technical manufacturer's data-sheet. A typical wind turbine usually works in four modalities which depend on the wind speed given in input (no wind speed, cut-in, rated, and cut-out wind speed), as shown in Fig. 7.7.

In particular, the following areas are considered

- area 1: wind speed values are lower than cut-in wind speed;

- area 2: wind speed values are comprised between cut-in wind speed and rated wind speed;

- area 3: wind speed values are comprised between rated wind speed and cut-out wind speed;

- area 4: wind speed values are greater than cut-out wind speed.

where

- cut-in speed: minimum speed which guarantees that wind turbine works properly;

- rated speed: minimum speed which guarantees that wind turbine works at nominal power;

- cut-out speed: wind turbine must be blocked if wind speed assumes values greater than the cut-out speed, in order to avoid structural damages.
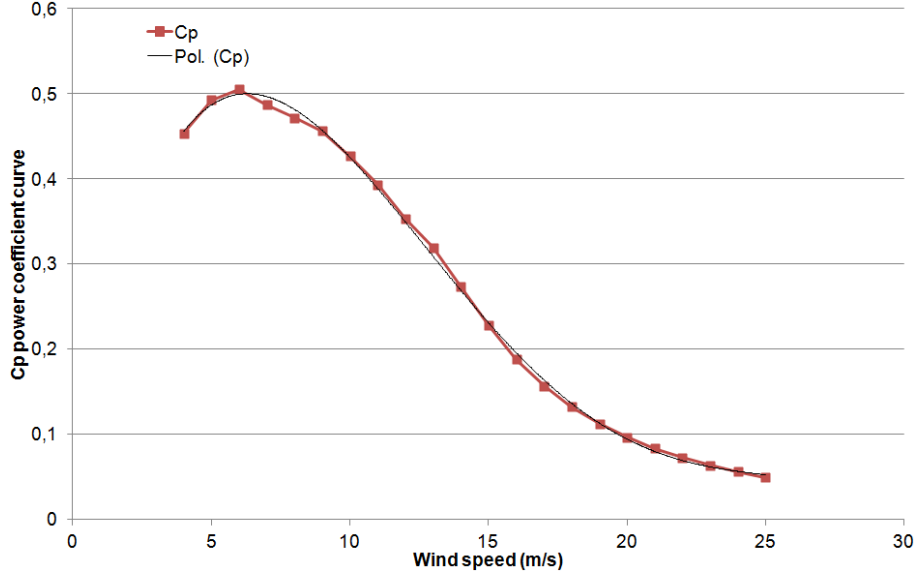
Figure 7.8: C_P power coefficient curve and its polynomial interpolation.

In the area 2, power output is calculated as follows

$$P = 0.5\rho C_P \pi R^2 (v_j^i)^3 \tag{7.15}$$

where

- ρ is the air density factor;

- C_P is the wind turbine power coefficient, which is a direct measure of its efficiency;

- $2R$ is the wind turbine diameter, given in technical manufacturer's data-sheet;

- v_j^i is the average wind speed for wind turbine i at time j.

C_P power coefficient depends on the technical characteristics of the wind turbine. A typical C_P power coefficient curve is shown in Fig. 7.8.

Based on Betz's Theory [Bet66], it is possible to calculate only the maximum value of C_P, which is about 0.59. The power curve cannot be easily reproduced, since it is determined considering the power coefficient curve. It is thus necessary to use the technical manufacturer's data-sheet power curve as an input for our wind data generator. This is a discrete power curve, where the correspondence wind speed-power is given. However, the input forecast wind speed value could not be found in the data-sheet.

For this reason, in our model we have introduced a novel and effective but not so complex approach to well approximate the power curve in all the four areas. We use a polynomial data interpolation algorithm to determine the power output associated with a given wind speed, according to the following steps:

1. C_P is determined for all the given data-sheet wind speeds and an assigned air density factor;

2. C_P is approximated with a polynomial curve;

3. C_P is re-calculated for all wind speeds and air densities, according to the interpolation equation;

4. the power associated with the input wind speed is determined, by substituting the value of C_P, calculated at step 3, in the power equation.

Fig. 7.8 shows the result of our polynomial interpolation algorithm for the power coefficient C_P applied on a real technical data-sheet (*Vestas V82* wind turbine).

7.3 Results and discussion

In this section we analyze how different Assignment formulations affect the quality of the solution and we present the most important simulation results obtained with the new generator.

7.3.1 Tuning the Assignment model

We analyze how different choices of the distance functions in the Assignment affect the quality of the solution, expressed by fitting properties. Fitting is defined as the measure of the difference between the average hourly observed wind speed curve and the re-assigned wind speed curve obtained with the Assignment algorithm. To carry out our analysis, we considered different types of Weibull distributions, for a fixed value of the scale parameter λ ($= 12$) and different values of the shape parameter k (Fig. 7.9):

- Weibull distribution A: $k = 1.95$;

- Weibull distribution B: $k = 1$;

- Weibull distribution C: $k = 3$;

- Weibull distribution D: $k = 1.2$.

These parameters have been chosen to take into account different aspects:

- λ parameter does not affect the shape of the Weibull distribution, but only its scale; for this reason, it is trivial to prove that λ does not affect the behavior of the Assignment algorithm. We have chosen $\lambda = 12$ as an average value in order to obtain a suitable average wind speed at the wind turbine's hub height;

- $k = 1$ and $k = 3$ represent the extremal values for the shape of the Weibull distribution, while $k = 1.2$ and $k = 1.95$ are two typical k parameters which represent a realistic wind speed Weibull distribution [BBL03].

Based on each of these Weibull distributions, we derived different types of hourly observed average wind speed curves (Fig. 7.10).

We performed 1000 simulations over a 24 hours time horizon with the new generator, considering all these curves in input. We did not modify the technical parameters of the wind turbine and the ARMA parameters, while we considered different functions of the assignment distances, as described below:
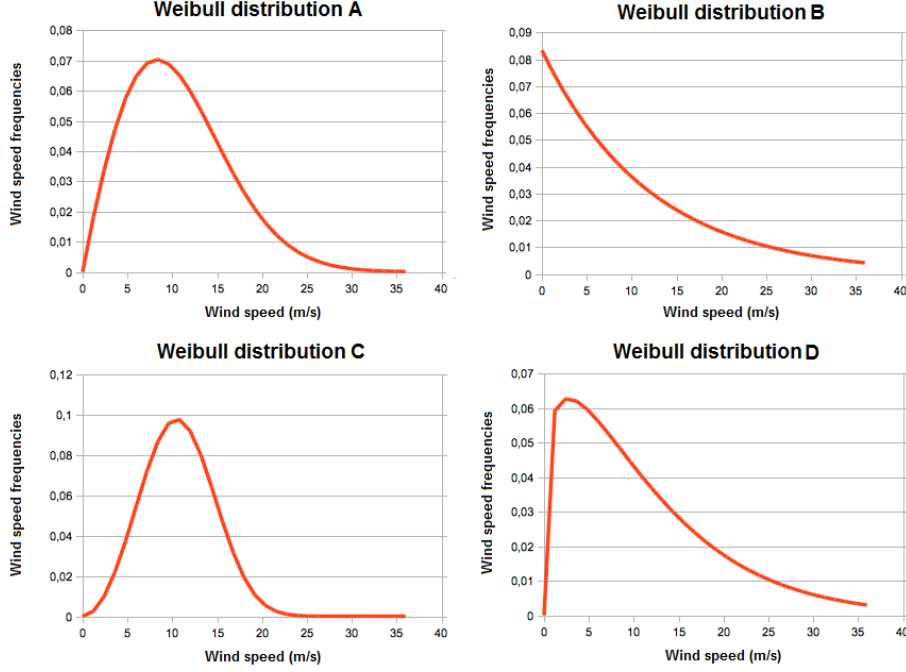
Figure 7.9: Weibull distributions considered in the simulation phase.

1. distance 1: $d_t = |\overline{v}_t - v_{rand,t}|$;

2. distance 2: $d_t = \frac{|\overline{v}_t - v_{rand,t}|}{2}$;

3. distance 3: $d_t = |\overline{v}_t^2 - v_{rand,t}^2|$;

4. distance 4: $d_t = (\overline{v}_t - v_{rand,t})^2$;

5. distance 5: $d_t = \frac{|\overline{v}_t - v_{rand,t}|}{4}$.

where $\overline{v}_t$ represents the average observed wind speed at time t, and $v_{rand,t}$ is the re-assigned wind speed at time t. The results obtained in the simulation phase are presented in the following sections.

Quality of the fitting and assignment distances

We study how the quality of the fitting is influenced by the function of the assignment distance. To calculate the quality of the fitting η we considered the formula $\eta = \sum_i^T \frac{|\overline{v}_t - v_{rand,t}|}{\overline{v}}$, where $\overline{v}$ is the average value of wind speed, observed in the given time horizon. Table 7.2 shows that η is influenced by the assignment distance. Smaller values of η correspond to a better quality of the fitting. Fig. 7.11, 7.12, 7.13, 7.14, and 7.15 show an example of how the fitting is subjected to variations, when different types of distances are considered. Fig. 7.16 shows the shape of the average of η, for all the types of distributions and curves (on the columns of the table 7.2). Distances 1 and 3 minimize the average value of η for each type of curve. Fig. 7.17 shows how
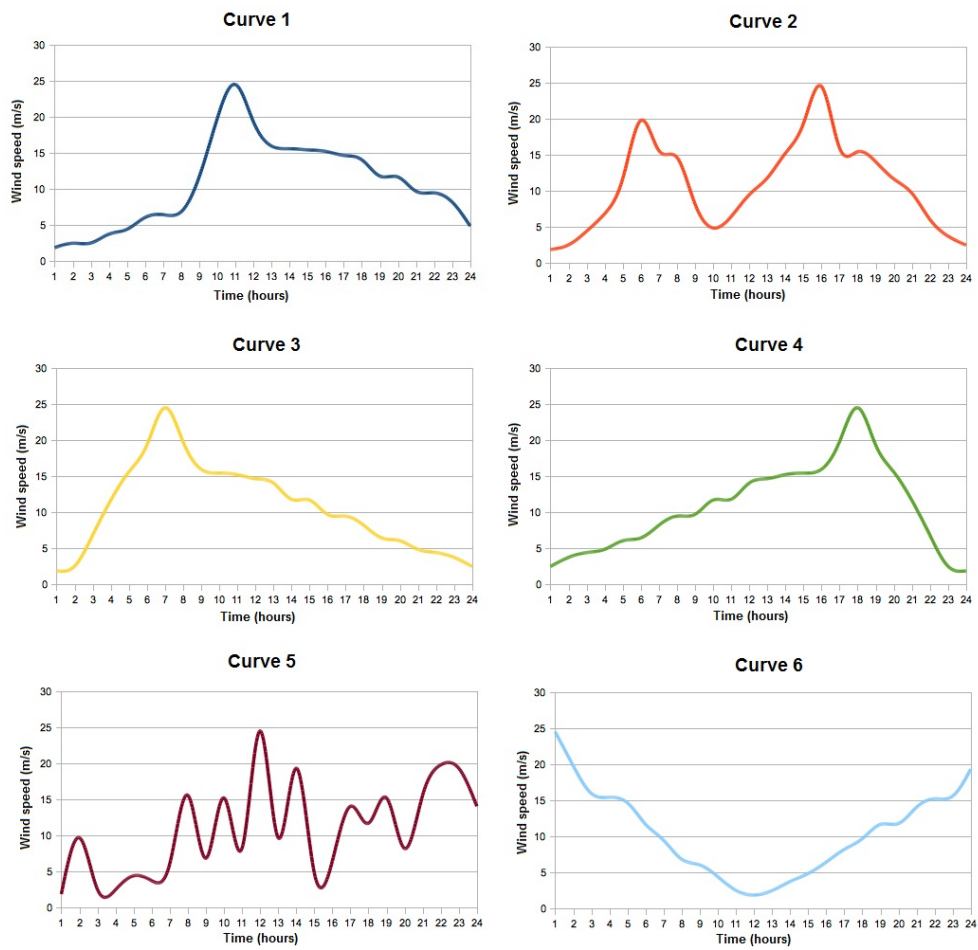
Figure 7.10: Average wind speed curves considered in the simulation phase.

Weibull	Curve	η (dist. 1)	η (dist. 2)	η (dist. 3)	η (dist. 4)	η (dist. 5)
A	1	7.67%	7.66%	7.97%	7.85%	8.94%
A	2	8.12%	8.01%	7.91%	7.94%	9.40%
A	3	7.58%	7.63%	8.15%	7.68%	9.93%
A	4	8.12%	7.80%	8.08%	7.87%	10.17%
A	5	9.96%	10.10%	10.03%	9.50%	10.87%
A	6	7.92%	8.00%	7.69%	7.94%	10.56%
B	1	7.40%	7.38%	7.48%	7.32%	8.98%
B	2	6.97%	7.26%	6.43%	10.91%	9.92%
B	3	6.74%	8.08%	6.57%	10.49%	8.72%
B	4	7.53%	7.55%	7.29%	10.47%	8.68%
B	5	6.89%	7.73%	7.24%	11.02%	9.40%
B	6	6.68%	7.28%	6.50%	10.95%	9.58%
C	1	8.45%	9.19%	8.50%	12.88%	11.73%
C	2	8.12%	8.84%	7.97%	12.52%	10.88%
C	3	4.03%	4.66%	4.50%	4.09%	12.42%
C	4	3.89%	4.03%	4.31%	4.28%	8.85%
C	5	3.87%	4.78%	4.12%	4.05%	11.95%
C	6	4.28%	4.19%	4.42%	4.24%	8.79%
D	1	4.10%	4.01%	3.83%	3.63%	6.91%
D	2	3.95%	4.16%	3.71%	3.63%	11.05%
D	3	3.79%	4.06%	3.90%	3.75%	9.40%
D	4	12.33%	12.60%	12.12%	16.80%	13.92%
D	5	11.34%	12.00%	11.17%	15.50%	13.46%
D	6	10.97%	12.02%	10.53%	15.71%	12.77%

Table 7.2: Values of η obtained with respect to the chosen assignment distance.

many times a given distance minimizes η for a certain distribution and curve (on the rows of the table 7.2). The larger probability to have the minimum η is given by the distance 3. Based on the results obtained, we observe that distance 3 ensures the best fitting for all the curves considered.

Quality of the fitting and shape of the average wind speed curves

We study how the quality of the fitting is influenced by the shape of the average curve. The results show that (Fig. 7.18) the quality of the fitting η is constant (Weibull A and B); the quality of the fitting η is influenced by the variation of the shape of the average wind speed curve (Weibull C and D). This result depends on the Weibull distribution; the distributions A and B and the shapes 1, 2, and 3 are characterized by a stronger persistence, which makes the operation of re-assignment simpler with random data. Since the parameter λ has been left unaltered during the simulations, the results show that the quality of the fitting is mildly dependent on the factor k of the Weibull distribution.

7.3.2   Simulating wind speed with the Assignment model

The simulation results described in this section have been obtained with the Assignment algorithm considering the distance 2. We have chosen this type of distance to simplify our calculations, even if it is not the best one, as shown previously. If wind speed values are random generated, considering only the Weibull distribution and neglecting wind speed persistence features, the random wind speed curve does not reflect the observed wind speed curve (Fig. 7.19). If wind speed values are generated solving the Assignment Problem, and considering both Weibull distribution and wind speed persistence features, the re-assigned wind speed curve reflects the observed wind speed realistically (Fig. 7.20).
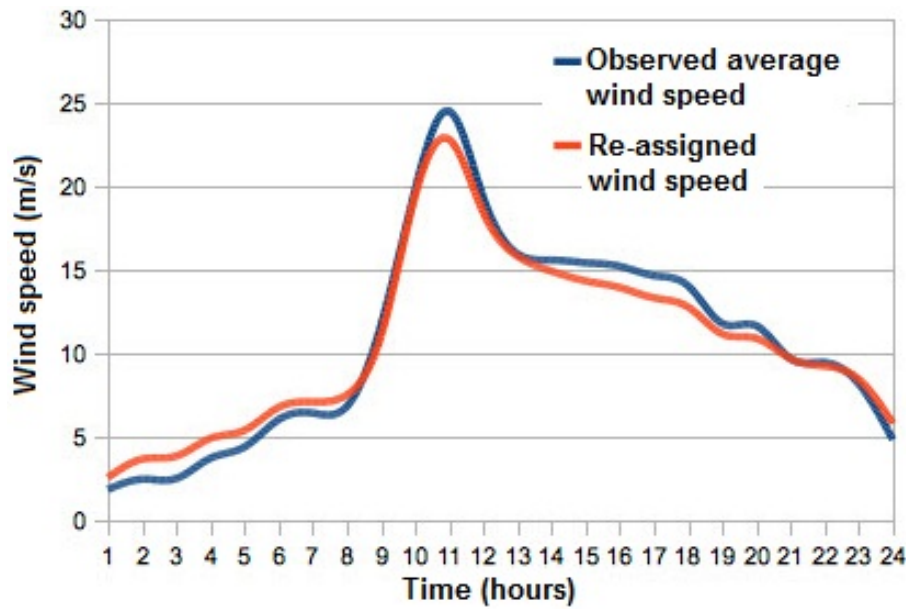
Figure 7.11: Fitting with distance 1.
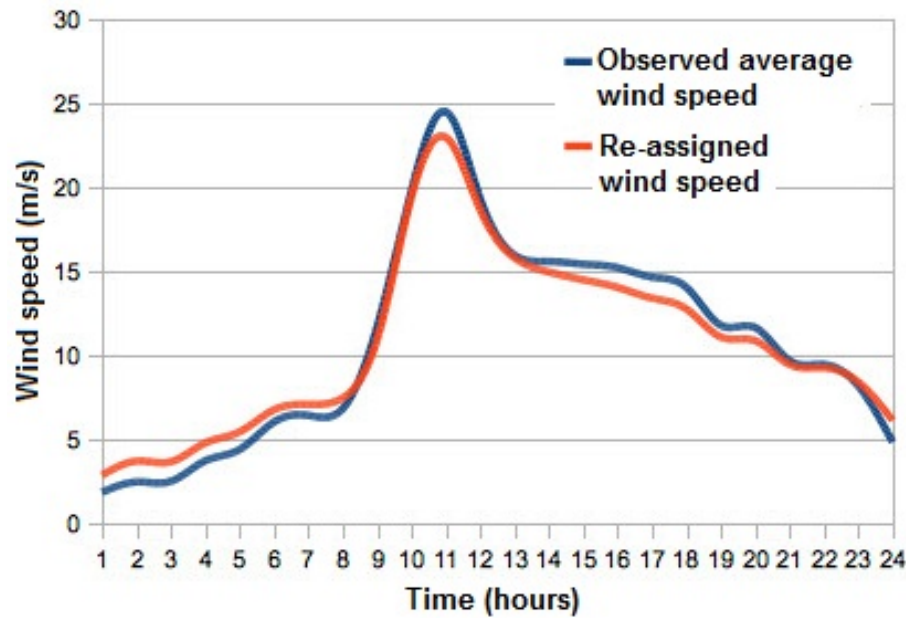
Figure 7.12: Fitting with distance 2.
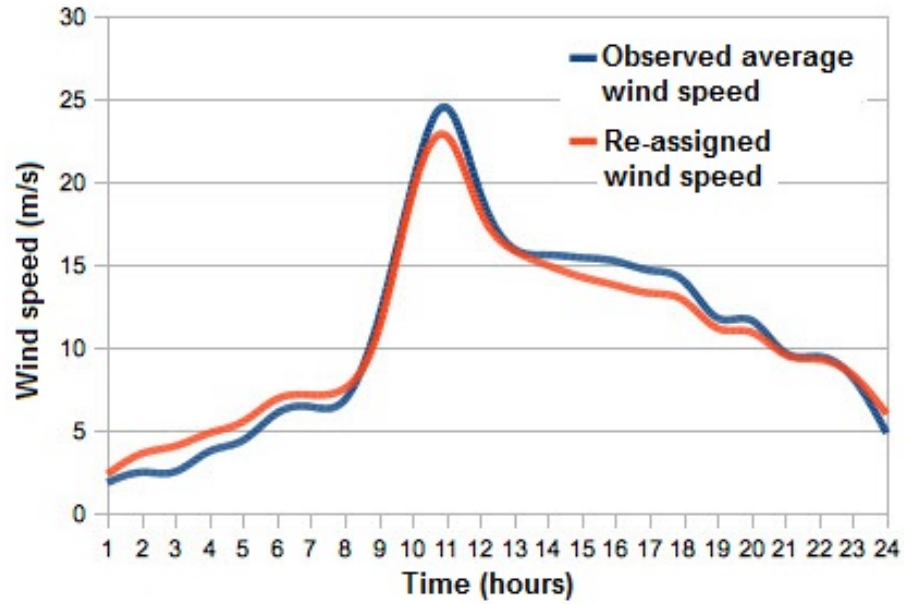
Figure 7.13: Fitting with distance 3.
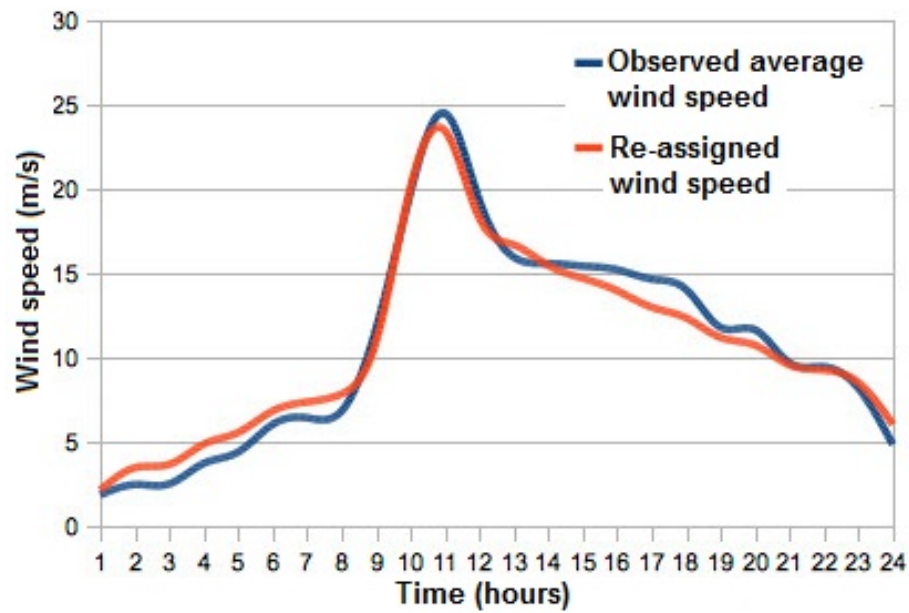
Figure 7.14: Fitting with distance 4.
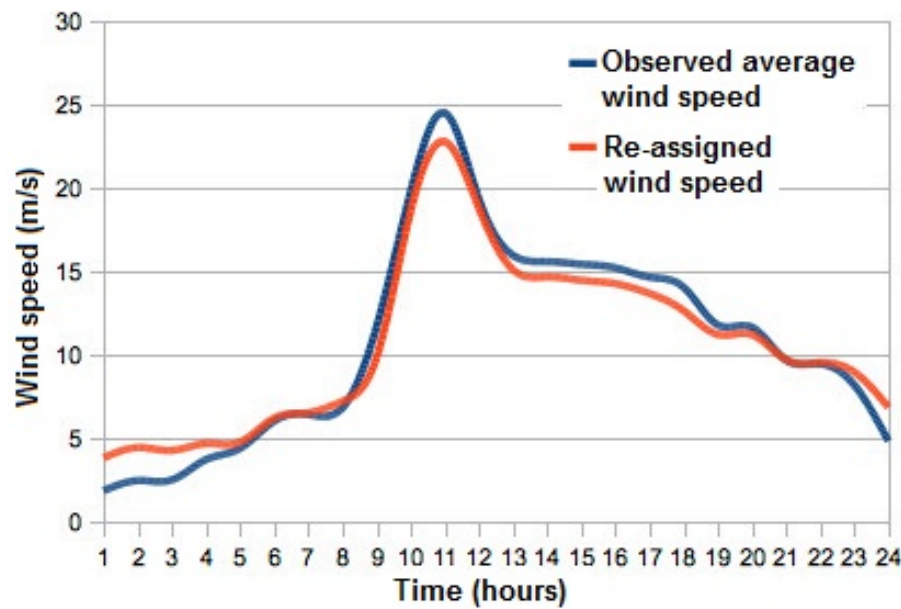
Figure 7.15: Fitting with distance 5.
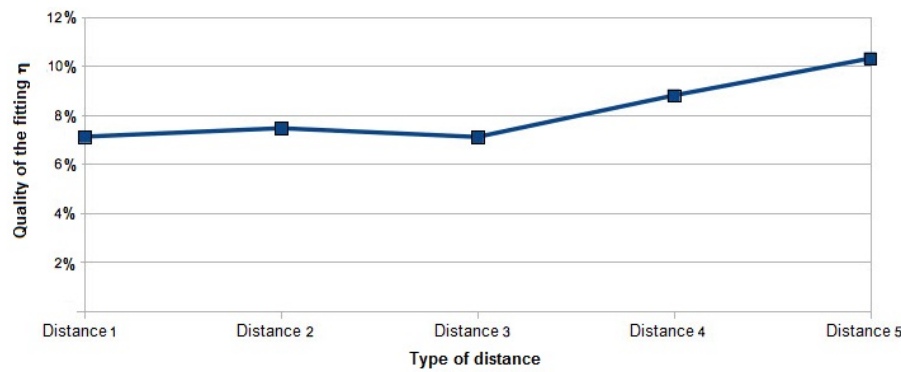
Figure 7.16: Quality of the fitting η for all the Weibull distributions and curves.
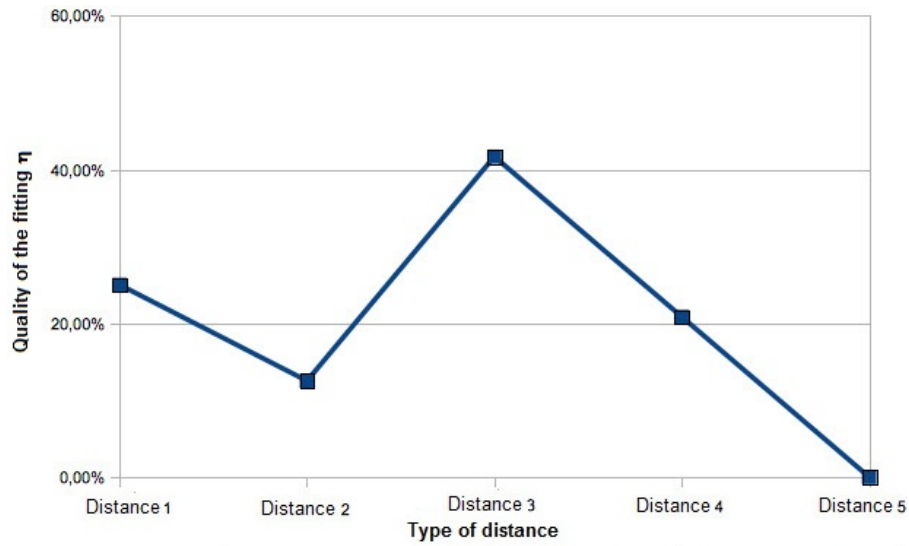
Figure 7.17: Quality of the fitting η for an assigned Weibull distribution and a given curve.
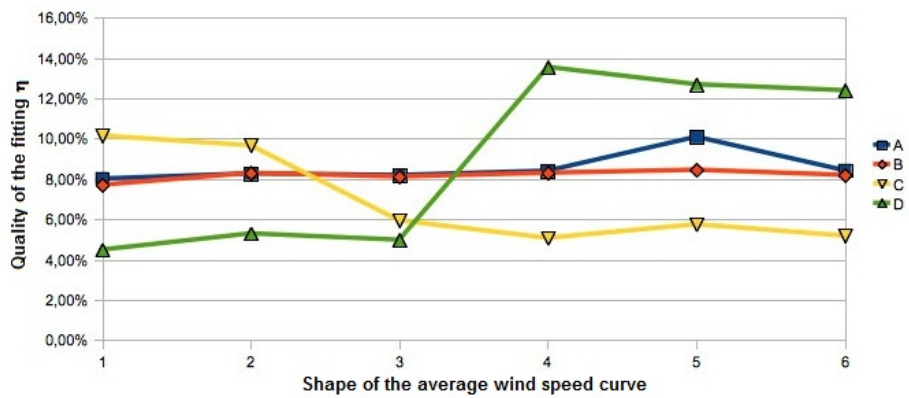
Figure 7.18: Quality of the fitting η with respect to the variation of the shape of the average curve.
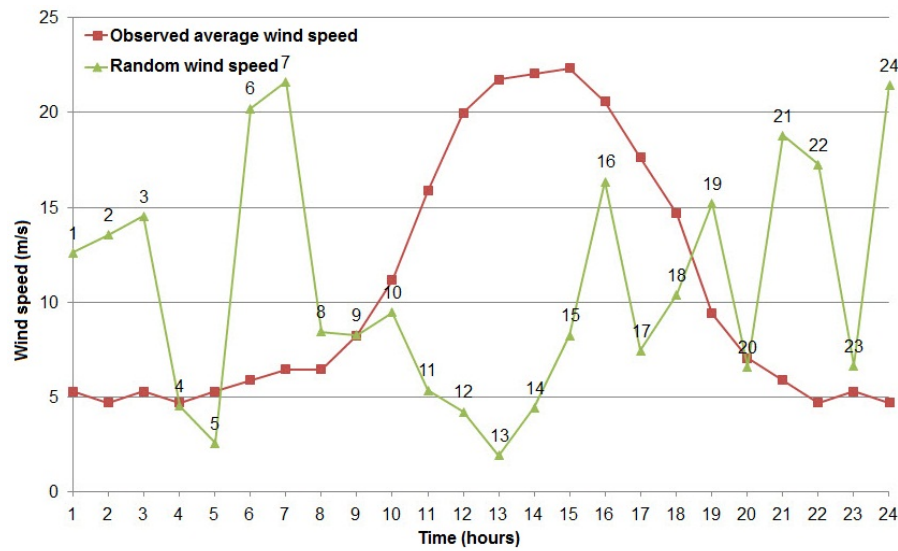
Figure 7.19: Wind speed results obtained with random generation.
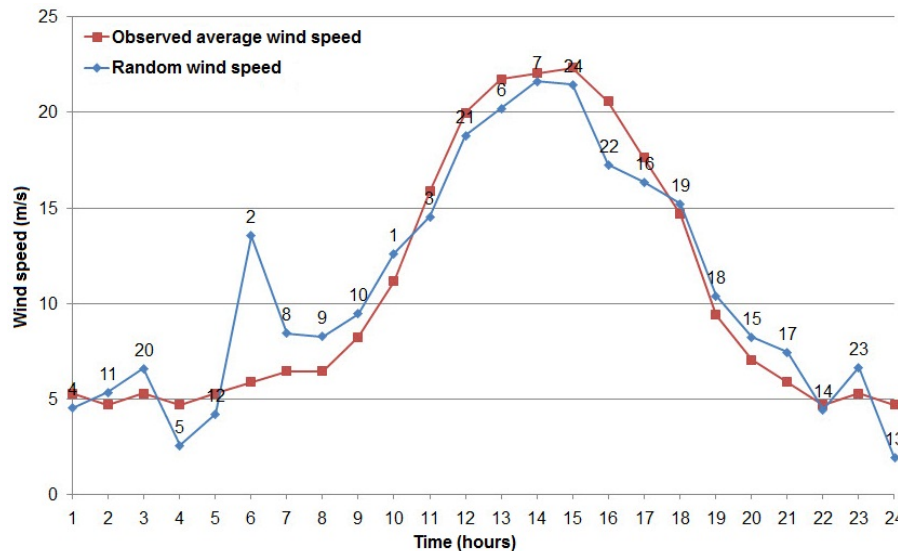
Figure 7.20: Wind speed results obtained with re-assignment.
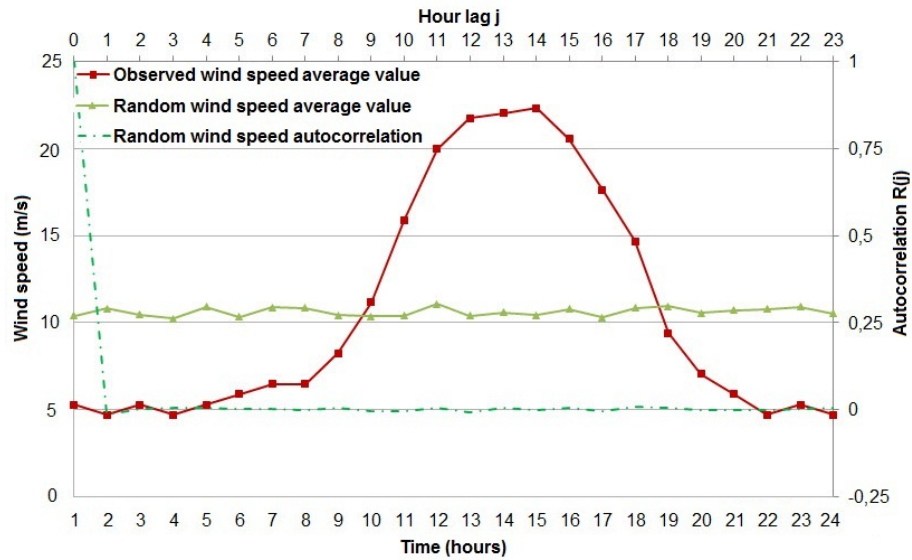
Figure 7.21: Simulation results obtained with random generation.
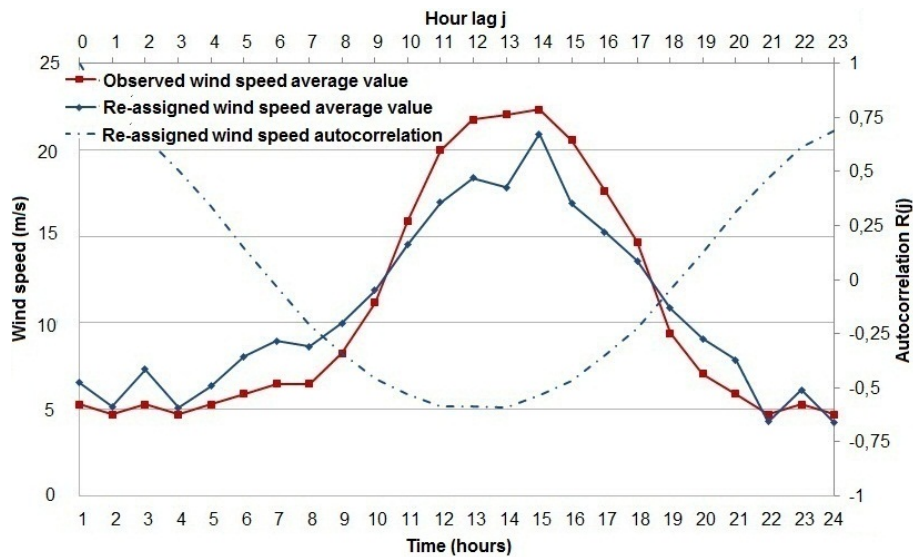
Figure 7.22: Simulation results obtained with re-assignment.
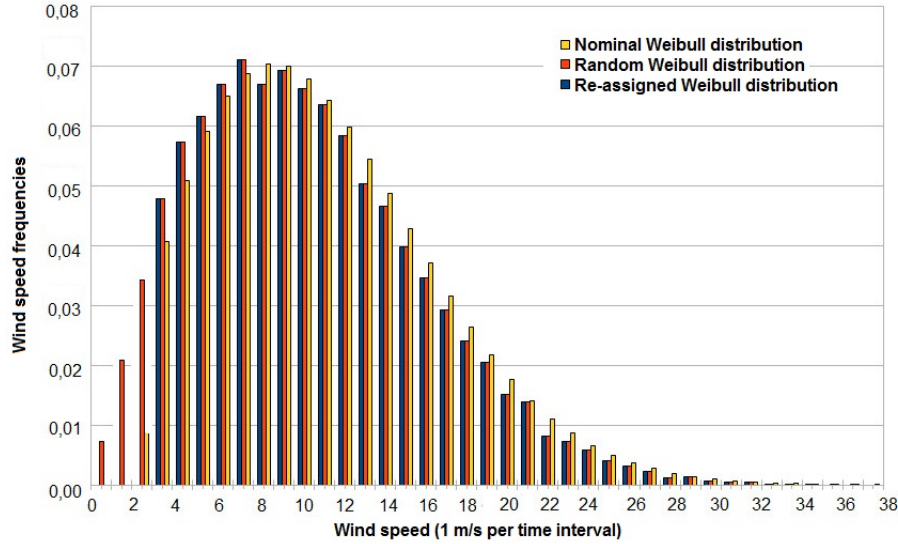
Figure 7.23: Nominal, random and re-assigned Weibull distributions.

If wind speed values are random generated, random wind speed average is constant and its auto-correlation tends to zero (Fig. 7.21). Thus, random wind speed does not reflect synoptic wind speed cycles and persistence features. If wind speed values are generated solving the Assignment Problem, re-assigned wind speed average is comparable to the observed wind speed average and re-assigned wind speed auto-correlation differs from zero (Fig. 7.22).

This means that re-assigned wind speed reflects synoptic wind speed cycles and persistence features. Fig. 7.23 compares the distributions of the observed hourly average, random, and reassigned wind speed. These distributions reflect a typical Weibull. Thus, performing the re-assignment considering wind speed persistence features does not alter the statistical characteristics of wind speed. Simulations results thereby show that formulations for the Assignment Problem represent a useful instrument to correctly model wind speed persistence features, which are fundamental to obtain proper wind speed and power forecasts.

7.3.3   Simulation results of the new synthetic wind data generator

In the simulation phase, the new generation model has been compared with a random one. The random model generates the synthetic wind speed curve applying a casual disturb to the observed average wind speed curve. In this operation, a normal distribution with amplitude equal to 60% of the average value of the observed wind speed curve is considered. For our simulations, we considered the hourly average wind speed curves observed in Catania, Italy, subject of the analysis shown in [BBL03]. To obtain realistic values of wind speed, this data has been normalized at the wind turbine hub height h, considering the following formula [Hei05]

$$v(h) = v_{10} \cdot \left(\frac{h}{h_{10}} \right)^a \tag{7.16}$$

where
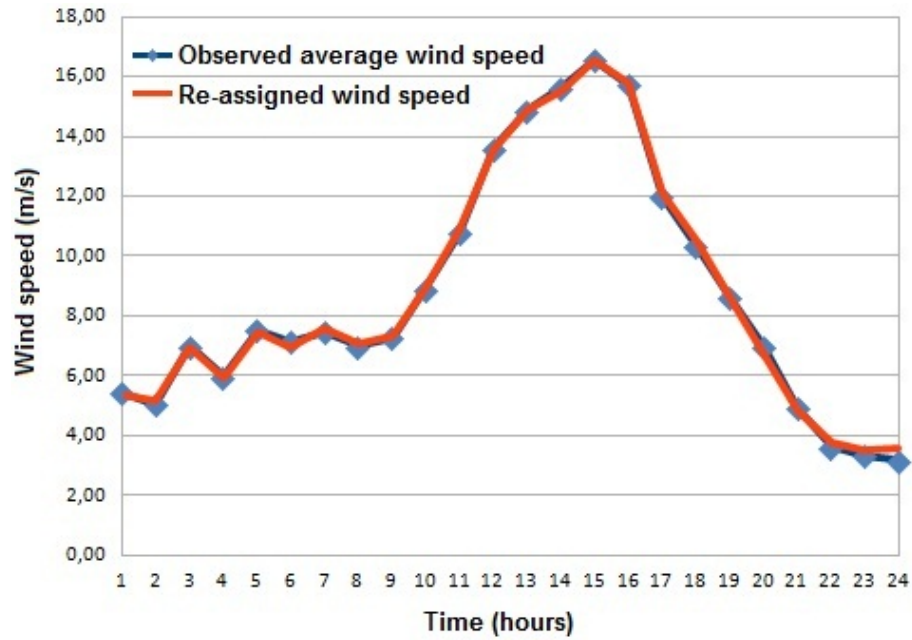
Figure 7.24: Wind speed curves obtained with random generation.
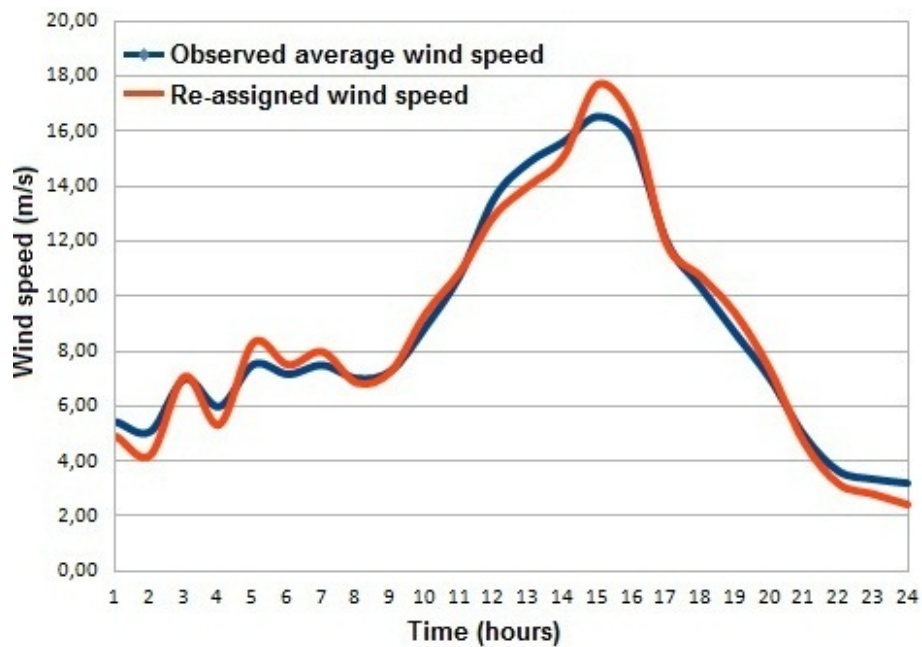
Figure 7.25: Wind speed curves obtained with re-assignment.
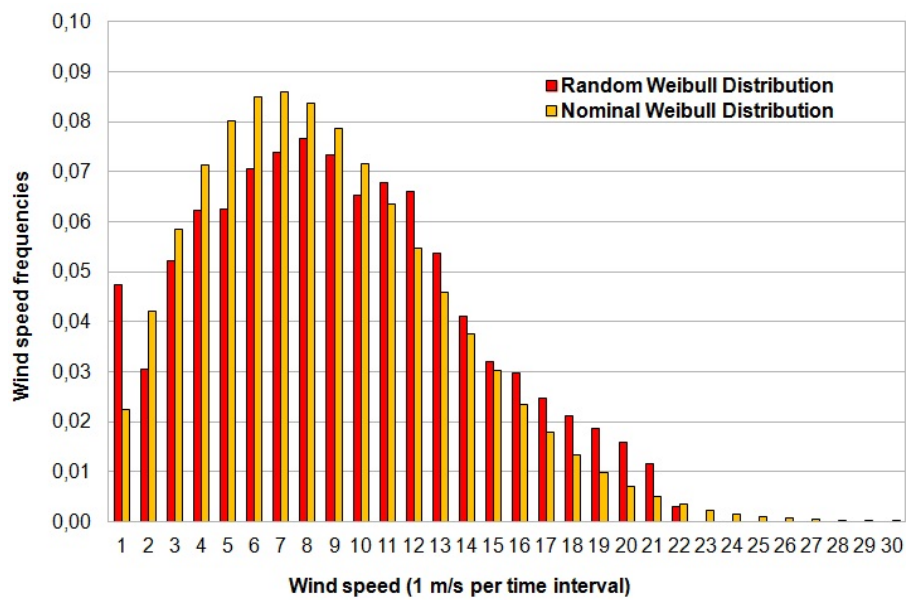
Figure 7.26: Weibull wind speed distributions obtained with random generation.
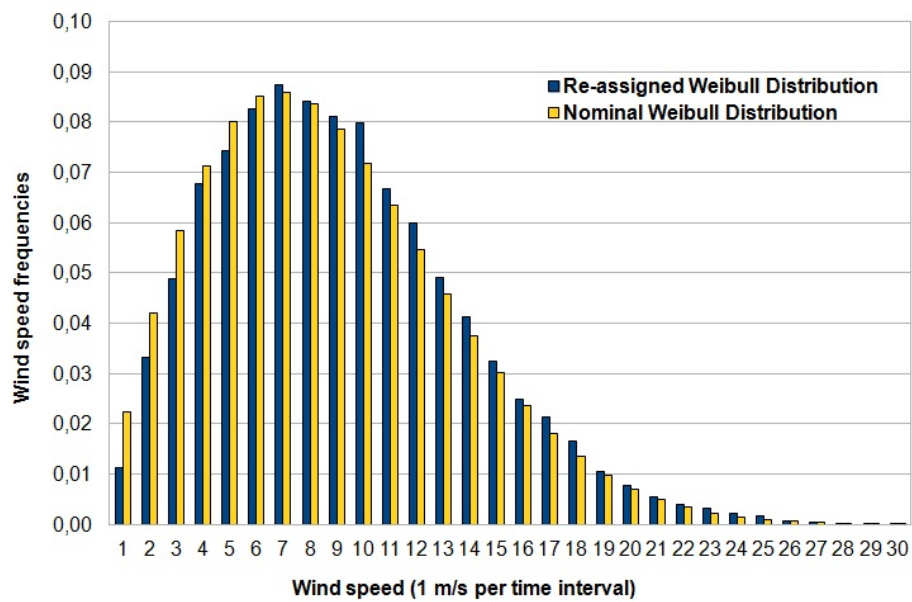
Figure 7.27: Weibull wind speed distributions obtained with re-assignment.

- $v(h)$ is wind speed at hub height h (m/s);

- v_{10} is wind speed at height $h_{10} = 10$ m (m/s);

- a is the Hellman exponent which depends on the coastal location, on the terrain complexity where wind turbines are located and on the stability of the air [KSW07].

We considered a time horizon consisting of one year, which has been divided into 4 slots, each comprising 90 days (3 months). Each slot is associated with a given observed hourly average wind speed curve, which respects a certain Weibull distribution with assigned λ and k parameters. This curve is the same in a given slot, while it changes when a different slot is considered. We performed 1000 simulations for each slot, taking in input a real wind turbine (Enercon E82 82m 2MW). For the ARMA parameters we considered $\alpha = 0.95$, $\beta = -0.60$, and $\sigma_z = 0.50$.

The random model perfectly approximates the hourly average observed wind speed curve (Fig. 7.24). This result is not surprising, as the casual disturb is almost annulled when the average operation is applied to the average curve itself. However, the distribution of the wind speed frequencies is degenerated at the extreme points (Fig. 7.26). The new model properly approximates the hourly average observed wind speed curve (Fig. 7.25). It guarantees an optimal distribution of the wind speed frequencies: re-assigned wind speed Weibull distribution is not altered (Fig. 7.27).

The random model produces a smoother average wind speed curve (Fig. 7.28). This model tends to underestimate the effect of the forecast error on wind power (Fig. 7.30). Nevertheless, at a local level, when a simulation slot is considered, wind speed has more peaks than the new proposed model (Fig. 7.34, 7.36, and 7.38). In fact, when the casual disturb is applied, wind speed tends to reach values near cut-out or below cut-in speed as effect of the degeneration of the Weibull distribution. This determines a wind power frequency distribution with higher probability on the extreme values (Fig. 7.32).

The new proposed model produces an average wind speed curve with marked peaks (Fig. 7.29). This model tends to overestimate the effect of the forecast error on wind power (Fig. 7.31). Nevertheless, at a local level, when a simulation slot is considered, wind speed presents better persistence characteristics (Fig. 7.35, 7.37, and 7.39). This is confirmed by the results on average forecast wind power, calculated as the average between the upper and the lower bound on power. In the case of the upper bound (lower bound), wind speed forecast error leads to an increase (reduction) in wind speed. These results are more realistic than those obtained with the random model (Fig. 7.40, 7.41, 7.42, 7.43, 7.44, and 7.45). In fact, even if power is strongly variable between a 24 hours time horizon and the following, it is cyclical in a single 24 hours time horizon. This is expected when we consider the same average wind speed curve in a limited time period (e.g. a week, a month, a season).

In the average power distribution, we observe that the value of 1 MW is associated with higher frequencies (Fig. 7.32 and 7.33). In fact, if wind speed is next cut-out and the forecast error is sufficiently high, the upper bound on wind speed is higher than cut-out, causing the block of the wind turbine (0 MW power), while the lower bound on wind speed is comprised in the rated range and produces the rated power (2 MW). If we do not consider this effect in our statistics on frequencies, the peak at 1 MW disappears; thus, it represents the statistical effect of wind speeds next cut-out associated with high forecast errors.

Based on the experiments conducted, we conclude that the new model:

- better approximates wind speed characteristics: Weibull distribution and autocorrelation are respected, average wind speed curve is approximated at optimality;
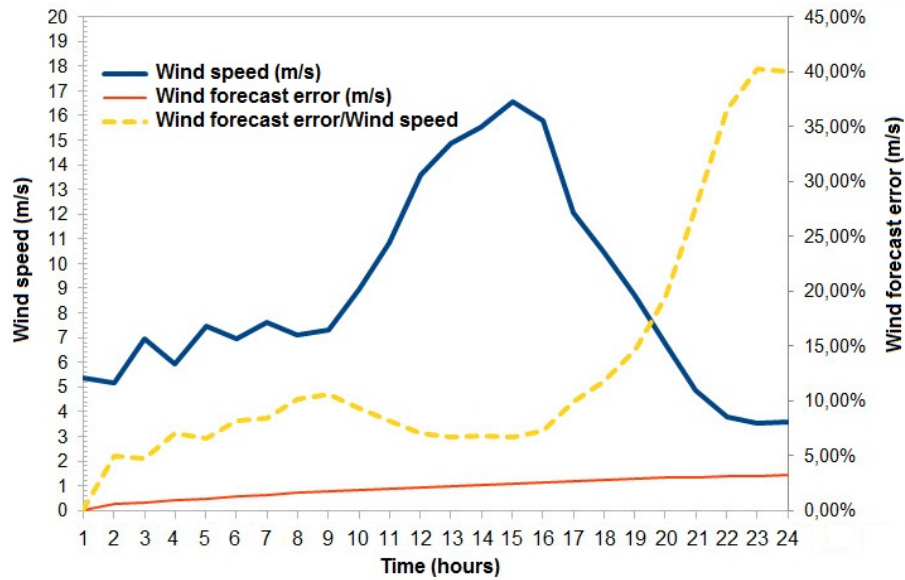
Figure 7.28: Wind speed forecast results obtained with random generation.
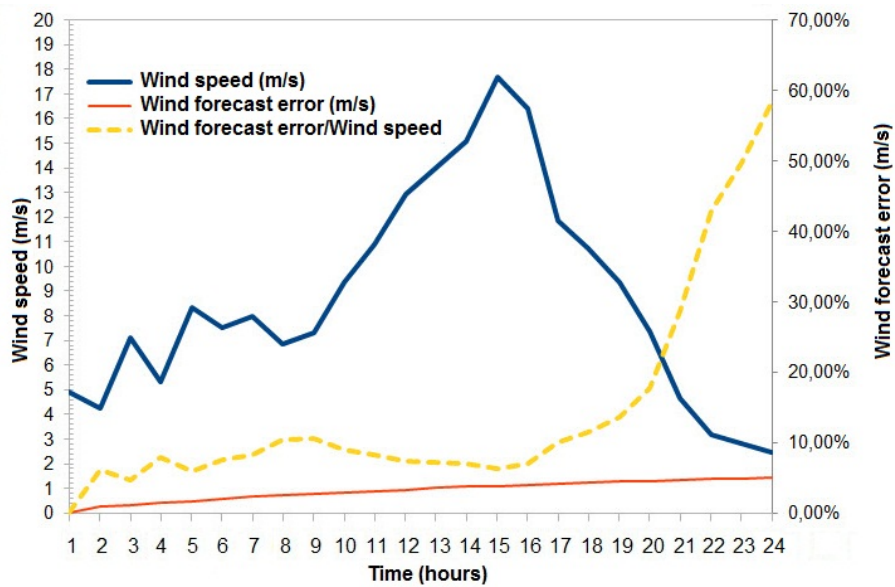
Figure 7.29: Wind speed forecast results obtained with re-assignment.
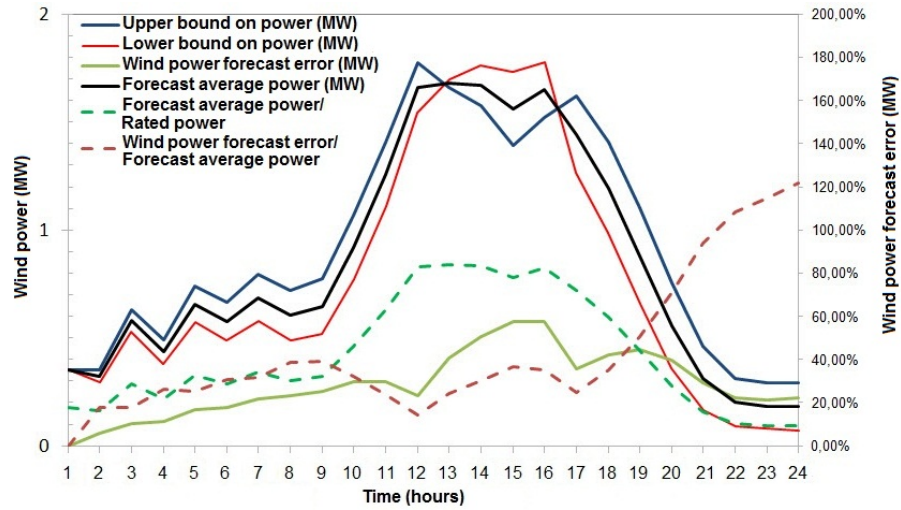
Figure 7.30: Wind power forecast results obtained with random generation.
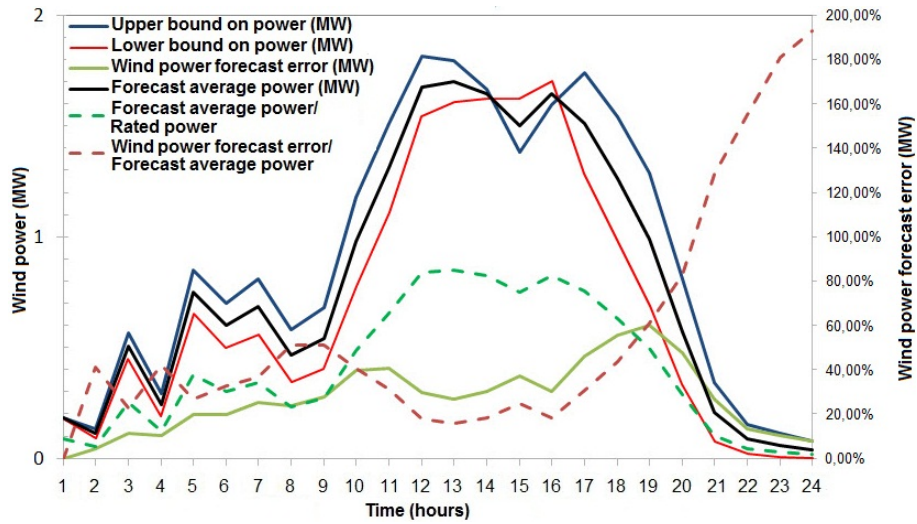
Figure 7.31: Wind power forecast results obtained with re-assignment.
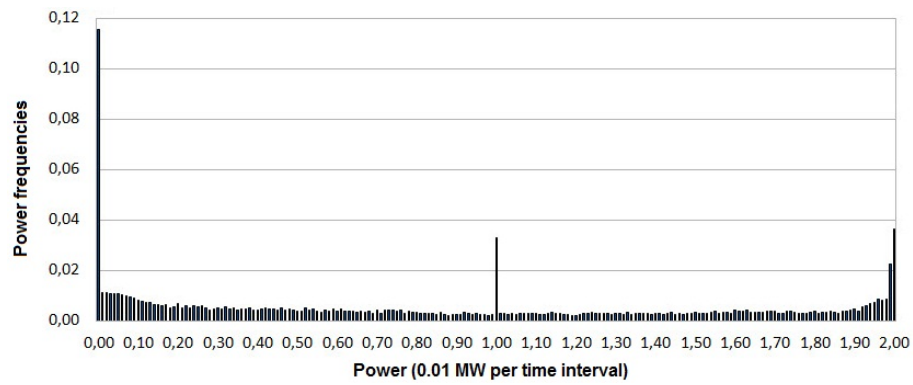
Figure 7.32: Wind power distributions obtained with random generation.
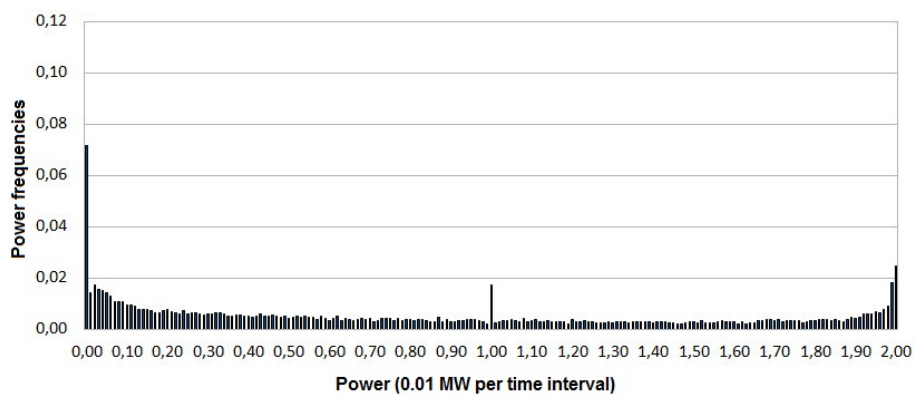
Figure 7.33: Wind power distributions obtained with re-assignment.

- generates synthetic wind speed data with better persistence features: the hourly average wind speed curve presents casual variations like the typical wind phenomena, but these variations are not uncorrelated, thus, wind memory effect is maintained (Fig. 7.35, 7.37, and 7.39);

- is more conservative in the generation of the synthetic wind power data: we can confirm this behavior of the model making a comparison between the hourly wind power curves and the estimation of the average hourly energy over all the simulations performed (Fig. 7.41, 7.43, and 7.45); this aspect is fundamental when this data is used as input to the generating units within a power production scheduling process such as UC.
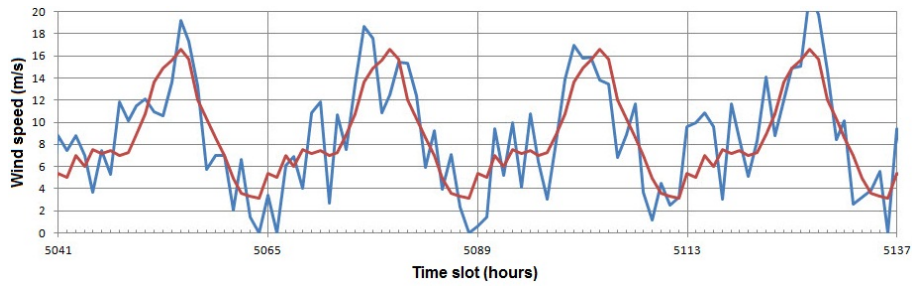
Figure 7.34: Wind speed obtained with random generation.
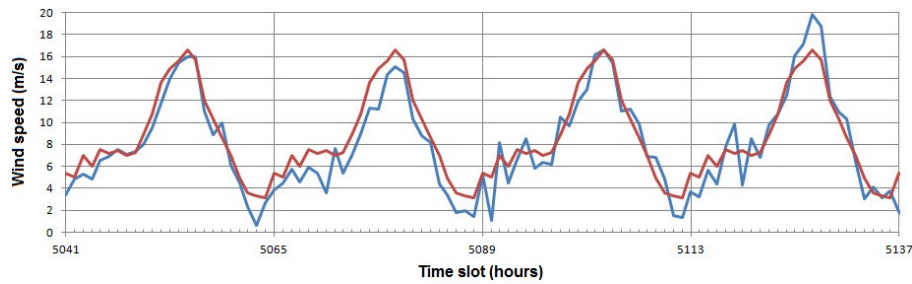
Figure 7.35: Wind speed obtained with re-assignment.
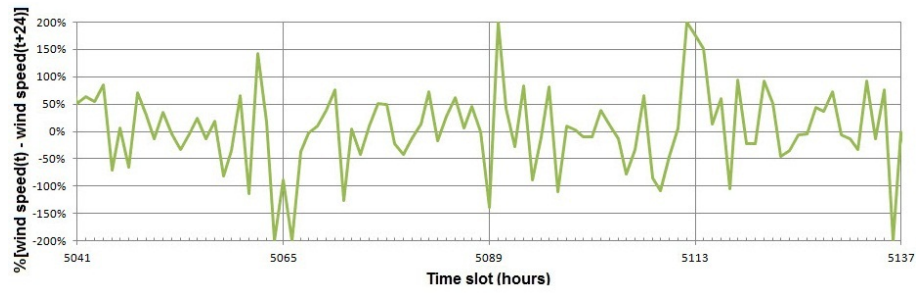
Figure 7.36: Wind speed shifting obtained with random generation.
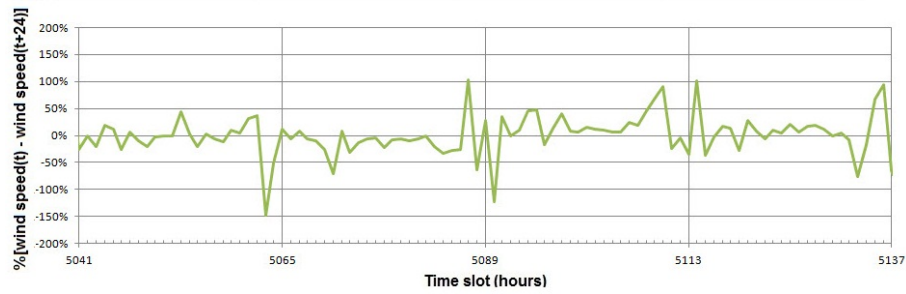
Figure 7.37: Wind speed shifting obtained with re-assignment.
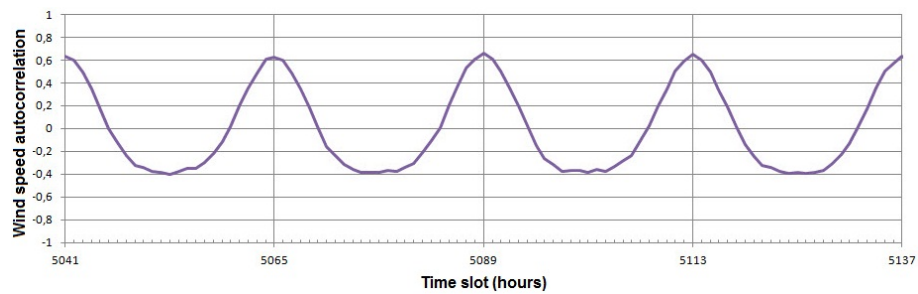
Figure 7.38: Wind speed autocorrelation obtained with random generation.
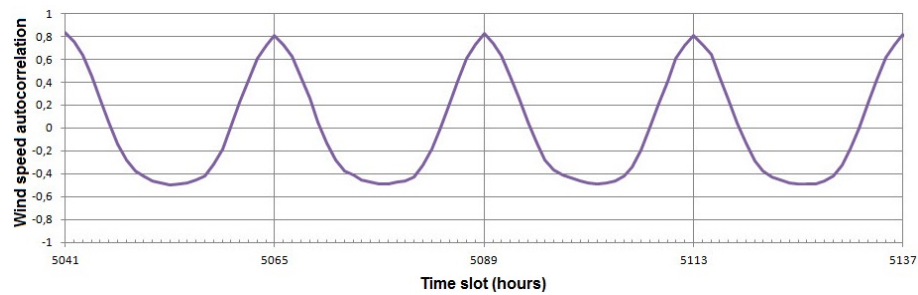
Figure 7.39: Wind speed autocorrelation obtained with re-assignment.
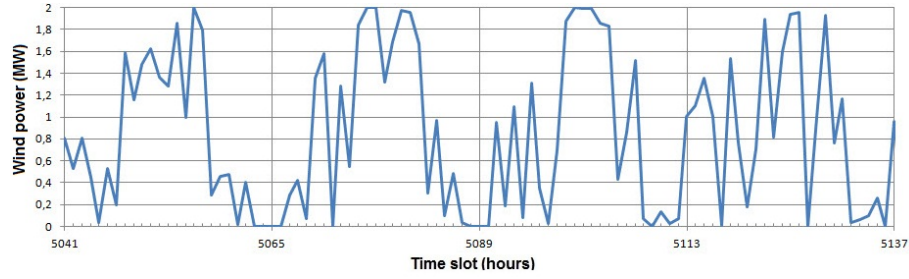
Figure 7.40: Wind power obtained with random generation.
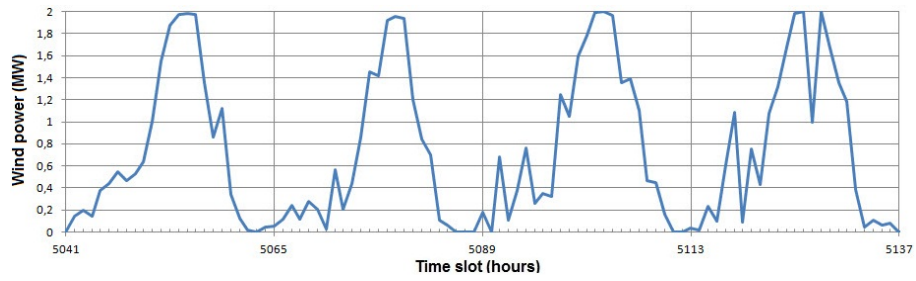
Figure 7.41: Wind power obtained with re-assignment.

Figure 7.42: Wind power shifting obtained with random generation.
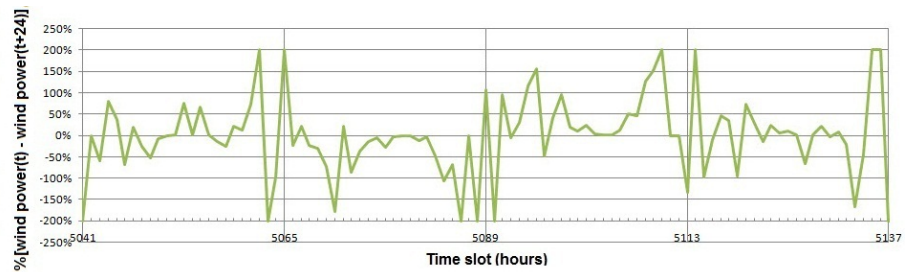
Figure 7.43: Wind power shifting obtained with re-assignment.
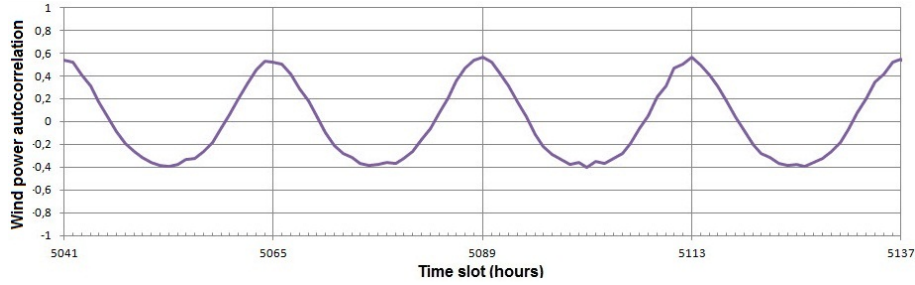
Figure 7.44: Wind power autocorrelation obtained with random generation.
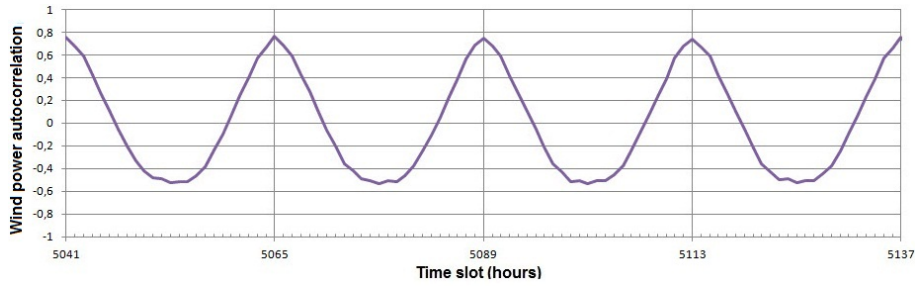
Figure 7.45: Wind power autocorrelation obtained with re-assignment.

7.4 Conclusions

In this chapter, a new model to generate synthetic wind data has been developed. Wind speed has been modeled as a Weibull distribution, while wind speed forecast error has been simulated using an ARMA time-series model. A mathematical formulation of the Assignment Problem has been used to model wind speed persistence features. Simulations results have shown that generating wind synthetic data in a pure random way is not sufficient to produce complete wind speed and power output forecasts, but an accurate generation model which considers all the wind characteristics, such as persistence features, is fundamental.

In the next chapter, wind synthetic data, generated with the proposed model, will be used to carry out simulations studies to individuate wind turbines operational parameters that mainly affect wind generators performances. An experimental function which expresses the average energy produced by a wind turbine in a 24 hours time horizon in a typical day will be determined, considering the main simulation parameters related with Weibull distribution and wind turbines.

As far as future work is concerned, the ARMA model used to determine the wind forecast error could be refined in order to take into account both the variability in space and in time. Regarding the solution of the Assignment Problem, we could consider a variable average curve, determined with an ARMA model, in order to simulate also the scenarios in which the persistence at long term decays.

Chapter 8

An enhanced approach to compute the average energy produced by a typical wind turbine

This chapter explains how the synthetic wind data, generated with the new model proposed in our research activities and presented in chapter 7, has been used to carry out simulations studies in order to individuate the wind turbines operational parameters that mainly affect the performances of the typical wind generators. In particular, we describe how to determine an experimental function which expresses the average energy produced by a wind turbine in a 24 hours time horizon in a typical day, considering the main simulation parameters related with the Weibull distribution and the technical characteristics of the wind turbines. In order to determine this function of the energy, we analyze first how the average energy produced by a wind turbine in a 24 hours time horizon of a typical day is influenced by the simulations parameters (and a combination of them), such as the Weibull distribution parameters (λ and k), the shape of the observed hourly average wind speed curve and the technical parameters of the wind turbine (rated speed v_r, cut-in speed v_{in}, cut-out speed v_{out}). In order to carry out our analysis, we have considered a set of Weibull distributions, with λ and k assigned parameters, and we have derived different average wind speed curves, analogously to what has been described in section 7.3.1 of chapter 7. For each of these curves, we have performed 1000 simulations with the proposed synthetic wind data generator, considering the values of the parameters λ and k of the Weibull distribution related with the average curve itself. For each type of curve, we have determined the value of the expression $\frac{E}{E_r}$, where:

- E is the energy produced by the wind turbine in a 24 hours time horizon;

- $E_r = P_r \cdot 24$ is the *rated* energy (P_r represents the *rated* power).

E_r represents the maximum energy that a wind turbine can produce, working at a *rated* power for 24 hours. In this case, the value of $\frac{E}{E_r}$, which represents the efficiency of the wind turbine, is equal to 1. This value is based on the assumption that the energy is constant in a given time period (usually equal to one hour), even if this is not proper realistic from a practical point of view. In fact, wind speed (and thus energy) can be subjected to variations in this time interval.

As mentioned before, the objective of this set of simulations is to find an experimental function of $\frac{E}{E_r}$, related with the main simulations parameters, such as λ, k and the rated speed v_r. The objective is thus to individuate a proper expression for $\frac{E}{E_r} = f(\frac{\lambda}{v_r}, k)$. In the function, we consider $\frac{\lambda}{v_r}$, because λ represents a wind speed from a dimensional point of view, since it is the scale factor of the Weibull distribution. For this reason, this representation of the energy is correct, since the average value of wind speed and the technical behavior of the wind turbine depend on the parameter λ.

8.1   Dependencies of the energy on wind speed and wind turbine parameters

In order to determine the function of the energy, we devoted our attention to:

- study the function of $\frac{E}{E_r}$, with respect to the variation of the shape of the observed hourly average wind speed curve (assuming that the parameters λ and k are constant);

- study the function of $\frac{E}{E_r}$, with respect to the variation of the assigned Weibull distribution (parameter k), considering different values of $\frac{\lambda}{v_r}$ (assuming that the parameter λ and the shape of the average curve are constant);

- study the function of $\frac{E}{E_r}$, with respect to the variation of $\frac{\lambda}{v_r}$, considering different values of the parameter k of the Weibull distribution (assuming that the parameter k and the shape of the average curve are constant);

- study the function of $\frac{E}{E_r}$, with respect to the variation of $\frac{v_{in}}{v_r}$ (assuming that the parameter k and the shape of the average curve are constant);

- study the function of $\frac{E}{E_r}$, with respect to the variation of $\frac{v_{out}}{v_r}$ (assuming that the parameter k and the shape of the average curve are constant).

The following sections describe the results obtained with the analysis of the aspects previously described.

8.1.1   How the energy depends on the shape of the average wind speed curve

For each Weibull distribution, we have analyzed how the function of the energy $\frac{E}{E_r}$ is influenced by the variation of the shape of the observed hourly average wind speed curve. It is possible to observe that the value of the energy does not depend on the shape of the average curve, as shown in Fig. 8.1. Nevertheless, the value of $\frac{E}{E_r}$ depends on the parameter k of the Weibull distribution. In fact, the amount of energy produced by the wind turbine tends to be larger for Weibull distributions of type A and C associated with a higher value of k.
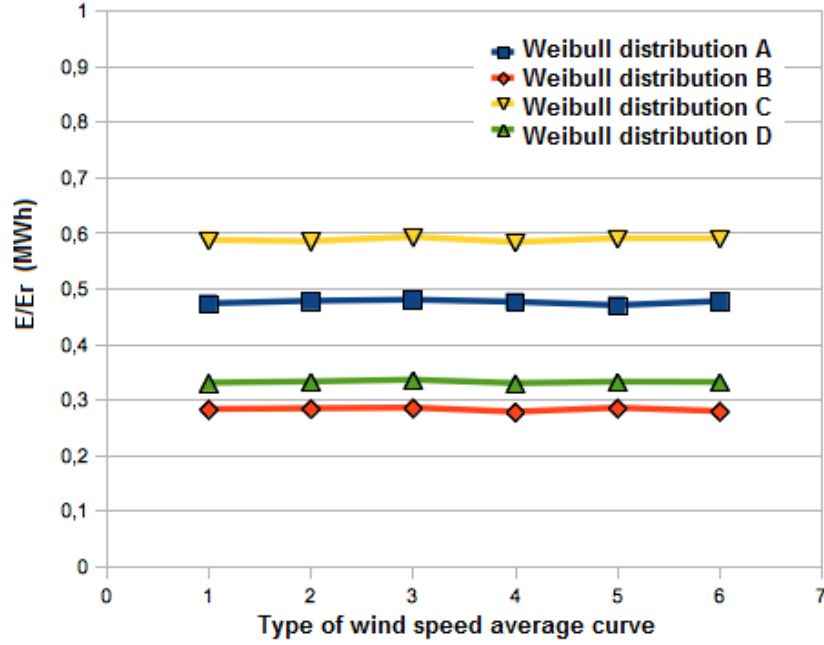
Figure 8.1: Form of $\frac{E}{E_r}$ with respect to the variation of the form of the average curve.

8.1.2 How the energy depends on the Weibull distribution parameters

In the previous section we have demonstrated that the value of the energy $\frac{E}{E_r}$ does not depend on the shape of the average curve. For this reason, we considered only one curve with a maximum peak, in order to perform our simulations to study the influences of the Weibull parameters on the energy. In particular, we considered:

- 2 assigned wind turbines with the following technical characteristics:
  $p_r = 2$ MW, $v_r = 16$, $v_{in} = 3.5$ $v_{out} = 25$;
  $p_r = 3$ MW, $v_r = 15$, $v_{in} = 3.5$ $v_{out} = 25$;

- the Weibull parameter λ varying within the set $\{1.6, 4.8, 12, 16, 20, 24\}$;

- the Weibull parameter k varying within the set $\{1, 1.2, 1.95, 3\}$.

With these parameters, we have performed 1000 simulations with the proposed synthetic wind data generator, obtaining 24 scenarios of 1000 iterations for each wind turbine. The values of the energy obtained in the simulation phase, respectively for the wind turbine of 2 MW and 3 MW, are shown in tables 8.1 and 8.2. We have thus analyzed how the function $\frac{E}{E_r}$ is influenced by the variation of the parameter k of the Weibull distribution, considering different values of $\frac{\lambda}{v_r}$ and vice versa. In particular, as mentioned above, we have analyzed the following two aspects:

- study the function of $\frac{E}{E_r}$, with respect to the variation of the assigned Weibull distribution (parameter k), considering different values of $\frac{\lambda}{v_r}$ and assuming that the parameter λ and the shape of the average curve are constant (figures 8.2 and 8.4);

- study the function of $\frac{E}{E_r}$, with respect to the variation of $\frac{\lambda}{v_r}$, considering different values of the parameter k of the Weibull distribution and assuming that the parameter k and the shape of the average curve are constant (figures 8.3 and 8.5).

The figures 8.2 and 8.4 show that the function $\frac{E}{E_r}$ for different values of $\frac{\lambda}{v_r}$ consists of a set of curves, of a logarithmic shape, which are dependent on the factor $\frac{\lambda}{v_r}$. The figures 8.3 and 8.5 show that the form of the function $\frac{E}{E_r}$ for different values of the parameter k consists of a set of several polynomial curves of fourth grade, which are dependent on the factor k. For this reason, it is possible to consider $\frac{E}{E_r}$ as a function of $\frac{\lambda}{v_r}$ and k, e.g., $\frac{E}{E_r} = f(\frac{\lambda}{v_r}, k)$, and determine it in a closed form, as described in section 8.2.

	$(\frac{\lambda}{v_r} = 0.1)$	$(\frac{\lambda}{v_r} = 0.3)$	$(\frac{\lambda}{v_r} = 0.75)$	$(\frac{\lambda}{v_r} = 1)$	$(\frac{\lambda}{v_r} = 1.25)$	$(\frac{\lambda}{v_r} = 1.5)$
k = 1	0.01	0.16	0.28	0.28	0.27	0.25
k = 1.2	0.01	0.14	0.33	0.33	0.3	0.28
k = 1.95	0	0.09	0.47	0.49	0.42	0.35
k = 3	0	0.07	0.59	0.64	0.52	0.37

Table 8.1: Values of the energy $\frac{E}{E_r}$ obtained for a wind turbine of 2 MW.

	$(\frac{\lambda}{v_r} = 0.11)$	$(\frac{\lambda}{v_r} = 0.32)$	$(\frac{\lambda}{v_r} = 0.80)$	$(\frac{\lambda}{v_r} = 1.07)$	$(\frac{\lambda}{v_r} = 1.33)$	$(\frac{\lambda}{v_r} = 1.5)$
k = 1	0.01	0.16	0.29	0.28	0.26	0.25
k = 1.2	0.01	0.14	0.33	0.33	0.31	0.28
k = 1.95	0	0.09	0.47	0.48	0.42	0.34
k = 3	0	0.07	0.59	0.64	0.52	0.37

Table 8.2: Values of the energy $\frac{E}{E_r}$ obtained for a wind turbine of 3 MW.

8.1.3   How the energy depends on cut-in and cut-out wind speeds

In order to study the function of the energy $\frac{E}{E_r}$ with respect to v_{in} and v_{out}, we have modified the technical curve of the wind turbine as shown in the figures 8.7 and 8.9, while the other simulation parameters have been left unaltered. Thus, we have analyzed how $\frac{E}{E_r}$ is influenced by the variation of the wind turbine technical parameters, such as the *cut-in speed v_{in}* and the *cut-out speed v_{out}*. In particular, the following two aspects have been considered:

- study the function of $\frac{E}{E_r}$, with respect to the variation of $\frac{v_{in}}{v_r}$ and assuming that the parameter k and the shape of the average curve are constant (Fig. 8.6);

- study the function of $\frac{E}{E_r}$, with respect to the variation of $\frac{v_{out}}{v_r}$ and assuming that the parameter k and the shape of the average curve are constant (Fig. 8.8).
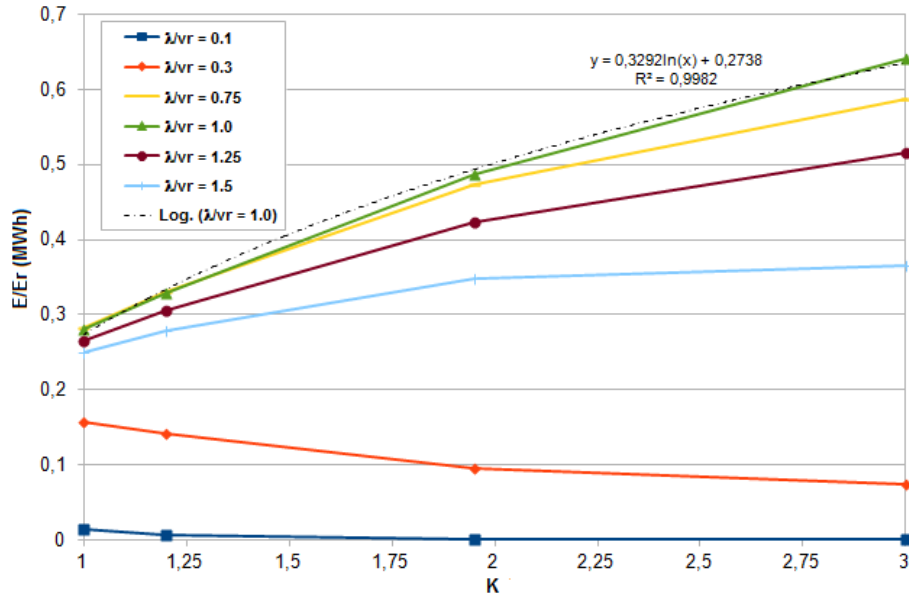
Figure 8.2: Function of the energy $\frac{E}{E_r}$ and Weibull distribution parameters (2 MW wind turbine).

Fig. 8.6 shows that when $\frac{v_{in}}{v_r}$ increases the value of the term $\frac{E}{E_r}$ decreases, e.g., the wind turbine does not produce a large amount of energy. This is due to the fact that when $\frac{v_{in}}{v_r}$ increases the range where the wind turbine works decreases, in terms of the area determined by the power
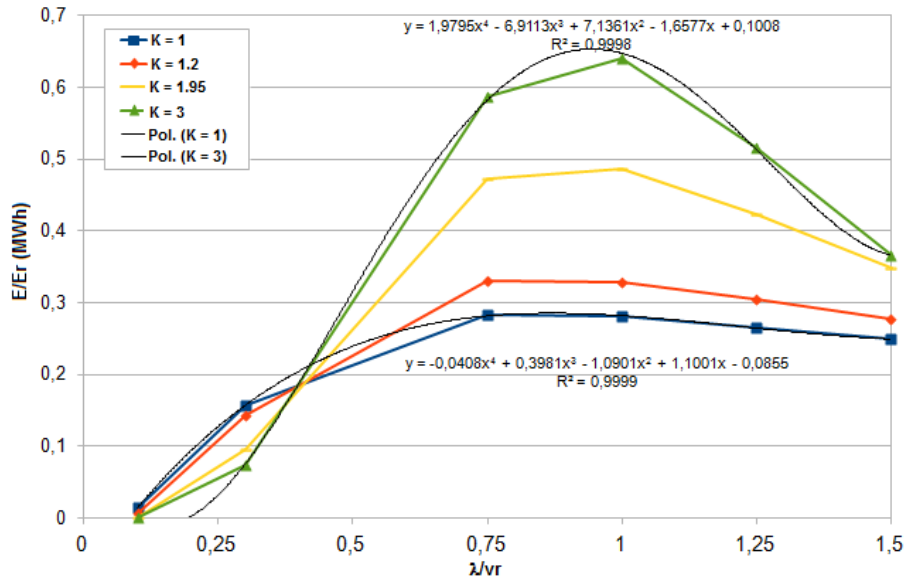
Figure 8.3: Function of the energy $\frac{E}{E_r}$ and parameter $\frac{\lambda}{v_r}$ (2 MW wind turbine).
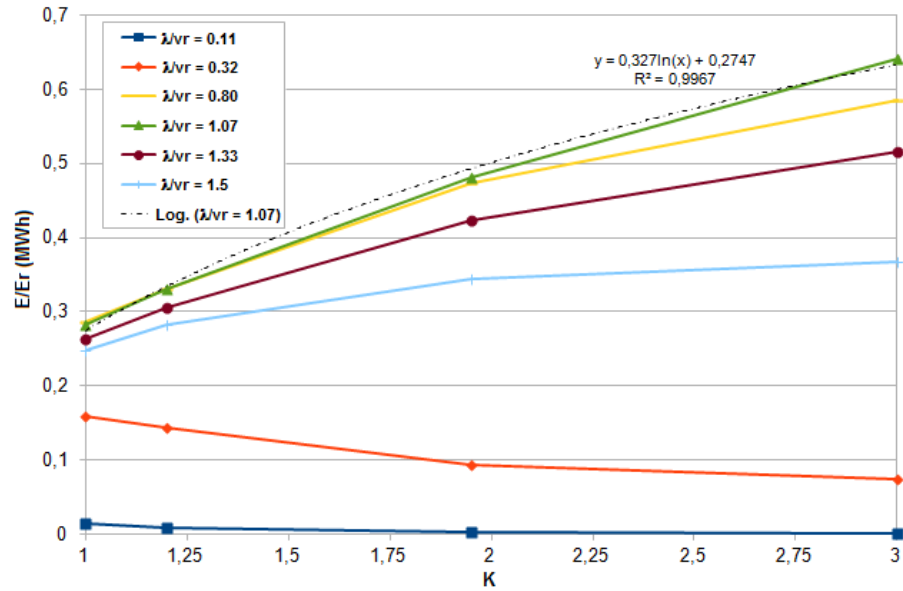
Figure 8.4: Function of the energy $\frac{E}{E_r}$ and Weibull distribution parameters (3 MW wind turbine).
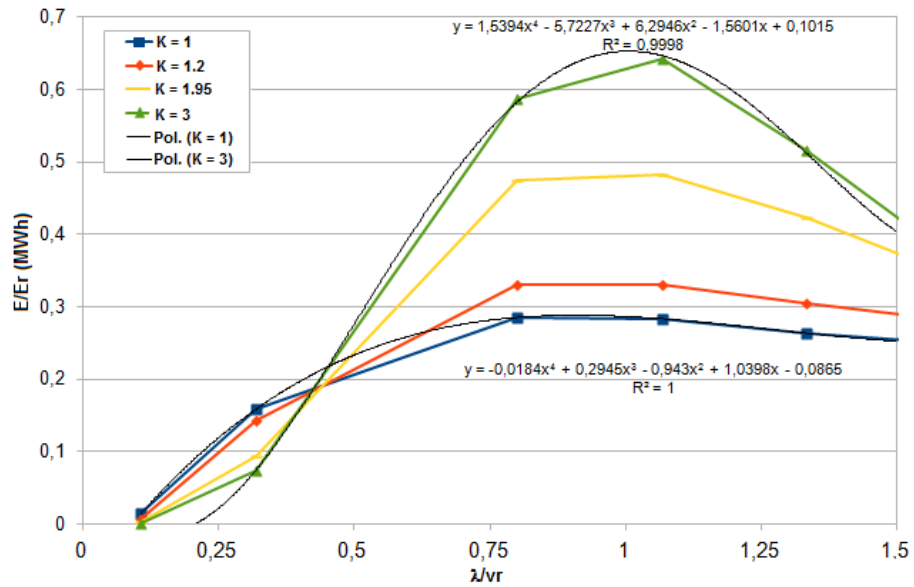
Figure 8.5: Function of the energy $\frac{E}{E_r}$ and parameter $\frac{\lambda}{v_r}$ (3 MW wind turbine).
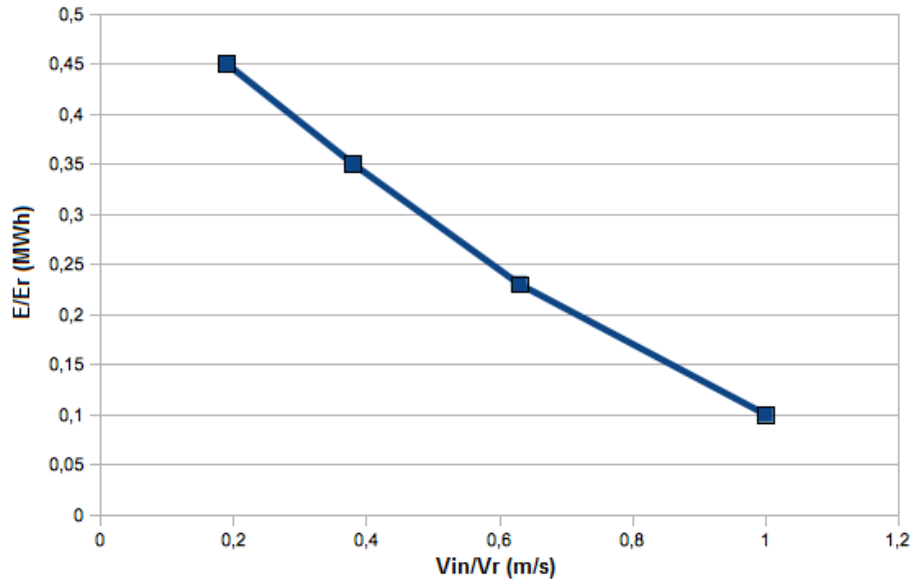
Figure 8.6: Function of the energy $\frac{E}{E_r}$ and parameter $\frac{v_{in}}{v_r}$.
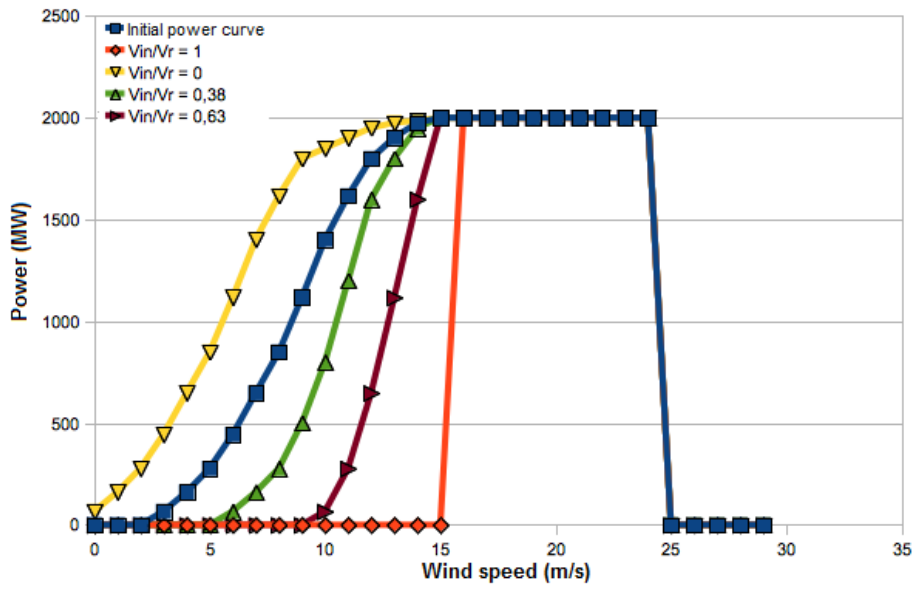
Figure 8.7: Power curve and parameter $\frac{v_{in}}{v_r}$.
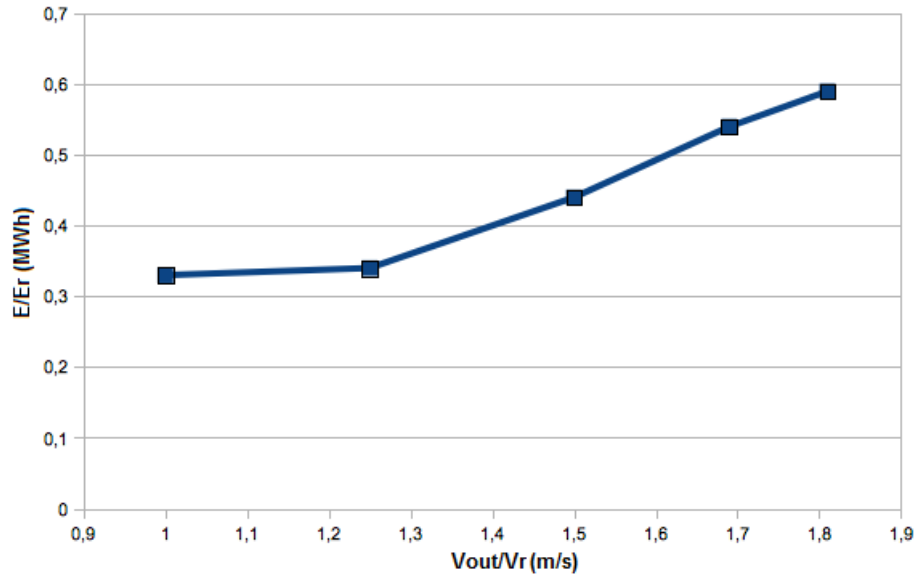
Figure 8.8: Function of the energy $\frac{E}{E_r}$ and parameter $\frac{v_{out}}{v_r}$.
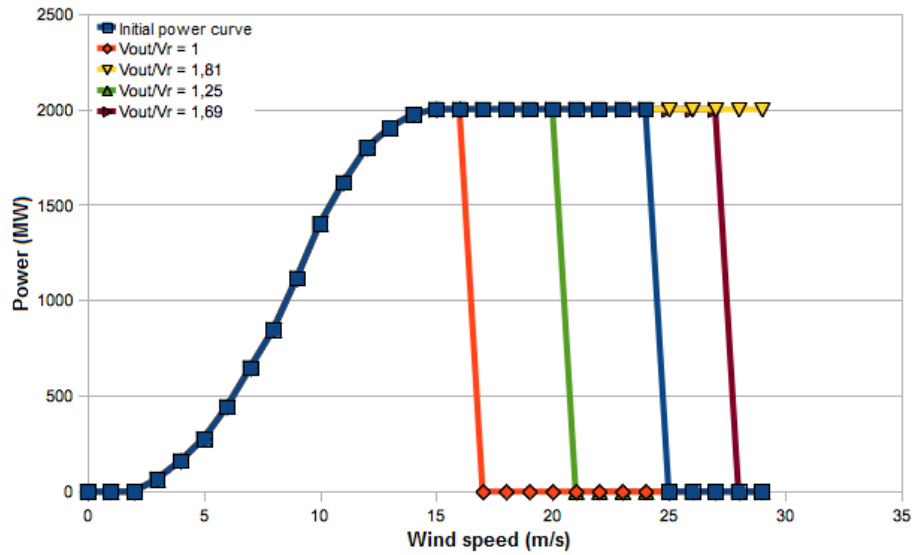
Figure 8.9: Power curve and parameter $\frac{v_{out}}{v_r}$.

curve, as shown in Fig. 8.7.

Fig. 8.8 shows that when $\frac{v_{out}}{v_r}$ increases then $\frac{E}{E_r}$ increases, e.g., the wind turbine produces more energy. This is due to the fact that when $\frac{v_{out}}{v_r}$ increases, the range where the wind turbine works increases, in terms of the area determined by the power curve, as shown in Fig. 8.9.

8.2 A novel model to compute the energy function

In section 8.1.2 we have analyzed how the function of the energy $\frac{E}{E_r}$ is influenced by the technical parameters of the wind turbine and the parameters of the assigned Weibull distribution. Figures 8.2, 8.3, 8.4 and 8.5 show that the function $\frac{E}{E_r}$ consists of a set of curves which depend on the parameter k of the assigned Weibull distribution and on the factor $\frac{\lambda}{v_r}$. It is thus possible to determine the function $\frac{E}{E_r} = f\left(\frac{\lambda}{v_r}, k\right)$ in a closed form and to demonstrate that this expression is valid for each type of wind turbine, if its technical parameters are known. Figures 8.3 and 8.5 show that

$$\frac{E}{E_r} = E\left(\frac{\lambda}{v_r}, k\right) = a\left(\frac{\lambda}{v_r}\right) ln\left(k\right) + b\left(\frac{\lambda}{v_r}\right) \tag{8.1}$$

where $a\left(\frac{\lambda}{v_r}\right)$ and $b\left(\frac{\lambda}{v_r}\right)$ are the values of the coefficients of the fourth grade polynomial function which approximates the energy curve $\frac{E}{E_r}$, which depend on the parameter $\frac{\lambda}{v_r}$ related with the assigned Weibull distribution. In the case in which $k = 1$, the expression (8.1) becomes

$$\frac{E}{E_r} = E\left(\frac{\lambda}{v_r}, k\right) = b\left(\frac{\lambda}{v_r}\right) \tag{8.2}$$

since $ln(k) = 0$ for $k = 1$. In the case in which $k = k'$, the expression (8.2) becomes

$$\frac{E}{E_r} = E\left(\frac{\lambda}{v_r}, k'\right) = a\left(\frac{\lambda}{v_r}\right) ln\left(k'\right) + b\left(\frac{\lambda}{v_r}\right) \tag{8.3}$$

By equaling the expression (8.2) with the (8.3), it is possible to calculate the value of $a\left(\frac{\lambda}{v_r}\right)$, as follows

$$a\left(\frac{\lambda}{v_r}\right) = \frac{E\left(\frac{\lambda}{v_r}, k'\right) - b\left(\frac{\lambda}{v_r}\right)}{ln\left(k'\right)} \tag{8.4}$$

where $b\left(\frac{\lambda}{v_r}\right)$ is expressed in a closed form by the (8.2).

Since we have obtained the forms of $a\left(\frac{\lambda}{v_r}\right)$ and $b\left(\frac{\lambda}{v_r}\right)$, it is thus possible to determine the value of $\frac{E}{E_r}$, by substituting these forms in (8.1). The expression (8.1) allows to determine the value of $\frac{E}{E_r}$ knowing the wind turbine technical parameters and the assigned Weibull distribution parameters. The following figures show that the functions of the energy calculated with the formula previously described are similar to the simulated functions shown in the figures 8.2, 8.3, 8.4 and 8.5. In particular, the figures 8.14 and 8.15 show the differences, in terms of percentages, between the function of the energy calculated with the formula and the simulated one. These differences are about 4%.
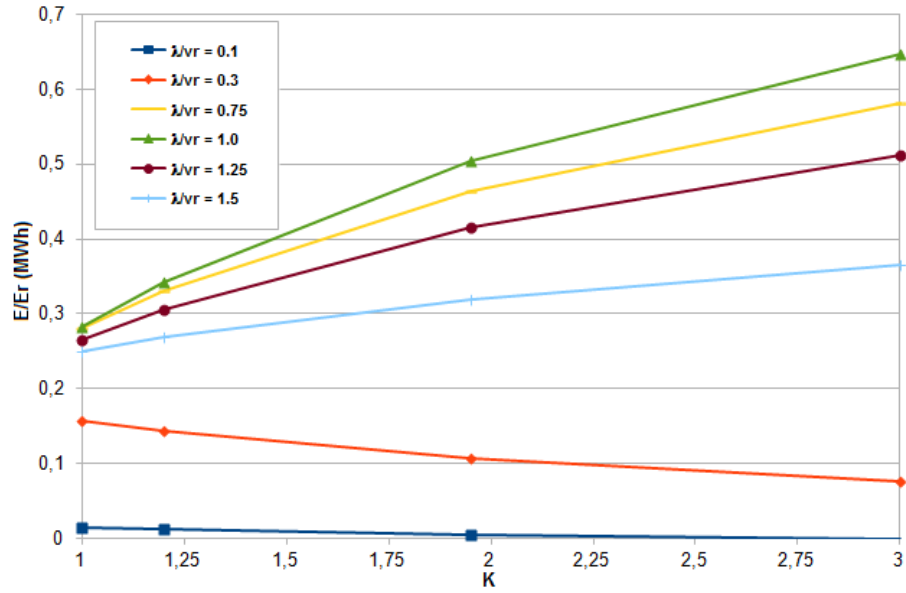
Figure 8.10: Calculated function of $\frac{E}{E_r}$ and Weibull parameters (2 MW wind turbine).
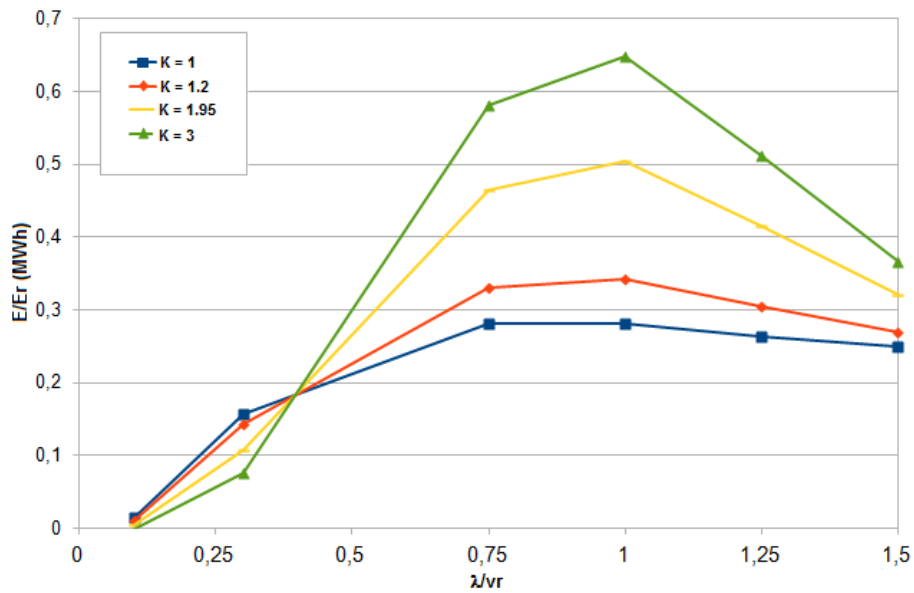
Figure 8.11: Calculated function of $\frac{E}{E_r}$ and parameter $\frac{\lambda}{v_r}$ (2 MW wind turbine).
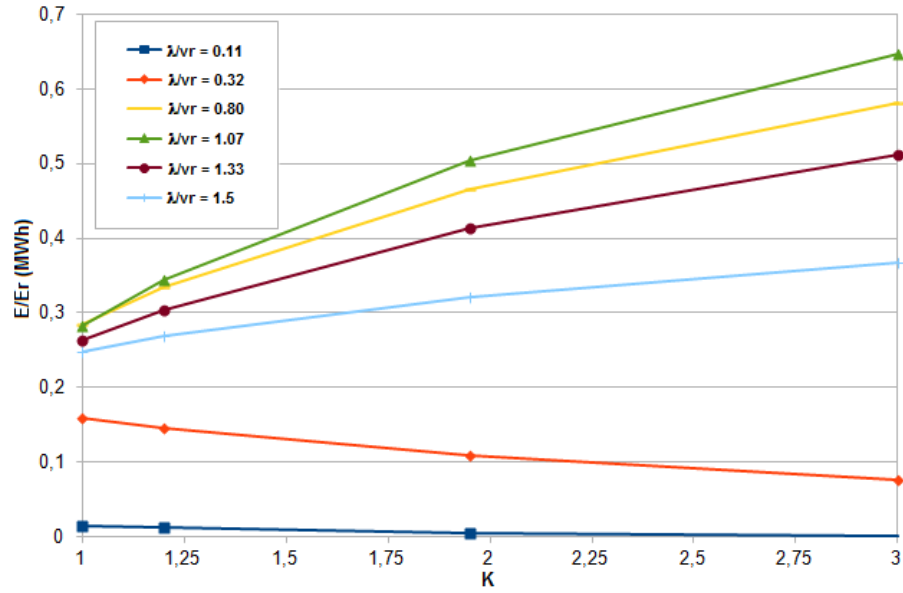
Figure 8.12: Calculated function of $\frac{E}{E_r}$ and Weibull parameters (3 MW wind turbine).
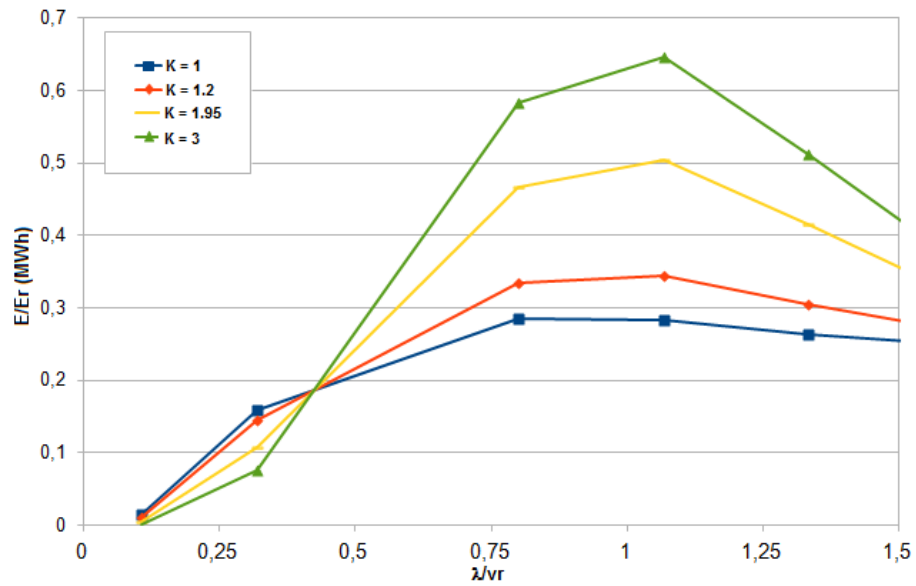
Figure 8.13: Calculated function of $\frac{E}{E_r}$ and parameter $\frac{\lambda}{v_r}$ (3 MW wind turbine).
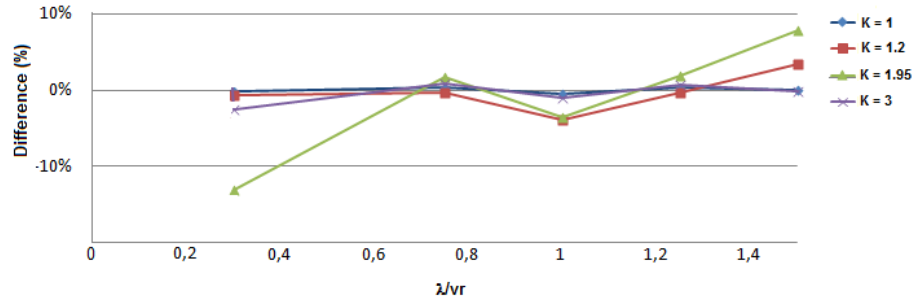
Figure 8.14: Differences between the calculated function of $\frac{E}{E_r}$ and the simulated function (2 MW wind turbine).
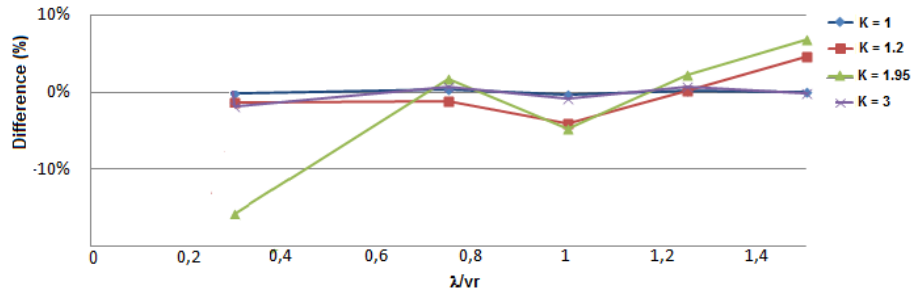
Figure 8.15: Differences between the calculated function of $\frac{E}{E_r}$ and the simulated function (3 MW wind turbine).

	$(\frac{\lambda}{v_r} = 0.1)$	$(\frac{\lambda}{v_r} = 0.3)$	$(\frac{\lambda}{v_r} = 0.75)$	$(\frac{\lambda}{v_r} = 1)$	$(\frac{\lambda}{v_r} = 1.25)$	$(\frac{\lambda}{v_r} = 1.5)$
k = 1	0.01	0.16	0.28	0.28	0.27	0.25
k = 1.2	0.01	0.14	0.33	0.33	0.3	0.28
k = 1.95	0	0.09	0.47	0.49	0.42	0.35
k = 3	0	0.07	0.59	0.64	0.52	0.37

Table 8.3: Values of $\frac{E}{E_r}$ simulated for a wind turbine of 2 MW.

	$(\frac{\lambda}{v_r} = 0.1)$	$(\frac{\lambda}{v_r} = 0.3)$	$(\frac{\lambda}{v_r} = 0.75)$	$(\frac{\lambda}{v_r} = 1)$	$(\frac{\lambda}{v_r} = 1.25)$	$(\frac{\lambda}{v_r} = 1.5)$
k = 1	0.01	0.16	0.28	0.28	0.26	0.25
k = 1.2	0.01	0.14	0.33	0.34	0.31	0.27
k = 1.95	0.01	0.11	0.46	0.5	0.42	0.32
k = 3	0	0.08	0.58	0.65	0.51	0.37

Table 8.4: Values of $\frac{E}{E_r}$ calculated with the formula for a wind turbine of 2 MW.

The following tables show, as an example, the values of $\frac{E}{E_r}$ simulated and calculated with the formula previously indicated, taking into account a wind turbine of 2 MW. We can observe that the values of the energy simulated and calculated with the formula are similar; this demonstrates that this formula well approximates the form of the energy.

8.3 Statistical analysis of the energy function

In the previous sections, we derived an experimental function which expresses the average energy produced by a wind turbine in a 24 hours time horizon in a typical day, considering the main simulation parameters related with Weibull distribution and wind turbines. Nevertheless, it has been necessary to verify the correctness and the effectiveness of the estimation of the experimental function $\frac{E}{E_r}$. In particular, it has been verified how the assigned simulation parameters influence this function, utilizing a proper statistical test. At the end, various correlation and regression analyses have been performed in order to individuate a normalized form of the function $\frac{E}{E_r}$ which can be applied to all the types of wind turbines. The following sections describe:

- the main characteristics of a statistical test and the motivations that lead to the choice of a particular statistical test, called ANOVA test;

- the analyses that have been performed in order to verify that the formula of the energy previously individuated is correctly expressed.

8.3.1 Choosing the most suitable statistical test

In order to verify the main parameters on which the wind turbine energy function $\frac{E}{E_r}$ depends, it is possible to utilize statistical tests. The objective of these tests is to verify if the values of the energy obtained in the simulation phase are different among themselves for casual reasons, or they are dependent on factors like Weibull distribution parameters (λ and k) and the wind turbine technical parameters (v_{in}, v_{out}, v_r).

Generally, a statistical test is an instrument used to analyze if groups of data obtained after some measurements are different among themselves for causal reasons or because they are dependent on some parameters. A statistical test is based on the **hypothesis zero**, according to which no differences exist between the groups of data with respect to the given parameter. According to the hypothesis zero, the group of data are equal and the difference that we observe is due to casual factors. The hypothesis zero can be true or false, so it is necessary to decide if we want to accept or refuse it, analyzing the data with the statistical test. If the result of the test is to refuse the hypothesis zero, then the observed difference is declared significant from a statistical point of view. If otherwise the result of the test is to accept the hypothesis zero, then the difference is not significant from a statistical point of view, because it is due to casual factors.

The results of a statistical test have a probability value. For this reason, the decision to refuse the hypothesis zero is probably correct, but it could be wrong. The measure of the risk to be wrong is the level of significance of the test. The level of significance of a test can be chosen by who performs the experiments. Nevertheless, usually, a level of probability equal to 0.05 (5%) or to 0.01 (1%) is chosen. This probability represents a quantitative estimation of the probability that the observed differences are due to casual factors. Different types of statistical tests exist; in our case, we applied the ANOVA test in order to verify if the energy $\frac{E}{E_r}$ is dependent on some given parameters, or if the differences between these values are due to casual factors, because:

- in our case, we have a large amount of data. Statistical test are suitable to analyze small amount of data, since the probability that the differences between the values obtained are due to causal factors decreases when we consider many data. Nevertheless, in our case, it is preferable to use an ANOVA test since it is suitable to verify the correctness of measurements obtained for a large amount of data;

- usually, statistical tests are used for two or three groups of data, since a great computational effort is required when the number of groups increase. In our case we prefer to use the ANOVA test, since we consider more than three groups of data and we consider also a large number of possible combinations of parameters (λ, k, v_r, v_{in}, v_{out}).

8.3.2   Applying the ANOVA test

In order to compare the values of the energy produced by various types of wind turbines, different values of $\frac{E}{E_r}$ have been considered, with respect to λ and k, obtaining the dependency on the rated speed v_r. These values have been organized into two series with rows that correspond to the couples of parameters and columns which are related with the different wind turbines. Then, the ANOVA test has been applied in order to verify that the difference of the values of the energy obtained in the different simulation is not due to casual factors, but it is caused by the dependencies on some parameters, such as λ, k, v_r, v_{in}, v_{out}. Then, the analysis of the variance of the matrix λ, k, v_r has been carried out. By applying the ANOVA test to the different groups of values obtained for the assigned wind turbines, we obtain a level of significance less than 5%, this demonstrates that the differences between the values of the energies are not due to causal factors. In particular, it has been possible to verify the following two aspects:

- the variations of the function $\frac{E}{E_r}$ are well described by the parameters λ, k for an assigned wind turbine generator, in fact, the significance test has given a positive result, since the level of significance is less than 5% with respect to the rows of the matrix on which the ANOVA test has been applied. For this reason, it is possible to affirm that $\frac{E}{E_r} = f(\lambda, k)$.

ANOVA test results

E/Er = f(λ,k)	3,83864E-65
E/Er = f(Vin, Vout, Vr)	1,7E-15

Figure 8.16: Results obtained applying the ANOVA test to the values of the energies.

- the variations of the function $\frac{E}{E_r}$ are well described by the wind turbine technical parameters, such as v_r, v_{in}, v_{out}, for assigned λ, k, in fact the significance test has given a positive result, since the level of significance is less than 5% with respect to the columns of the matrix on which the ANOVA test has been applied. For this reason, it is possible to affirm that $\frac{E}{E_r} = f(\lambda, k, v_r, v_{in}, v_{out})$.

Table 8.16 resumes all the results obtained by applying the ANOVA test on the values of the energy obtained in the simulation phase for each of the 6 wind turbines considered.

Analysis of the coefficients of the polynomial functions

As described previously, the ANOVA test has demonstrated that the energy depends not only on the parameters of the Weibull distribution (λ e k), but it depends also on the wind turbine technical characteristics (v_r, v_{in}, v_{out}). Furthermore, the shape of the function of the energy, for all the wind turbines, is logarithmic with respect to the factor k and it is a fourth grade polynomial function with respect to the variation of $\frac{\lambda}{v_r}$.

It is thus necessary to study how the energy depends on the wind turbines technical parameters and on a combination of them. In particular, the dependencies of the polynomial function coefficients $a(\frac{\lambda}{v_r})$ and $b(\frac{\lambda}{v_r})$ on the wind turbine technical parameters have been analyzed.

As far as the coefficients a are concerned, a correlation analysis has been performed for each coefficient of the polynomial curve, with respect to the following wind turbine technical parameters and their possible combination: v_r, v_{in}, v_{out}, $v_r - v_{in}$, $v_r - v_{out}$, $v_{out} - v_{in}$. Figures 8.17 and 8.18 resume the correlation analysis of each coefficient of the polynomial curve, with respect to the wind turbine technical parameters and their possible combinations, according to the grade of the approximating curve. It is possible to observe that the coefficients present a dependency on the parameter v_r or on a combination of the wind turbine technical parameters that always includes the term v_r, while dependencies on the coefficients of the parameter v_{out} are not present.

As far as the coefficients b are concerned, a correlation analysis has been performed for each coefficient of the polynomial curve, with respect to the following wind turbine technical parameters and their possible combinations: v_r, v_{in}, v_{out}, $v_r - v_{in}$, $v_r - v_{out}$, $v_{out} - v_{in}$. Figures 8.19 and 8.20 resume the correlation analysis of each coefficient of the polynomial curve, with respect to the wind turbines technical parameters and their possible combinations, according to the grade of the approximating curve. It is possible to observe that the coefficients present dependencies on different combination of wind turbine technical parameters which include the terms v_r, v_{in} e v_{out}.

Correl.	c1 Vr	c2 Vin	c3 Vout	c4 Vr-Vin	c5 Vr-Vout	c6 Vout-Vin
a1	95%	10%	-16%	92%	86%	-17%
a2	-96%	-8%	10%	-94%	-82%	10%
a3	98%	1%	1%	97%	76%	1%
a4	-93%	24%	-20%	-99%	-59%	-23%
a5	5%	-97%	45%	29%	-29%	63%

Figure 8.17: Correlation analysis of the coefficients a with fourth grade approximating curve.

Correl.	c1 Vr	c2 Vin	c3 Vout	c4 Vr-Vin	c5 Vr-Vout	c6 Vout-Vin
a1	-99%	-2%	-23%	-98%	-61%	-20%
a2	92%	-11%	49%	94%	36%	46%
a3	-77%	25%	-72%	-83%	-8%	-70%
a4	78%	-23%	69%	84%	11%	66%

Figure 8.18: Correlation analysis of the coefficients a with third grade approximating curve.

Correl.	c1 Vr	c2 Vin	c3 Vout	c4 Vr-Vin	c5 Vr-Vout	c6 Vout-Vin
b1	26%	-2%	85%	27%	-41%	76%
b2	15%	16%	-84%	11%	73%	-78%
b3	-40%	-20%	69%	-35%	-82%	66%
b4	36%	-3%	-26%	37%	47%	-22%
b5	87%	9%	32%	85%	45%	26%

Figure 8.19: Correlation analysis of the coefficients b with fourth grade approximating curve.

Correl.	c1 Vr	c2 Vin	c3 Vout	c4 Vr-Vin	c5 Vr-Vout	c6 Vout-Vin
b1	98%	13%	-4%	94%	80%	-7%
b2	-99%	-8%	-7%	-96%	-72%	-4%
b3	92%	-12%	37%	94%	45%	36%
b4	-12%	66%	-87%	-29%	53%	-92%

Figure 8.20: Correlation analysis of the coefficients b with third grade approximating curve.

8.4   Results and discussion

Since we have individuated the dependencies of the coefficients of the polynomial functions $a(\frac{\lambda}{v_r})$ and $b(\frac{\lambda}{v_r})$ on the wind turbine technical parameters, it is possible to estimate their values.

Thus, it is possible to calculate the form of the energy function by the formula:

$$\frac{E}{E_r} = E\left(\frac{\lambda}{v_r}, k\right) = a\left(\frac{\lambda}{v_r}\right) ln\left(k\right) + b\left(\frac{\lambda}{v_r}\right) \tag{8.5}$$

and compare these values of the energy with the measured ones obtained in the simulation phase. By analyzing the resulting data, it is possible to verify that:

- the curves of the energy present the same logarithmic form (with respect to k) and polynomial form (with respect to $\frac{\lambda}{v_r}$), this derives from the definition of the function itself, as shown in the example of Fig. 8.21;

- utilizing the different combinations of the fourth and third grade polynomial functions a and b, it is possible to verify that the best estimations are obtained considering the fourth grade polynomial function for $a(\frac{\lambda}{v_r})$ and the third grade polynomial function for $b(\frac{\lambda}{v_r})$. This reflects the form of the measured functions of $\frac{E}{E_r}$ for each wind turbine;

- the values of the energy that have been calculated considering the estimated parameters differ from the values of the simulated values according to the wind turbine chosen. In particular, normalizing the form of the power curve with respect to the P_r, as shown in Fig. 8.22, we obtain three sets of wind turbines:

  1. a set containing wind turbines 1,2,6. For these turbines the estimation model which uses the fourth grade polynomial function $a(\frac{\lambda}{v_r})$ and the third grade polynomial function $b(\frac{\lambda}{v_r})$ works correctly: the forms of the function $\frac{E}{E_r}$ are well separated with respect to k and λ and the approximation is acceptable for a large range. An example is shown in Fig. 8.23;

  2. a set containing wind turbines 3,5. For these turbines the estimation model which uses the fourth grade polynomial function $a(\frac{\lambda}{v_r})$ and the third grade polynomial function $b(\frac{\lambda}{v_r})$ sometimes does not work correctly. The form of the function $\frac{E}{E_r}$ is individuated only if the values of the Weibull distribution for k less than 2 and λ less than 1 are considered, however these are the ranges where wind turbines are more frequently utilized. An example is shown in Fig. 8.24;

  3. a set containing wind turbine 4. For this turbine the estimation model is not adequate. In fact, the normalized form of the power curve is different from the others and for this reason it represents an exception which is not properly managed. An example is shown in Fig. 8.25.

According to these considerations, probably there exists a strong dependence of the coefficients of the polynomial functions $a(\frac{\lambda}{v_r})$ and $b(\frac{\lambda}{v_r})$ on the form of the power curve in the non linear part (between v_{in} and v_r) which is mainly represented by linear combinations of the characteristic wind speeds (in order to express their dependency on the shape coefficient of the linear curve that approximates this part), but, in order to have a more accurate estimation model, more complex combinations of the parameters of the wind turbine should be considered.
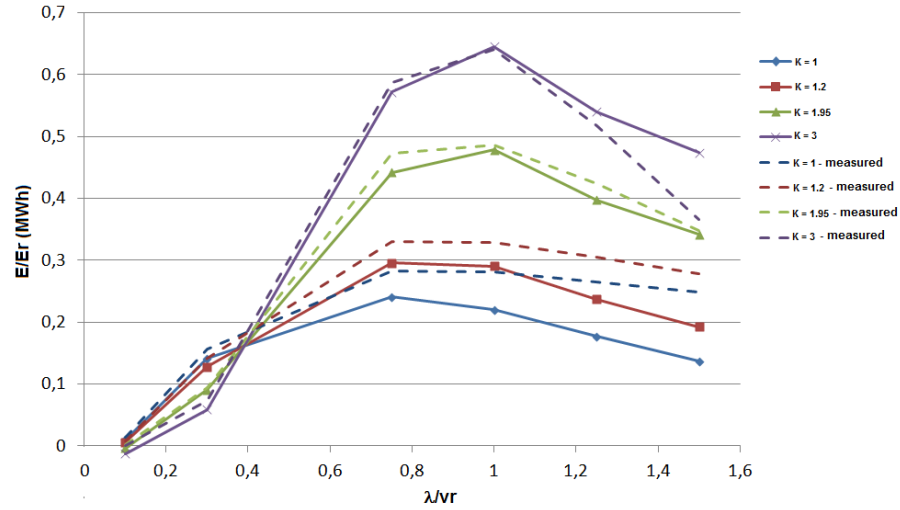
Figure 8.21: Form of the function $\frac{E}{E_r}$ for wind turbine 1 (with respect to λ).
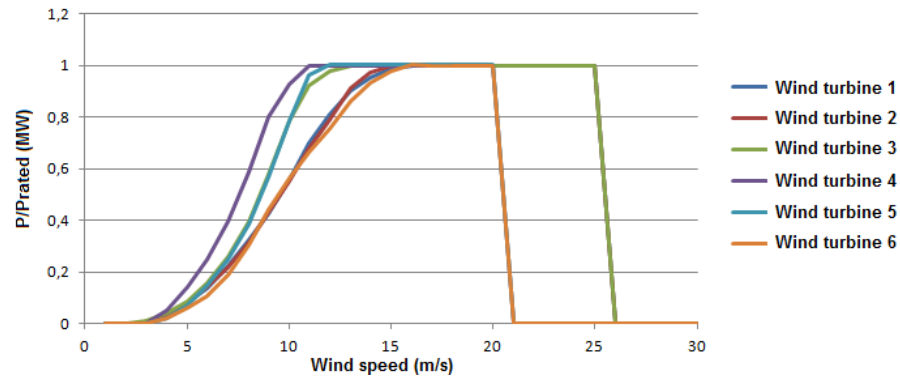
Figure 8.22: Form of the power curve normalized with respect to P_r.
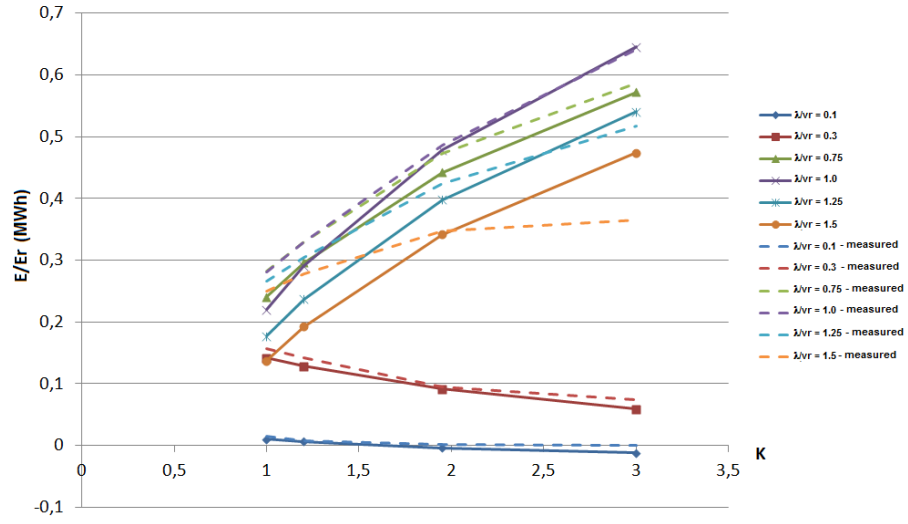
Figure 8.23: Form of the function $\frac{E}{E_r}$ for wind turbine 1 (with respect to k).
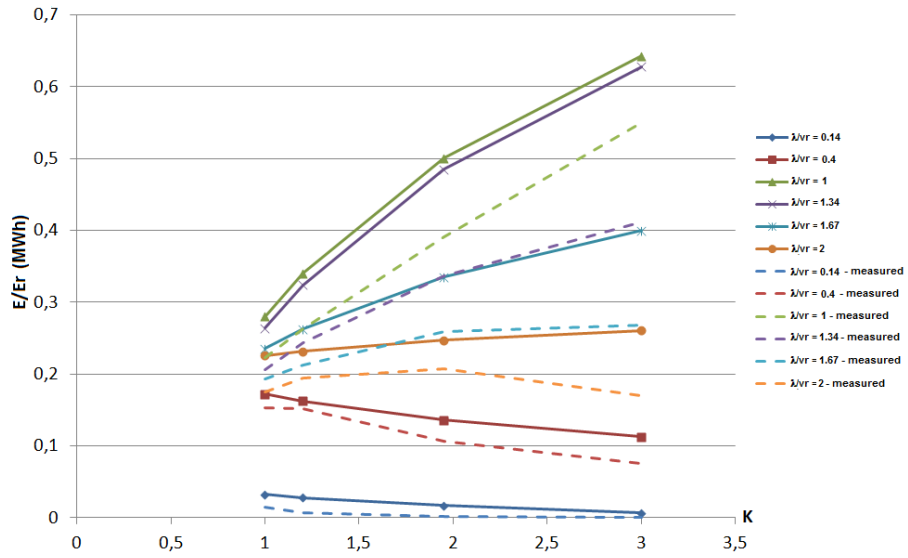
Figure 8.24: Form of the function $\frac{E}{E_r}$ for wind turbine 3 (with respect to k).
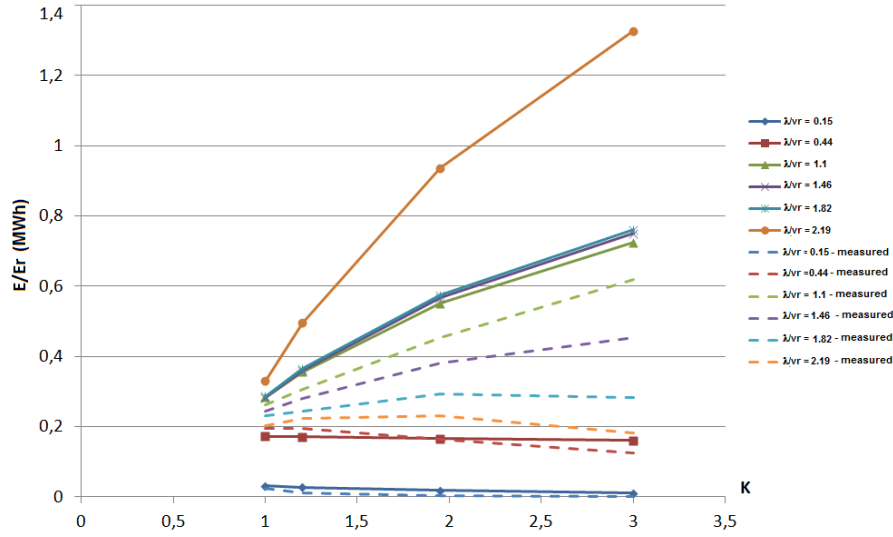
Figure 8.25: Form of the function $\frac{E}{E_r}$ for wind turbine 4 (with respect to k).

8.5   Conclusions

In this chapter, the wind synthetic data, generated with the new generation model proposed in chapter 7, has been used to carry out simulations studies to individuate the wind turbines operational parameters that mainly affect the wind generators performances. An experimental function which expresses the average energy produced by a wind turbine in a 24 hours time horizon in a typical day has been determined, considering the main simulation parameters related with Weibull distribution and wind turbines. This function represents a very useful instrument, since, when the energy production of a wind park is scheduled, it is fundamental to have proper methodologies to determine the average energy that a site will produce, in order to obtain an economical return of the investment. In our case, we have studied how the energy depends on some key parameters. This analysis has been summarized with an analytical expression to determine the value of the average energy considering only a few data easy to retrieve from the geographical site where wind turbines are located. Moreover, this type of expression allows to simplify the models of energy production planning when systems consisting of conventional units and wind generators are considered.

As far as future work is concerned, we will exploit the new synthetic wind data generation model to study the dependencies of the energy function on more wind turbine technical parameters that we have not considered so far in order to simplify the analysis. Furthermore, the data set used in the simulation phase could be extended in order to perform a larger number of simulations. This could be very interesting and useful, since it could be easy to determine a function of the energy that realistically reflects the behavior of the wind turbines and that takes into account all their technical parameters. Furthermore, this new model to compute the energy could be used to determine the input data for the GWUC model, to perform proper simulations on realistic data.

Part IV

Conclusions and Bibliography

Conclusions and directions for future work

For many years, researchers from mathematics, operations research and engineering have focused their attention on applying mathematical modeling and optimization techniques to solve the optimization problems related to the efficient operating and planning of energy generation systems. Optimizing the scheduling of electric energy production is a fundamental process, which gives to the energy utilities the possibility to control the total production costs and maximize the expected net profit from the market, taking into account both the uncertainty related to the forecast energy demand load and the uncertainty related to not conventional energy sources, such as wind or solar power plants [Nai08].

Different types of optimization problems are considered and solved for the efficient scheduling of the energy production. The problem solved in the medium-term period (days and weeks) is known as Unit Commitment Problem (UC). Its objective is to determine the best combination of generating units in terms of their status (committed or uncommitted) and their output (power). This schedule has to satisfy the forecast demand at minimum total production cost, under the operating, technical and environmental system constraints.

Models for UC are usually characterized by a combination of several difficulties like the presence of continuous and binary decision variables at the same time, very large-scale problem dimension, non-linearities (for instance, in fuel costs modeling) and uncertainty of problem data (for example, in load demand forecasts, fuel pricing models, stream flows to reservoirs and generating units failures). For this reason, the literature has proposed numerous simplified variants of models and algorithms for UC so far.

Part of our research activities focused mainly on modeling aspects related with the production and the scheduling of electrical systems. In particular, we have analyzed the limits and the simplifications mainly used in the classical UC models presented in the literature. Traditional UC models (energy-based models) make two main hypotheses: the power can be instantaneously adjusted; the power output is constant in a assigned interval (i.e. of 1 hour), so energy produced in each hour is equal to the power level multiplied by 1 hour. These assumptions greatly simplify the model, because energy and power can be represented by the same variable, but they do not realistically reflect the actual behavior of the generating units.

In our research activities, we have defined more realistic mathematical formulations than the ones proposed in the literature, overcoming the drawbacks of the UC energy-based models. In particular, we have proposed new Mixed-Integer Quadratic Programming (MIQP) models for UC, where decision variables represent power levels instead of energy. The basic assumption of these models is that the unit is always ramping linearly during each time period. This means that the

power increases - or decreases - uniformly from a given time instant to the following during all the period. The energy is computed by assuming linear ramp-up and ramp-down trajectories, i.e., piecewise-linear continuous power curves whose integral (the produced energy) can be easily computed.

Simulations results have shown that in the proposed models the trajectories of power constructed by the model and the energy decisions are surely feasible, since the physical constraints on power are directly modeled. Furthermore, even if these formulations require to use more constraints and more variables, the resulting MIQP problems can be easily solved at optimality with commercial solvers, exploiting their mathematical characteristics.

In our research activities we have proposed also new UC models integrated with the Economic Dispatch Problem (ED), where the variables are associated with the power levels, that are assumed to change linearly in each time period, while the energy levels are then computed accordingly. This has enabled us to derive a more realistic model that can represent more effectively the constraints imposed on the units in order, for example, to avoid mechanical stresses to the rotors for conventional units, or to avoid the use of more units in peak hours. The results obtained have shown that a simulator based on this new model can be effective to compare the flexibility, efficiency and effectiveness of different UC solutions in the adaptation to actual electricity demand (load) in an electrical system, real time. The results have also shown that in the simulation phase it's important to correctly set the parameters which determine the transformation of the power-demand profile used in UC problem into the energy-demand profile used in the simulator. These parameters have to take into account the characteristics of the power-demand profile in order to avoid marked asperities of the load curve itself. In these cases, simulators generally work better since they use the units status of the UC solution.

As far as future work is concerned, we will test the behavior of the new proposed UC models, both from a computational and an operational point of view, with the new Reduced Economic Dispatch (RED) simulator developed, in order to analyze the differences between the various formulations, in terms of the quality of the solution, in a real-time electrical system. In the simulation phase, more input data instances with more generating units and different load profiles will be considered. In order to study these differences, it could be necessary to perform several simulations on real time problems. The aim of these simulations is to compare the flexibility, the efficiency and the effectiveness of the UC solutions in the adaptation to the actual load in a real time electrical system. The formulations that could be taken into account in this analysis could be represented not only by the new models for UC proposed in this dissertation, but also by the models for UC with spinning reserve constraints and robust optimization considerations. The objective, for instance, could be to demonstrate that robust UC formulations are more flexible in the adaptation to the load profile with respect to the UC formulations with spinning reserve constraints. Furthermore, the RED simulator developed could be used to compare the solutions obtained with an energy-based discontinuous UC model integrated with RED and the new continuous power-based models proposed in this thesis, demonstrating that the continuous models better reflect the real behavior of the generating units.

The integration of wind energy sources into conventional electrical system is growing in importance, due to its economical and environmental development benefits; nevertheless, particular attention must be devoted to the related practical operational aspects. This leads to the necessity to modify the current procedures, such as the UC and the ED, to take into account large amounts of wind power production.

Part of our research activities focused on the development of a new UC model in presence of wind energy sources. In particular, a generalized form of the UC problem, called *Generalized Wind*

Unit Commitment Problem - (GWUC), which takes into account conventional generating units (like thermal and hydro power plants) and wind turbines, has been proposed. The model is based on the concept of subsets of units: it is possible to choose only a part of the available generators, making a dynamic modification of the given set of generating units, in order to determine the best configuration of generators (optimal mix), minimizing the total production cost and satisfying the energy demand. In this way, subset constraints can be used as external requirements, for instance related to regulatory laws, such as limited number of units of a particular type, risk limits associated with not programmable sources, emissions constraints, geographical distribution requirements, reliability and security constraints, transmission constraints. In all these cases we do not know *a priori* which is the single unit that is not committed, hence the classical UC model is not applicable, while the GWUC model could represent a valid approach.

The most important results obtained show that, in contrast to the classical UC models and the typical wind UC models, in the GWUC formulation wind generating units are integrated in the solution of the UC problem and furthermore they are also associated with risk considerations, correlated with the forecast error which can be controlled (limited). Moreover, as far as emissions considerations are concerned, the GWUC model chooses for the optimal mix the units that posses the lowest value of emissions, e.g., the units that are more 'virtuous' from this point of view, regardless the absolute value of CO_2 that they will emit after producing a certain amount of energy. This aspect differentiates the GWUC model with subset constraints from a classical UC model with 'emission control', where the emissions are considered as a cost in the objective function.

As far as future work is concerned, it could be very interesting to consider a larger number of subsets of generating units in the GWUC formulation, in order to analyze the behavior of the model in terms of the quality of the solution obtained and in terms of computational times. Furthermore, we could consider a higher number of wind turbines in our model in order to analyze how the solution is influenced by the use of wind sources. Moreover, other additional constraints on wind turbines could be considered in the formulation in order to improve the modeling of the realistic behavior of the wind units, from a practical and an operational point of view. Interconnections, security, and reliability aspects could be also taken into account in order to improve the GWUC formulation; furthermore, the model of the risk related with the utilization of wind energy sources could be refined, considering also detailed economical considerations. It could be also very interesting to formulate the GWUC as a power-based continuous model, taking into account the assumptions explained in chapter 4, in order to analyze how the solution obtained is effective for the efficient operation and planning of a real time electrical system. The GWUC could be also modeled taking into account robust optimization considerations: it could represent a very interesting aspect since robust optimization techniques could be easily applied to model the risk correlated with the utilization of wind energy sources.

Furthermore, wind generation requires complex forecasting techniques which take into account wind speed, wind direction, hub height, geographical conditions, wind farm size, wind turbine technical and operational characteristics and others, in order to provide accurate forecasts on wind production. For these reasons, new generation models for synthetic wind data are needed, in order to properly generate forecasts of wind speed and power. This data is fundamental in simulations carried out to analyze and improve the performances of wind generating units, individuating the technical parameters of wind turbines that directly affect power production.

For these reasons, part of our research activities focused also on developing a new model to generate realistic synthetic wind data. In this model, wind speed is assumed to behave as a Weibull distribution, while wind speed forecast error is simulated using First-Order Auto-Regressive Mov-

ing Average - ARMA time-series models. A formulation of the Assignment Problem is used to model wind speed persistence features, which, as shown by simulation results, are essential to properly obtain wind speed and power output forecasts. Simulations results have shown that generating wind synthetic data in pure random way is not sufficient to produce complete wind speed and power output forecasts, but an accurate generation model which considers all the wind characteristics, such as persistence features, is fundamental. Wind synthetic data, generated with the new generation model proposed, has been used to carry out simulations studies to individuate wind turbines operational parameters that mainly affect wind generators performances.

An experimental function which expresses the average energy produced by a wind turbine in a 24 hours time horizon in a typical day has been determined, considering the main simulation parameters related with Weibull distribution and wind turbines. This function represents a very useful tool, since, when the energy production of a wind park is scheduled, it is fundamental to have proper methodologies to determine the average energy that a site will produce, in order to obtain an economical return of the investment. In our case, we have studied how the energy depends on some key parameters. This analysis has been summarized with an analytical expression to determine the value of the average energy considering only a few data easy to retrieve from the geographical site where wind turbines are located. Moreover, this type of expression allows to simplify the models of energy production planning when systems consisting of conventional units and wind generators are considered.

As far as future work is concerned, in the new synthetic wind data generator, the ARMA model used to determine the wind forecast error could be refined in order to take into account both the variability in space and in time. Regarding the solution of the Assignment Problem, we could consider a variable average curve, determined with an ARMA model, in order to simulate also the scenarios in which the persistence at long term decays.

We will exploit the new synthetic wind data generation model to study the dependencies of the energy function on more wind turbine technical parameters that we have not considered so far in order to simplify the analysis. Furthermore, the data set used in the simulation phase could be extended in order to perform a larger number of simulations. This could be very interesting and useful, since it could be easy to determine a function of the energy that realistically reflects the behavior of the wind turbines and that takes into account all their technical parameters. Furthermore, this new model to compute the energy could be used to determine the input data for the GWUC model, and perform proper simulations on realistic data.

Publications

Technical Reports

1. A. Naimo. A novel model for power Unit Commitment in presence of wind energy sources. Technical Report R. 12-14, IASI-CNR, 10/2012.

2. A. Naimo. A new synthetic wind forecast data generation model. Technical Report R. 11-32, IASI-CNR, 12/2011.

3. A. Frangioni, C. Gentile, F. Lacalandra, A. Naimo. Unit Commitment models with power variables. Technical Report R. 11-26, IASI-CNR, 11/2011.

Bibliography

[AA13]   N. Amjady and M. R. Ansari. Hydrothermal Unit Commitment with AC constraints by a new solution method based on Benders Decomposition. *Energy Conversion and Management*, 65:57–65, 2013.

[AC04]   J. Arroyo and A. Conejo. Modeling of start-up and shut-down power trajectories of thermal units. *IEEE Transactions on Power Systems*, 19(3):1562–1568, 2004.

[AIS⁺89]   K. Aoki, M. Itoh, T. Satoh, K. Nara, and M. Kanezashi. Optimal long-term Unit Commitment in large scale systems including fuel constrained thermal and pumped-storage hydro. *IEEE Transactions on Power Systems*, 4(3):1065–1073, 1989.

[ANE11]   ANEMOS. ANEMOS: a success story of European research. *http://www.anemos-plus.eu/*, 2011.

[ANP95]   U. D. Annakkage, T. Numnonda, and N. C. Pahalawaththa. Unit Commitment by parallel simulated annealing. *Proc. Inst. Elect. Eng. Gen. Transm. Dist.*, 142:595–600, 1995.

[AOS02]   A. Arce, T. Ohishi, and T. Soares. Optimal dispatch of generating units of the itaip hydroelectric plant. *IEEE Transactions on Power Systems*, 17(1):154–158, 2002.

[AP71]   A. K. Ayoub and A. D. Patton. Optimal thermal generating Unit Commitment. *IEEE Transactions on Power Apparatus and Systems*, PAS-90(4):1752–1756, 1971.

[ASI87]   K. Aoki, , T. Satoh, and M. Itoh. Unit Commitment in large scale power systems including fuel constrained thermal and pumped-storage hydro. *IEEE Transactions on Power Systems*, 2(4):1077–1084, 1987.

[Aut04]   Danish Energy Authority. Energy in Denmark 2003. *Danish Authority Report*, 2004.

[BBL03]   S Bivona, R Burlon, and C Leone. Hourly wind speed analysis in Sicily. *Renewable Energy*, 28(9):1371–1385, 2003.

[BD46]   R. E. Bellman and S. E. Dreyfus. *Applied dynamic programming*. Princeton University Press, New Jersey, pp. 4-16, 1946.

[BDM09]   R Burkard, M Dell'Amico, and S Martello. *Assignment Problems*. Society for Industrial and Applied Mathematics - SIAM, Philadelphia, 2009.

[BDO04]   M. Bazilian, E. Denny, and M. O'Malley. Challenges of increased wind energy penetration in Ireland. *Wind Engineering*, 28(1):43–56, 2004.

[Bet66]   A Betz. *Introduction to the Theory of Flow Machines*. D. G. Randall, Trans., Oxford: Pergamon Press, 1966.

[BF86]   D. Bond and B. Fox. Optimal thermal unit scheduling using improved dynamic programming algorithm. *IEEE Proceedings - Generation, Transmission and Distribution*, 133(1):1–5, 1986.

[BFLN03]   A. Borghetti, A. Frangioni, F. Lacalandra, and C. Nucci. Lagrangian heuristics based on disaggregated bundle methods for hydrothermal Unit Commitment. *IEEE Transactions on Power Systems*, 18:313–323, 2003.

[BG75]   R. M. Burns and C. A. Gibson. Optimization of priority lists for a Unit Commitment program. In *Proc. IEEE Power Eng. Soc. Summer Meeting*, 1975.

[BG80]   L. F. B. Baptistella and J. C. Geromel. Decomposition approach to problem of Unit Commitment schedule for hydrothermal systems. *IEEE Proceedings-D*, 127(6):250–258, 1980.

[BG08]   F. Bouffard and F. Galiana. Stochastic security for operations planning with significant wind power generation. *IEEE Transactions on Power Systems*, 23(2):306–316, 2008.

[BH85]   P. P. J. Van Den Bosch and G. Honderd. A solution of the Unit Commitment problem via decomposition and dynamic programming. *IEEE Transactions on Power Apparatus and Systems*, 104(7):1684–1690, 1985.

[BK09]   Kevin Brokish and James Kirtley. Pitfalls of modeling wind power using Markov chains. In *IEEE/PES Power Systems Conference and Exposition, PSCE '09*, pages 1–6, 2009.

[BKS$^+$12]   A. Bhardwaj, V.K. Kamboj, V.K. Shukla, B. Singh, and P. Khurana. Unit Commitment in electrical power system - a literature review. In *IEEE International Power Engineering and Optimization Conference (PEDCO) Melaka, Malaysia, 2012*, pages 275–280, 2012.

[BLRS01]   L. Bacaud, C. Lemarchal, A. Renaud, and C. Sagastizbal. Bundle methods in stochastic optimal power management: a disaggregated approach using preconditioners. *Computational Optimization and Applications*, 20(3):227–244, 2001.

[BLS$^+$13]   D. Bertsimas, E. Litvinov, X.A. Sun, J. Zhao, and T. Zheng. Adaptive Robust Optimization for the Security Constrained Unit Commitment Problem. *IEEE Transactions on Power Systems*, 28(1):52–63, 2013.

[Boo05]   A Boone. Simulation of short-term wind speed forecast errors using a multi-variate ARMA(1,1) time-series model. Master's thesis, Dept. of Electrical Engineering, Electric Power Systems Stockholm, Sweden, Royal Institute of Technology, 2005.

[Bro06]   L. Brown. *Plan B 2.0: Rescuing a planet under stress and a civilization in trouble. Chapter 10: Stabilizing Climate*. Earth Policy Institute, 2006.

[BS97]   X. Bai and S. M. Shahidehpour. Extended neighborhood search algorithm for constrained Unit Commitment. *International Journal of Electric Power and Energy Systems*, 19(5):349–356, 1997.

[BTK12]   A. Bhardwaj, N. Singh Tung, and V. Kamboj. Unit Commitment in power system: A review. *International Journal of Electrical and Power Engineering*, 6:51–57, 2012.

[CA91]   E. Castillo and E. Alvarez. *Expert Systems: Uncertainty and Learning.* U.K.: Computational Mechanics Publications, 1991.

[CA06]   M. Carrion and J. M. Arroyo. A computationally efficient mixed integer linear formulation for the thermal Unit Commitment problem. *IEEE Transactions on Power Systems*, 21(3):1371–1378, 2006.

[CB90]   N. Chowdhury and R. Billinton. Unit Commitment in interconnected generating systems using a probabilistic technique. *IEEE Transactions on Power Systems*, 5:1231–1238, 1990.

[CBC99]   A. I. Cohen, V. Brandwajn, and S. K. Chang. Security constrained Unit Commitment for open market. *Proc. 21st IEEE Power Eng. Soc. Int. Conf. Power Ind. Comput. Applicat.*, pages 39–44, 1999.

[CCS12]   C. Christopher Columbus, K. Chandrasekaran, , and Sishaj P. Simon. Nodal ant colony optimization for solving profit based Unit Commitment problem for GEN-COs. *Applied Soft Computing*, 12(1):145–160, 2012.

[CHR12]   C. Corchero, F. J. Heredia, and J. C. Rubiano. Optimal electricity market bidding strategies considering emission allowances. In *9th International Conference on the European Energy Market (EEM)*, pages 1–8, 2012.

[CHSP12]   K. Chandrasekarana, S. Hemamalinib, Sishaj P. Simona, and Narayana Prasad Padhy. Thermal Unit Commitment using binary-real coded artificial bee colony algorithm. *Electric Power Systems Research*, 84(1):109–119, 2012.

[CLL00]   C. P. Cheng, C. W. Liu, and C. C. Liu. Unit Commitment by Lagrangian Relaxation and genetic algorithm. *IEEE Transactions on Power Systems*, 15:707–714, 2000.

[CMMF05]   J. Catalo, S. Mariano, V. Mendes, and L. Ferreira. Parametrization effect on the behavior of a head dependent hydro chain using a nonlinear model. *Electric Power System Research*, 76:404–412, 2005.

[Com97]   European Commission. Energy for the future: Renewable sources of energy, white paper for a community strategy and action plan. *COM(97) 599 final*, 1997.

[CPM10]   J. Catalo, H. Pousinho, and V. Mendes. Scheduling of head dependent cascaded reservoirs considering discharge ramping constraints and start/stop of units. *International Journal of Electrical Power and Energy Systems*, 32(8):904–910, 2010.

[CSGTXB10]   Yoreley Cancino-Solrzano, Antonio J. Gutirrez-Trashorras, and Jorge Xiberta-Bernat. Analytical methods for wind persistence: Their application in assessing the best site for a wind farm in the State of Veracruz, Mexico. *Renewable Energy*, 35(12):2844–2852, 2010.

[CSK78]   Ross B Corotis, Arden B Sigl, and Joel Klein. Probability models of wind velocity magnitude and persistence. *Solar Energy*, 20(6):483–493, 1978.

[CW87]   A. I. Cohen and S. H. Wan. A method for solving the fuel constrained Unit Commitment problem. *IEEE Transactions on Power Systems*, PWRS-2:608–614, 1987.

[CW02]   H. Chen and X. Wang. Cooperative evolutionary algorithm for Unit Commitment. *IEEE Transactions on Power Systems*, 16:128–133, 2002.

[CY83]   A. I. Cohen and M. Yoshimura. A branch and bound algorithm for Unit Commitment. *IEEE Transactions on Power Apparatus and Systems*, PAS-102:444–451, 1983.

[DE76]   T. S. Dillon and G. T. Eagan. The application of combinatorial methods to the problems of maintenance scheduling and Unit Commitment in large power systems. *IFAC Symposium on Large Scale Systems, Udine, Italy*, 1976.

[DEKT78]   T. S. Dillon, K. W. Edwin, H. D. Kochs, and R. J. Taud. Integer programming approach to the problem of optimal Unit Commitment with probabilistic reserve determination. *IEEE Transactions on PAS*, 97(6):2154–2166, 1978.

[dEn03]   Red Electrica de España. El sistema electrico español en 2003. *Red Electrica de España Report*, 2003.

[Den07]   E. Denny. *A Cost Benefit Analysis of Wind Power*. Master's thesis, School of Electrical, Electronic and Mechanical Engineering, National University of Ireland, University College Dublin, Ireland, 2007.

[DM94]   D. Dasgupta and D. R. McGregor. Thermal Unit Commitment using genetic algorithms. *Proc. Inst. Elect. Eng., Gen. Transm. Dist.*, 141:459–465, 1994.

[dMEG]   Gestore del Mercato Elettrico GME. http://www.mercatoelettrico.org/.

[DMN03]   K. Deng, A. W. Moore, and M. C. Nechyba. Learning to recognize time series: Combining ARMA models with memory-based learning. *The Robotics Institute, Carnegie Mellon University*, 2003.

[dPdERA05] Associacion de Productores de Energias Renovables (APPA). España cierra 2004 superando los 8.200 MW de potencia eolica instalada. *Nota de Prensa 2005-01-28*, 2005.

[DT05]   R. Deepak and S. Takriti. Minimum up/down polytopes of the Unit Commitment problem with start-up costs. *Tech. Rep. RC23628, IBM Research Division*, 2005.

[EIA04]   EIA. Energy information administration (EIA): international energy outlook. *EIA Report*, 2004.

[Eir04]   EirGrid. Impact of wind power generation in Ireland on the operation of conventional plant and the economic implications. *EirGrid Report*, 2004.

[End05]   C. Ender. Wind energy use in Germany: Status 31.12.2004. *DEWI Magazin, Deutsches Windenergie-Institut DEWI, 26*, 2005.

[Eth06]   J. R. Etherington. The case against windfarms. *Country Guardian's Report*, 2006.

[EWE12]   The European Wind Energy Association EWEA. Basic cost of wind energy. *EWEA Reports*, 2012.

[FBC95]   A. Farag, S. Baiyat, and T. C. Cheng. Economic load dispatch multiobjective optimisation procedures using linear programming techniques. *IEEE Transactions on Power Systems*, 10(2):731–738, 1995.

[FdS06]   E. Finardi and E. da Silva. Solving the hydro Unit Commitment problem via Dual Decomposition and Sequential Quadratic Programming. *IEEE Transactions on Power Systems*, 21(2):835–844, 2006.

[FdSS05]   E. Finardi, E. da Silva, and C. Sagastizbal. Solving the Unit Commitment problem of hydropower plants via Lagrangian Relaxation and Sequential Quadratic Programming. *Computational and Applied Mathematics*, 24(3):317–341, 2005.

[FG06]   A. Frangioni and C. Gentile. Perspective cuts for a class of convex 0-1 mixed integer programs. *Mathematical Programming*, 106(2):225–236, 2006.

[Fly03]   D. Flynn. Thermal power plant simulation and control, 1st edition. *IEE Power and Energy Series, IEE, London*, 43, 2003.

[GBK03]   G. Giebel, R. Brownsword, and G. Kariniotakis. The state of the art in short term prediction of wind power, a literature overview. *Project Anemos, Contract No. ENK5-CT-2002-00665, http://anemos.cma.fr*, 2003.

[GHA+06]   R. Gross, P. Hemptonstall, D. Anderson, T. Green, M. Leach, and J. Skea. The costs and impacts of intermittency: An assessment of the evidence on the costs and impacts of intermittent generation on the British electricity network. *A report of the Technology and Policy Assessment Function of the UK Energy Research Centre*, 2006.

[GHSHG03]   P. Gardiner, H. H. Snodin, A. Higgins, and S. M. Goldrick. The impacts of increased levels of wind penetration on the electricity systems of the Republic of Ireland and northern Ireland. *(3096/GR/04)*, 2003.

[Gij96]   T. Gijengedal. Emission constrained Unit Commitment. *IEEE Transactions on Energy Conversion*, 11(1):132–138, 1996.

[GLKB03]   G. Giebel, L. Landberg, G. Kariniotakis, and R. Brownsword. State of the art on methods and software tools for short term prediction of wind energy production. *In: European Wind Energy Conference and Exhibition EWEC. Madrid, Spain*, 2003.

[GLYA92]   X. Guan, P. B. Luh, H. Yan, and J. A. Amalfi. An optimization based method for Unit Commitment. *International Journal of Electrical Power and Energy Systems*, 14(1):9–17, 1992.

[GR12]   M. Govardhan and R. Roy. Evolutionary computation based Unit Commitment using hybrid priority list approach. In *IEEE International Conference on Power and Energy (PECon)*, pages 245–250, 2012.

[GSHG03]   P. Gardner, H. Snodin, A. Higgins, and S. M. Goldrick. The impacts of increased levels of wind penetration on the electricity systems of the Republic of Ireland and Northern Ireland. *Final Report to the Commission for Energy Regulation/OFREG by Garrad Hassan 3096/GR/04*, 2003.

[GTPdF98]   A Garcia, J L Torres, E Prieto, and A de Francisco. Fitting wind speed distributions: a case study. *Solar Energy*, 62(2):139–144, 1998.

[Gup86]   B K Gupta. Weibull parameters for annual and monthly wind speed distributions for five locations in India. *Solar Energy*, 37(6):469–471, 1986.

[Guy71]   J. D. Guy. Security constrained Unit Commitment. *IEEE Transactions on Power Apparatus and Systems*, 90(3):1385–1389, 1971.

[HAMS98]   A. H.Mantawy, Y. L. Abdel-Magid, and S. Z. Selim. A simulated annealing algorithm for Unit Commitment. *IEEE Transactions on Power Systems*, 13:197–204, 1998.

[HB86]   H. Habibollahzadeh and J. A. Bubenko. Application of decomposition techniques to short-term operation planning of hydrothermal power system. *IEEE Transactions on PWRS*, 1(1):41–47, 1986.

[HCP+00]   N. Hatziargyriou, G. Contaxis, M. Papadopoulos, B. Papadias, M. Maots, J. P. Lopes, E. Nogaret, G. Kariniotakis, J. Halliday, G. Dutton, P. Dokopoulos, A. Bakirtzis, A. Androutsos, J. Stefanakis, and A. Gigantidou. Operation and control of island systems - the Crete case. *In: IEEE Power Engineering Society Winter Meeting*, 2000.

[Hei05]   S Heier. *Grid Integration of Wind Energy Conversion Systems*. Chichester: John Wiley and Sons, 2005.

[Hel05]   D. Helm. *Climate change policy, 1st Edition*. Oxford University Press, Oxford, UK, 2005.

[Hen77]   Joseph P Hennessey. Some aspects of wind power statistics. *Journal of Applied Meteorology*, 16(2):119–128, 1977.

[HHWS88]   W. J. Hobbs, G. Hermon, S. Warner, and G. B. Sheble. An enhanced dynamic approach for Unit Commitment. *IEEE Transactions on Power Systems*, 3(3):1201–1205, 1988.

[HJW71]   H. H. Happ, R. C. Johnson, and W. J. Wright. Large scale hydrothermal Unit Commitment method and results. *IEEE Transactions on Power Apparatus and Systems*, 90(3):1373–1384, 1971.

[HKH66]   K. Hara, M. Kimiura, and N. Honda. A method for planning economic Unit Commitment and maintenance of thermal power systems. *IEEE Transactions on Power Apparatus and Systems*, PAS-85:427–436, 1966.

[Hol04]   H. Holttinen. The impact of large scale wind power production on the Nordic electricity system. *VTT publications 554. Julkaisija, VTT technical research centre of Finland*, 2004.

[HRNC01]   B. Hobbs, M. Rothkopf, R. O' Neill, and H. Chao. *The next generation of Unit Commitment models.* Boston: Kluwer Academic Press, 2001.

[HSLH91]   Y. Y. Hsu, C. C. Su, C. C. Liang, and C. T. Huang. Dynamic security constrained multi-area Unit Commitment. *IEEE Transactions on Power Systems*, 6(3):1049–1055, 1991.

[Hua01]   S. J. Huang. Enhancement of hydroelectric generation scheduling using ant colony system based optimization approaches. *IEEE Trans. Energy Conversion*, 16:296–301, 2001.

[Hua13]   Cong Hui Huang. Enhanced artificial intelligence algorithm for optimal Unit Commitment problem. *Applied Mechanics and Materials*, 3087(284-287), 2013.

[HYH98]   K. Y. Huang, H. T. Yang, and C. L. Huang. A new thermal Unit Commitment approach using constraint logic programming. *IEEE Transactions on Power Systems*, 13:936–945, 1998.

[IEA12]   The International Energy Agency IEA. Co2 emissions from fuel combustion. *IEA Reports*, 2012.

[IoLES04] Institute of Electrical IEEE/CIGRE and Electronics Engineers/International Council on Large Electric Systems. Joint task force on stability terms and definitions. Definition and classification of power system stability. *IEEE Transactions on Power Systems*, 19(2):1387–1401, 2004.

[JBRF13]   M. Zareian Jahromi, M.M. Hosseini Bioki, M. Rashidinejad, and R. Fadaeinedjad. Solution to the Unit Commitment problem using an artificial neural network. *Turkish Journal of Electrical Engineering and Computer Sciences*, 21:198–212, 2013.

[JHMG78]   C G Justus, W R Hargraves, A Mikhail, and D Graber. Methods for estimating wind speed frequency distributions. *Journal of Applied Meteorology*, 17(3):350–385, 1978.

[JHY76]   C G Justus, W R Hargraves, and A Yalcin. Nationwide assessment of potential output from wind-powered generators. *Journal of Applied Meteorology*, 15(7):673–678, 1976.

[JKTH99]   K. A. Juste, H. Kita, E. Tanaka, and J. Hasegawa. An evolutionary programming solution to the Unit Commitment problem. *IEEE Transactions on Power Systems*, 14:1452–1459, 1999.

[KHM92]   S. Kuloor, G. S. Hope, and O. P. Malik. Environmentally constrained Unit Commitment. *IEEE Proceedings Generation, Transmission and Distribution*, 139(2):122–128, 1992.

[KK12]   M. Kaur and R. Kaur. Fuzzy logic and neural network approach to short term thermal Unit Commitment. *People's Journal of Science and Technology*, 2(1), 2012.

[KK13]   R. Uday Kishan and P. Seshu Kumar. Thermal Unit Commitment using fuzzy logic. *International Journal of Engineering Research and Technology*, 2(1), 2013.

[KP07]   S. S. Kumar and V. Palanisamy. A dynamic programming based fast computation
           hopfield neural network for Unit Commitment and Economic Dispatch. *Electric
           Power Systems Research*, 77(8):917–925, 2007.

[KS04]   D. Kirschen and G. Strbac. *Fundamentals of Power system economics*. Wiley and
           Sons Ltd., West Sussex, England, 2004.

[KS10]   A. Khodaei and M. Shahidehpour. Transmission Switching in Security-Constrained
           Unit Commitment. *IEEE Transactions on Power Systems*, 25(4):1937–1945, 2010.

[KSF66]   R. H. Kerr, J. L. Scheidt, and A. J. Fontana. Unit Commitment. *IEEE Transactions
           on Power Apparatus and Systems*, PAS-85:417–421, 1966.

[KSW07]   Martin Kaltschmitt, Wolfgang Streicher, and Andreas Wiese. *Renewable energy:
           technology, economics, and environment*. Springer, 2007.

[KW94]   P. Kall and S. W. Wallace. *Stochastic Programming*. John Wiley and Sons, Chich-
           ester, 1994.

[LBG97]   S. Lefton, P. Besuner, and G. Grimsrud. Understand what it really costs to cycle
           fossil-fired units. *Power*, 141(2):41–42, 1997.

[LC91]   F. N. Lee and Q. Chen. Unit Commitment risk with sequential rescheduling. *IEEE
           Transactions on Power Systems*, 6:1017–1023, 1991.

[LCT02]   W. M. Lin, F. S. Chen, and M. T. Tsay. An improved Tabu Search for Economic
           Dispatch with multiple minima. *IEEE Trans. Power Syst.*, 17:108–112, 2002.

[LDCG83]   K. D. Lee, J. T. Day, B. L. Cooper, and E. W. Gibbons. A global optimization
           method for scheduling thermal generation, hydro generation, and economy pur-
           chase. *IEEE Trans. Power App. Syst.*, PAS-102:1983–1986, 1983.

[Lee88]   F. N. Lee. Short term Unit Commitment: a new method. *IEEE Transactions on
           Power Systems*, 3:421–428, 1988.

[Lee89]   F. N. Lee. A fuel constrained Unit Commitment method. *IEEE Transactions on
           Power Systems*, 4(3):1208–1218, 1989.

[Lee91]   F. N. Lee. The application of commitment utilization factor (CUF) to thermal Unit
           Commitment. *IEEE Transactions on Power Systems*, 6:691–698, 1991.

[LF92]   F. N. Lee and Q. Feng. Multi area Unit Commitment. *IEEE Transactions on Power
           Systems*, 7(2):591–598, 1992.

[LG13]   M.M. Lotfi and S.F. Ghaderi. A compromised multi-objective solution using fuzzy
           mixed integer goal programming for market-based short-term Unit Commitment
           problem. *Journal of the Operational Research Society*, 172, 2013.

[LHA94]   F. N. Lee, J. Huang, and R. Adapa. Multi-area Unit Commitment via sequential
           method and a dc power flow network model. *IEEE Transactions on Power Systems*,
           9:279–287, 1994.

[LJBP82]   G. S. Lauer, N. R. Sandell Jr, N. R. Bertsekas, and T. A. Posbergh. Solution of large scale optimal Unit Commitment problems. *IEEE Transactions on Power Apparatus and Systems*, PAS-101:79–96, 1982.

[LJS$^+$98]   C. Li, R. B. Johnson, A. J. Svoboda, C. Tseng, and E. Tsu. A robust Unit Commitment algorithm for hydro-thermal optimization. *IEEE Transactions on Power Systems*, 13:1051–1056, 1998.

[LK00]   R. H. Liang and F. C. Kang. Thermal generating Unit Commitment using an extended mean field annealing neural network. *Proc. Inst. Elect. Eng., Gen. Transm. Dist.*, 147:164–170, 2000.

[LKPvdS10]   A. Lojowska, D. Kurowicka, G. Papaefthymiou, and L. van der Sluis. Advantages of ARMA-GARCH wind speed time series modeling. In *2010 IEEE 11th International Conference on Probabilistic Methods Applied to Power Systems (PMAPS)*, pages 83–88, 2010.

[lLCMMG12]   J. lvarez Lpez, J.L. Ceciliano-Meza, I.G. Moya, and R.N. Gmez. A MIQCP formulation to solve the Unit Commitment problem for large-scale power systems. *International Journal of Electrical Power and Energy Systems*, 36(1):68–75, 2012.

[LLM04]   J. Lee, J. Leung, and F. Margot. Min-up/min-down polytopes. *Discrete Optimization*, 1:77–85, 2004.

[LLX02]   X. Lei, E. Lerch, and C. Y. Xie. Frequency security constrained short term Unit Commitment. *Elect. Power Syst. Res.*, 60:193–200, 2002.

[LN84]   D. Lidgate and K. M. Nor. Unit Commitment in a thermal generation system with multiple pumped storage power stations. *International Journal of Electrical Power and Energy Systems*, 6(2):101–111, 1984.

[Low66]   P. G. Lowery. Generating Unit Commitment by dynamic programming. *IEEE Transactions on Power Apparatus and Systems*, 85(5):422–426, 1966.

[LPZ13]   Y.F. Li, N. Pedroni, and E. Zio. A memetic evolutionary multi-objective optimization method for environmental power Unit Commitment. *IEEE Transactions on Power Systems*, PP(99):1–10, 2013.

[LS93]   S. Li and S. M. Shahidehpour. Promoting the application of expert systems in short-term Unit Commitment. *IEEE Transactions on Power Systems*, 3:286–292, 1993.

[LS03]   Z. Li and M. Shahidehpour. Generation scheduling with thermal stress constraints. *IEEE Transactions on Power Systems*, 18(4):1402–1409, 2003.

[LS05]   B. Lu and M. Shahidehpour. Unit Commitment with flexible generating units. *IEEE Transactions on Power Systems*, 20(2):1022–1034, 2005.

[LSFL10]   A. Lotfjou, M. Shahidehpour, Yong Fu, and Zuyi Li. Security-Constrained Unit Commitment with AC/DC transmission systems. *IEEE Transactions on Power Systems*, 25(1):531–542, 2010.

[MAMS98]   A. H. Mantawy, Y. L. Abdel-Magid, and S. Z. Selim. Unit Commitment by Tabu Search. *Proc. Inst. Elect. Eng., Gen. Transm. Dist.*, 145(1):56–64, 1998.

[MAMS99]   A. H. Mantawy, Y. L. Abdel-Magid, and S. Z. Selim. Tabu Search and Simulated Annealing for the Unit Commitment problem. *IEEE Trans. Poer Syst.*, 14:829–836, 1999.

[Mee84]   H. P. Van Meeteren. Scheduling of generation and allocation of fuel using dynamic and linear programming. *IEEE Transactions on Power Apparatus and Systems*, 103(7):1562–1568, 1984.

[MELR12]   G. Morales-Espana, J.M. Latorre, and A. Ramos. Tight and compact MILP formulation of start-up and shut-down ramping in Unit Commitment. *IEEE Transactions on Power Systems*, 28(2):1288–1296, 2012.

[MK77]   A. Muckstadt and S. A. Koenig. An application of Lagrangian Relaxation to scheduling in power-generation systems. *Operation Research*, 25(3):387–403, 1977.

[MK95]   M. Mazumdar and A. Kapoor. Stochastic method for power generation system production costs. *Electrical Power Systems Research*, 35:93–100, 1995.

[MM00]   H. Mori and O. Matsuzaki. Embedding the priority into into Tabu Search for Unit Commitment. In *Proc. IEEE Winter Meeting*, 2000.

[MQ00]   M. Madrigal and V. H. Quintana. An interior point/cutting plane method to solve Unit Commitment problems. *IEEE Transactions on Power Systems*, 15(3):1022–1027, 2000.

[MS83]   A. Merlin and P. Sandrin. A new method for Unit Commitment at Electricite De France. *IEEE Transactions on Power Apparatus and Systems*, PAS-102:1218–1225, 1983.

[MS96]   T. T. Maifeld and G. B. Sheble. Genetic-based Unit Commitment algorithm. *IEEE Transactions on Power Systems*, 11:1359–1370, 1996.

[MS98]   H. Ma and S. M. Shahidehpour. Transmission constrained Unit Commitment based on Benders Decomposition. *International Journal of Electrical Power and Energy Systems*, 20(4):287–294, 1998.

[MS99]   H. Ma and S. M. Shahidehpour. Unit Commitment with transmission security and voltage constraints. *IEEE Transactions on Power Systems*, 14:757–764, 1999.

[MSH02]   A. H. Mantawy, S. A. Soliman, and M. E. El Hawary. A new Tabu Search algorithm for the long term hydro scheduling problem. *Proc. Large Eng. Syst. Conf. Power Eng.*, pages 29–34, 2002.

[MSW88]   S. Mokhtari, J. Singh, and B. Wollenberg. A Unit Commitment expert system. *IEEE Transactions on Power Systems*, 3(1):272–277, 1988.

[MU96]   H. Mori and T. Usami. Unit Commitment using Tabu Search with restricted neighborhood. *Proc. Intell. Syst. Applicat. Power Syst.*, pages 422–427, 1996.

[Nai08]   A. Naimo. *Modelli e algoritmi di ottimizzazione robusta per la gestione operativa di centrali elettriche.* Master's thesis, Dipartimento di Informatica e Automazione DIA, Universit di Roma Tre, Italy, 2008.

[NaIG87]   R. Nieva and A. Inda abd I. Guillen. Lagrangian reduction of search range for large scale Unit Commitment. *IEEE Transactions on PWRS*, 2(2):465–473, 1987.

[NGH+04]   P. Norgard, G. Giebel, H. Holttinen, L. Soder, and A. Petterteig. Fluctuations and predictability of wind and hydropower. *Deliverable D2.1. Riso-R-1443(EN)*, 2004.

[NIF86]   R. Nieva, A. Inda, and J. Frausto. Cht: a digital computer package for solving short term hydro-thermal coordination and Unit Commitment problems. *IEEE Transactions on Power Apparatus and Systems*, PAS-1:168–174, 1986.

[NK94]   I. J. Nagrath and D.P. Kothari. *Power System Engineering.* Tata McGraw Hill Publishing Co, New Delhi, 1994.

[NM02]   H. A. Nielsen and H. Madsen. Analyse og simulering af prdiktionsfejl for vindenergiproduktion ved indmelding til nordpool. *Informatics and Mathematical Modelling, Technical University of Denmark, Lyngby, Denmark*, 2002.

[NNM02]   H. A. Nielsen, T. S. Nielsen, and H. Madsen. On on-line systems for short-term forecasting for energy systems. *Proceedings of the OR 2002 Conference, pp. 265-271*, 2002.

[OAV12]   J. Ostrowski, M.F. Anjos, and A. Vannelli. Tight Mixed Integer Linear Programming formulations for the Unit Commitment Problem. *IEEE Transactions on Power Systems*, 27(1):39–46, 2012.

[OI97]   S. O. Orero and M. R. Irving. Large scale Unit Commitment using an hybrid genetic algorithm. *International Journal of Electric Power and Energy Systems*, 19(1):45–55, 1997.

[OS90]   Z. Ouyang and S. M. Shahidehpour. Short-term Unit Commitment expert system. *Electric Power Systems Research*, 20(1):1–13, 1990.

[OS91]   Z. Ouyang and S. M. Shahidehpour. An intelligent dynamic programming for Unit Commitment application. *IEEE Transactions on Power Systems*, PWRS-6(3):1203–1209, 1991.

[otETD07]   Department of the Enterprise Trade and Investment (DETI). A study into the economic renewable energy resource in northern Ireland and the ability of the electricity network to accommodate renewable generation up to 2010. *Available: www.energy.detini.gov.uk.*, 2007.

[Pad99]   N. P. Padhy. A new fuzzy expert decision making approach for Unit Commitment with reliable risk reserve and emission constraints. *J. Energy Environment*, 1:25–36, 1999.

[Pad04]   N. P. Padhy. Unit Commitment: a bibliographical survey. *IEEE Transactions on Power Systems*, 19(2):1196–1205, 2004.

[Par01]   European Parliament. Directive 2001/77/EC on the promotion of electricity pro-
             duced from renewable energy sources in the internal electricity market. *EUP Di-
             rective*, 2001.

[PC76]   C. K. Pang and H. C. Chen. Optimal short term thermal Unit Commitment. *IEEE
             Transactions on Power Apparatus and Systems*, 95(4):1336–1346, 1976.

[PP95]   N. P. Padhy and S. R. Paranjothi. Application of expert system for short-term Unit
             Commitment problem. *Proc. Nat. Syst. Conf., Agra, India*, pages 443–447, 1995.

[PP03]   J. Pedersen and B. E. Peter. Simulation model including stochastic behavior of
             wind. *Fourth International Workshop on Large-Scale Integration of Wind Power
             and Transmission Networks for Offshore Wind Farms, Billund, Denmark*, 2003.

[PRP95]   N. P. Padhy, V. R. Ramachandran, and S. R. Paranjothi. Fuzzy decision system for
             short-term Unit Commitment problem. *Proc. Nat. Conf. Neural Networks Fuzzy
             Syst., Chennai, India*, pages 287–298, 1995.

[PRP99]   N. P. Padhy, V. R. Ramachandran, and S. R. Paranjothi. Fuzzy decision system for
             Unit Commitment risk analysis. *International Journal of Power Energy Systems*,
             19(2):180–185, 1999.

[PSA81]   C. K. Pang, G. B. Sheble, and F. Albuyeh. Evaluation of dynamic programming
             bases methods and multiple area representation for thermal Unit Commitment.
             IEEE Transactions on Power Apparatus and Systems, 100(3):1212–1218, 1981.

[RB99]   A. Rudolf and R. Bayrleithner. A genetic algorithm for solving the Unit Com-
             mitment problem of a hydro-thermal power system. *IEEE Transactions on Power
             Systems*, 14:1460–1468, 1999.

[RdMC89]   J S Rohatgi, A L R de Meiros, and R A Cavalcanti. Statistical testing of Weibull and
             other frequency distributions of wind speed variations for different sites. In *EWEC
             '89, Proceedings of European Wind Energy Conference and Exhibition, Brazil: Peter
             Peregrino Ltd*, pages 880–883, 1989.

[RHH94]   S Rehman, T O Halawani, and T Husain. Weibull parameters for wind speed
             distribution in Saudi Arabia. *Solar Energy*, 53(6):473–479, 1994.

[RMM02]   A. Rajan, C. C. Mohan, and M. R. Manivannan. Neural based Tabu Search method
             for solving Unit Commitment problem. *Proc. 5th Int. Conf. Power Syst. Manage.
             Contr.*, pages 180–185, 2002.

[RPS09]   P.A. Ruiz, C. R. Philbrick, and P.W. Sauer. Wind power day-ahead uncertainty
             management through stochastic Unit Commitment policies. In *Proceedings Power
             Systems Conference and Exhibition, Seattle, Wash.*, 2009.

[RPZ+09]   P.A. Ruiz, C. R. Philbrick, E. Zak, K.W. Cheung, and P.W. Sauer. Uncertainty
             management in the Unit Commitment problem. *IEEE Transactions on Power
             Systems*, 24(2):642–651, 2009.

[Sal07]   S. Salam. Unit Commitment solution methods. *World Academy of Science, Engi-
             neering and Technology*, 35:320–325, 2007.

[SAS13]   M. Samiee, N. Amjady, and H. Sharifzadeh. Security constrained Unit Commitment of power systems by a new combinatorial solution strategy composed of enhanced harmony search algorithm and numerical optimization. *International Journal of Electrical Power and Energy Systems*, 44(1):471–481, 2013.

[SCHG80]   R. R. Shoults, S. K. Chang, S. Helmick, and W. M. Grady. A practical approach to Unit Commitment, Economic Dispatch and savings allocation for multiple area pool operation with import/export constraints. *IEEE Transactions on Power Apparatus and Systems*, PAS-99:625–635, 1980.

[SCL94]   D. Srinivasan, C. S. Chang, and A. C. Liew. Multi-objective generation scheduling using fuzzy optimal search technique. *IEEE Proceedings*, 141(3):233–242, 1994.

[SDPM04]   J. Smith, E. DeMeo, B. Parsons, and M. Milligan. Wind power impact on electric power system costs: summary and perspective on work to date. *In: Global WINDPOWER Conference. Chicago, Illinois*, 2004.

[SDSK13]   B. Saravanan, S. Das, S. Sikri, and D.P. Kothari. A solution to the Unit Commitment problem - a review. *Frontiers in energy*, 2013.

[SEK02]   N. S. Sisworahardjo and A. A. El-Kaib. Unit Commtiment using ant colony search algorithm. *Proc. 2002 Large Eng. Syst. Conf. Power Eng.*, pages 2–6, 2002.

[SH91]   C. C. Su and Y. Y. Hsu. Fuzzy dynamic programming: an application to Unit Commitment. *IEEE Transactions on PWRS*, 6(3):1231–1237, 1991.

[Sha95]   J. J. Shaw. A direct method for security-constrained Unit Commitment. *IEEE Transactions on Power Systems*, 10:1329–1342, 1995.

[She96]   G. B. Sheble. Unit Commitment by genetic algorithm with penalty methods and a comparison of lagrangian search and genetic algorithm-economic dispatch example. *International Journal of Power Energy Systems*, 18(6):339–346, 1996.

[SHN91]   M. S. Salam, A. R. Hamdan, and K. M. Nor. Integrating an expert system into a thermal Unit Commitment algorithm. *IEEE Proceedings-Generation, Transmission and Distribution*, 138(6):553–559, 1991.

[SM12]   S. Soliman and A.H. Mantawy. Economic Dispatch (ED) and Unit Commitment Problems (UCP): Formulation and solution algorithms. *Modern Optimization Techniques with Applications in Electric Power Systems Energy Systems*, pages 185–279, 2012.

[Sod93a]   L. Soder. Modeling of wind power forecast uncertainty. In *Proceedings of the European Community Wind Energy Conference, 8 - 12 March 1993, Lubeck-Travemunde, pp. 786 - 789*, 1993.

[Sod93b]   L. Soder. Reserve margin planning in a wind-hydro-thermal power system. *IEEE Transactions on Power Systems*, 8:564–571, 1993.

[Sod04]   L Soder. Simulation of wind speed forecast errors for operation planning of multi-area power systems. In *8th International Conference on Probabilistic Methods Applied to Power Systems, Iowa State University, United States*, pages 723–728, 2004.

[SPG03]   Y. R. Sood, N. P. Padhy, and H. O. Gupta. Discussion on optimal power flow by enhanced genetic algorithms. *IEEE Transactions on Power Systems*, 18:1219, 2003.

[SPR87]   W. L. Snyder, H. D. Powell, and J. C. Rayburn. Dynamic programming approach to Unit Commitment. *IEEE Transactions on Power Systems*, 2(2):339–351, 1987.

[SPS97]   S. Saneifard, N. R. Prasad, and H. A. Smolleck. A fuzzy logic approach to Unit Commitment. *IEEE Transactions on Power Systems*, 12:988–995, 1997.

[SS79]   M J M Stevens and P T Smulders. The estimation of the parameters of the Weibull wind speed distribution for wind energy utilization purposes. *Wind Engineering*, 3(2):132–145, 1979.

[ST10]   Terna S.p.A. and Gruppo Terna. Dati statistici sull'energia elettrica in Italia. *Statistiche sul sistema elettrico italiano - Terna S.p.A.*, 2010.

[Sta04]   Windstats Newsletter Staff. How wind power can reach large scale penetration into Europe's power grid. *Windstats Newsletter*, 17(4), 2004.

[SWK+91]   H. Sasaki, M. Watanabe, J. Kubokawa, N. Yorina, and R. Yokoyama. A solution method of Unit Commitment by artificial neural network. *Proc. IEEE Power Eng. Soc. Summer Meeting*, 1991.

[SWY92]   H. Sasaki, M. Watanabe, and R. Yokoyama. A solution method of Unit Commitment by artificial neural networks. *IEEE Transactions on Power Systems*, 7:974–981, 1992.

[SY02]   K. S. Swarup and S. Yamashiro. Unit Commitment solution methodology using genetic algorithm. *IEEE Transactions on Power Systems*, 17:87–91, 2002.

[TB00]   S. Takriti and J. R. Birge. Using Integer Programming to refine Lagrangian-based Unit Commitment solutions. *IEEE Transactions on Power Systems*, 15:151–156, 2000.

[TBB13]   N.S. Tung, A.B. Bhadoria, and A. Bhardwa. Start up cost constraint optimization using Lagrangian algorithm for unit schedule in electrical power system. *International Journal of enhanced research in science, technology and engineering*, 1(2), 2013.

[TBL96]   S. Takriti, J. R. Birge, and E. Long. A stochastic model for the Unit Commitment problem. *IEEE Transactions on Power Systems*, 11:1497–1508, 1996.

[TDM07]   A. Tuohy, E. Denny, and M. O' Malley. Rolling Unit Commitment for systems with significant installed wind capacity. In *2007 IEEE Lausanne Power Tech, July 1-5 2007*, pages 130–1385, 2007.

[TMDM09]   A. Tuohy, P. Meibom, E. Denny, and M. O' Malley. Unit Commitment for systems with significant wind penetration. *IEEE Transactions on Power Systems*, 24(2):592–601, 2009.

[TMM08]   A. Tuohy, P. Meibom, and M. O' Malley. Benefits of stochastic scheduling for power systems with significant installed wind power. In *Proc. 10th Int. Conf. Probabilistic Methods Applied to Power Systems (PMAPS), Mayaguez, Puerto Rico*, 2008.

[TS89]   S. K. Tong and S. M. Shahidehpour. Combination of Lagrangian-Relaxation and linear-programming approaches for fuel-constrained Unit Commitment problems. *Proc. Inst. Elect. Eng., Gen. Transm. Dist.*, 136:162–174, 1989.

[TS90a]   S. K. Tong and S. M. Shahidehpour. Hydro thermal Unit Commitment with probabilistic constraints using segmentation method. *IEEE Transactions on Power Systems*, 5:276–282, 1990.

[TS90b]   S. K. Tong and S. M. Shahidehpour. An innovative approach to generation scheduling in large scale hydrothermal power systems with fuel constrained units. *IEEE Transactions on Power Systems*, 5(2):665–673, 1990.

[Tse96]   C. L. Tseng. *On Power System Generation Unit Commitment Problems*. PhD thesis, UC Berkeley, December 1996.

[Tur78]   A. Turgeon. Optimal scheduling of thermal generating units. *IEEE Transactions on Automatic Control*, 23(6):1000–1005, 1978.

[UGP$^+$07] B. C. Ummels, M. Gibescu, E. Pelgrum, W.L. Kling, and A.J. Brand. Impacts of wind power on thermal generation Unit Commitment and dispatch. *IEEE Transactions on Energy Conversion*, 22(1):44–51, 2007.

[VGP03]   P. Venkatesh, R. Gnanadass, and N. P. Padhy. Comparison and application of evolutionary programming techniques to combined economic emission dispatch with line flow constraints. *IEEE Transactions on Power Systems*, 18:688–692, 2003.

[VL91]   S. Vemuri and L. Lemonidis. Fuel constrained Unit Commitment. *IEEE Transactions on Power Systems*, 7:410–415, 1991.

[WAB81]   J. G. Waight, F. Albuyeh, and A. Bose. Scheduling of generation and reserve margin using dynamic and linear programming. *IEEE Transactions on Power Apparatus and Systems*, 100(5):2226–2230, 1981.

[WD91]   K. P. Wong and K. Doan. Artificial intelligence algorithm for daily scheduling of thermal generators. *Proc. Inst. Elect. Eng. Gen. Transm. Dist.*, 138(6):518–534, 1991.

[WIL05]   WILMAR. General overview of WILMAR project. *http://www.wilmar.risoe.dk/*, 2005.

[WM97]   M. P. Walsh and M. J. O. Malley. Augmented Hopfield network for Unit Commitment and Economic Dispatch. *IEEE Transactions on Power Systems*, 12:1765–1774, 1997.

[WS93]   C. Wang and S. Shahidehpour. Effects of ramp-rate limits on Unit Commitment and Economic Dispatch. *IEEE Transactions on Power Systems*, 8(3):1341–1350, 1993.

[WS94]   C. Wang and S. Shahidehpour. Ramp-rate limits in Unit Commitment and Economic Dispatch incorporating rotor fatigue effect. *IEEE Transactions on Power Systems*, 9(3):1539–1545, 1994.

[WS95]   C. Wang and S. Shahidehpour. Optimal generation scheduling with ramping costs. *IEEE Transactions on Power Systems*, 10(1):60–67, 1995.

[WS08]   J. Wang and M. Shahidehpour. Security-constrained Unit Commitment with volatile wind power generation. *IEEE Transactions on Power Systems*, 23(3):1319–1327, 2008.

[WSKI95]   S. J. Wang, S. M. Shahidehpour, D. S. Kirschen, and G. D. Irasarri. Short term generation scheduling with transmission and environmental constraints using an augmented Lagrangian Relaxation. *IEEE Transactions on Power Systems*, 10(3):1294–1301, 1995.

[Wu11]   Lei Wu. A tighter piecewise linear approximation of quadratic cost curves for Unit Commitment Problems. *IEEE Transactions on Power Systems*, 26(4):2581–2583, 2011.

[WW84]   A. J. Wood and B. F. Wollenberg. *Power Generation, Operation and Control.* John Wiley and Sons, New York, N. Y., 1984.

[WW94]   K. P. Wong and Y. W. Wong. Short term hydro thermal scheduling part I: simulated annealing approach. *Proc. Inst. Elect. Eng. Gen. Transm. Dist.*, 141:497–501, 1994.

[WWE11]   WWEC-2011. World wind energy report 2010. In *10th World Wind Energy Conference and Renewable Energy Exhibition, Greening Energy: Converting Deserts into Powerhouses, Cairo, Egypt*, pages 1–23, 31 October - 2 November 2011.

[XGK01]   H. X.S., H. Gooi, and D. Kirshen. Dynamic Economic Dispatch: feasible and optimal solutions. *IEEE Transactions on Power Systems*, 16(1), 2001.

[YKCCCL13] Wu Yuan-Kang, Huang Chih-Cheng, and Lin Chun-Liang. Resolution of the Unit Commitment problems by using the hybrid Taguchi-ant colony system algorithm. *International Journal of Electrical Power and Energy Systems*, 49:188–198, 2013.

[YLGR93]   H. Yan, P. B. Luh, X. Guan, and P. M. Rogan. Scheduling of hydrothermal power systems. *IEEE Transactions on Power Systems*, 8(3):1358–1365, 1993.

[YYH96]   H. T. Yang, P. C. Yang, and C. L. Huang. Evolutionary programming based Economic Dispatch for units with non smooth fuel costs functions. *IEEE Transactions on Power Systems*, 11:112–118, 1996.

[YYH97]   H. Yang, P. Yang, and C. Huang. A parallel genetic algorithm approach to solving the Unit Commitment problem: implementation on the transputer networks. *IEEE Transactions on Power Systems*, 12:661–668, 1997.

[ZG88]   F. Zhuang and F. D. Galiana. Toward a more rigorous and practical Unit Commitment by Lagrangian Relaxation. *IEEE Transactions on Power Systems*, 3:763–773, 1988.

List of Figures

List of Tables